Finite Element Methods for Geometric Problems

Dissertation

zur

Erlangung des Doktorgrades (Dr.rer.nat.)

der

Mathematisch-Naturwissenschaftlichen Fakultät

der

Rheinischen Friedrich-Wilhelms-Universität Bonn

vorgelegt von

Alexander Helmut-Wilhelm Raisch

aus

Reutlingen

Bonn, Juni 2012

Angefertigt mit Genehmigung der Mathematisch-Naturwissenschaftlichen Fakultät der
Rheinischen Friedrich-Wilhelms Universität Bonn

1. Gutachter: Prof. Dr. Sören Bartels

2. Gutachter: Prof. Dr. Martin Rumpf

Tag der Promotion: 04. September 2012

Erscheinungsjahr: 2012

Publications. Parts of this thesis have been published as preprints at the Collaborative Research Center (SFB) 611:

S.Bartels, G.Dolzmann, R.H.Nochetto and A.Raisch. *Finite Element Methods for Director Fields on Flexible Surfaces*. SFB preprint 2011.

A.Raisch. *Mixed Method for Conformally Invariant Variational Problems*. SFB preprint 2012.

Introduction

Geometric problems and nonlinear partial differential equations on manifolds or subdomains of the euclidean space have attracted many mathematicians within the last twenty years and even prior to that. The modelling of biological, chemical or physical processes like the demixing of alloys or emulsions, the action on the shape of human cells by certain surfactants sitting on the membrane or the alignment of liquid crystals due to internal and external forces lead to interesting mathematical problems whose answers are often far outside our theoretical understanding. But there are also almost ancient questions that are worth the effort to address. For instance, Plateau's problem, raised by Joseph-Louis Lagrange in 1760, or the more general version of finding surfaces with a prescribed mean curvature and a given boundary curve.

Right at the interface between applied sciences and mathematics the importance of numerical simulations drastically rose in recent years. Not only that a large part of an engineers work today or the development in modern industry is unthinkable without computer science but also mathematicians from all different areas are inspired by numerical methods and experiments that often provide predictions beyond theory.

Where do geometric problems arise?

From Plateau's problem to conformally invariant elliptic energies

The above mentioned problem of filling the interior of a given loop with a surface of least area has intrigued many scientists and occurs in the description of soap bubbles [49] or in modern architecture to name but a few applications.

One of the most well known examples in architecture is the olympic stadium in Munich. When studying optimal shapes of roofs, Frei Paul Otto tested different wireframe models that he plunged into a soap sud to look how the soap film spans the interspace.

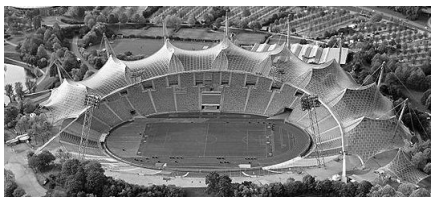

Olympic stadium Munich, 1972: One of the major works of Frei Paul Otto.

Mathematically this problem can be formulated as to find a map u from the two-dimensional unit ball $B_1(0)$ into the three-dimensional euclidean space $\mathbb{R}^3$, satisfying

$$-\Delta u = 2H(u)\partial_x u \times \partial_y u \tag{1}$$

in $B_1(0)$ and $u(\partial B_1(0)) = \Gamma$ on the boundary, where Γ is a given curve. Here H is the prescribed mean curvature and $\times$ denotes the usual three dimensional cross product. This equation appears as the Euler-Lagrange equation of

$$E^H(u) := \frac{1}{2}\int_{B_1(0)} |\nabla u|^2 \,\mathrm{d}x + \frac{3}{2}\int_{B_1(0)} Q(u)\partial_x u \times \partial_y u \,\mathrm{d}x, \tag{2}$$

where $Q : \mathbb{R}^3 \to \mathbb{R}^3$ and $H : \mathbb{R}^3 \to \mathbb{R}$ are related by $\operatorname{tr} DQ = \frac{1}{3}H$. The energy E^H in turn, is a special case of the conformally invariant elliptic energy

$$E(u) := \frac{1}{2}\int_{B_1(0)} |\nabla u|^2 + \omega(u)(\partial_x u, \partial_y u)\,\mathrm{d}x, \tag{3}$$

where u is a map with values in a manifold N and ω is a 2-form on N. Conformal invariance is to be understood as $E(u \circ \varphi) = E(u)$ for any conformal map $\varphi : B_1(0) \to B_1(0)$.

For $\omega = 0$ the functional (3) is called Dirichlet energy and stationary points satisfy the harmonic map equation

$$-\Delta u = A_N(u)[\nabla u, \nabla u], \tag{4}$$

where A_N denotes the second fundamental form of N. See [72] for a derivation of this identity or have a look at the famous reports on harmonic maps [35, 34] and the references therein. Because of the conformal invariance of the Dirichlet energy we have that with u also $u \circ \varphi$ for conformal φ is a solution of this equation.

Compactness results for approximations of solutions of such nonlinear partial differential equations have always been a difficult task. Although there are techniques to circumvent missing regularity properties [25, 40, 59, 72] there are many situations in which convergence is not clear. Minimizing sequences of the Dirichlet energy for instance are bounded in $W^{1,2}$, hence only weak convergence of the gradients in L^2 is given. This is not enough to ensure that weak limits of approximating sequences are solutions of the limit equation (4), because the right-hand side is quadratic in the gradient. A compactness result for the harmonic map equation was done in [44], using moving frames. The existence of these frames can be ensured either if the target manifold N is parallelizable or if it is of class C^4. Compactness of approximations of solutions of the Euler-Lagrange equations of (3) was shown in [68]. The key to proving this result is that every critical point of E satisfies an equation of the form

$$-\Delta u = \Omega \bullet \nabla u, \tag{5}$$

where $\Omega \in L^2(M, so(n) \otimes \mathbb{R}^2)$, that is, for all $i, j \in \{1, \dots, n\}$, $\Omega^{ij} = -\Omega^{ji} \in L^2(B_1(0), \mathbb{R}^2)$. The skew symmetry of Ω is used to prove a new compensation property and derive far reaching compactness and regularity results, see the Theorems 2.1.1 - 2.1.4 in Chapter 1. We point out that the proposition of Theorem 2.1.1 is that solutions of 5 are continuous and note that by establishing this continuity result a conjecture of E. Heinz [43] on surfaces of prescribed mean curvature and a conjecture by S. Hildebrandt [46, 47] which says that critical points of energies of the form (3) in 2-dimensions are continuous was proved in the affirmative.

Modelling cells and analyzing shape functionals

Understanding cells and their behavior in the presence of chemical and physical forces has become a field enjoying great interest in the last twenty years. One of the first works concerning a prescription of red blood cells is [45]. Almost all of the mathematical models deal with an energy of the form

$$E(\Gamma) := \frac{1}{2}\int_{\Gamma} c_H(H - H_0)^2 + c_K K\,\mathrm{d}x, \tag{6}$$

where $\Gamma \subset \mathbb{R}^3$ is a closed surface identified with the cell membrane, H is the mean curvature of Γ, K the Gaussian curvature, the constants c_H, c_K are the associated moduli of elasticity and H_0 is the so called spontaneous curvature that locally affects the shape of the surface. If we stay within one topological class of surfaces the integral over the Gaussian curvature K is constant by the theorem of Gauss-Bonnet and can therefore be neglected in the analysis. Furthermore, we note that for $H_0 = 0$, $c_H = 1$ and $c_K = 0$ we obtain the Willmore functional. We refer the reader to [77] for basic facts about Riemannian geometry and the Willmore functional and the works of [18, 54, 70] for existence theorems of Willmore surfaces and estimates on the energy. Numerical investigations and schemes for the L^2-gradient flow, also known as Willmore flow, can be found in [9, 10, 31, 62].

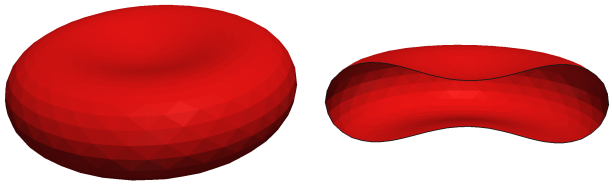

Discocytes as stationary points of the Willmore functional $W(\Gamma) = \frac{1}{2}\int_\Gamma H^2\,dx$ under the constraint of prescribed surface area and enclosed volume. First introduced in [45] this energy models the shape of red blood cells in the absence of outer forces.

Mathematically the definition of the L^2-gradient flow has to be formulated in a proper way, that is, a first task is to choose an appropriate metric space, characterize variations of Γ and determine the gradient of E, see for example [77] or for more general shape functionals see [29] and Chapter 1. Let $H_0 = const$ and $c_H = 1$, then the L^2-gradient flow for the normal velocity v of Γ leads to a fourth order nonlinear partial differential equation on an evolving surface

$$v = \Delta_\Gamma H + (H - H_0)|\nabla_\Gamma \nu|^2 - \frac{1}{2}(H - H_0)^2 H. \tag{7}$$

Treating such kind of equations analytically and numerically is a very delicate issue. Most of the numerical schemes exhibit crucial drawbacks. For example one cannot find an energy law which would yield stability of the scheme and guarantee energy reduction, or they exhibit unfavorable tangential movements that lead to defects in the mesh.

Contributions of this work

The mixed formulation

We denote by $\mathcal{T}_h$ a regular triangulation of the polygonal domain $M \subset \mathbb{R}^2$ and by $\mathcal{N}_h$ the set of nodes. We present a mixed finite element method for (5) using the MINI-element $\left(V^h_{mini}, \mathcal{S}^1(\mathcal{T}_h)\right)$, see [4] for details. We compute $(p_h, u_h) \in [V^h_{mini}]^{n\times 2} \times [\mathcal{S}^1(\mathcal{T}_h)]^n$ satisfying $u_h(z) \in N$ for all $z \in \mathcal{N}_h$ and solving

$$(p_h; \sigma_h) + \quad (\operatorname{div} \sigma_h, u_h) \;= \int_{\partial M} u_{D,h}\sigma_h \bullet \nu_{\partial M} \mathrm{d}x, \tag{8}$$

$$(\operatorname{div} p_h, v_h) + (\Omega_h \bullet p_h, v_h) \;= \qquad 0, \tag{9}$$

for all $(\sigma_h, v_h) \in [V^h_{mini}]^{n\times 2} \times [\mathcal{S}^1(\mathcal{T}_h)]^n$. We would like to apply the above mentioned compactness result to show that accumulation points of the sequence $(p_h, u_h)_h$ yield solutions of (5). Unfortunately the proof makes both use of integration by parts and gradient structures. The first fact prevents us from using a discretization of the form

$$(\nabla u_h; \nabla v_h) - (\Omega_h \bullet \nabla u_h, v_h) \;=\; 0, \tag{10}$$

with u_h piecewise linear, because ∇u_h is then piecewise constant and jump terms across the inner edges occur at the integration by parts. The latter fact causes error terms including $||\nabla u_h - p_h||_{L^2(M)}$ for which we have no convergence to zero in general. Fortunately $p_h \in [V^h_{mini}]^{n\times 2}$ is the L^2-projection of ∇u_h and therefore

$$||\nabla u_h - p_h||_{L^2(M)} = \inf_{\sigma_h \in [V^h_{mini}]^{n\times 2}} ||\nabla u_h - \sigma_h||_{L^2(M)}. \tag{11}$$

It turns out that for two meshes $\mathcal{T}_{h_1}, \mathcal{T}_{h_2}$ with $h_2 = o(h_1)$ and any uniformly bounded sequence $(u_{h_1})_{h_1} \subset W^{1,2}(M; \mathbb{R}^n)$ satisfying $u_{h_1} \in [\mathcal{S}^1(\mathcal{T}_{h_1})]^n$ for every $h_1 > 0$ we have that

$$\inf_{\sigma_{h_2}} ||\sigma_{h_2} - \nabla u_{h_1}||_{L^2(M)} \to 0 \quad \text{as} \quad h_1 \to 0, \tag{12}$$

where the infimum is taken over all $\sigma_{h_2} \in [V^{h_2}_{mini}]^{n\times 2}$. Thus if $N \subset \mathbb{R}^n$ is a C^3 submanifold and under appropriate conditions on the sequences $(\Omega_{h_{1,2}})_{h_{1,2}}$, $(p_{h_2})_{h_2}$ and $(u_{h_1})_{h_1}$ we establish the following theorem.

Theorem I. *Let $\mathcal{T}_{h_1}$ and $\mathcal{T}_{h_2}$ be two sequences of quasiuniform triangulations with mesh-sizes $h_2 = o(h_1)$ and for $h_1, h_2 > 0$ let $(p_{h_2}, u_{h_1}, \Omega_{h_{1,2}}) \in [V^{h_2}_{mini}]^{n\times 2} \times [\mathcal{S}^1(\mathcal{T}_{h_1})]^n \times L^2(M; so(n) \otimes \mathbb{R}^2)$ satisfy $u_{h_1}(z) \in N$ for all $z \in \mathcal{N}_{h_1}$ and*

$$(p_{h_2}; \sigma_{h_2}) + \quad (\operatorname{div} \sigma_{h_2}, u_{h_1}) \;=\; \int_{\partial M} u_{D,h_1} \sigma_{h_2} \bullet \nu_{\partial M} \, dx, \tag{13}$$

$$(\operatorname{div} p_{h_2}, v_{h_1}) + (\Omega_{h_{1,2}} \bullet p_{h_2}, v_{h_2}) \;=\; 0, \tag{14}$$

for all $(\sigma_{h_2}, v_{h_1}) \in [V^{h_2}_{mini}]^{n\times 2} \times [\mathcal{S}^1(\mathcal{T}_{h_1})]^n$. Assume that $||p_{h_2}||_{H(\operatorname{div})} + ||\nabla u_{h_1}||_{L^2} + ||\Omega_{h_{1,2}}||_{L^2} \le C_0$, and $u_{D,h_1} \to u_D$ in $L^2(\partial M; \mathbb{R}^n)$ as $h_1 \to 0$. Then every weak accumulation point of the sequence $(p_{h_2}, u_{h_1}, \Omega_{h_{1,2}})_{h_{1,2}}$ satisfies

$$(p\,;\, \sigma) + (\operatorname{div} \sigma, u) \;=\; \int_{\partial M} u_D \sigma \bullet \nu_{\partial M} \, dx, \tag{15}$$

$$(\operatorname{div} p, v) + (\Omega \bullet p, v) \;=\; 0, \tag{16}$$

for all $(\sigma, v) \in H(\operatorname{div}; \mathbb{R}^{n\times 2}) \times L^2(M; \mathbb{R}^n)$.

As mentioned above we could not establish a convergence proof for the $P1$-method under the usual assumption $||\nabla u_h||_{L^2} + ||\Omega_h||_{L^2} \le C_0$. However, if we take a slightly stronger bound on $(u_h, \Omega_h)_h$ for granted we obtain the desired compactness.

Theorem II. *Let $\mathcal{T}_h$ be a sequence of quasiuniform triangulations of M and for $h > 0$ let $(u_h, \Omega_h) \in [\mathcal{S}^1(\mathcal{T}_{h_1})]^n \times L^2(M; so(n) \otimes \mathbb{R}^2)$ satisfy $u_h(z) = u_{D,h}(z)$ for all $z \in \mathcal{N}_h \cap \partial M$, $u_h(z) \in N$ for all $z \in \mathcal{N}_h$ and*

$$(\nabla u_h, \nabla v_h) - (\Omega_h \bullet \nabla u_h, v_h) = 0, \tag{17}$$

for all $v_h \in [\mathcal{S}^1_0(\mathcal{T}_h)]^n$. Assume that $||\nabla u_h||_{L^{2+\theta}} + ||\Omega_h||_{L^{2+\theta}} \le C_0$, for some $\theta > 0$ and $u_{D,h} \to u_D$ in $L^2(\partial M; \mathbb{R}^n)$ as $h \to 0$. Then every weak accumulation point of the sequence $(u_h, \Omega_h)_h$ satisfies

$$(\nabla u, \nabla v) - (\Omega \bullet \nabla u, v) = 0 \tag{18}$$

for all $v \in W^{1,2}_0(M; \mathbb{R}^n)$.

Equipped with these results we discuss the approximation of harmonic maps and surfaces of prescribed mean curvature.

Harmonic maps

Solutions of the mixed system in the continuous setting can be characterized as saddle points of the augmented energy

$$\widetilde{E}(p, u) := \frac{1}{2} \int_M |p|^2 \, \mathrm{d}x + \int_M \operatorname{div} p \bullet u \, \mathrm{d}x + \int_M \omega(u)(\partial_x u, \partial_y u) \, \mathrm{d}x - \int_{\partial M} u_D p \bullet \nu_{\partial M} \, \mathrm{d}x, \tag{19}$$

where $p : M \to \mathbb{R}^{n\times 2}$, $u : M \to N$ and $u_D : \partial M \to \mathbb{R}^n$ defines the boundary conditions. For the approximation of harmonic maps we set $\omega = 0$ and replace u_D by $u_{D,h_1} \in [\mathcal{S}^1(\mathcal{T}_{h_1})]^n$ satisfying $u_{D,h_1} \to u_D$ in $L^2(\partial M; \mathbb{R}^n)$ as $h_1 \to 0$ to obtain the discrete energy $\widetilde{E}_{h_{1,2}}$. We call $(p_{h_2}, u_{h_1}) \in [V^{h_2}_{mini}]^{n\times 2} \times [\mathcal{S}^1(\mathcal{T}_{h_1})]^n$ a discrete harmonic pair if $u_{h_1}(z) \in N$ for all $z \in \mathcal{N}_{h_1}$ and if (p_{h_2}, u_{h_1}) is a saddle point of $\widetilde{E}_{h_{1,2}}$. This means that for all $(\sigma_{h_2}, v_{h_1}) \in [V^{h_2}_{mini}]^{n\times 2} \times [\mathcal{S}^1(\mathcal{T}_{h_1})]^n$ that satisfy $v_{h_1}(z) \in N$ for all $z \in \mathcal{N}_{h_1}$, we have

$$\widetilde{E}_{h_{1,2}}(p_{h_2}, v_{h_1}) \le \widetilde{E}_{h_{1,2}}(p_{h_2}, u_{h_1}) \le \widetilde{E}_{h_{1,2}}(\sigma_{h_2}, u_{h_1}). \tag{20}$$

We show that discrete harmonic pairs satisfy a compactly perturbed system of the form (13) - (14) and deduce a weak compactness result.

Theorem III. *Let $\mathcal{T}_{h_1}$ and $\mathcal{T}_{h_2}$ be two sequences of quasiuniform triangulations with mesh-sizes $h_2 = o(h_1)$ and for $h_1, h_2 > 0$ let $(p_{h_2}, u_{h_1}) \in [V^{h_2}_{mini}]^{n\times 2} \times [\mathcal{S}^1(\mathcal{T}_{h_1})]^n$ satisfy $u_{h_1}(z) \in N$ for all $z \in \mathcal{N}_{h_1}$. Moreover, let (p_{h_2}, u_{h_1}) be a sequence of saddle points of the energy*

$$\widetilde{E}_{h_{1,2}}(p_{h_2}, u_{h_1}) := \frac{1}{2}\int_M |p_{h_2}|^2\,dx + \int_M \operatorname{div} p_{h_2} \bullet u_{h_1}\,dx - \int_{\partial M} u_{D,h_1} p_{h_2} \bullet \nu_{\partial M}\,dx. \tag{20}$$

Assume that $||p_{h_2}||_{H(\mathrm{div})} + ||u_{h_1}||_{W^{1,2}} \leq C_0$, and $u_{D,h_1} \to u_D$ in $L^2(\partial M; \mathbb{R}^n)$ as $h_1 \to 0$. Then every weak accumulation point of the sequence $(p_{h_2}, u_{h_1})_{h_{1,2}}$ satisfies $p = \nabla u$ and $u \in W^{1,2}(M, \mathbb{R}^n)$ is a harmonic map into N, subject to the boundary conditions $u|_{\partial M} = u_D$.

A convergence proof for the approximation of harmonic maps with finite differences on planar lattices can be found in [64]. Some techniques from [64] have been generalized to finite element methods in [13]. Therein, $u_h \in [\mathcal{S}^1(\mathcal{T}_h)]^n$ is called a discrete harmonic map if it satisfies $u_h(z) \in N$ for all $z \in \mathcal{N}_h$ and

$$(\nabla u_h; \nabla v_h) = 0, \tag{21}$$

for all $v_h \in [\mathcal{S}^1(\mathcal{T}_h)]^n$ satisfying $v_h(z) \in T_{u_h(z)}N$ for all $z \in \mathcal{N}_h$. Main ingredients of the convergence proof are the moving frame technique from [44] and concentration compactness principles for finite elements which we recall for our purpose in Section 1.6. These arguments play an important role in our proofs, too, and we use them to show that occuring error terms converge to distributions whose support is a countable discrete subset of M. By [40] it follows that these Dirac measures are identically zero. If N is a unit sphere the high symmetry simplifies the proof of convergence not only in the continuous case, but also in the discrete setting as can be seen in [12] for the above mentioned discretization or in [17] for an equivalent weak formulation and its discretization. Referring to Theorem II we establish a compactness result for the $P1$-method under the stronger assumption that $(u_h)_h \subset W^{1,2+\theta}(M; \mathbb{R}^n)$ is uniformly bounded for some $\theta > 0$.

Theorem IV. *Let $\mathcal{T}_h$ be a sequence of quasiuniform triangulations of M and for $h > 0$ let $u_h \in [\mathcal{S}^1(\mathcal{T}_h)]^n$ be such that $u_h(z) = u_{D,h}(z)$ for all $z \in \mathcal{N}_h \cap \partial M$, $u_h(z) \in N$ for all $z \in \mathcal{N}_h$ and let u_h solve (21). Assume that $||\nabla u_h||_{L^{2+\theta}} \leq C_0$ for some $\theta > 0$ and $u_{D,h} \to u_D$ in $L^2(\partial M, \mathbb{R}^n)$ for $h \to 0$, then every weak accumulation point of the sequence $(u_h)_h$ is a harmonic map into N, subject to the boundary condition $u|_{\partial M} = u_D$.*

For a classification of the results from [12, 13] and the compactness results in this thesis we propose the following table. Columns 1, 2 and 4 refer to the standard $P1$-method while column 3 refers to the mixed method.

	$\|\|\nabla u_h\|\|_{L^2} \leq C_0$	$\|\|\nabla u_h\|\|_{L^{2+\theta}} \leq C_0$	$\|\|\nabla u_{h_1}\|\|_{L^2} \leq C_0$, $\|\|p_{h_2}\|\|_{H(\mathrm{div})} \leq C_0$	$\|\|\nabla u_h\|\|_{L^2} \leq C_0$, N is a sphere
[12, 13]	✓ 1),2)	✓ 1),2)		✓
Thesis		✓ 3)	✓ 3),4)	

The different numbers at the checkmarks ✓ denote that some of the following properties have to be fulfilled to guarantee compactness: 1) $\mathcal{T}_h$ is logarithmically right angeled 2) N is a C^4 submanifold or parallelizable 3) N is a C^3 submanifold 4) the two mesh-sizes satisfy $h_2 = o(h_1)$

In [48] a saddle point approach for the computation of harmonic maps is studied, using the functional

$$F(u, \lambda) := \frac{1}{2}\int_M |\nabla u|^2\,\mathrm{d}x + \int_M \lambda \bullet f(u)\,\mathrm{d}x. \tag{22}$$

Here $f : \mathbb{R}^n \to \mathbb{R}^k$ is such that $N := \{x \in \mathbb{R}^n : f(x) = 0\}$. Let $u \in W^{2,2}(M; \mathbb{R}^n) \cap W^{1,\infty}$ be a harmonic map into $N \subset \mathbb{R}^n$. It is shown that there exists $u_h \in [\mathcal{S}^1(\mathcal{T}_h)]^n$ in a small neighborhood of

$\mathcal{I}_h u$ satisfying

$$||u_h - u||_{W^{1,2}} \leq Ch. \tag{23}$$

Surfaces of prescribed mean curvature

Our method applies directly to the problem of finding surfaces of prescribed mean curvature $H \in L^\infty(\mathbb{R}^3)$. These parametrizations $u : B_1(0) \to \mathbb{R}^3$ are solutions of (1) and satisfy $u(\partial B_1(0)) = \Gamma$, where $\Gamma \subset \mathbb{R}^3$ is an arbitrary, possibly knotted boundary curve. If the 2-form ω is such that $2\mathrm{d}\omega = H(u)\mathrm{d}u_1\mathrm{d}u_2\mathrm{d}u_3$ and N is replaced by the whole $\mathbb{R}^3$ then solutions of (1) are stationary points of the general conformal invariant elliptic energy (3). For the discretization we consider polygonal approximations B_h of the unit disk, and two sequences of quasiuniform triangulations $\mathcal{T}_{h_1}$ and $\mathcal{T}_{h_2}$ with $h_2 \leq h_1$ and $h_2 = o(h_1)$ are such that $\cup_{\mathcal{T}_{h_2}} T_{h_2} = \cup_{\mathcal{T}_{h_1}} T_{h_1} = B_{h_1}$.

Theorem V. *Consider two sequences of triangulations $\mathcal{T}_{h_1}$ and $\mathcal{T}_{h_2}$ of B_{h_1} with $h_2 = o(h_1)$ and for $h_1, h_2 > 0$ let $(p_{h_2}, u_{h_1}) \in [V^{h_2}_{mini}]^{n\times 2} \times [\mathcal{S}^1(\mathcal{T}_{h_1})]^n$ be a saddle point of the energy*

$$\widetilde{E}_{h_{1,2}}(p_{h_2}, u_{h_1}) := \frac{1}{2}\int_{B_{h_1}} |p_{h_2}|^2\, dx + \int_{B_{h_1}} \operatorname{div} p_{h_2} \bullet u_{h_1}\, dx + \int_{B_{h_1}} \omega(u_{h_1})(\partial_x u_{h_1}, \partial_y u_{h_1})\, dx - \int_{\partial B_{h_1}} u_{D,h_1} p_{h_2} \bullet \nu_{\partial M}\, dx. \tag{24}$$

Assume that $||p_{h_2}||_{H(\mathrm{div})} + ||u_{h_1}||_{W^{1,2}} \leq C_0$, and $u_{D,h_1} \to u_D$ in $L^2(\partial M; \mathbb{R}^n)$ as $h_1 \to 0$. Then every weak accumulation point of the sequence $(p_{h_2}, u_{h_1})_{h_{1,2}}$ satisfies $p = \nabla u$ and $u \in W^{1,2}(M, \mathbb{R}^n)$ is a solution of (1) and satisfies $u|_{\partial M} = u_D$.

There is a large amount of important literature addressing this problem that we can not cover here, so we refer the reader only to [41, 72] for an analytical overview as well as the references in [68] and [72]. A substantial treatment from the numerical point of view was done in [33]. Especially the Plateau problem ($H = 0$) has found considerable attention in applied mathematics and numerics, see for example [42].

Geometric flows and applications from biology

We work on a novel model for the evolution of biomembranes driven by the L^2-gradient flow. An elasticity functional is introduced and describes the coupling of a director field on a membrane and its curvature. It has the form

$$E(\Gamma, n) = \int_\Gamma \Big(\frac{1}{2}\big|\mathrm{div}_\Gamma \nu - \delta \mathrm{div}_\Gamma n\big|^2 + \frac{\lambda}{2}\big|\nabla_\Gamma n\big|^2\Big)\mathrm{d}x, \tag{25}$$

where div_Γ and ∇_Γ are the tangential divergence and gradient operators and $\lambda > 0$. After the discussion of a linearization of (25) in the Monge gauge we exploit the qualitative behavior of graphs. Turning to the nonlinear model we deduce a variation of E and formulate the relaxation dynamics. If v_Γ denotes the normal velocity of Γ and $\frac{\delta E}{\delta \Gamma}$ the variation of E with respect to Γ then the evolution of Γ, in a rough notation, is given by $v_\Gamma = -\frac{\delta E}{\delta \Gamma}$. For the discretization in the closed surface case we employ parametric finite elements and primarily use a scheme developed in [10]. We compute the discrete surface Γ_h^j at time t_j as a parametrization over the surface Γ_h^{j-1} at time t_{j-1}. If X_h^{j-1} and X_h^j are the identity maps on Γ_h^{j-1} and Γ_h^j respectively then the normal velocity of the discrete surface at time t_{j-1} is approximated by

$$v_h^{j-1} \approx \frac{1}{\tau}\Big(X_h^j - X_h^{j-1}\Big) \bullet \nu_h^{j-1}, \tag{26}$$

where ν_h^{j-1} is the discrete outer normal on Γ_h^{j-1}. We denote by $\Psi_{E,h}^{j,j-1}$ a semi-implicit discretization of the variation $\frac{\delta E}{\delta \Gamma}$ which depends on the director field and on the discrete scalar mean curvatures

H_h^{j-1} and H_h^j of Γ_h^{j-1} and Γ_h^j respectively. For the evolution of the surface in the discrete setting we compute in every step the parametrization $X_h^j \in [\mathcal{S}^1(\Gamma_h^{j-1})]^3$ of Γ_h^j and the discrete mean curvature $H_h^j \in \mathcal{S}^1(\Gamma_h^{j-1})$ of Γ_h^j as solutions of

$$\frac{1}{\tau}\Big((X_h^j - X_h^{j-1}) \bullet \nu_h^{j-1}, \phi_h\Big) = -\Big(\Psi_{E,h}^{j,j-1}, \phi_h\Big), \tag{27}$$

$$\Big(\nabla_{\Gamma_h^{j-1}} X_h^j, \nabla_{\Gamma_h^{j-1}} \eta_h\Big) = -\Big(H_h^j, \eta_h \bullet \nu_h^{j-1}\Big), \tag{28}$$

for all $\eta_h \in [\mathcal{S}^1(\Gamma_h^{j-1})]^3$ and all $\phi_h \in \mathcal{S}^1(\Gamma_h^{j-1})$. While (27) is a discretization of $v_\Gamma = -\frac{\delta E}{\delta \Gamma}$, equation (28) traces back to the crucial equality $\Delta_\Gamma \mathrm{id}_\Gamma = H\nu$ and relates the identity map on a surface and its curvature. This idea was first used in [30] for a finite element treatment of evolutionary surfaces. For the evolution of the director field we employ the $P1$-method which is well-defined and convergent also on curved surfaces, see [13] for details.

Overview of the thesis

The outline of this work is as follows. After introducing some basic notation and elementary differential geometry we define the used finite element spaces in Chapter 1. In Chapter 2 we start with a summary of the results from [68] and cite the convergence proof that inspired the first part of this work. After that we propose proofs of Theorem I and II.

In Chapter 3 we apply the results from Chaper 2 to harmonic pairs and discrete harmonic maps and devise an iterative scheme for the numerical realization. In Chapter 4 we define a mixed formulation of (1) and analyze its convergence before deducing an iterative scheme. In the last chapter of this thematically first block we illustrate the performance of our numerical schemes.

In Chapter 6 we start our work on shape functionals and biomembranes with an introduction to the numerical treatment of the Willmore flow. We proceed with the derivation of our elasticity functional and analyze the linearized model. Finally, we formulate the L^2-gradient flow for the nonlinear model and carry out several numerical experiments.

Open questions

There remain interesting questions in the mathematical neighborhood of harmonic maps which we did not address within this dissertation project. We highlight some of them in this section. As far as the author knows there is no uniqueness result for discrete harmonic maps with values in arbitrary submanifolds, neither for the $P1$-method nor for the mixed method. One possible approach to this question is [50], where a maximum principle for the geodesic distance of two different solutions is proved.

As we work with mixed finite elements one may ask whether discretizations using other stable elements lead to comparable compactness results, for example the lowest order Raviert-Thomas space [67]. In light of the $P1$-method from [13] and the discussed mixed method we propose the following discrete formulation.

Compute $(p_h, u_h) \in [\mathcal{RT}^0(\mathcal{T}_h)]^{n\times 2} \times [\mathcal{L}^0(\mathcal{T}_h)]^n$ *such that* $u_h\Big|_T \in N$ *for all* $T \in \mathcal{T}_h$ *and*

$$(p_h; \sigma_h) + (\operatorname{div} \sigma_h, u_h) = \int_{\partial M} u_{D,h}\sigma_h \bullet \nu_{\partial M}\, dx, \tag{29}$$

$$(\operatorname{div} p_h, v_h) = 0, \tag{30}$$

for all $\sigma_h \in [\mathcal{RT}^0(\mathcal{T}_h)]^{n\times 2}$ *and all* $v_h \in [\mathcal{L}^0(\mathcal{T}_h)]^n$ *satisfying* $v_h\Big|_T \in T_{u_h|_T}N$ *for all* $T \in \mathcal{T}_h$.

The advantage of such an approximation is that we have $u_h \in N$ almost everywhere in stead of $u_h \in N$ almost nowhere, as in the $P1$ setting or the mixed formulation using the MINI-element.

Finally we note that there exists a compactness result for n-harmonic maps with values in general submanifolds, see [75]. If N is a unit sphere there is a convergent finite element scheme available for n-harmonic maps, see [7]. As far as the author knows no discrete version for arbitrary target manifolds exists.

Acknowledgements

I would like to express my sincere gratitude to my advisor Prof. Dr. Sören Bartels for this interesting research project and the support of my Ph.D. studies. I appreciate the stimulating and revealing discussions during the last three years. I acknowledge his support for the participation at several summer schools, seminars and conferences that broadened my mathematical horizon.

Furthermore, I acknowledge support by the DFG through the Collaborative Research Center (SFB) 611 *Singular Phenomena and Scaling in Mathematical Models*.

Thanks to Clemens Kienzler and Patrick Schreier for proofreading parts of this dissertation. Moreover, I am thankful for Patricks help with any type of MATLAB problems and the efficient vectorization of the algorithms. Especially in the implementation of the simulations with different mesh sizes.

Finally, I am deeply grateful to my beloved Annalie, for her support within the last years. Her unbounded patience and support in mathematically hard times gave me the requisite perseverance.

Contents

Chapter 1.

Background and Analytical tools

Finite element methods for geometric problems and partial differential equations on submanifolds occured in a great variety in recent years [1, 10, 11, 13, 14, 17, 21, 26, 27, 30, 31, 33, 36, 42, 64]. This section is devouted to a short overview over the techniques we use and to introduce basic notations.

We provide basics in differential geometry, analytical tools for the numerical treatment of partial differential equations, triangulations of curved surfaces and we introduce the finite element setting for the different examples examined.

1.1. Basic notation

Standard notation is adopted throughout this work. We denote by $a \bullet b$ the standard inner product of two vectors $a, b \in \mathbb{R}^n$ and for matrices $p, \sigma \in \mathbb{R}^{n\times\ell}$ we set $p : \sigma := \mathrm{tr}(p^T\sigma) = \sum_{i=1}^{n}\sum_{j=1}^{\ell} p_{ij}\sigma_{ij}$. Furthermore $(\cdot;\cdot)$ is the standard L^2-inner product over the domain $M \subset \mathbb{R}^2$ and $(W^{m,p}(M;\mathbb{R}^\ell), ||\cdot||_{W^{m,p}})$ denotes the (m,p)-Sobolev space of vector-valued functions. For $n \in \mathbb{N}$ let $so(n)$ denote the set of antisymmetric matrices, that is, $so(n) = \{A = (a_{ij})_{i,j=1,\dots,n} \in \mathbb{R}^{n\times n} : a_{ij} = -a_{ji}\}$. Then the tensor product of $so(n)$ with $\mathbb{R}^2$ is defined as follows

$$so(n) \otimes \mathbb{R}^2 := \{\Omega \in \mathbb{R}^{n\times n\times 2} : \Omega^{ij} = -\Omega^{ji} \in \mathbb{R}^2 \ \forall i, j = 1, \dots, n\}.$$

As was shown in [68], the Euler-Lagrange equations, corresponding to two-dimensional conformally invariant energy functionals take the form

$$-\Delta u = \Omega \bullet \nabla u,$$

with some $\Omega \in L^2(M; so(n) \otimes \mathbb{R}^2)$. By this short notation we mean that the mapping $u : M \to \mathbb{R}^n$ satisfies

$$-\Delta u^i = \sum_{j=1}^{n} \Omega^{ji} \bullet \nabla u^j$$

for all $i = 1, \dots, n$. As we will see in the convergence proof we have the auxiliary matrix equation

$$\nabla A - A\Omega = \nabla^\perp B,$$

where $A, B : M \to \mathbb{R}^{n\times n}$ and $\nabla^\perp = [-\partial_y, \partial_x]^T$ is the rotated gradient. The above equation is to be understood as

$$\nabla A_{ij} - \sum_{k=1}^{n} A_{ik}\Omega^{kj} = \nabla^\perp B_{ij}$$

for $i, j = 1, \dots, n$. Throughout this work $C > 0$ is a generic positive h-independent constant which may take different values at different locations. The subscripts inv and P indicate that the constants C_{inv} and C_P stem from an inverse estimate and the Poincaré inequality respectively.

1.2. Elementary differential geometry

We give a short summary of basic definitions and statements about submanifolds in $\mathbb{R}^n$. We refer the reader to [13],[56] and [57] or the lectures notes [63] for details concerning this summary of technical

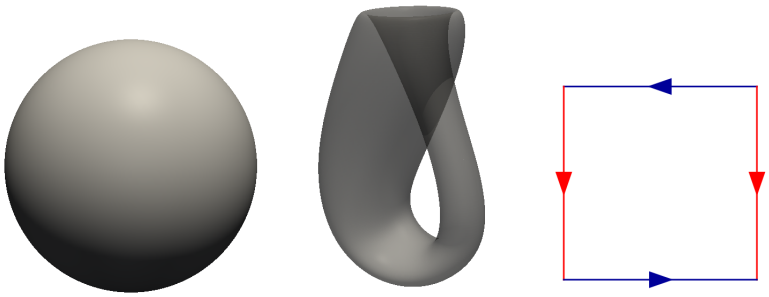

Figure 1.1.: Two examples for orientable and non-orientable surfaces: The standard sphere $\mathbb{S}^2$ (left) and the so-called Klein bottle (middle) which is topologically obtained by glueing together the edges of the unit square in the directions indicated in the right figure.

tools from differential geometry and finite elements. The lecture notes provide also a profound discussion on geometric evolution problems like the mean curvature flow. The simulation of membranes and cells in Chapter 6 are an example for an evolution problem steming from biology.

Definition 1.2.1 *(Simple submanifold) Let $\ell \geq 1$, $n \geq 2$ and $k \leq d$. A set $E \subset \mathbb{R}^n$ is a simple k-dimensional C^ℓ submanifold, if there exists an open set $V \subset \mathbb{R}^k$ and an injective C^ℓ-map $X : V \to \mathbb{R}^n$ such that $\operatorname{rank}\left(\frac{\partial X}{\partial \xi_1}, \ldots, \frac{\partial X}{\partial \xi_k}\right) = k$ and $X(V) = E$. Moreover $X^{-1} : E \to V$ has to be continuous. We call X a parametrization of E.*

Definition 1.2.2 *(Tangent space) Let E be a simple k-dimensional C^ℓ-submanifold. The tangent space at $p \in E$ is defined by*

$$T_x E := \operatorname{span}\left(\frac{\partial X}{\partial \xi_1}, \ldots, \frac{\partial X}{\partial \xi_k}\right),$$

where X is a parametrization.

Definition 1.2.3 *(Submanifold) A set $N \subset \mathbb{R}^n$ is a k-dimensional C^ℓ submanifold, if for every $p \in N$ there exists a k-dimensional neighbourhood $U(p)$ of p such that $N \cap U(p)$ is a simple k-dimensional submanifold.*

Definition 1.2.4 *(Orientable surface) A set $\Gamma \subset \mathbb{R}^n$ is an orientable C^ℓ surface, if it is a $n-1$-dimensional C^ℓ submanifold and if there exists a continuous map $\nu : \Gamma \to \mathbb{R}^n$ such that*

$$\nu(p) \perp T_p\Gamma \text{ and } |\nu(p)| = 1,$$

for all $p \in \Gamma$.

We assume now, that $\Gamma \subset \mathbb{R}^n$ is a $n-1$-dimensional compact and orientable surface. We want to define the tangential differential operators on surfaces and introduce the notion of curvature and volume on Γ. We call a function $f : \Gamma \to \mathbb{R}$ differentiable if for every point $p \in \Gamma$ and every parametrization $X : V \subset \mathbb{R}^{n-1} \to \Gamma \cap U(p)$ the composition $f \circ X$ is differentiable.

Definition 1.2.5 *(First fundamental form) Let $X : V \to U(x_0) \cap \Gamma$ be a local parametrization. Then the first fundamental form is defined as*

$$g_{ij} := \frac{\partial X}{\partial \xi_i} \bullet \frac{\partial X}{\partial \xi_j}.$$

Definition 1.2.6 *(Tangential gradient and divergence) Let Γ be a $n-1$-dimensional surface in $\mathbb{R}^n$. Suppose that for every $p \in \Gamma$ there exists an open set U in $\mathbb{R}^n$ containing p and a C^1 function $\tilde{f} : U \to \mathbb{R}$ with $\tilde{f}\Big|_{U\cap\Gamma} = f\Big|_{U\cap\Gamma}$. Then the tangential gradient of f is defined as*

$$\nabla_\Gamma f(p) = (\mathrm{Id} - \nu(p) \otimes \nu(p))\nabla \tilde{f}(p),$$

where $\nu(p)$ is a unit normal. Note that this definition is independent of the local parametrization and the choice of the unit normal. Let $w \in C^1(\Gamma;\mathbb{R}^n)$ and $\tilde{w} \in C^1(U,\mathbb{R}^n)$ where $\tilde{w}\big|_{U\cap\Gamma} = w\big|_{U\cap\Gamma}$. We define the tangential divergence as

$$\operatorname{div}_\Gamma w(p) = \operatorname{div}\tilde{w}(p) - \nu^T(p)D\tilde{w}(p)\nu(p).$$

For later purposes we compute the defined operators in local coordinates. Let X be a local parametrization of Γ, $\xi \in V$ and $p \in X(V) = U(p)\cap\Gamma$ such that $X(\xi) = p$. Then the vectors

$$v^i = \sum_{j=1}^{d-1} \frac{\partial X}{\partial \xi_j}(g^{-1/2}(\xi))_{ij}$$

form an orthonormal basis of $T_p\Gamma$. We write g^{ij} for the (i,j)-th entry of the inverse of g_{ij}, that is, we have $\sum\limits_{k=1}^{n-1} g^{ik}g_{kj} = \delta_{ij}$.

Lemma 1.2.7 *(Rerpresentation of $\operatorname{div}_\Gamma$ and ∇_Γ) Let $f : \Gamma \to \mathbb{R}$ and $w : \Gamma \to \mathbb{R}^n$ be differentiable and let X be a local parametrization. Then we have that*

$$(\nabla_\Gamma f)\circ X = \sum_{i=1}^{n-1}\sum_{j=1}^{n-1} g^{ij}\frac{\partial}{\partial\xi_j}(f\circ X)\frac{\partial X}{\partial\xi_i}$$

and

$$(\operatorname{div}_\Gamma w)\circ X = \sum_{i=1}^{n-1}\sum_{j=1}^{n-1} g^{ij}\frac{\partial X}{\partial\xi_i}\bullet\frac{\partial}{\partial\xi_j}(w\circ X)$$

Proof. For the representation of $\nabla_\Gamma f$ we note that

$$\frac{\partial}{\partial\xi_j}(f\circ X) = (\nabla f)\circ X \bullet \frac{\partial X}{\partial\xi_j} = (\nabla_\Gamma f)\circ X \bullet \frac{\partial X}{\partial\xi_j},$$

where the first equality is the chain rule and the second one stems from the fact, that the normal part of the gradient vanishes. Since $\nabla_\Gamma f$ is tangent to Γ there exist $(a_i)_{i=1,\dots,n-1} \subset \mathbb{R}$ such that $\nabla_\Gamma f = \sum_i a_i\frac{\partial X}{\partial\xi_i}$. We multiply this equality with $\frac{\partial X}{\partial\xi_j}$ to obtain the identity

$$\frac{\partial}{\partial\xi_j}(f\circ X) = \sum_i a_i g_{ij},$$

and therefore $a_i = \sum_j g^{ij}\frac{\partial}{\partial\xi_j}(f\circ X)$. We conclude

$$(\nabla_\Gamma f)\circ X = \sum_{i=1}^{n-1} a_i\frac{\partial X}{\partial\xi_i} = \sum_{i,j=1}^{n-1} g^{ij}\frac{\partial}{\partial\xi_j}(f\circ X)\frac{\partial X}{\partial\xi_i}.$$

For the representation of the divergence we complete the orthonormal basis of the tangent space $v^1,\dots,v^{n-1}$ to a basis of $\mathbb{R}^n$ by adding the normal vector field $v^n := \nu$. For an extension $\tilde{w} : \mathbb{R}^n \to \mathbb{R}^n$ of w we have that

$$\begin{aligned}\operatorname{div}\tilde{w} = \operatorname{tr} D\tilde{w} &= \sum_{i=1}^{n} v_i^T D\tilde{w}v_i = \sum_{i=1}^{n-1} v_i^T D\tilde{w}v_i + \nu^T D\tilde{w}\nu \\ &= \sum_{i,j,k=1}^{n-1} g_{ij}^{(-1/2)}g_{ik}^{(-1/2)}X_j^T D\tilde{w}X_k + \nu^T D\tilde{w}\nu = \sum_{j,k=1}^{n-1} g^{jk}\frac{\partial}{\partial\xi_j}(w\circ X)\bullet X_k + \nu^T D\tilde{w}\nu.\end{aligned}$$

□

In order to integrate functions on a given surface Γ we need to define the volume element. Let $E' \subset \mathbb{R}^k$ and let $X : E' \to E$ be a local parametrization of $E \subset \Gamma$. Let g_{ij} be the first fundamental form and set $g = \det g_{ij}$. Then, the $n-1$-dimensional Hausdorff measure of E is

$$\mathcal{H}^{n-1}(E) = \int_{E'} \sqrt{g} \mathrm{d}\xi.$$

Suppose further that $f : E \to \mathbb{R}$ is a measurable function. Then

$$\int_E f \,\mathrm{d}\mathcal{H}^{n-1} = \int_{E'} (f \circ X)(\xi)\sqrt{g(\xi)}\mathrm{d}\xi.$$

If we want to integrate a function $f : \Gamma \to \mathbb{R}$ on the whole surface Γ we work with a partition of unity. That is, we have a finite covering of Γ consisting of open sets $(U_i)_{i=1,\dots,L} \subset \mathbb{R}^n$, a family of open sets $(V_i)_{i=1,\dots,L} \subset \mathbb{R}^{n-1}$ and parametrizations $(X^i)_{i=1,\dots,L}$ such that $X^i : V^i \to \Gamma \cap U^i$. Furthermore, there are functions $\phi^i \in C_0^\infty(\Gamma \cap U^i)$ for $i = 1, \dots, L$ such that $\sum_{i=1}^L \phi^i(p) = 1$ for every $p \in \Gamma$. The integral of f over Γ is then computed as follows

$$\int_\Gamma f \,\mathrm{d}\mathcal{H}^{n-1} = \sum_{i=1}^L \int_\Gamma f\phi^i \,\mathrm{d}\mathcal{H}^{n-1} = \sum_{i=1}^L \int_{\Gamma \cap U^i} f\phi^i \,\mathrm{d}\mathcal{H}^{n-1}.$$

Every summand on the right-hand side can now be computed by the introduced proceeding for simple submanifolds. Before we state the integration by parts formula on curved surfaces we need to define the second fundamental form and the mean curvature, which we do for genereal submanifolds.

Definition 1.2.8 *Let $N \subset \mathbb{R}^n$ be a k-dimensional submanifold, let $p \in N$ and let $X : V \to U(p) \cap N$ be a local parametrization. Let $\nu^{k+1}, \dots, \nu^n$ be local normal fields that span the normal space of N at p. We define the scalar second fundamental form at $p = X(\xi) \in N$ as*

$$A_{ij}(p) = -\sum_{\ell=k+1}^n \frac{\partial}{\partial \xi_i}(\nu^\ell \circ X)(\xi) \bullet \frac{\partial X}{\partial \xi_j}(\xi),$$

and the vector valued second fundamental form is given by

$$\mathbf{A}_{ij} = -\sum_{\ell=k+1}^n \frac{\partial}{\partial \xi_i}(\nu^\ell \circ X) \bullet \frac{\partial X}{\partial \xi_j}\, \nu^\ell \circ X.$$

The mean curvature and the mean curvature vector are then defined as follows

$$H = \sum_{i,j=1}^k g^{ij} A_{ij}, \quad \mathbf{H} = \sum_{i,j=1}^k g^{ij} \mathbf{A}_{ij}.$$

Note that for a surface Γ we have

$$H = -\sum_{i,j=1}^k g^{ij} \frac{\partial}{\partial \xi_i}(\nu \circ X)(\xi) \bullet \frac{\partial X}{\partial \xi_j}(\xi) = -(\mathrm{div}_\Gamma \nu) \circ X.$$

Thus, with this definition the unit sphere $\mathbb{S}^2$ has mean curvature -2. For a surface $\Gamma \subset \mathbb{R}^n$ without boundary and a vector valued function $w : \Gamma \to \mathbb{R}^n$ we state the Gauss theorem

$$\int_\Gamma \mathrm{div}_\Gamma w + w \bullet \mathbf{H} \,\mathrm{d}\mathcal{H}^{n-1} = 0,$$

and if w is tangent to Γ almost everywhere we have

$$\int_\Gamma \mathrm{div}_\Gamma w \,\mathrm{d}\mathcal{H}^{n-1} = 0.$$

The proof of this theorem and an introduction to measure theory on surfaces can be found in the lecture notes [2]. Since we work with the Willmore functional and some related problems in three dimensions we provide some more statements for surfaces and we restrict ourselves to the case that $n = 3$ so that $\Gamma \subset \mathbb{R}^3$ is a 2-dimensional surface. Let $V \subset \mathbb{R}^2$ be open and $X : V \to \mathbb{R}^3$, $(\xi_1, \xi_2) \mapsto X(\xi_1, \xi_2)$ be a local parametrization of Γ. We recall quickly the above made definitions in the new setting. If $X_i := \frac{\partial X}{\partial \xi_i}$, for $i = 1, 2$, the induced metric on Γ is given by $g_{ij} = X_i \bullet X_j$. The inverse of g_{ij} is g^{ij} and the square root of g^{ij} is $g_{ij}^{(-1/2)}$, i.e., $\sum_k g_{ik}^{(-1/2)} g_{jk}^{(-1/2)} = g^{ij}$. The unit outer normal is $\nu = \frac{X_1 \times X_2}{|X_1 \times X_2|}$, and the second fundamental form is $A_{ij} = -\partial_i \nu \bullet X_j$. If f and w are scalar- and vector-valued functions on Γ, then the tangential gradient and divergence in local coordinates are

$$(\nabla_\Gamma f) \circ X = \sum_{i,j} g^{ij} \frac{\partial}{\partial \xi_j} (f \circ X) X_i, \qquad (\mathrm{div}_\Gamma w) \circ X = \sum_{i,j} g^{ij} \frac{\partial}{\partial \xi_i} (w \circ X) \bullet X_j. \tag{1.2.1}$$

It is now easy to check for all functions f, f_1, and f_2 the identities

$$(\nabla_\Gamma f_1 \bullet \nabla_\Gamma f_2) \circ X = \sum_{i,j} g^{ij} \frac{\partial}{\partial \xi_i} (f_1 \circ X) \frac{\partial}{\partial \xi_j} (f_2 \circ X), \qquad X_i \bullet (\nabla_\Gamma f) \circ X = \frac{\partial}{\partial \xi_i} (f \circ X). \tag{1.2.2}$$

We note that the tangential gradient $\nabla_\Gamma w$ of a vector field w is a square matrix in $\mathbb{R}^{3\times 3}$ whose i-th row is the tangential gradient of the i-th component of w. If w is tangential, then it can be equivalently written as

$$w = \sum_k (v_k \bullet w) v_k = \sum_{i,j,k} g_{ik}^{(-1/2)} g_{jk}^{(-1/2)} w \bullet X_i X_j = \sum_{i,j} g^{ij} w \bullet X_i X_j.$$

Applying this expression to the tangential vector $\frac{\partial}{\partial \xi_k} \nu$ yields the Weingarten equations

$$\frac{\partial \nu}{\partial \xi_k} = -\sum_{i,j} g^{ij} A_{ki} X_j. \tag{1.2.3}$$

The Laplace-Beltrami operator $\Delta_\Gamma f = \mathrm{div}_\Gamma \nabla_\Gamma f$ has the following expression in local coordinates

$$\Delta_\Gamma f = \frac{1}{\sqrt{g}} \sum_{i,j} \frac{\partial}{\partial \xi_i} \left(\sqrt{g} g^{ij} \frac{\partial}{\partial \xi_j} f \right) = \sum_{i,j} g^{ij} \frac{\partial^2 f}{\partial \xi_i \partial \xi_j} - \sum_{i,j,k} g^{ij} \Gamma_{ij}^k \frac{\partial f}{\partial \xi_k}, \tag{1.2.4}$$

where the functions Γ_{ij}^k are the Christoffel symbols corresponding to the metric g_{ij}, satisfying

$$\Gamma_k^{ij} = \frac{1}{2} \sum_\ell g^{kl} \left(\frac{\partial g_{j\ell}}{\partial \xi_i} + \frac{\partial g_{i\ell}}{\partial \xi_j} + \frac{\partial g_{ij}}{\partial \xi_\ell} \right).$$

Let ϕ be a smooth real-valued function on Γ and $s \in (-\varepsilon, \varepsilon)$, $\varepsilon > 0$ small enough. A normal variation of Γ is given by the map

$$X_s(\xi_1, \xi_2) = X(\xi_1, \xi_2) + s\phi(X(\xi_1, \xi_2))\nu$$

with values in a tubular neighborhood of Γ. We calculate now the variation of several geometric quantities and we denote the variation with a prime, that is, if $f = f_s$ we write $f' := \partial_s|_{s=0} f_s$.

Lemma 1.2.9 *Let $\Gamma \subset \mathbb{R}^3$ be a surface and let X be a parametrization. Consider a normal variation $(X_s)_{-\varepsilon<s<\varepsilon}$ of Γ as defined above. Then the variations of $g_{ij}, g^{ij}, \nu, \sqrt{g}$ and H are*

$$\begin{aligned}
(g_{ij})' &= -2\phi A_{ij}, \\
(g^{ij})' &= 2\phi \sum_{k,\ell} g^{ik} g^{\ell j} A_{k\ell}, \\
\nu' &= -\nabla_\Gamma \phi, \\
(\sqrt{g})' &= -\phi H \sqrt{g}, \\
H' &= \Delta_\Gamma \phi + \phi |\nabla_\Gamma \nu|^2.
\end{aligned}$$

Proof. (i) We compute

$$(g_{ij})' = \frac{\mathrm{d}}{\mathrm{d}s}\Big|_{s=0}(X_i)_s \bullet (x_j)_s = \frac{\mathrm{d}}{\mathrm{d}s}\Big|_{s=0}\frac{(\partial X + s\phi\nu)}{\partial\xi_i}\bullet\frac{(\partial X + s\phi\nu)}{\partial\xi_j} = \phi\Big(\frac{\partial\nu}{\partial\xi_i}\bullet\frac{\partial X}{\partial\xi_j}+\frac{\partial X}{\partial\xi_i}\bullet\frac{\partial\nu}{\partial\xi_j}\Big) = -2\phi A_{ij}.$$

(ii) Note that $\sum_k g^{ik}g_{kj} = \delta_{ij}$, where δ_{ij} denotes the Kronecker delta. Hence $\frac{\mathrm{d}}{\mathrm{d}s}\big|_{s=0}\sum_k g^{ik}g_{kj} = 0$. We obtain

$$\sum_k (g^{ik})' g_{kj} + g^{ik}(g_{kj})' = 0.$$

In matrix notation, where $G = (g_{ij})_{i,j=1,2}$, this means $(G^{-1})'G + G^{-1}G' = 0$, thus, $(G^{-1})' = -G^{-1}G'G^{-1}$ or expressed in the entries of G, G' and G^{-1}

$$(g^{ij})' = -\sum_{k\ell} g^{ik}(g_{k\ell})' g^{\ell j} = 2\phi\sum g^{ik}g^{j\ell}A_{k\ell}.$$

(iii) We use that $\nu \bullet X_i = 0$, for $i = 1, 2$ to obtain $\nu' \bullet X_i + \nu \bullet (X_i)' = 0$. With $(X_i)' = \nu\frac{\partial\phi}{\partial\xi_i} + \frac{\partial\nu}{\partial\xi_i}\phi$ we see that

$$\nu' \bullet X_i + \nu \bullet (X_i)' = \nu' \bullet X_i + \nu \bullet (\nu\frac{\partial\phi}{\partial\xi_i} + \frac{\partial\nu}{\partial\xi_i}\phi) = \nu' \bullet X_i + \frac{\partial\phi}{\partial\xi_i},$$

since $|\nu|^2 = 1$ and $\nu \perp \frac{\partial\nu}{\partial\xi_i}$. Now, $0 = \frac{1}{2}(|\nu|^2)' = \nu \bullet \nu'$ and therefore we have the existence of $(a_j)_{j=1,2} \subset \mathbb{R}$ such that $\nu' = \sum_j a_j X_j$. We multiply this equation with X_i and proceed as above to see, that $a_j = -\sum_i g^{ij}\frac{\partial\phi}{\partial\xi_i}$. Finally we conclude

$$\nu' = \sum_j a_j X_j = -\sum_{ij} g^{ij}\frac{\partial\phi}{\partial\xi_i}X_j = -\nabla_\Gamma\phi.$$

(iv) We recall that for $A \in C^1(\mathbb{R}, \mathbb{R}^{n\times n})$, with $A(0)$ regular, we have

$$\frac{\mathrm{d}}{\mathrm{d}s}\Big|_{s=0}\sqrt{\det A(s)} = \frac{1}{2}\sqrt{\det A(0)}\,\mathrm{trace}\Big[A^{-1}(0)\frac{\mathrm{d}}{\mathrm{d}s}\Big|_{s=0}A(s)\Big].$$

We give a short proof of this identity at the end of (iv) and conclude already for the variation of the determinant

$$\frac{\mathrm{d}}{\mathrm{d}s}\Big|_{s=0}\sqrt{g_s} = \frac{1}{2}\sqrt{g}\,\mathrm{trace}\Big[g^{ij}(g_{ij})'\Big] = \frac{1}{2}\sqrt{g}\sum_{ij} g^{ij}(g_{ij})' = -\phi\sqrt{g}\sum_{ij} g^{ij}A_{ij} = -\phi H\sqrt{g}.$$

For the proof of the derivative of the determinant we suppose first, that $A(0) = I$. Then

$$\begin{aligned}\frac{\mathrm{d}}{\mathrm{d}s}\Big|_{s=0}\det A(t) &= \frac{\mathrm{d}}{\mathrm{d}s}\Big|_{s=0}\sum_{\sigma\in S^n}\mathrm{sgn}(\sigma)\frac{\mathrm{d}}{\mathrm{d}s}\Big|_{s=0}\prod_{i=1}^n a_{i\sigma(i)}(t)\\ &= \sum_{\sigma\in S^n}\mathrm{sgn}(\sigma)\sum_{j=1}^n\prod_{i\neq j} a_{i,\sigma(i)}(0)\dot{a}_{j\sigma(j)}(0)\\ &= \sum_{j=1}^n \dot{a}_{jj}(0) = \mathrm{trace}\,\dot{A}(0),\end{aligned}$$

where we used that $a_{j,\sigma(j)}(0) = \delta_{j,\sigma(j)}$ which is only different from zero if $\sigma(j) = j$ for all $j \in \{1, \ldots, n\}$. Hence the sum over all permutations $\sigma \in S^n$ vanishes and $sgn(\mathrm{id}) = 1$. For the general case we introduce $B(t) := A^{-1}(0)A(t)$ and note that $B(0) = I$. The desired identity follows then by the chain rule and the multiplicity of the determinant, that is, $\det(A^{-1}(0)A(t)) = (\det A(0))^{-1}\det A(t)$.
(v) We recall the Gauss formula for the second derivative of X

$$X_{ij} = \sum_k \Gamma_{ij}^k X_k + A_{ij}\nu.$$

Then $\nu \bullet X_{ij} = \nu \bullet A_{ij}\nu = A_{ij}$ and we compute

$$(A_{ij})' = \nu' \bullet X_{ij} + \nu \bullet (X_{ij})' = -\sum_k \Gamma_{ij}^k \frac{\partial \phi}{\partial \xi_k} + \nu \bullet (X_{ij})'.$$

For the second summand we recall that

$$(X_{ij})' = \frac{\partial^2 \phi}{\partial \xi_i \partial \xi_j}\nu + \frac{\partial \phi}{\partial \xi_i}\frac{\partial \nu}{\partial \xi_j} + \frac{\partial \phi}{\partial \xi_j}\frac{\partial \nu}{\partial \xi_i} + \phi \frac{\partial^2 \nu}{\partial \xi_i \partial \xi_j},$$

giving

$$\begin{aligned}\nu \bullet (X_{ij})' &= \frac{\partial^2 \phi}{\partial \xi_i \partial \xi_j} + \phi \nu \bullet \frac{\partial^2 \nu}{\partial \xi_i \partial \xi_j} = \frac{\partial^2 \phi}{\partial \xi_i \partial \xi_j} - \phi \frac{\partial \nu}{\partial \xi_i} \bullet \frac{\partial \nu}{\partial \xi_j} \\ &= \frac{\partial^2 \phi}{\partial \xi_i \partial \xi_j} - \phi \sum_{k\ell} g^{k\ell} A_{ik} A_{j\ell},\end{aligned}$$

where we use the Weingarten equations in the last step. Now, we have everything together to compute the variation of the curvature:

$$\begin{aligned}H' &= \sum_{ij} (g^{ij})' A_{ij} + g^{ij} (A_{ij})' \\ &= 2\phi \sum_{i,j,k,\ell} g^{ik} g^{lj} A_{k\ell} A_{ij} + \sum_{i,j} g^{ij} \Big(\nu' \bullet X_{ij} + \nu \bullet (X_{ij})' \Big) \\ &= 2\phi \sum_{i,j,k,\ell} g^{ik} g^{lj} A_{k\ell} A_{ij} - \sum_{i,j,k} g^{ij} \Gamma_{ij}^k \frac{\partial \phi}{\partial \xi_k} + \sum_{i,j} g^{ij} \frac{\partial^2 \phi}{\partial \xi_i \partial \xi_j} - \phi \sum_{i,j,k,\ell} g^{ij} g^{k\ell} A_{ik} A_{j\ell} \\ &= \Delta_\Gamma \phi + \phi \sum_{i,j,k,\ell} g^{ij} g^{k\ell} A_{ik} A_{j\ell} = \Delta_\Gamma \phi + \phi |\nabla_\Gamma \nu|^2.\end{aligned}$$

Here, again, we incorporated the Weingarten equation to obtain the identity

$$|\nabla_\Gamma \nu|^2 = \sum_{i,j,k,\ell} g^{ij} g^{k\ell} A_{ik} A_{j\ell}.$$

□

As a direct conclusion of the previous lemma we state the first variation of a shape dependent integral.

Lemma 1.2.10 *Let $\Gamma \subset \mathbb{R}^3$ be a surface and let X be a local parametrization. Consider a normal variation Γ_s of Γ, defined through $X_s(\xi_1, \xi_2) = X(\xi_1, \xi_2) + s\phi(X(\xi_1, \xi_2))\nu$. Then, for a smooth function $f : \Gamma \to \mathbb{R}$ and the integral*

$$I(\Gamma) := \int_\Gamma f \, d\mathcal{H}^2,$$

the first variation is given by

$$\langle I(\Gamma), \phi \rangle := \frac{d}{ds}\Big|_{s=0} I(\Gamma_s) = \int_\Gamma f' \, d\mathcal{H}^2 - \int_\Gamma f H \phi \, d\mathcal{H}^2.$$

Proof. We have that

$$\int_{\Gamma_s} f \, \mathrm{d}\mathcal{H}^2 = \int_V f \circ X_s(y) \sqrt{g_s(y)} \, \mathrm{d}y,$$

and therefore

$$\begin{aligned}\frac{\mathrm{d}}{\mathrm{d}s}\Big|_{s=0} \int_{\Gamma_s} f \, \mathrm{d}\mathcal{H}^2 &= \int_V \Big[\frac{\mathrm{d}}{\mathrm{d}s}\Big|_{s=0} (f \circ X_s)\Big] \sqrt{g_s} \mathrm{d}y + \int_V f \circ X_s \Big[\frac{\mathrm{d}}{\mathrm{d}s}\Big|_{s=0} \sqrt{g_s}\Big] \mathrm{d}y \\ &= \int_\Gamma f' \, \mathrm{d}\mathcal{H}^2 - \int_\Gamma f H \phi \, \mathrm{d}\mathcal{H}^2.\end{aligned}$$

□

We finish this subsection with the variation of a conformally invariant elliptic energy including a 2-form. In [68] it is shown that every stationary point of such an energy is continuous. We remark, that the standard Dirichlet energy for functions with values in a submanifold $N \subset \mathbb{R}^n$ is obtained when neglecting the differential form. Before we state the lemma we note that we can pull back the 2-form ω, defined on the submanifold N, to a 2-form $\tilde{\omega} := \pi_N^* \omega$ defined in a small neighborhood of N. Let $p \in \mathbb{R}^n$ be in that neighborhood of N and let $v, w \in \mathbb{R}^n$, then

$$\tilde{\omega}(p)(v, w) := \omega(\pi_N(p))(D\pi_N(v), D\pi_N(w)).$$

Let $(e_i)_{i=1,\dots,n}$ be the chanonical basis of $\mathbb{R}^n$ and $q \in N$. We then define $\lambda^i_{j,\ell}(q) := \mathrm{d}\tilde{\omega}(q)(e_i, e_j, e_\ell)$.

Lemma 1.2.11 *Let $N \subset \mathbb{R}^n$ be a C^2 submanifold. Let ω be a C^1 2-form on N such that the L^∞-norm of $d\omega$ is bounded. Every critical point of the energy*

$$E(u) := \frac{1}{2} \int_M |\nabla u|^2 \, dx + \int_M \omega(u)(\partial_x u, \partial_y u) \, dx \tag{1.2.5}$$

satisfies

$$-\Delta u + \mathbf{A}(u)[\nabla u, \nabla u] + \sum_{j,\ell} \lambda_{j,\ell}(u) \partial_x u^j \partial_y u^\ell = 0.$$

Here $\lambda_{j,\ell}(u) \in \mathbb{R}^n$ is the vector with components $\lambda^i_{j,\ell}(u)$, for $i = 1, \dots, n$, and $\mathbf{A}$ is the vector valued second fundamental form.

Proof. If $\omega = 0$ the Euler-Lagrange equations corresponding to the energy E yield

$$-\Delta u(x) \perp T_{u(x)} N \text{ for all } x \in M.$$

Therefore there exist functions $\eta_{k+1}, \dots, \eta_n$ such that

$$-\Delta u(x) - \sum_{m=k+1}^{n} \eta_m(x) \nu^m \circ u(x) = 0 \text{ for all } x \in M.$$

We multiply the equation with $\nu^m \circ u(x)$ for an $m \in \{k+1, \dots, n\}$ and obtain

$$\eta_m(x) = -\Delta u(x) \bullet \nu^m \circ u(x) = -\mathrm{div}\Big(\underbrace{\nabla u(x) \bullet \nu^m \circ u(x)}_{=0}\Big) + \nabla u^T (D\nu^m) \nabla u.$$

For $a, b \in T_{u(x)} N$ we have the representation $a = \sum_i a^i X_i$ and $b = \sum_j b^j X_j$ for a local parametrization X of N. The second fundamental form applied to a, b at $u(x) \in N$ is defined as $\mathbf{A}(u)[a, b] := \sum_{ij} a^i b^j \mathbf{A}_{ij}$. This yields

$$\begin{aligned} A(u)[a, b] = \sum_{ij} a^i b^j \mathbf{A}_{ij} &= \sum_{ij} \sum_m a^i b^j \frac{\partial X}{\partial \xi_i} \bullet \frac{\partial \nu^m}{\partial \xi_j} \\ &= \sum_m \sum_{ij} a^i b^j \frac{\partial X}{\partial \xi_i} \bullet D\nu^m \Big(\frac{\partial X}{\partial \xi_j}\Big) \\ &= \sum_m a \bullet D\nu^m b. \end{aligned}$$

Thus, in local coordinates we have

$$\begin{aligned} \sum_{i=k+1}^{n} \eta_i(x) \nu^i \circ u(x) &= \sum_k \sum_m \partial_k u D\nu^m \partial_k u \nu^i \circ u(x) \\ &= \sum_k \sum_m \partial_k u \bullet D\nu^m (\partial_k u) \nu^i \circ u(x) \\ &= \sum_k \mathbf{A}(u)[\partial_k u, \partial_k u] =: \mathbf{A}(u)[\nabla u, \nabla u]. \end{aligned}$$

We show how to compute the variation of $\int_M \omega(u)(\partial_x u, \partial_y u)\,\mathrm{d}x$ for maps with values in a submanifold of $\mathbb{R}^3$. Similar calculations lead to the Euler-Lagrange equations in higher dimensions (see [44]). We claim that

$$\frac{\mathrm{d}}{\mathrm{d}s}\Big|_{s=0} \int_M \tilde{\omega}(u+s\phi)(\partial_x(u+s\phi), \partial_y(u+s\phi))\,\mathrm{d}x = \int_M \mathrm{d}\tilde{\omega}(\phi, \partial_x u, \partial_y u)\,\mathrm{d}x,$$

where $\phi \in C_0^\infty(M;\mathbb{R}^n)$ is such that $\phi(x) \in T_{u(x)}N$ for all $x \in M$. Then the assertion follows from the identity

$$\mathrm{d}\tilde{\omega}(\phi, \partial_x u, \partial_y u) = \sum_{i,j,\ell=1}^{n} \lambda^i_{j,\ell}(u)\phi^i \partial_x u^j \partial_y u^\ell.$$

To proof the claim we compute

$$\begin{aligned}\frac{\mathrm{d}}{\mathrm{d}s}\Big|_{s=0} \int_M \tilde{\omega}(u+s\phi)(\partial_x(u+s\phi), \partial_y(u+s\phi))\,\mathrm{d}x \;=\; &\int_M \tilde{\omega}(u)(\partial_x\phi, \partial_y u)\,\mathrm{d}x \;+\; \int_M \tilde{\omega}(u)(\partial_x u, \partial_y\phi)\,\mathrm{d}x \\ &+ \int_M \frac{\mathrm{d}}{\mathrm{d}s}\Big|_{s=0} \tilde{\omega}(u+s\phi)(\partial_x u, \partial_y u)\,\mathrm{d}x.\end{aligned}$$

In local coordinates we can write $\tilde{\omega} = Q_1 \mathrm{d}x_2 \wedge \mathrm{d}x_3 + Q_2 \mathrm{d}x_3 \wedge \mathrm{d}x_1 + Q_3 \mathrm{d}x_1 \wedge \mathrm{d}x_2$, where $(\mathrm{d}x_i)_{i=1,2,3}$ is the dual basis to the standard basis $(e_i)_{i=1,2,3}$ in $\mathbb{R}^3$. Thus, we compute

$$\begin{aligned}\frac{\mathrm{d}}{\mathrm{d}s}\Big|_{s=0} \tilde{\omega}(u+s\phi)(\partial_x u, \partial_y u) \;=\; &\frac{\mathrm{d}}{\mathrm{d}s}\Big|_{s=0} Q_1(u+s\phi)\mathrm{d}x_2 \wedge \mathrm{d}x_3(\partial_x u, \partial_y u) \\ &+ \frac{\mathrm{d}}{\mathrm{d}s}\Big|_{s=0} Q_2(u+s\phi)\mathrm{d}x_3 \wedge \mathrm{d}x_1(\partial_x u, \partial_y u) \\ &+ \frac{\mathrm{d}}{\mathrm{d}s}\Big|_{s=0} Q_3(u+s\phi)\mathrm{d}x_1 \wedge \mathrm{d}x_2(\partial_x u, \partial_y u) = \phi^T DQ(\partial_x u \times \partial_y u),\end{aligned}$$

where $Q = [Q_1, Q_2, Q_3]^T$ and $DQ = (\nabla Q_i)_{i=1,2,3} = (\partial_j Q_i)_{i,j=1,2,3}$ is the Jacobian of Q. For the whole variation we obtain

$$\frac{\mathrm{d}}{\mathrm{d}s}\Big|_{s=0} \int_M \tilde{\omega}(u+s\phi)(\partial_x(u+s\phi), \partial_y(u+s\phi))\,\mathrm{d}x = \int_M \phi^T DQ(\partial_x u \times \partial_y u) + Q\bullet(\partial_x\phi \times \partial_y u) + Q\bullet(\partial_x u \times \partial_y\phi)\,\mathrm{d}x.$$

First, we look at all terms containing Q_1 or ∇Q_1

$$\int_B v \bullet \nabla Q_1(\partial_x u_2 \partial_y u_3 - \partial_x u_3 \partial_y u_2) + Q_1(\partial_x v_2 \partial_y u_3 - \partial_x v_3 \partial_y u_2) + Q_1(\partial_x u_2 \partial_y v_3 - \partial_x u_3 \partial_y v_2)\,\mathrm{d}x =: (I).$$

Integration by parts in the second and third summand of (I) gives by the chain rule

$$-\int_B \partial_x u \bullet \nabla Q_1(v_2 \partial_y u_3 - v_3 \partial_y u_2)\,\mathrm{d}x - \int_B \partial_y u \bullet \nabla Q_1(v_3 \partial_x u_2 - v_2 \partial_x u_3)\,\mathrm{d}x,$$

where the terms with 2nd derivatives of u cancel out. We set $\det(i,j) := \det \begin{bmatrix} \partial_x u_i & \partial_y u_i \\ \partial_x u_j & \partial_y u_j \end{bmatrix}$ and get

$$\begin{aligned}(I) \;=\; &\int_B \partial_1 Q_1 v_1 \det(2,3)\,\mathrm{d}x + \int_B (\partial_2 Q_1 v_2 + \partial_3 Q_1 v_3)\det(2,3)\,\mathrm{d}x \\ &- \int_B (\partial_1 Q_1 \det(1,3) + \partial_2 Q_1 \det(2,3))v_2\,\mathrm{d}x \\ &- \int_B (-\partial_1 Q_1 \det(1,2) + \partial_3 Q_1 \det(2,3))v_3\,\mathrm{d}x \\ = \;&\int_B \partial_1 Q_1 v_1 \det(2,3) - \partial_1 Q_1 v_2 \det(1,3) + \partial_1 Q_1 v_3 \det(1,2))\,\mathrm{d}x \\ = \;&\int_B \partial_1 Q_1\, v \bullet (\partial_x u \times \partial_y u)\,\mathrm{d}x.\end{aligned}$$

An analog computation for the terms with Q_i and ∇Q_i for $i = 2, 3$ gives the full variation

$$\frac{\mathrm{d}}{\mathrm{d}s}\Big|_{s=0} \int_M \pi_N^* \omega(u + t\phi)(\partial_x(u + t\phi), \partial_y(u + t\phi))\,\mathrm{d}x \;=\; \int_M (\operatorname{trace} DQ)\,\phi \bullet (\partial_x u \times \partial_y u)\mathrm{d}x.$$

We note that

$$(\operatorname{tr} DQ)\,\phi \bullet (\partial_x u \times \partial_y u) = (\operatorname{trace} DQ)\,\mathrm{d}x_1 \wedge \mathrm{d}x_2 \wedge \mathrm{d}x_3(\phi, \partial_x u, \partial_y u) = \mathrm{d}\tilde{\omega}(u)(\phi, \partial_x u, \partial_y u),$$

which yields the claim. □

Remark 1.2.12 *As we will see later the functional for surfaces of prescribed mean curvature in $\mathbb{R}^3$ is given by*

$$E(u) := \frac{1}{2}\int_{B_1(0)} |\nabla u|^2\,dx + \frac{2}{3}\int_M Q(u) \bullet (\partial_x u \times \partial_y u)\,dx,$$

where $u : B_1(0) \subset \mathbb{R}^2 \to \mathbb{R}^3$ and $Q : \mathbb{R}^3 \to \mathbb{R}^3$. We can write the second integral as

$$\int_M Q(u) \bullet (\partial_x u \times \partial_y u)\,dx = \int_M w(u)(\partial_x u, \partial_y u)\,dx,$$

with the 2-form $\omega = Q_1\,dx_2 \wedge dx_3 + Q_2\,dx_3 \wedge dx_1 + Q_3\,dx_1 \wedge dx_2$. We introduce $H := \frac{1}{3}\operatorname{tr} DQ$ and obtain that $d\omega = 3H\,dx_1 \wedge dx_2 \wedge dx_3$ and $\frac{2}{3}d\omega(u)(\phi, \partial_x u, \partial_y u) = 2H(u)\phi \bullet (\partial_x u \times \partial_y u)$. The Euler-Lagrange equation for the above defined integral are

$$-\Delta u = 2H(u)\partial_x u \times \partial_y u.$$

1.3. Finite element spaces

In this section we present the finite element spaces we work with. We recall, that $M \subset \mathbb{R}^2$ is always assumed to be a polygonal Lipschitz domain. When handling with shape functionals and biomembranes we consider a twodimensional surface $\Gamma \subset \mathbb{R}^3$ that will always be of topologial type of a sphere. We denote by $\mathcal{T}_h$ a regular triangulation [24] of M into triangles of maximal diameter $h > 0$. We say that $\mathcal{T}_h$ is *weakly acute* if the sum of every pair of angles opposite to an interior edge is bounded by π and if the angle opposite to every edge on the boundary is less than or equal to $\pi/2$.

We define the finite element spaces

$$\mathcal{S}^1(\mathcal{T}_h) := \{\phi_h \in C(\overline{M}) :\, \phi_h|_T \text{ affine for all } T \in \mathcal{T}_h\} \cap W^{1,2},$$

$$\mathcal{S}_0^1(\mathcal{T}_h) := \{\phi_h \in C(\overline{M}) :\, \phi_h|_T \text{ affine for all } T \in \mathcal{T}_h\} \cap W_0^{1,2}.$$

With the nodal basis $(\varphi_z :\, z \in \mathcal{N}_h)$ the bubble function associated to an element $T \in \mathcal{T}_h$ with vertices $z_1, z_2, z_3 \in \mathcal{N}_h$ is defined by $b_T = \varphi_{z_1}\varphi_{z_2}\varphi_{z_3}$ and we set

$$\mathcal{B}^3(\mathcal{T}_h) := \{\phi_h = \sum_{T \in \mathcal{T}_h} \alpha_T b_T \;:\; (\alpha_T)_{T \in \mathcal{T}_h} \subset \mathbb{R}\}.$$

Finally we define the MINI-element for our discretization of the mixed formulation

$$V_{mini}(\mathcal{T}_h) := V_{mini}^h := \mathcal{S}^1(\mathcal{T}_h) \oplus \mathcal{B}^3(\mathcal{T}_h),$$

and proof that the inf-sup condition is satisfied for the discrete mixed formulation of the Poisson problem, see [4] for details. Before that, we state the definition of some important interpolators.

Definition 1.3.1 *We define the nodal interpolant and Clément interpolant*

$$\mathcal{I}_h : C(M) \to \mathcal{S}^1(\mathcal{T}), \quad u \mapsto \sum_{z \in \mathcal{N}_h} u(z)\varphi_z$$
$$\mathcal{J}_h : L^1_{loc}(M) \to \mathcal{S}^1(\mathcal{T}), \; u \mapsto \sum_{z \in \mathcal{N}_h} u_z \varphi_z,$$

where $u_z := \frac{1}{|\omega_z|}\int_{\omega_z} u(x)\,dx$ *is the mean value of* u *on a node-patch* $\omega_z := \operatorname{supp}\varphi_z$, $z \in \mathcal{N}_h$. *The* L^2*-projection on* $P_0^h : L^2(M) \to V^h_{mini}$ *is defined through*

$$(P_0^h(\eta), \sigma_h) = (\eta, \sigma_h) \text{ for all } \sigma_h \in V^h_{mini}.$$

Remark 1.3.2 *One can show the estimates*

$$||h^{-2}(v - \mathcal{I}_h v)||_{L^2} + ||h^{-1}\nabla(v - \mathcal{I}_h)||_{L^2} \leq C||D^2 v||_{L^2},$$

and

$$||h^{-1}(v - \mathcal{J}_h v)||_{L^2} + ||\nabla \mathcal{J}_h v||_{L^2} \leq C'||\nabla v||_{L^2},$$

for $v \in W^{2,2}(M)$ *and* $C, C' > 0$. *The proof of the estimate for the Clément interpolant uses a scaling law and a compactness result. For the nodal interpolant the Bramble-Hilbert lemma is employed, see [22] for details.*

Lemma 1.3.3 *Let* $M \subset \mathbb{R}^2$ *be a polygonal Lipschitz domain and* $\mathcal{T}_h$ *be a regular triangulation of* M. *Let* $\ell_1 \in \left([V^h_{mini}]^2\right)'$ *and* $\ell_2 \in \left(\mathcal{S}^1(\mathcal{T}_h)\right)'$, *then the problem of finding* $(p_h, u_h) \in [V^h_{mini}]^2 \times \mathcal{S}^1_0(\mathcal{T}_h)$ *such that*

$$\begin{aligned}(p_h, q_h) + (\operatorname{div} q_h, u_h) &= \ell_1(q_h)\\ (\operatorname{div} p_h, v_h) &= \ell_2(v_h)\end{aligned}$$

for all $(q_h, v_h) \in [V^h_{mini}]^2 \times \mathcal{S}^1_0(\mathcal{T}_h)$ *admits a unique solution.*

Proof. Clearly it suffices to show, that there exists a solution, since the uniqueness follows from linearity. We define

$$b : W^{1,2}(M;\mathbb{R}^2) \times L^2(M) \to \mathbb{R}, \qquad (q, v) \mapsto \int_M (\operatorname{div} q)\, v \,\mathrm{d}x,$$

and note that there exists $\beta > 0$ such that

$$\inf_{v \in L^2(M)\setminus\{0\}} \sup_{q \in W^{1,2}\setminus\{0\}} \frac{b(q,v)}{||q||_{W^{1,2}}||v||_{L^2}} \geq \beta.$$

For details of the proof of this claim see [22]. We will construct a Fortin interpolant $\Pi_h : W^{1,2}(M;\mathbb{R}^2) \to [V^h_{mini}]^2$ that satisfies

- $||\Pi_h q||_{W^{1,2}} \leq C||q||_{W^{1,2}}$ for $q \in W^{1,2}(M;\mathbb{R}^2)$, and
- $b(q - \Pi_h q, v) = 0$ for all $q \in W^{1,2}(M;\mathbb{R}^2)$ and $v \in L^2(M)$.

Then, by Fortin's criterion we obtain

$$\begin{aligned}\beta\,||v_h|| \quad &\leq \sup_{q \in W^{1,2}\setminus\{0\}} \frac{b(q, v_h)}{||q||_{W^{1,2}}||v_h||_{L^2}} = \sup_{q \in W^{1,2}\setminus\{0\}} \frac{b(\Pi_h q, v_h)}{||q||_{W^{1,2}}||v_h||_{L^2}}\\ &\leq C \sup_{q \in W^{1,2}\setminus\{0\}} \frac{b(\Pi_h q, v_h)}{||\Pi_h q||_{W^{1,2}}||v_h||_{L^2}} \leq C \sup_{q_h \in [V_{mini}]^2\setminus\{0\}} \frac{b(q_h, v_h)}{||q_h||_{W^{1,2}}||v_h||_{L^2}},\end{aligned}$$

which is the inf-sup condition. For the construction of the interpolant we mainly follow the lines in [4]. Let $p \in L^2(M;\mathbb{R}^2)$ and define $\mathcal{J}_h p \in [\mathcal{S}^1(\mathcal{T}_h)]^2$ to be the Clément interpolant of p. For $T \in \mathcal{T}_h$ we set $\alpha_T = (60/|T|)\int_T (p - \mathcal{J}_h p)\,\mathrm{d}x$ and finally, the Fortin operator $\Pi_h : L^2(M;\mathbb{R}^2) \to [V^h_{mini}]^2$ is defined through

$$\Pi_h p := \mathcal{J}_h p + \sum_{T\in\mathcal{T}_h} \alpha_T b_T.$$

We first prove the second property, that is for $p \in W^{1,2}(M;\mathbb{R}^2)$ and $v_h \in \mathcal{S}^1_0(\mathcal{T}_h)$ we have

$$b(p - \Pi_h p, v_h) = 0.$$

To proof this we integrate by parts and see that it suffices to show

$$\int_T p - \Pi_h p\,\mathrm{d}x = 0 \quad \text{for all } T \in \mathcal{T}_h.$$

We conclude

$$\begin{aligned}
\int_T p - \Pi_h p\,\mathrm{d}x &= \int_T p\mathrm{d}x - \int_T \mathcal{J}_h p\mathrm{d}x - \alpha_T \int_T b_T \mathrm{d}x \\
&= \int_T p\mathrm{d}x - \int_T \mathcal{J}_h p\mathrm{d}x - (60/|T|)\int_T (p - \mathcal{J}_h p)\,\mathrm{d}x \int_T b_T \mathrm{d}x \\
&= \int_T p\mathrm{d}x - \int_T \mathcal{J}_h p\mathrm{d}x - \int_T p\,\mathrm{d}x + \int_T \mathcal{J}_h p\,\mathrm{d}x = 0,
\end{aligned}$$

where we used the fact that $\int_T b_T\,\mathrm{d}x = |T|/60$. Boundedness of the operator follows from the estimate

$$|T|^{-1/2}||\mathcal{J}_h p - p||_{L^2(T)} + ||\nabla(\mathcal{J}_h p - p)||_{L^2(T)} \le C||\nabla p||_{L^2(T)}.$$

for $T \in \mathcal{T}_h$. We compute

$$\begin{aligned}
||\Pi_h p - p||^2_{L^2(T)} &= \int_T \Big|\mathcal{J}_h p + \Big(\frac{60}{|T|}\int_T \mathcal{J}_h p - p\,\mathrm{d}x\Big) b_T - p\Big|^2 \mathrm{d}x \\
&\le 2\int_T \Big|\mathcal{J}_h p - p\Big|^2 \mathrm{d}x + \frac{7200}{|T|^2}\Big(\int_T \Big|\mathcal{J}_h p - p\Big|\,\mathrm{d}x\Big)^2 \int_T |b_T|^2\,\mathrm{d}x \\
&= 2||\mathcal{J}_h p - p||^2_{L^2(T)} + \frac{20}{7}|T|^{-1}\Big(\int_T \Big|\mathcal{J}_h p - p\Big|\,\mathrm{d}x\Big)^2 \\
&\le \frac{34}{7}||\mathcal{J}_h p - p||^2_{L^2(T)},
\end{aligned}$$

where we used $\int_T |b_T|^2\,\mathrm{d}x = \frac{|T|}{2520}$ and the Cauchy-Schwarz inequality. Now, we estimate the H^1-seminorm

$$\begin{aligned}
||\nabla(\Pi_h p - p)||^2_{L^2(T)} &= \int_T \Big|\nabla\mathcal{J}_h p + \Big(\frac{60}{|T|}\int_T \mathcal{J}_h p - p\,\mathrm{d}x\Big)\nabla b_T - \nabla p\Big|^2 \mathrm{d}x \\
&\le 2||\nabla(\mathcal{J}_h p - p)||^2_{L^2(T)} + \frac{7200}{|T|^2}\Big(\int_T \Big|\mathcal{J}_h p - p\Big|\,\mathrm{d}x\Big)^2 \int_T |\nabla b_T|^2\,\mathrm{d}x \\
&\le 2||\nabla(\mathcal{J}_h p - p)||^2_{L^2(T)} + \frac{480}{|T|h_T^{-2}}\Big(\int_T \Big|\mathcal{J}_h p - p\Big|\,\mathrm{d}x\Big)^2 \\
&\le 2||\nabla(\mathcal{J}_h p - p)||^2_{L^2(T)} + \frac{480}{h_T^2}||\mathcal{J}_h p - p||^2_{L^2(T)} \le C||\nabla p||^2_{L^2(T)}.
\end{aligned}$$

Here we used Cauchy-Schwarz inequality, the estimate $\int_T |\nabla b_T|^2\,\mathrm{d}x \le \frac{|T|}{15h_T^2}$ and the approximation property of the Clément interpolant. Summing up the above estimates over all $T \in \mathcal{T}_h$ yields the assertion. □

Remark 1.3.4 *Let $T_{ref} := \mathrm{conv}\{(0,0),(1,0),(0,1)\}$ be the standard reference triangle and $T = \mathrm{conv}\{z_1,z_2,z_3\} \in \mathcal{T}_h$ be arbitrary. Then $\Phi : \mathbb{R}^2 \to \mathbb{R}^2$, $x \mapsto (z_2-z_1, z_3-z_1)x + z_1$ is a parametrization of T. We have that $g_{ij} = \frac{\partial \Phi}{\partial x_i} \bullet \frac{\partial \Phi}{\partial x_j}$ and $g = \det(g_{ij}) = 4|T|^2$ and for $f \in L^1_{loc}(M)$*

$$\int_T f \, d\mathcal{H}^2 = \int_{T_{ref}} f \circ \Phi \sqrt{g} \, dx = 2|T| \int_{T_{ref}} f \circ \Phi \, dx.$$

This yields

$$\int_T b_T \, dx = 2|T| \int_{T_{ref}} (\varphi_1\varphi_2\varphi_3) \circ \Phi \, dx = 2|T| \int_0^1 \int_0^{1-y} xy(1-x-y) \, dx\, dy = |T|/60,$$

and $\int_T |b_T|^2 \, dx = |T|/2520$.

1.4. The requirement of two meshes

Given $u_h \in [\mathcal{S}^1(\mathcal{T}_h)]^n$ we introduce the auxiliary variable $p_h \in \mathbb{V}$ via

$$(p_h; \sigma_h) \, - \, (\sigma_h; \nabla u_h) = 0 \quad \text{for all } \sigma_h \in \mathbb{V}, \tag{1.4.1}$$

that is, $p_h = P_0^h(\nabla u_h)$. For a minimizing sequence $(u_h)_h \subset W^{1,2}(M;\mathbb{R}^n)$, with $u_h \in \mathcal{A}(\mathcal{T}_h)$ for $h > 0$, of the introduced energy (**??**) we know that $||\nabla u_h|| \leq C$ and hence $||p_h||_{L^2} \leq C$. For our proof we require that $\nabla u_h - p_h \to 0$ in L^2 as $h \to 0$. However, the bounds on $(\nabla u_h)_h$ and $(p_h)_h$ only provide weakly convergent subsequences so that the strong convergence of the difference is not satisfied in general. The idea is to use two different meshes for the different variables, namely for $h_1 \geq h_2$ we consider two quasiuniform triangulations $\mathcal{T}_{h_1}$ and $\mathcal{T}_{h_2}$ of M. Given $u_{h_1} \in [\mathcal{S}^1(\mathcal{T}_{h_1})]^n$ we define $p_{h_2} := P_0^{h_2}(\nabla u_{h_1}) \in [V^{h_2}_{mini}]^{n\times 2}$ and see that

$$||p_{h_2} - \nabla u_{h_1}||_{L^2} = \inf_{\sigma_{h_2} \in [V^{h_2}_{mini}]^{n\times 2}} ||\sigma_{h_2} - \nabla u_{h_1}||_{L^2},$$

since p_{h_2} is the L^2-projection of ∇u_{h_1}. For fixed h_1 it holds

$$\inf_{\sigma_{h_2}} ||\sigma_{h_2} - \nabla u_{h_1}||_{L^2} \to 0$$

as $h_2 \to 0$. We can therefore take a diagonal sequence $h_2(h_1) \to 0$ for $h_1 \to 0$ such that

$$||p_{h_2(h_1)} - \nabla u_{h_1}||_{L^2} \to 0 \quad \text{as} \quad h_1 \to 0.$$

In Lemma 1.4.2 we prove a quantitive relation between the two meshes which is optimal in the sense that there exists a counter example with $h_1 = h_2$ where no strong convergence in L^2 can be deduced.

Remark 1.4.1 *Consider $M = \mathbb{T}^2$ with fundamental domain $D = (0,1)^2$ and a uniform triangulation $\mathcal{T}_h$ of D with $h = \frac{\sqrt{2}}{2N}$, which corresponds to $2N^2$ triangles. Then the set of nodes of D is given by*

$$\mathcal{N}_h := \{z_{i+(N+1)j} = (i/N, j/N) \in \overline{M} \, : \, i,j = 0,\dots,N\},$$

where we identify nodes on $\{0\}\times(0,1)$ and $(0,1)\times\{0\}$ with nodes on $\{1\}\times(0,1)$ and $(0,1)\times\{1\}$. We define the periodic function $u_h(z_{i,j}) := (-1)^{i+j}h$ and note that $(u_h)_h \subset W^{1,2}(\mathbb{T}^2)$ as well as $\nabla u_h \rightharpoonup 0$ in $L^2(\mathbb{T})^2$ as $h \to 0$. Then we compute $\int_{\mathbb{T}^2} \partial_x u_h \, \varphi_z \, dx = \int_{\mathbb{T}^2} \partial_y u_h \, \varphi_z \, dx = 0$ for all $z \in \mathcal{N}_h$. Let $M_1, M_{1,3}$ and $M_3 = \mathrm{diag}\, \frac{|T|}{2520}$ denote the mass matrices corresponding to the L^2-inner products of $(p_{\mathcal{S}^1}, \sigma_{\mathcal{S}^1})$, $(p_{\mathcal{S}^1}, \sigma_{\mathcal{B}^3})$ and $(p_{\mathcal{B}^3}, \sigma_{\mathcal{B}^3})$. Then the computation of the auxiliary variable $p_h = p_{\mathcal{S}^1} + p_{\mathcal{B}^3}$ leads to

$$M_1 \, p_{\mathcal{S}^1} + M_{1,3}^T \, p_{\mathcal{B}^3} = 0, \quad M_{1,3} \, p_{\mathcal{S}^1} + M_3 \, p_{\mathcal{B}^3} = \frac{|T|}{180} \nabla u_h.$$

Since M_3 is diagonal we compute $p_{\mathcal{B}^3} = 14\nabla u_h - \frac{2520}{|T|} M_{1,3}\, p_{\mathcal{S}^1}$, expressed in the basis $(b_T)_T$ of $\mathcal{B}_h^3$. We plug this into the first equation and obtain

$$(M_1 - \frac{2520}{|T|} M_{1,3}^T M_{1,3})\, p_{\mathcal{S}^1} = 0,$$

since $M_{1,3}^T \nabla u_h = 0$. The matrix $M_1 - \frac{2520}{|T|} M_{1,3}^T M_{1,3}$ is positive definite and therefore we check that $p_{\mathcal{S}^1} = 0$. Thus $p_h = p_{\mathcal{B}^3} = 14 \sum_T \nabla u_h|_T b_T$ and $||p_h - \nabla u_h||_{L^2}^2 = \sum_T (\frac{7}{90} - \frac{14}{90} + 1)|T| \left|\nabla u_h\right|^2 = \frac{83}{90} ||\nabla u_h||_{L^2}^2$. Since $(\nabla u_h)_h$ does not converge strongly we do not have $\nabla u_h - p_h \to 0$ in $L^2(\mathbb{T}^2)$ as $h \to 0$.

Lemma 1.4.2 *Consider two sequences of regular triangulations $\mathcal{T}_{h_1}, \mathcal{T}_{h_2}$ of M such that $h_2 = o(h_1)$, i.e., $\lim_{h_1 \to 0} \frac{h_2}{h_1} = 0$. Furthermore let $(u_{h_1})_{h_1} \subset W^{1,2}(M)$ be bounded and let $u_{h_1} \in \mathcal{S}^1(\mathcal{T}_{h_1})$ for all $h_1 > 0$. Then*

$$||P_0^{h_2}(\nabla u_{h_1}) - \nabla u_{h_1}||_{L^2(M)} = \inf_{\sigma_{h_2} \in [V_{mini}^{h_2}]^2} ||\sigma_{h_2} - \nabla u_{h_1}||_{L^2(M)} \to 0 \quad as \quad h_1 \to 0.$$

Proof. Let $p_{h_2} \in [V_{mini}^{h_2}]^2$ be defined through $p_{h_2}(z) := \nabla u_{h_1}\Big|_{T_{h_1}}$ for $z \in \mathcal{N}_{h_2}$, $T_{h_1} \in \mathcal{T}_{h_1}$ and $z \in T_{h_1}$. If $z \in \mathcal{N}_{h_2} \cap \mathcal{N}_{h_1}$ then we set $p_{h_2}(z) := \nabla u_{h_1}\Big|_{T_{h_1}}$ for $T_{h_1} \subset \omega_z^{h_1}$ arbitrary. Then for $T \in \mathcal{T}_{h_2}$ with $T \subset T_{h_1}$ and $T \cap \partial T_{h_1} = \emptyset$ we have $p_{h_2}\Big|_T = \nabla u_{h_1}\Big|_T$ so that

$$||p_{h_2} - \nabla u_{h_1}||_{L^2(T)} = 0.$$

We define $\omega_{T_{h_1}}$ to be the patch of triangles $\tilde{T}_{h_1} \in \mathcal{T}_{h_1}$ having non-empty intersection with T_{h_1} and deduce

$$\begin{aligned}
\int_{T_{h_1}} |p_{h_2} - \nabla u_{h_1}|^2 \,\mathrm{d}x \;&\leq \sum_{\substack{T \in \mathcal{T}_{h_2} \\ T \cap \partial T_{h_1} \neq \emptyset}} \int_{T \cap T_{h_1}} |p_{h_2} - \nabla u_{h_1}|^2 \,\mathrm{d}x \\
&\leq C \sum_{\substack{T \in \mathcal{T}_{h_2} \\ T \cap \partial T_{h_1} \neq \emptyset}} \int_{T \cap T_{h_1}} 1 \,\mathrm{d}x \sum_{\widetilde{T}_{h_1} \in \omega_{T_{h_1}}} \left|\nabla u_{h_1}\Big|_{\widetilde{T}_{h_1}}\right|^2 \\
&\leq C h_1^{-2} ||\nabla u_{h_1}||_{L^2(\omega_{T_{h_1}})}^2 \sum_{\substack{T \in \mathcal{T}_{h_2} \\ T \cap \partial T_{h_1} \neq \emptyset}} \int_{T \cap T_{h_1}} 1 \,\mathrm{d}x.
\end{aligned}$$

We use the estimates $|T \cap T_{h_1}| \leq C h_2^2$ and $\mathrm{card}\{T \in \mathcal{T}_{h_2} : T \cap \partial T_{h_1} \neq \emptyset\} \leq C \frac{|\partial T_{h_1}|}{|T|} \leq C \frac{h_1}{h_2}$ to obtain

$$\begin{aligned}
\int_{T_{h_1}} |p_{h_2} - \nabla u_{h_1}|^2 \,\mathrm{d}x \;&\leq\; C h_1^{-2} h_2^2 \frac{h_1}{h_2} ||\nabla u_{h_1}||_{L^2(\omega_{T_{h_1}})}^2 \\
&\leq C \frac{h_2}{h_1} ||\nabla u_{h_1}||_{L^2(\omega_{T_{h_1}})}^2.
\end{aligned}$$

Finally we arrive at

$$\inf_{\sigma_{h_2} \in [V_{mini}^{h_2}]^2} ||\sigma_{h_2} - \nabla u_{h_1}||_{L^2(M)} \leq ||p_{h_2} - \nabla u_{h_1}||_{L^2(M)} \leq C C_{overlap} \sqrt{\frac{h_2}{h_1}} ||\nabla u_{h_1}||_{L^2(M)} \to 0$$

as $h_1 \to 0$. Here the constant $C_{overlap}$ accounts for the finite overlap, that is, each triangle T_{h_1} belongs only to finitely many patches $\omega_{T_{h_1}}$. □

For a better readability we will use from now on only one index h whenever the different mesh-sizes do not cause any further problems. Note that inverse estimates in the stability proof of our numerical scheme only occur in the larger mesh-size h_1.

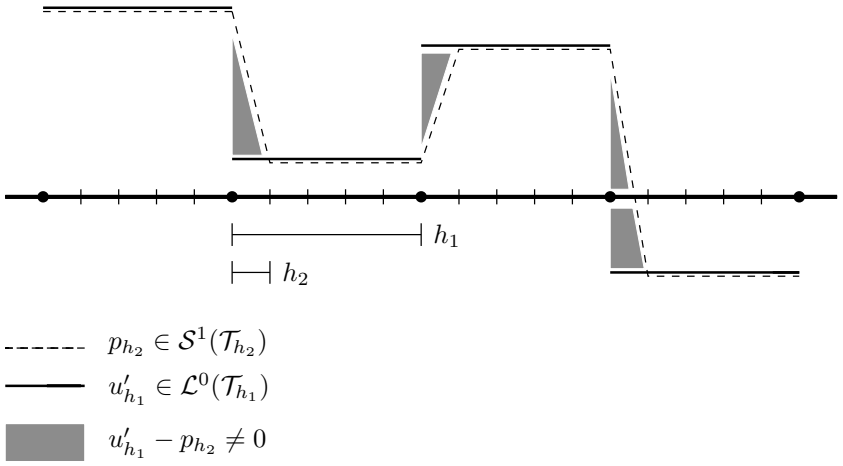

Figure 1.2.: One dimensional sketch of the construction of p_{h_2}. The support of the error $||u'_{h_1} - p_{h_2}||_{L^2}$ sits on a strip of thickness h_2 (gray) around the edges (black dots) of the coarser grid $\mathcal{T}_{h_1}$.

1.5. Finite element functions with values in a submanifold

Let $N \subset \mathbb{R}^n$ be a k-dimensional C^2-submanifold. We define the finite element space of functions with values in N

$$\mathcal{A}(\mathcal{T}_h) := \{u_h \in [\mathcal{S}^1(\mathcal{T}_h)]^n \,:\, u_h(z) \in N \text{ for all } z \in \mathcal{N}_h\},$$

and for given $u_h \in \mathcal{A}(\mathcal{T}_h)$ we set

$$\mathcal{F}[u_h] := \{\eta_h \in [\mathcal{S}^1_0(\mathcal{T}_h)]^n \,:\, \eta_h(z) \in T_{u_h(z)}N \text{ for all } z \in \mathcal{N}_h \setminus \partial M\}.$$

In the case $N = \mathbb{S}^2 \subset \mathbb{R}^3$ we have

$$\mathcal{A}(\mathcal{T}_h) = \{u_h \in [\mathcal{S}^1(\mathcal{T}_h)]^3 \,:\, |u_h(z)| = 1 \text{ for all } z \in \mathcal{N}_h\},$$

and

$$\mathcal{F}[u_h] = \{\eta_h \in [\mathcal{S}^1_0(\mathcal{T}_h)]^3 \,:\, \eta_h(z) \bullet u_h(z) = 0 \text{ for all } z \in \mathcal{N}_h \setminus \partial M\}.$$

Given a C^2 submanifold $N \subset \mathbb{R}^n$ there exists a tubular neighborhood $U_{\delta_N} := \{q \in \mathbb{R}^n \,:\, \operatorname{dist}(q, N) < \delta_N\}$ of N for some $\delta_N > 0$ such that the projection of $x \in U_{\delta_N}$ to N is well-defined. If N is of class C^ℓ for $\ell \geq 2$ we have that the projection $\pi_N : U_{\delta_N} \to N$ is a $C^{\ell-1}$ map and satisfies

$$|q - \pi_N(q)| = \operatorname{dist}(q, N) \quad \text{for all} \quad q \in U_{\delta_N}.$$

Moreover we have the identities $D\pi_N(p)\Big|_{T_pN} = \mathrm{id}\Big|_{T_pN}$ for $p \in N$, and $D\pi_N(p)\nu = 0$ for $\nu \in \mathbb{R}^n$ such that $\nu \perp T_pN$. For every $q \in N$ there exist compactly supported $C^{\ell-1}$-vector fields $\nu_{k+1}, \ldots, \nu_n : U(q) \to \mathbb{R}^n$ which span the normal bundle of N in a neighborhood $U(q) \subset N$, that is, for $y \in U(q)$ we have $\operatorname{span}(\nu_{k+1}(y), \ldots, \nu_n(y)) = N_yN$. The family of sets $(U(q))_{q\in N}$ builds a covering of N so that there exists a finite subcover $U_1, \ldots, U_K$. We show that local computations in the discrete setting can always be done within one support of a local frame.

Lemma 1.5.1 *Let $(u_h)_h \subset W^{1,2}(M;\mathbb{R}^n)$ be a uniformly bounded sequence with $u_h \in \mathcal{A}(\mathcal{T}_h)$ for all $h > 0$ and $\delta := \min_{i=1,\ldots,K} \operatorname{diam} U_i$. There exists $h_0 > 0$ such that for all $h < 0$ and for almost every $x \in M$ there exists $z_x \in \mathcal{N}_h$ and $\ell \in \{1, \ldots, K\}$ such that $x \in \omega_{z_x}$ and $\pi_N(u_h(\omega_{z_x})) \subset U_\ell$. Moreover we have for every $y \in \omega_{z_x}$ that*

$$\operatorname{span}(\nu^\ell_{k+1}(\pi_N(u_h(y))), \ldots, \nu^\ell_n(\pi_N(u_h(y)))) = N_{\pi_N(u_h(y))}N.$$

Proof. We set

$$\Sigma_{\delta,h} := \{z \in \mathcal{N}_h \,:\, ||\nabla u_h||_{L^2(\omega_z)} > C_{inv}\delta\},$$

where $C_{inv} > 0$ is the constant from the inverse estimate $h_z||\nabla u_h||_{L^\infty(\omega_z)} \leq C_{inv}||\nabla u_h||_{L^2(\omega_z)}$. We note that $\operatorname{card}\Sigma_{\delta,h} \leq C\delta^{-2}$ for all $h > 0$ and, therefore, $\Sigma_{\delta,h} \to \Sigma_\delta = \{x_1^\delta, \dots, x_{L^\delta}^\delta\}$, $L^\delta \in \mathbb{N}$, for $x_1^\delta, \dots, x_{L^\delta}^\delta \in M$ as $h \to 0$. For each $x \in M \setminus \Sigma_\delta$ there exists h_0 such that for every $h < h_0$ there exists $z_x \in \mathcal{N}_h \setminus \Sigma_{\delta,h}$ with $x \in \omega_{z_x}$. Then we have for all $\widetilde{x} \in \omega_{z_x}$

$$|u_h(x) - u_h(\widetilde{x})| \leq h_{z_x}||\nabla u_h||_{L^\infty(\omega_{z_x})} \leq C_{inv}^{-1}||\nabla u_h||_{L^2(\omega_{z_x})} \leq \delta,$$

hence $\pi_N(u_h(\omega_{z_x})) \subset U_\ell$ for some $\ell \in \{1, \dots, K\}$ and for every $y \in \omega_{z_x}$ we have

$$\operatorname{span}(\nu_{k+1}^\ell(\pi_N(u_h(y))), \dots, \nu_n^\ell(\pi_N(u_h(y)))) = N_{\pi_N(u_h(y))}N.$$

□

Let $f : \mathbb{R}^k \to \mathbb{R}^n$ be a local parametrization of N, where k is the dimenison of N. A Taylor expansion at $p = f(x) \in N$ in every component of f yields

$$p^i = f^i(x) = p^i(x_0) + (x - x_0)\nabla f^i(x_0) + (x - x_0)^T D^2 f^i(\tilde{x}^i)(x - x_0), \quad i = 1, \dots, n,$$

with some $(\tilde{x}^i)_{i=1,\dots,n} \subset \mathbb{R}^k$ and $p_0 = f(x_0)$. Multiplying the equation with $\nu \in \mathbb{R}^n$ such that $\nu \perp T_{p_0}N$, we obtain

$$(p - p_0) \bullet \nu \leq C_N|p - p_0|^2,$$

since $\nabla f^i(x_0) \in T_{p_0}N$, $i = 1, \dots, n$. Here C_N depends on the curvature of N and the Lipschitz constant of f^{-1}. This estimate can be used to show that

$$\partial_{x_i} u_h|_T \bullet \nu \leq Ch_T\,|\nabla u_h|_T|^2 \quad i = 1, 2, \tag{1.5.1}$$

if $u_h \in \mathcal{A}(\mathcal{T}_h)$, $T \in \mathcal{T}_h$ and $\nu \in T_{u_h(z)}N$ for $z \in T$. If $T = \operatorname{conv}((0,0),(0,h),(h,0))$ and $\nu \in T_{u_h(0,0)}N$ then

$$\partial_{x_1} u_h|_T \bullet \nu = \frac{1}{h}(u_h(h,0) - u_h(0,0)) \bullet \nu \leq C\frac{1}{h}|u_h(h,0) - u_h(0,0)|^2 = Ch|\partial_{x_1} u_h|_T|^2,$$

for the general case see [13]. For the characterization of the discrete Lagrangian multipliers it will be usefull to define the partition of a given testfunction into tangential and normal part.

Lemma 1.5.2 *Let $u_h \in \mathcal{A}(\mathcal{T}_h)$, $\eta \in L^\infty(M;\mathbb{R}^n) \cap W^{1,2}$ and $\eta_h = \mathcal{J}_h\eta$. We define η_h^{nor} through*

$$\eta_h^{nor}(z) := \sum_{i=k+1}^{n} \nu_i(u_h(z)) \bullet \eta_h(z)\nu_i(u_h(z)) \text{ for all } z \in \mathcal{N}_h, \tag{1.5.2}$$

and $\eta_h^{tan} := \eta_h - \eta_h^{nor}$. Then $\eta_h^{tan} \in \mathcal{F}[u_h]$ and $\eta_h^{nor} \in L^\infty(M;\mathbb{R}^n) \cap W^{1,2}$. Moreover, we have the following estimate

$$||\nabla\eta_h^{nor}||_{L^2} \leq C(||\nabla u_h||_{L^2}||\eta||_{L^\infty} + ||\nabla\eta||_{L^2}),$$

where $C > 0$ depends only on the geometry of $\mathcal{T}_h$ and the curvature of N but not on the mesh-size $h > 0$.

Proof. *(Of the claim).* We use that $\sum_{z\in\mathcal{N}_h} \nabla\varphi_z = 0$ and compute for $x \in M$

$$\begin{aligned}
|\nabla\eta_h^{nor}(x)| &= \left|\sum_{z\in\mathcal{N}_h}\sum_{i=k+1}^{n} \nu_i^\ell(u_h(z)) \bullet \eta_h(z)\nu_i^\ell(u_h(z)) \otimes \nabla\varphi_z(x)\right| \\
&= \left|\sum_{z\in\mathcal{N}_h}\sum_{i=k+1}^{n} \left[\nu_i^\ell(u_h(z)) \bullet \eta_h(z)\nu_i^\ell(u_h(z)) - \nu_i^\ell(\pi_N(u_h(x))) \bullet \eta_h(x)\nu_i^\ell(\pi_N(u_h(x)))\right] \otimes \nabla\varphi_z(x)\right| \\
&\leq C_N \sum_{z\in\mathcal{N}_h} h_z(|\nabla u_h(x)|||\eta||_{L^\infty(M)} + |\nabla\eta(x)|)|\nabla\varphi_z(x)| \\
&\leq C_{N,\mathcal{T}_h}(|\nabla u_h(x)|||\eta||_{L^\infty(M)} + |\nabla\eta(x)|),
\end{aligned}$$

where C_N is an upper bound on the curvature of N. We take the square on both sides and integrate over M to arrive at

$$||\nabla \eta_h^{nor}||_{L^2}^2 \leq C(||\nabla u_h||_{L^2}^2 ||\eta||_{L^\infty}^2 + ||\nabla \eta||_{L^2}^2).$$

□

Lemma 1.5.3 *Consider $u_h \in \mathcal{A}(\mathcal{T}_h)$, $A_h \in L^\infty(M;\mathbb{R}^{n\times n}) \cap W^{1,2}$ and a C^1-normal field ν on N. We define the discrete normal field $[\nu(u_h)]_h := \sum_{z\in\mathcal{N}_h} \nu(u_h(z))\varphi_z$, and for $\eta \in C^1(M;\mathbb{R}^n)$ we set*

$$\begin{aligned}[A_h^T\eta]_h &:= \sum_{z\in\mathcal{N}_h} \frac{1}{|\omega_z|}\left(\int_{\omega_z} A_h^T(x)\,dx\right)\eta(z)\varphi_z \\ &= \sum_{z\in\mathcal{N}_h} A_{h,z}^T \eta(z)\varphi_z.\end{aligned}$$

Then the following estimates hold:

$$\begin{aligned}
||\nu(u_h(z)) - [\nu(u_h)]_h||_{L^2(\omega_z)} &\leq C_{\kappa_N} C_{\mathcal{T}_h} h_z ||\nabla u_h||_{L^2(\omega_z)}, \\
||A_{h,z} - A_h||_{L^2(\omega_z)} &\leq C_P h_z ||\nabla A_h||_{L^2(\omega_z)}, \\
||\eta(z) - \eta(\bullet)||_{L^\infty(\omega_z)} &\leq h_z ||\nabla \eta||_{L^\infty(\omega_z)}, \\
||[A_h^T\eta]_h(z) - [A_h^T\eta]_h||_{L^2(\omega_z)} &\leq C_{\mathcal{T}_h}(h_z^2 ||A_h||_{L^\infty}||\nabla\eta||_{L^\infty} + h_z||\nabla A_h||_{L^2(\omega_z)}|\eta(z)|).
\end{aligned}$$

Proof. We may assume that $\pi_N(u_h(\omega_z)) \subset \operatorname{supp}\nu$ and compute for the first inequality

$$\begin{aligned}
||\nu(u_h(z)) - [\nu(u_h)]_h||_{L^2(\omega_z)}^2 &= \int_{\omega_z} |\nu(u_h(z)) - \sum_{z'\in\mathcal{N}_h\cap\omega_z} \nu(u_h(z'))\varphi_{z'}|^2\,\mathrm{d}x \\
&\leq \sum_{z'\in\mathcal{N}_h\cap\omega_z} \int_{\omega_z\cap\omega_{z'}} |\nu(u_h(z)) - \nu(u_h(z'))|^2\,\mathrm{d}x \\
&\leq 2\sum_{z'\in\mathcal{N}_h\cap\omega_z} \int_{\omega_z\cap\omega_{z'}} |\nu(u_h(z)) - \nu(\pi_N(u_h(x)))|^2 \\
&\qquad + |\nu(\pi_N(u_h(x))) - \nu(u_h(z'))|^2\,\mathrm{d}x \\
&\leq C_N \sum_{z'\in\mathcal{N}_h\cap\omega_z} \int_{\omega_z\cap\omega_{z'}} |u_h(z) - \pi_N(u_h(x))|^2 + |\pi_N(u_h(x)) - u_h(z')|^2\,\mathrm{d}x \\
&\leq C_{\kappa_N} C_{\mathcal{T}_h} h_z^2 ||\nabla u_h||_{L^2(\omega_z)}^2,
\end{aligned}$$

where the last step is an application of Lemma 1.5.6. The second estimate follows from Poincaré's inequality for functions with zero mean value on ω_z and the third one is an application of Taylor's formula. The last estimate is just a combination of the previous ones. □

Remark 1.5.4 *Note, that for the definition of $[\nu(u_h)]_h$ we need no global continuity of the normal field.*

Finally we mention two important statements on discrete vector fields with values in the submanifold N, proofs can be found in [13]. The first lemma shows that a sequence $(u_h)_h \subset W^{1,2}(M;\mathbb{R}^n)$ with $u_h \in \mathcal{A}(\mathcal{T}_h)$ for all $h \geq 0$ exhibits a weakly converging subsequence in $W^{1,2}$ whos accumulation points $u \in W^{1,2}(M;\mathbb{R}^n)$ satisfy $u(x) \in N$ for almost every $x \in M$. The second lemma states that $\pi_N \circ u_h : M \to N$ is Lipschitz continuous if $u_h \in \mathcal{A}(\mathcal{T}_h)$ and π_N is a C^1 map.

Lemma 1.5.5 *Suppose that $(u_h)_{h\geq 0}$ is bounded sequence in $W^{1,2}(M;\mathbb{R}^n)$ such that for each $h > 0$ we have $u_h \in \mathcal{A}_h(\mathcal{T}_h)$. Then, every weak accumulation point $u \in W^{1,2}(M;\mathbb{R}^n)$ of the sequence satisfies $u(x) \in N$ for almost every $x \in M$.*

Lemma 1.5.6 *Let $(u_h)_{h>0} \subset W^{1,2}(M;\mathbb{R}^n)$ be such that $u_h \in \mathcal{A}(\mathcal{T}_h)$ for all $h > 0$ and $u_h \rightharpoonup u$ in $W^{1,2}$ as $h \to 0$. Then there exists $h_0 > 0$ such that for all $h \leq h_0$ and almost every $x \in M$ it holds $\operatorname{dist}(u_h(x), N) < \delta_N$, and if $x \in \omega_z$ for $z \in \mathcal{N}_h$ we have the estimate*

$$|\pi_N(u_h(x)) - u_h(z)| \leq C_N h_z |\nabla u_h(x)|.$$

Proof. From Lemma 1.5.5 we knot that the continuous functional $f_h : x \mapsto \operatorname{dist}(u_h(x), N)$ converges to zero almost everywhere as $h \to 0$. Hence, there exists $h_0 > 0$ such that $\operatorname{dist}(u_{h_0}(x), N) < \delta_N$ for almost every $x \in M$. Consider now $z \in \mathcal{N}_h$ and $x \in \omega_z$. A Taylor expansion yields

$$\pi_N(u_h(x)) = \pi_N(u_h(z)) + (x - z)^T \nabla(\pi_N(u_h(\zeta))),$$

for some $\zeta \in \{y \in M : \exists t \in [0,1]\, y = tz + (1-t)x\}$. We conclude

$$|\pi_N(u_h(x)) - u_h(z)| \leq ||D\pi_N||_{L^\infty} h_z |\nabla u_h(x)|,$$

where we used the fact that $\nabla u_h(x) = \nabla u_h(\zeta)$ since u_h is piecewise affine. □

1.6. Auxiliary results from measure theory

For the sake of completness we state two elementary results from measure theory. We refer to [13] for the proofs. Parts of these statements and proofs are generalizations of the finite difference methods from [64] to the finite element setting.

Lemma 1.6.1 *Let $(F_\ell)_{\ell\in\mathbb{N}}$ be a bounded sequence in $C(\overline{M})^*$. If for each $\ell \in \mathbb{N}$ the support of F_ℓ is finite, i.e., $F_\ell = \sum_{j=1}^{L_\ell} a_j^\ell \delta_{x_j^\ell}$ for $L_\ell \in \mathbb{N}$ and $a_j^\ell \in \mathbb{R}$, $x_j^\ell \in \overline{M}$, $j = 1, 2, \ldots, L_\ell$ and if $F_\ell \to F$ strongly as $\ell \to \infty$ for some $F \in C(\overline{M})^*$, i.e.*

$$\sup_{\eta\in C(\overline{M}):||\eta||_{L^\infty(M)}\leq 1} \langle F_\ell - F, \eta\rangle \to 0$$

as $\ell \to \infty$, then there exist $(a_j)_{j\in\mathbb{N}} \subset \mathbb{R}$ and $(x_j)_{j\in\mathbb{N}} \subset \overline{M}$ such that $F = \sum_{j=1}^\infty a_j \delta_{x_j}$. If $\sum_{j=1}^{L_\ell} |a_j^\ell|^s \leq C_1$ for some $s > 0$ and all $\ell \in \mathbb{N}$ then $F = \sum_{j=1}^\infty |a_j|^s \leq C_1$.

Lemma 1.6.2 *Let $(F_h)_{h>0}$ be a bounded sequence in $C(\overline{M})^*$. Suppose that there exist $C > 0$ and $L \in \mathbb{N}$ such that for each $h > 0$ and all $\eta \in C^1(\overline{M})$ we have*

$$|F_h(\eta)| \leq Ch||\nabla\eta||_{L^\infty(\overline{M})} + \sum_{j=1}^{L} \rho_j^h |\eta(x_j^h)|$$

for $\rho_j^h \in \mathbb{R}$ and $x_j^h \in \overline{M}$ for $j = 1, 2, \ldots, L$. Then there exist $L' \leq L$ and $\rho_j \in \mathbb{R}$, $y_j \in \overline{M}$, $j = 1, 2, \ldots, L'$ such that for a subsequence which is not relabeled we have

$$F_h \rightharpoonup^* \sum_{j=1}^{L'} \rho_j \delta_{y_j}$$

as $h \to 0$. If $s \in (0, 1]$ and $\sum_{j=1}^L |\rho_j^h|^s \leq C_1$ for all $h > 0$ then $\sum_{j=1}^{L'} |\rho_j|^s \leq C_1$.

We point out how to use the above results in order to show that the occuring error terms in Theorem 2.2.1 converge to a sum of Dirac measures. The statement is a variation of Lemma 4.7 from [11] and the proof is esentially the same.

Lemma 1.6.3 *Let $(g_h)_{h>0} \subset L^2(\overline{D};\mathbb{R}^n)$ and $(f_h)_{h>0}\Big([\mathcal{S}^1(\mathcal{T}_h)]^n\Big)^*$ be uniformly bounded sequences and $\eta \in C^1(\overline{D};\mathbb{R}^n)$. Suppose that we have for $\eta_h := \mathcal{I}_h\eta$ the estimate*

$$|f_h(\eta_h)| \leq C'h||\nabla\eta||_{L^\infty} + C'' \sum_{z\in\mathcal{N}_h} ||g_h||^3_{L^2(\omega_z)}|\eta(z)|,$$

then there exist $(a_\iota)_{\iota\in\mathbb{N}} \subset \mathbb{R}^n$ and $(y_\iota)_{\iota\in\mathbb{N}} \subset \overline{D}$ such that $\sum_{\iota\in\mathbb{N}} |a_\iota|^{2/3} \leq C$ and for an appropriate subsequence (which is not relabeled) and every $\eta \in C^\infty(\overline{D};\mathbb{R}^n)$ we have, as $h \to 0$

$$f_h(\mathcal{I}_h\eta) \;\to\; \sum_{\iota\in\mathbb{N}} a_\iota \bullet \eta(y_\iota).$$

Proof. We can expand $(f_h)_h$ to a uniform bounded sequence in $C(\overline{M};\mathbb{R}^n)^*$ via $\eta \mapsto f_h(\mathcal{I}_h\eta)$. Thus, there exists subsequence for which we have $f_h \rightharpoonup^* f$ as $h \to 0$. For fixed $\delta > 0$ we define

$$\Sigma_{\delta,h} := \{z \in \mathcal{N}_h \,:\, ||g_h||_{L^2(\omega_z)} > \delta\}.$$

Then, the cardinality of the set $\Sigma_{\delta,h}$ is uniformly bounded with respect to h and therefore, for an appropriate sequence we have

$$\Sigma_{\delta,h} \to \{x_1^\delta, x_2^\delta, \ldots, x_{L^\delta}^\delta\}.$$

as $h \to 0$. With $f_h^{i,z} := f_h(\varphi_z e_i) \in \mathbb{R}$ for each $z \in \mathcal{N}_h$, where $\{e_1,\ldots,e_n\}$ is the standard orthonormal base of $\mathbb{R}^n$, we have

$$f_h(\eta_h) = \sum_{z\in\Sigma_{\delta,h}} f_h^z \bullet \eta(z) + \sum_{z\in\mathcal{N}_h\setminus\Sigma_{\delta,h}} f_h^z \bullet \eta(z) =: f_{\delta,h}^1(\eta) + f_{\delta,h}^2(\eta).$$

For $f_{\delta,h}^2$ we conclude

$$|f_{\delta,h}^2(\eta)| \leq C'h||\nabla\eta||_{L^\infty} + C\delta||\eta||_{L^\infty},$$

and, therefore, $f_{\delta,h}^2 \rightharpoonup^* f_\delta^2$ in $C(\overline{D};\mathbb{R}^n)^*$ as $h \to 0$ with $f_\delta^2 \in C(\overline{D};\mathbb{R}^n)^*$ such that $||f_\delta^2||_{C(\overline{D};\mathbb{R}^n)^*} \leq C\delta$. An application of Lemma 1.6.2 provides the convergence of $f_{\delta,h}^1$ as $h \to 0$, i.e. $f_{\delta,h}^1 \rightharpoonup^* f_\delta^1 = \sum_{j=1}^{L'} \rho_j^\delta \delta_{x_j^\delta}$. We thus have

$$||f - f_\delta^1||_{C(\overline{D};\mathbb{R}^n)^*} \leq C\delta.$$

Employing Lemma 1.6.1 we verify the assertion. □

Chapter 2.

Mixed formulation

We aim at adapting the convergence result for 2-dimensional conformally invariant nonlinear elliptic partial differential equation following the ideas in [68]. After providing a proof we discuss two specifications of the theorem in Chapter 3 and Chapter 4. First we look at harmonic maps into submanifolds of $\mathbb{R}^n$ and second we consider the equation for surfaces of variable prescribed mean curvature. At the end of this Chapter we establish ties between the compactness result for the mixed formulation using MINI-elements and the P^1-method.

2.1. Weak compactness in the continuous setting

We give a short overview of the compactness result from [68] which we adapt to our discrete system. We consider nonlinear elliptic energy functionals of the form

$$E(u) = \int_{D^2} |\nabla u|^2 + \omega(u)(\partial_x u, \partial_y u)\,\mathrm{d}x$$

where ω is a 2-form, $D^2 \subset \mathbb{R}^2$ the unit disk, and $u : D^2 \to N$. Every critical point of E in $W^{1,2}(D^2; N)$ satisfies an equation of the form

$$-\Delta u = \Omega \bullet \nabla u \text{ in } D^2, \tag{2.1.1}$$

with $\Omega \in L^2(D^2; so(n) \otimes \mathbb{R}^2)$, cf. Theorem I.2 in [68]. For a better understanding of the following chapters we state the main theorems from [68] which we need and quote the proof of the compactness result as this inspired the proof in the discrete setting.

Theorem 2.1.1 ([68], Theorem I.1) *Let $n \in \mathbb{N}$. For every $\Omega = (\Omega^{ij})_{1\le i,j\le n}$ in $L^2(D^2, \mathrm{so}(n)\otimes\mathbb{R}^2)$, every $u \in W^{1,2}(D^2, \mathbb{R}^n)$ solving*

$$-\Delta u = \Omega \bullet \nabla u \qquad \text{in } D^2 \tag{2.1.2}$$

is continuous where the contracted notation using coordinates stands for: for all $i = 1, \dots, n$, $-\Delta u^i = \sum_{j=1}^n \Omega^{ij} \bullet \nabla u^j$.

Theorem 2.1.2 ([68], Theorem I.3) *Let $n \in \mathbb{N}$. Let $\Omega = (\Omega^{ij})_{1\le i,j\le n}$ in $L^2(D^2, \mathrm{so}(n) \otimes \mathbb{R}^2)$ and let $A \in L^\infty(D^2, \mathbb{R}^{n\times n}) \cap W^{1,2}$ and $B \in W^{1,2}(D^2, \mathbb{R}^{n\times n})$ satisfying*

$$\nabla_\Omega A := \nabla A - \Omega A = \nabla^\perp B,$$

where $\nabla^\perp = [-\partial_2, \partial_1]^T$. Then every solution to (2.1.2) satisfies the following conservation law

$$\operatorname{div}(A\nabla u + B\nabla^\perp u) = 0. \tag{2.1.3}$$

Theorem 2.1.3 ([68], Theorem I.4) *There exists $\varepsilon(n) > 0$ and $C(n)$ such that for every $\Omega = (\Omega^{ij})_{1\le i,j\le n}$ in $L^2(D^2, \mathrm{so}(n) \otimes \mathbb{R}^2)$ satisfying*

$$\int_{D^2} |\Omega|^2\,dx \le \varepsilon(n),$$

there exists $A \in L^\infty(D^2, \mathbb{R}^{n\times n}) \cap W^{1,2}$ and $B \in W^{1,2}(D^2, \mathbb{R}^{n\times n})$ satisfying

1.
$$\int_{D^2} |\nabla A|^2 + |\nabla A^{-1}|^2 + ||\mathrm{dist}(A, \mathrm{SO}(n))||^2_{L^\infty} \leq C(n) \int_{D^2} |\Omega|^2 dx,$$

2.
$$\int_{D^2} |\nabla B|^2 dx \leq C(n) \int_{D^2} |\Omega|^2 dx,$$

3.
$$\nabla_\Omega A := \nabla A - \Omega A = \nabla^\perp B.$$

Theorem 2.1.4 ([68], Theorem I.5) *Let $\Omega_h \in L^2(D^2, \mathrm{so}(n) \otimes \mathbb{R}^2)$ such that Ω_h weakly converges in L^2 to some Ω. Let f_h be a sequence in $\left(W^{1,2}(D^2, \mathbb{R}^n)\right)'$ which converges to 0 in $\left(W^{1,2}\right)'$ and u_h be a bounded sequence in $W^{1,2}(D^2, \mathbb{R}^n)$ solving*

$$-\Delta u_h = \Omega_h \bullet \nabla u_h + f_h \qquad \text{in } D^2.$$

Then, there exists a (not relabeled) subsequence u_h which weakly converges in $W^{1,2}$ to a solution of (2.1.2).

Proof. *(of Theorem 2.1.4)* There exist subsequences and functions $\Omega \in L^2(D^2; so(n) \otimes \mathbb{R}^2)$ and $u \in W^{1,2}(D^2; N)$ such that $\Omega_h \rightharpoonup \Omega$ and $u_h \to u$ in L^2 as $h \to 0$, see [3] for questions concerning statements from functional analysis. Let $\lambda < 1$ and $\varepsilon(n)$ be given by Theorem 2.1.3. To every $x \in B_\lambda(0)$ we assign $r_{x,h} \leq 1 - |x|$ such that $\int_{B_{r_{x,h}}(x)} |\Omega_h|^2 \, \mathrm{d}x = \varepsilon(n)$ or $r_{x,h} = 1 - |x|$ in case $\int_{B_{r_{x,h}}(x)} |\Omega_h|^2 \, \mathrm{d}x < \varepsilon(n)$. $\{B_{r_{x,h}}(x)\}$ for every $x \in B_\lambda(0)$ realizes of course a covering of $B_\lambda(0)$. We extract a Vitali covering from it which ensures that every point in $B_\lambda(0)$ is covered by a number of balls bounded by a universal number. Since $\int_{D^2} |\Omega_h|^2 \, \mathrm{d}x$ is uniformly bounded, the number of balls in each such a Vitali covering for each $h > 0$ is also uniformly bounded and, modulo extraction of a subsequence, we can assume that it is fixed and equal to K independent of n. Let $\{B_{r_{i,h}}(x_{i,h})\}_{i=1,\dots,K}$ be this covering. Modulo extraction of a subsequence we can always assume that each sequence $x_{i,h}$ converges in $\overline{B_\lambda(0)}$ to a limit x_i and that each sequence $r_{i,h}$ converges to a non negative number r_i (which could be zero of course). We claim that $-\Delta u = \Omega \bullet \nabla u$ on each $B_{r_i}(x_i)$. Let $A_{i,h}$ and $B_{i,h}$ be given by Theorem 2.1.3 in $B_{r_{i,h}}(x_{i,h})$ for Ω_h. We have

$$\mathrm{div}\Big(A_{i,h} \nabla u_h + B_{i,h} \nabla^\perp u_h\Big) = -A_{i,h} f_h \text{ in } B_{r_{i,h}}(x_{i,h}),$$

where $A_{i,h}$ and $B_{i,h}$ satisfy

$$\nabla A_{i,h} - A_{i,h} \Omega_h = \nabla^\perp B_{i,h}.$$

We can extract a subsequence such that each of the couples $(A_{i,h}, B_{i,h})$ weakly converge in $W^{1,2}$ to some limit (A_i, B_i) in every $B_{r_i}(x_i)$. Because of the weak convergence in $W^{1,2}$ we have strong convergence in L^2 and

$$\begin{aligned} A_{i,h} \nabla u_h + B_{i,h} \nabla^\perp u_h \quad &\to \quad A_i \nabla u + B_i \nabla^\perp u, \\ \nabla A_{i,h} - A_{i,h} \Omega_h - \nabla^\perp B_{i,h} \quad &\to \quad \nabla A_i - A_i \Omega_h - \nabla^\perp B_i, \end{aligned}$$

as well as $-A_{i,h} f_h \to 0$ in the sense of distribution. Combining these identities we obtain that

$$\mathrm{div}\Big(A_i \nabla u + B_i \nabla^\perp u\Big) = 0 \text{ in } B_{r_i}(x_i),$$

and

$$\nabla A_i - A_i \Omega_h = \nabla^\perp B_i \text{ in } B_{r_i}(x_i).$$

Thus,

$$A_i \Big[\Delta u + \Omega \bullet \nabla u\Big] = 0 \text{ in } B_{r_i}(x_i)$$

After extracting a subsequence we have pointwise convergence of $A_{i,h}$ almost everywhere. Since $||\mathrm{dist}(A_i, SO(d))||_{L^\infty} \leq C\varepsilon(n)$ and the set of invertible matrices is open we get the invertibility of A_i and, therefore

$$\Delta u + \Omega \bullet \nabla u = 0 \text{ in } B_{r_i}(x_i).$$

It is clear that every point in $B_\lambda(0)$ is in the closure of the union of the $B_{r_i}(x_i)$. Let x be a point which is none of the $B_{r_i}(x_i)$. It seats on the boundary of one of the $B_{r_i}(x_i)$. For convexity reason, it has to seat at the boundary of at least 2 different circles. Two different circles can intersect at only finitely many points, since there are finitely many circles, only finitely many points in $B_\lambda(0)$ can be outside the union of the $B_{r_i}(x_i)$. Thus the distribution $\Delta u + \Omega \bullet \nabla u$ is supported at at mostly finitely many points. Since $\Delta u + \Omega \bullet \nabla u \in (W^{1,2})' + L^1$ it is identically zero on $B_\lambda(0)$. Since this holds for every $\lambda < 1$ we have proved the Theorem. □

2.2. A compactness result for the mixed method

Assumption (BC). Let M be a polygonal Lipschitz domain and $(\mathcal{T}_h)_h$ be a sequence of quasiuniform triangulations of M. Consider $u_D \in L^2(\partial M; \mathbb{R}^n)$ and suppose that there exists a sequence $(u_{D,h})_h \subset W^{1,2}(M; \mathbb{R}^n) \cap L^2(\partial M; \mathbb{R}^n)$ such that $u_{D,h} \in \mathcal{A}(\mathcal{T}_h)$ for all $h > 0$ and $u_{D,h} \to u_D$ in $L^2(\partial M; \mathbb{R}^n)$ for $h \to 0$.

Theorem 2.2.1 *Let M be a polygonal Lipschitz domain and $(\mathcal{T}_{h_1})_{h_1}, (\mathcal{T}_{h_2})_{h_2}$ be two sequences of quasiuniform triangulations of M with mesh-sizes $h_2 = o(h_1)$. Suppose that (BC) holds. Let $(p_{h_2}, u_{h_1}) \in [V^{h_2}_{mini}]^{n\times 2} \times \mathcal{A}(\mathcal{T}_h)$ and $(\Omega_{h_{1,2}})_{h_{1,2}} \subset L^2(M; so(n) \otimes \mathbb{R}^2)$ be such that*

$$||p_{h_2}||_{H(\mathrm{div})} + ||u_{h_1}||_{W^{1,2}} + ||\Omega_{h_{1,2}}||_{L^2} \leq C_0,$$

where the constant $C_0 > 0$ is independent of the mesh-sizes $h_1, h_2 > 0$. If in addition

$$\begin{aligned} (p_{h_2}; \sigma_{h_2}) + \quad (\mathrm{div}\, \sigma_{h_2}, u_{h_1}) &= \int_{\partial M} u_{D,h_1} \sigma_{h_2} \bullet \nu_{\partial M}\, dx, \\ (\mathrm{div}\, p_{h_2}, v_{h_1}) + (\Omega_{h_{1,2}} \bullet p_{h_2}, v_{h_2}) &= 0, \end{aligned}$$

for all $(\sigma_{h_2}, v_{h_1}) \in [V^{h_2}_{mini}]^{n\times 2} \times [\mathcal{S}^1(\mathcal{T}_{h_1})]^n$ and all $h_1, h_2 \geq 0$, then every weak accumulation point of the sequence $(p_{h_2}, u_{h_1}, \Omega_{h_{1,2}})_{h_{1,2}}$ satisfies

$$(p\,;\,\sigma) + (\mathrm{div}\, \sigma, u) = \int_{\partial M} u_D \sigma \bullet \nu_{\partial M}\, dx, \tag{2.2.1}$$

$$(\mathrm{div}\, p, v) + (\Omega \bullet p, v) = 0, \tag{2.2.2}$$

for all $(\sigma, v) \in H(\mathrm{div}; \mathbb{R}^{n\times 2}) \times L^2(M; \mathbb{R}^n)$.

Remark 2.2.2 *For every weak accumulation point of $(p_h, u_h)_h$ from Theorem 2.2.1 we have $p = \nabla u$ so that u is a weak solution of $-\Delta u = \Omega \bullet \nabla u$ in M and $u = u_D$ on ∂M. Applying now Theorem 2.1.1 yields continuity of u.*

Proof. (i) The limit $h_1, h_2 \to 0$ in the first equation is straight forward and leads to

$$(p\,;\,\sigma) + (\mathrm{div}\, \sigma\,,\, u) = \int_{\partial M} u_D \sigma \bullet \nu_{\partial M} \mathrm{d}x,$$

for all $\sigma \in H(\mathrm{div}; \mathbb{R}^{n\times 2})$. Therefore, $\nabla u = p$ as well as $u \in N$ almost everywhere and $u|_{\partial M} = u_D$. From now on we use only one index $h > 0$ for the discrete variables.
(ii) As in [68] we localize the problem. For every $x \in M$ there exists a scalar $\rho_{x,h} > 0$ such that $||\Omega_h||_{L^2(B_{\rho_{x,h}}(x))} \leq \varepsilon(n)$, where $\varepsilon(n)$ is the constant from Theorem 2.1.3. Arguing as in the proof of

Theorem 2.1.4 we end up with a uniform bounded finite covering consisting of $B_{\rho_{1,h}}(x_{1,h}), \dots B_{\rho_{L,h}}(x_{L,h})$ with $L \in \mathbb{N}$, $\rho_{j,h} \to \rho_j \geq 0$ and $x_{j,h} \to x_j$ for a (not relabeled) subsequence $h \to 0$. For $\lambda < 1$ we show convergence on every $B_{\lambda\rho_j}(x_j)$, $j = 1, \dots, L$. In the following we neglect the index j since the given arguments are independent of these. Furthermore we set $D := B_{\lambda\rho}(x)$.
(iii) From $||\Omega_h||_{L^2(D)} \leq \varepsilon(n)$ we deduce with Theorem 2.1.3 the existence of $A_h \in L^\infty(D;\mathbb{R}^{n\times n}) \cap W^{1,2}$ and $B_h \in W^{1,2}(D;\mathbb{R}^{n\times n})$ satisfying $\nabla A_h - A_h\Omega_h = \nabla^\perp B_h$ on D and $||A_h||_{L^\infty} + ||A_h||_{W^{1,2}} + ||B_h||_{W^{1,2}} + ||\mathrm{dist}(A_h, SO(n))||_{L^\infty} \leq C\varepsilon(n)$. Let $\eta \in C^0(\overline{D};\mathbb{R}^n)$. We test the second equation with

$$\begin{aligned}[A_h^T\eta]_h &:= \sum_{z\in\mathcal{N}_h} \frac{1}{|\omega_z|}\left(\int_{\omega_z} A_h^T(x)\,\mathrm{d}x\right)\eta(z)\varphi_z \\ &= \sum_{z\in\mathcal{N}_h} A_{h,z}^T\eta(z)\varphi_z,\end{aligned}$$

and obtain

$$(\mathrm{div}\, p_h\,,\, A_h^T\eta) + (\Omega_h \bullet \nabla u_h\,,\, A_h^T\eta) = \Lambda_h^1(\eta) + \Lambda_h^2(\eta) + \Lambda_h^3(\eta), \tag{2.2.3}$$

where we define Λ_h^1, Λ_h^2 and $\Lambda_h^3 : C^0(\overline{D},\mathbb{R}^n) \to \mathbb{R}$ through

$$\begin{aligned}\Lambda_h^1(\eta) :=\ & \sum_{z\in\mathcal{N}_h}\int_{\omega_z} \mathrm{div}\, p_h(x)(A_{z,h}^T - A_h^T(x))\eta(z)\varphi_z(x)\,\mathrm{d}x \\ &+ \sum_{z\in\mathcal{N}_h}\int_{\omega_z} \mathrm{div}\, p_h(x)A_h^T(x)(\eta(z)-\eta(x))\varphi_z(x)\,\mathrm{d}x,\end{aligned}$$

$$\begin{aligned}\Lambda_h^2(\eta) :=\ & \sum_{z\in\mathcal{N}_h}\int_{\omega_z} \Omega_h(x) \bullet \nabla u_h(x)(A_{z,h}^T - A_h^T(x))\eta(z)\varphi_z(x)\,\mathrm{d}x \\ &+ \sum_{z\in\mathcal{N}_h}\int_{\omega_z} \Omega_h(x) \bullet \nabla u_h(x)A_h^T(x)(\eta(z)-\eta(x))\varphi_z(x)\,\mathrm{d}x\end{aligned}$$

and

$$\Lambda_h^3(\eta) := (\Omega_h \bullet (\nabla u_h - p_h), A_h^T\eta).$$

(iv) We show in Lemma 2.2.3 that $f_h := \Lambda_h^1 + \Lambda_h^2 + \Lambda_h^3 \in C(\overline{D};\mathbb{R}^n)^*$ is uniformly bounded and that for all $\eta \in C^1(\overline{D};\mathbb{R}^n)$

$$|f_h(\eta)| \leq Ch||\eta||_{W^{1,\infty}} + C'\sum_{z\in\mathcal{N}_h}\gamma_{h,z}^3|\eta(z)| + C''||p_h - \nabla u_h||_{L^2},$$

where for each $z \in \mathcal{N}_h$

$$\gamma_{h,z} := \max\{||\nabla u_h||_{L^2(\omega_z)}, ||\nabla A_h||_{L^2(\omega_z)}, ||\Omega_h||_{L^2(\omega_z)}\}.$$

We can directly apply the auxiliary results from measure theory in Appendix **??** to obtain the convergence of f_h to a sum of Dirac measures.
(v) Integration by parts in the first summand of 2.2.3 yields

$$-(\nabla u_h\,,\, \nabla(A_h^T\eta)) + (\Omega_h \bullet \nabla u_h\,,\, A_h^T\eta) = f_h(\eta) + (p_h - \nabla u_h, \nabla(A_h^T\eta)).$$

Owing to the additional equation $\nabla A_h - A_h\Omega_h = \nabla^\perp B_h$ on the left-hand side we have

$$(\nabla^\perp B_h \bullet \nabla u_h, \eta) + (A_h\nabla u_h, \eta) = f_h(\eta) + (p_h - \nabla u_h, \nabla(A_h^T\eta)).$$

Using the convergence of $\nabla u_h - p_h \to 0$ and the results from Lemma 2.2.3 and Appendix **??** the right-hand side converges to a sum of Dirac measures. It remains to verify the convergence of $(\nabla^\perp B_h \bullet \nabla u_h, \eta)$. This follows directly from integration by parts

$$\int_D \nabla u_h \bullet (\eta\nabla^\perp B_h)\,\mathrm{d}x = -\int_D u_h \mathrm{div}\,(\eta\nabla^\perp B_h)\,\mathrm{d}x = -\int_D u_h\nabla\eta \bullet \nabla^\perp B_h\,\mathrm{d}x.$$

Since $u_h \to u$ strongly in L^2 and $\nabla^\perp B_h \rightharpoonup \nabla^\perp B$ weakly in L^2 we obtain

$$(\nabla^\perp B_h \bullet \nabla u_h, \eta) = -(u_h \nabla^\perp B_h, \nabla\eta) \to -(u\nabla^\perp B, \nabla\eta) = (\nabla^\perp B \bullet \nabla u, \eta).$$

We conclude the existence of $(a_\iota)_{\iota\in\mathbb{N}} \subset \mathbb{R}^n$ and $(x_\iota)_{\iota\in\mathbb{N}} \subset D$ such that

$$(\nabla^\perp B \bullet \nabla u, \eta) + (A\nabla u, \nabla\eta) = \sum_{\iota\in\mathbb{N}} a_\iota \bullet \eta(x_\iota),$$

in the limit $h \to 0$. The left-hand side is in $L^1 + H^{-1}$ which contains no Dirac-measures, see [40] for details. Thus $a_\iota = 0$ for all $\iota \in \mathbb{N}$ and we get

$$\operatorname{div}(B\nabla^\perp u + A\nabla u) = 0 \quad \text{on } D, \tag{2.2.4}$$

in the sense of distribution.
(vi) We have $A_h \rightharpoonup A$, $B_h \rightharpoonup B$ in $W^{1,2}$ and $\Omega_h \rightharpoonup \Omega$ in L^2. Therefore we obtain the convergence of the additional equation in the sense of distribution. Incorporating, thus, $\nabla A - A\Omega = \nabla^\perp B$ into (2.2.4) yields

$$A[\operatorname{div} p + \Omega \bullet p] = A[\Delta u + \Omega \bullet \nabla u] = 0 \quad \text{on } D.$$

Since $||\operatorname{dist}(A, SO(n))||_{L^\infty} \leq C\varepsilon(n)$, and the set of regular matrices in $\mathbb{R}^{n\times n}$ is open, we conclude that A is regular and see that (p, u) solves (2.2.1) - (2.2.2) on D.
(iv) The parameter $\lambda < 1$ was arbitrary so that we obtain the equation on every ball $B_{\rho_j}(x_j)$, $j = 1, \dots, L$. The support of the distribution $\operatorname{div} p + \Omega \bullet p$ is a subset of $M \setminus \bigcup_{j=1,\dots,L} B_{\rho_j}(x_j)$ which is a finite collection of single points. As above we conclude that $\operatorname{div} p + \Omega \bullet p = 0$ on M since $L^1 + H^{-1}$ contains no Dirac-measures. □

Lemma 2.2.3 *Let $f_h := \Lambda_h^1 + \Lambda_h^2 + \Lambda_h^3 \in C(\overline{D}; \mathbb{R}^n)^*$ be the functional from the proof of Theorem 2.2.1. We claim that $(f_h)_h \subset C(\overline{D}; \mathbb{R}^n)^*$ is uniformly bounded and that for all $\eta \in C^1(\overline{D}; \mathbb{R}^n)$ we have*

$$|f_h(\eta)| \leq Ch||\eta||_{W^{1,\infty}} + C' \sum_{z\in\mathcal{N}_h} \gamma_{h,z}^3 |\eta(z)| + C''||p_h - \nabla u_h||_{L^2},$$

where for each $z \in \mathcal{N}_h$

$$\gamma_{h,z} := \max\{||\nabla u_h||_{L^2(\omega_z)}, ||\nabla A_h||_{L^2(\omega_z)}, ||\Omega_h||_{L^2(\omega_z)}\},$$

and the constants $C, C', C'' > 0$ depend on inverse estimates, Poincaré's inequality and $\varepsilon(n)$.

Proof. From the uniform estimates

$$||p_h||_{H(\operatorname{div})} + ||u_h||_{W^{1,2}} \leq C_0$$

and

$$||A_h||_{L^\infty} + ||A_h||_{W^{1,2}} \leq C||\Omega_h||_{L^2} \leq C\varepsilon(n)$$

we see directly that $(f_h)_h$ is bounded in $C(\overline{D}; \mathbb{R}^n)^*$. From Taylor's formula we obtain for $x \in \omega_z$ that

$$|\eta(z) - \eta(x)| \leq |z - x|||\nabla\eta||_{L^\infty} \leq h_z||\nabla\eta||_{L^\infty}.$$

Next we use Poincaré's estimate for functions with zero mean value to conclude

$$||A_{h,z} - A_h||_{L^2(\omega_z)} \leq C_P h_z ||\nabla A_h||_{L^2(\omega_z)}.$$

Finally we combine the above estimates with the inverse inequality $||\nabla u_h||_{L^\infty(\omega_z)} \leq C_{inv} h_z^{-1} ||\nabla u_h||_{L^2(\omega_z)}$ to see

$$\begin{aligned}
|\Lambda_h^1(\eta)| \leq & \sum_{z\in\mathcal{N}_h} \int_{\omega_z} |\operatorname{div} p_h (A_{z,h}^T - A_h^T)\eta(z)\varphi_z| \,\mathrm{d}x \\
& + \sum_{z\in\mathcal{N}_h} \int_{\omega_z} |\operatorname{div} p_h A_h^T(\eta(z)-\eta)\varphi_z| \,\mathrm{d}x \\
\leq & \; C_P \sum_{z\in\mathcal{N}_h} h_z ||\operatorname{div} p_h||_{L^2(\omega_z)} ||\nabla A_h||_{L^2(\omega_z)} ||\eta||_{L^\infty} \\
& + \sum_{z\in\mathcal{N}_h} h_z ||\operatorname{div} p_h||_{L^2(\omega_z)} ||A_h||_{L^2(\omega_z)} ||\nabla\eta||_{L^\infty} \\
\leq & \; Ch||\eta||_{W^{1,\infty}},
\end{aligned}$$

as well as

$$\begin{aligned}
|\Lambda_h^2(\eta)| \leq & \sum_{z\in\mathcal{N}_h} \int_{\omega_z} |\Omega_h \bullet \nabla u_h (A_{z,h}^T - A_h^T)\eta(z)\varphi_z| \,\mathrm{d}x \\
& + \sum_{z\in\mathcal{N}_h} \int_{\omega_z} |\Omega_h \bullet \nabla u_h A_h^T(\eta(z)-\eta)\varphi_z| \,\mathrm{d}x \\
\leq & \; C_P \sum_{z\in\mathcal{N}_h} h_z ||\Omega_h||_{L^2(\omega_z)} ||\nabla u_h||_{L^\infty(\omega_z)} ||\nabla A_h||_{L^2(\omega_z)} |\eta(z)| \\
& + \sum_{z\in\mathcal{N}_h} h_z ||\Omega_h||_{L^2(\omega_z)} ||\nabla u_h||_{L^2(\omega_z)} ||A_h||_{L^\infty(\omega_z)} ||\nabla\eta||_{L^\infty} \\
\leq & \; Ch||\eta||_{W^{1,\infty}} + C' \sum_{z\in\mathcal{N}_h} \gamma_{h,z}^3 |\eta(z)|,
\end{aligned}$$

and

$$\Lambda_h^3(\eta) \leq C'' ||p_h - \nabla u_h||_{L^2}.$$

This yields

$$|f_h(\eta)| \leq |\Lambda_h^1(\eta)| + |\Lambda_h^2(\eta)| + |\Lambda_h^3(\eta)| \leq Ch||\eta||_{W^{1,\infty}} + C' \sum_{z\in\mathcal{N}_h} \gamma_{h,z}^3 |\eta(z)| + C''||p_h - \nabla u_h||_{L^2}.$$

□

2.3. A compactness result for the P^1-method

A natural choice for the P^1-discretization of equation (2.1.1) is: Compute $u_h \in \mathcal{A}(\mathcal{T}_h)$ such that $u_h(z) = u_{D,h}(z)$ for all $z \in \mathcal{N}_h \cap \partial M$ and

$$(\nabla u_h, \nabla v_h) + (\Omega_h \bullet \nabla u_h, v_h) = 0$$

for all $v_h \in [\mathcal{S}_0^1(\mathcal{T}_h)]^n$. If we ask for a little more regularity of the sequences u_h and Ω_h then compactness of the P^1-method, using Theorem 2.1.4, can be established.

Theorem 2.3.1 *Let M be a polygonal Lipschitz domain and $(\mathcal{T}_h)_h$ be a sequence of quasiuniform triangulations of M. Let $\theta > 0$, $u_h \in \mathcal{A}(\mathcal{T}_h)$ and $\Omega_h \in L^2(M; so(n) \otimes \mathbb{R}^n)$ be such that*

$$||\nabla u_h||_{L^{2+\theta}} + ||\Omega_h||_{L^{2+\theta}} \leq C_0,$$

where the constant $C_0 > 0$ is independent of the mesh-size $h > 0$. If in addition $u_h(z) = u_{D,h}(z)$ for all $z \in \mathcal{N}_h$, where $u_{D,h} \in [\mathcal{S}^1(\mathcal{T}_h)]^n$ suffices $u_{D,h} \to u_D$ in $L^2(\partial M; \mathbb{R}^n)$ as $h \to 0$, and

$$(\nabla u_h, \nabla v_h) - (\Omega_h \bullet \nabla u_h, v_h) = 0$$

for all $v_h \in [\mathcal{S}^1_0(\mathcal{T}_h)]^n$, then every weak accumulation point of the sequence $(u_h, \Omega_h)_{h>0}$ satisfies $u \in N$ almost everywhere,

$$(\nabla u, \nabla v) \; - \; (\Omega \bullet \nabla u, v) \; = \; 0$$

for all $v \in W^{1,2}_0(M;\mathbb{R}^n)$ and $u = u_D$ on ∂M.

Proof. (i) First we consider an auxiliary triangulation $\mathcal{T}_{\tilde{h}}$ of M with mesh-size $\tilde{h} = o(h^\beta)$ where $\beta > 1$ will be chosen later. We introduce the auxiliary variable $p_{\tilde{h}} := P_0^{\tilde{h}} \nabla u_h \in [V^{\tilde{h}}_{mini}]^{n\times 2}$ and note that

$$||p_{\tilde{h}} - \nabla u_h||_{L^2} \leq C\sqrt{h^{\beta-1}}||\nabla u_h||_{L^2},$$

as can be seen from the proof of Lemma 1.4.2. Furthermore, we can decompose $p_{\tilde{h}} = p^\perp_{\tilde{h}} + p^\top_{\tilde{h}}$ where $p^\top_{\tilde{h}} \in Z_{\tilde{h}} := \{\sigma_{\tilde{h}} \in [V^{\tilde{h}}_{mini}]^{n\times 2} : (\operatorname{div}\sigma_{\tilde{h}}, v_h) = 0 \text{ for all } v_h \in [\mathcal{S}^1(\mathcal{T}_h)]^n\}$ and $p^\perp_{\tilde{h}} \in Z^\perp_{\tilde{h}}$, that is $(p^\perp_{\tilde{h}}, \sigma_{\tilde{h}}) = 0$ for all $\sigma_{\tilde{h}} \in Z_{\tilde{h}}$. We note that

$$||p_{\tilde{h}} - \nabla u_h||^2_{L^2} = ||p^\perp_{\tilde{h}} - \nabla u_h||^2_{L^2} + ||p^\top_{\tilde{h}}||^2_{L^2},$$

by orthogonality and, therefore, we have that $p^\top_{\tilde{h}} \to 0$ in L^2 as $h \to 0$. For $p^\perp_{\tilde{h}}$ we have by the inf-sup condition that

$$||p^\perp_{\tilde{h}}||_{H(\operatorname{div})} \leq \gamma ||\operatorname{div} p_{\tilde{h}}||_{([\mathcal{S}^1(\mathcal{T}_h)]^n)'}.$$

(ii) After a localization procedure as in the proof of Theorem 2.2.1 we consider a ball $D \subset M$ such that $||\Omega_h||_{L^2(D)} \leq \varepsilon(n)$ and corresponding matrices $A_h \in L^\infty(D;\mathbb{R}^{n\times n}) \cap W^{1,2}$ and $B_h \in W^{1,2}(D;\mathbb{R}^{n\times n})$. We test the equation with $[A_h^T\eta]_h$ for some $\eta \in C^\infty_0(D;\mathbb{R}^n)$ and obtain

$$(\nabla u_h, \nabla v_h) - (\Omega_h \bullet u_h, v_h) + \Psi_h(\eta) = 0, \tag{2.3.1}$$

where $\Psi_h \in C(M;\mathbb{R}^n)^*$ is defined through

$$\Psi_h(\eta) := (\nabla u_h - p^\perp_{\tilde{h}}, \nabla([A_h^T\eta]_h - A_h^T\eta)) - (\operatorname{div} p^\perp_{\tilde{h}}, [A_h^T\eta]_h - A_h^T\eta) + (\Omega_h \bullet \nabla u_h, [A_h^T\eta]_h - A_h^T\eta).$$

The first term vanishes as $h \to 0$ since $(\nabla([A_h^T\eta]_h - A_h^T\eta))_{h>0}$ is bounded in L^2 and $\nabla u_h - p^\perp_{\tilde{h}} \to 0$ in L^2 as $h \to 0$. The third term can be treated as in the proof of Theorem 2.2.1, for the second we compute

$$\begin{aligned}
(\operatorname{div} p^\perp_{\tilde{h}}, [A_h^T\eta]_h - A_h^T\eta) &\leq C_P \sum_{z\in\mathcal{N}_h} h_z ||\operatorname{div} p^\perp_{\tilde{h}}||_{L^2(\omega_z)} ||\nabla A_h||_{L^2(\omega_z)} ||\eta||_{L^\infty} \\
&\quad + \sum_{z\in\mathcal{N}_h} h_z ||\operatorname{div} p^\perp_{\tilde{h}}||_{L^2(\omega_z)} ||A_h||_{L^2(\omega_z)} ||\nabla\eta||_{L^\infty} \\
&\leq Ch ||\operatorname{div} p^\perp_{\tilde{h}}||_{L^2} \Big(||A_h||_{L^2} ||\nabla\eta||_{L^\infty} + ||\nabla A_h||_{L^2} ||\eta||_{L^\infty} \Big).
\end{aligned}$$

We claim that $h^{1-\theta/2}||\operatorname{div} p^\perp_{\tilde{h}}||_{L^2} \leq C$ for a constant $C > 0$ depending on $||\nabla u_h||_{L^{2+\theta}}$ and $||\Omega_h||_{L^{2+\theta}}$. Then,

$$(\operatorname{div} p^\perp_{\tilde{h}}, [A_h^T\eta]_h - A_h^T\eta) \leq C\varepsilon(n) h^{\theta/2} ||\eta||_{W^{1,\infty}} \to 0$$

as $h \to 0$. To proof the claim we estimate

$$\begin{aligned}
||\operatorname{div} p^\perp_{\tilde{h}}||_{L^2} &\leq \gamma^{-1} ||\operatorname{div} p^\perp_{\tilde{h}}||_{([\mathcal{S}^1(\mathcal{T}_h)]^n)'} \\
&= \gamma^{-1} \sup_{v_h \in [\mathcal{S}^1_0(\mathcal{T}_h)]^n} \frac{(\operatorname{div} p^\perp_{\tilde{h}}, v_h)}{||v_h||_{L^2}} \\
&\leq \gamma^{-1} \sup_{v_h \in [\mathcal{S}^1_0(\mathcal{T}_h)]^n} \frac{(p^\perp_{\tilde{h}} - \nabla u_h, \nabla v_h)}{||v_h||_{L^2}} + \gamma^{-1} \sup_{v_h \in [\mathcal{S}^1_0(\mathcal{T}_h)]^n} \frac{(\nabla u_h, \nabla v_h)}{||v_h||_{L^2}} \\
&\leq \gamma^{-1} C h^{1/2(\beta-1)} ||\nabla u_h||_{L^2} \sup_{v_h \in [\mathcal{S}^1_0(\mathcal{T}_h)]^n} \frac{||\nabla v_h||_{L^2}}{||v_h||_{L^2}} + \gamma^{-1} \sup_{v_h \in [\mathcal{S}^1_0(\mathcal{T}_h)]^n} \frac{(\Omega_h \bullet \nabla u_h, v_h)}{||v_h||_{L^2}} \\
&\leq C' h^{1/2(\beta-3)} + \gamma^{-1} ||\Omega_h \bullet \nabla u_h||_{L^2}.
\end{aligned}$$

Then,

$$\begin{aligned} h^{1-\theta/2}||\operatorname{div} p_{\tilde{h}}^{\perp}||_{L^2} &\leq C' h^{1/2(\beta-1-\theta)} + \gamma^{-1} h^{1-\theta/2} ||\Omega_h \bullet \nabla u_h||_{L^2} \\ &\leq C' h^{1/2(\beta-1-\theta)} + \gamma^{-1} \Big(h||\nabla u_h||_{L^\infty} \Big)^{1-\theta/2} ||\Omega_h||_{L^{2+\theta}} ||\nabla u_h||_{L^{2+\theta}}^{\theta/2} \\ &\leq C' h^{1/2(\beta-1-\theta)} + C_{inv} \gamma^{-1} ||\nabla u_h||_{L^2}^{1-\theta/2} ||\Omega_h||_{L^{2+\theta}} ||\nabla u_h||_{L^{2+\theta}}^{\theta/2} \\ &\leq C' h^{1/2(\beta-1-\theta)} + C'' ||\nabla u_h||_{L^{2+\theta}} ||\Omega_h||_{L^{2+\theta}}. \end{aligned}$$

Thus, for $\beta \geq 1+\theta$ we can conclude the claim. As in the proof of Theorem 2.2.1 we know that Ψ_h converges to a sum of Dirac measures. We use the auxiliary equation $\nabla A_h - A_h \Omega_h = \nabla^{\perp} B_h$ in (2.3.1) and conclude the existence of a (not relabeled) subsequence of $(u_h, \Omega_h)_h$ converging to a solution of $\Delta u + \Omega \bullet \nabla u = 0$ in D. The rest of the proof is exactly the same as in Theorem 2.2.1. □

Remark 2.3.2 *The proof of Theorem 2.3.1 shows that we can also require*

$$||p_{h_2}||_{L^2} + ||\nabla u_{h_1}||_{L^{2+\theta}} + ||\Omega_{h_{1,2}}||_{L^{2+\theta}} \leq C_0$$

in Theorem 2.2.1 to obtain compactness of approximating sequences.

Chapter 3.

Harmonic maps

First we give a definition of harmonic pairs into submanifolds of $\mathbb{R}^n$ as saddle points of a certain energy. Then we provide the corresponding Euler-Lagrange equation in a mixed form. We proceed with a discretization and apply the results of Chapter 2 for a compactness result. Finally we introduce an iterative algorithm for the numerical realization.

3.1. A compactness result for discrete harmonic pairs

Definition 3.1.1 *Let $M \subset \mathbb{R}^2$ be a Lipschitz domain and $u_D \in L^2(\partial M)$. A pair of functions $(p,u) \in H(\mathrm{div}, \mathbb{R}^{n\times 2}) \times W^{1,2}(M;\mathbb{R}^n)$ is called a (weakly) harmonic pair into N, subject to the boundary data $u|_{\partial M} = u_D$, if $u(x) \in N$ for almost every $x \in M$ and if it is a saddle point of the energy $\widetilde{E}: H(\mathrm{div}, \mathbb{R}^{n\times 2}) \times W^{1,2}(M;\mathbb{R}^n) \to \mathbb{R}$,*

$$(\sigma, v) \mapsto \frac{1}{2}\int_M |\sigma|^2 dx + \int_M \mathrm{div}\,\sigma \bullet v \, dx - \int_{\partial M} u_D \sigma \bullet \nu_{\partial M}\, dx$$

with respect to perturbations of the form $(p+\mu, \pi_N(u+\phi))$ for $\mu \in H(\mathrm{div}, \mathbb{R}^{n\times 2})$ and $\phi \in L^\infty(M;\mathbb{R}^n) \cap W_0^{1,2}$ that are compactly supported in M. Here, $\nu_{\partial M}: \partial M \to \mathbb{R}^2$ is the unit outer normal to M.

Proposition 3.1.2 *Suppose that $N \subset \mathbb{R}^n$ is a compact k-dimensional C^2 submanifold without boundary. A pair of functions $(p,u) \in H(\mathrm{div}, \mathbb{R}^{n\times 2}) \times W^{1,2}(M;\mathbb{R}^n)$ is a harmonic pair into N, subject to the boundary conditions $u|_{\partial M} = u_D$, if and only if $u(x) \in N$ for almost every $x \in M$ and one of the following equivalent conditions is satisfied:*

1. *For all $\sigma \in H(\mathrm{div}; \mathbb{R}^{n\times 2})$ and all $v \in L^2(M;\mathbb{R}^n)$ satisfying $v(x) \in T_{u(x)}N$ for almost every $x \in M$ we have*

$$\begin{aligned} (p\,;\,\sigma) + (\mathrm{div}\,\sigma, u) &= \int_{\partial M} u_D \sigma \bullet \nu_{\partial M}\, dx \\ (\mathrm{div}\, p, v) &= 0. \end{aligned}$$

2. *For all $\sigma \in H(\mathrm{div}; \mathbb{R}^{n\times 2})$ and all $v \in L^\infty(M;\mathbb{R}^n) \cap W_0^{1,2}$ we have*

$$(p\,;\,\sigma) + (\mathrm{div}\,\sigma, u) = \int_{\partial M} u_D \sigma \bullet \nu_{\partial M}\, dx \tag{3.1.1}$$

$$(\mathrm{div}\, p, v) + (A_N(u)[\nabla u, \nabla u], v) = 0. \tag{3.1.2}$$

where A_N denotes the second fundamental form on N.

Remark 3.1.3 *Let $p, \sigma \in \mathbb{R}^{n\times 2}$, $u \in \mathbb{R}^n$ and $\nu_{\partial M} \in \mathbb{R}^2$. Then the above expressions stand for*

$$(p\,;\,\sigma) = \sum_{i=1}^{n}\sum_{j=1}^{2} p_{ij}\sigma_{ij}, \quad (\mathrm{div}\,\sigma, u) = \sum_{i=1}^{n}\sum_{j=1}^{2} \partial_j \sigma_{ij} u_i, \quad u_D\,\sigma \bullet \nu_{\partial M} = \sum_{i=1}^{n}\sum_{j=1}^{2} u_D^i \sigma_{ij} \nu_j.$$

For a proof of Proposition 3.1.2 we refer the reader to [13],[44] or [72]. We will now give a definition of what we call a discrete harmonic pair.

Definition 3.1.4 *Let $M \subset \mathbb{R}^2$ be a polygonal Lipschitz domain and $\mathcal{T}_h$ a quasiuniform triangulation of M. Assume that (BC) holds. We say that $(p_h, u_h) \in [V^h_{mini}]^{n\times 2} \times \mathcal{A}(\mathcal{T}_h)$ is a discrete harmonic pair, subject to the boundary conditions $u_h = u_{D,h}$ on ∂M, if it is a saddle point of the energy $\widetilde{E}_h : [V^h_{mini}]^{n\times 2} \times \mathcal{A}(\mathcal{T}_h) \to \mathbb{R}$,*

$$(\sigma_h, v_h) \mapsto \frac{1}{2}||\sigma_h||^2_{L^2} + (\operatorname{div}\sigma_h, v_h) + \int_{\partial M} u_{D,h}\sigma_h \bullet \nu_{\partial M}\, dx,$$

that means, for arbitrary $(\sigma_h, v_h) \in [V^h_{mini}]^{n\times 2} \times \mathcal{A}(\mathcal{T}_h)$

$$\widetilde{E}(p_h, v_h) \le \widetilde{E}(p_h, u_h) \le \widetilde{E}(\sigma_h, u_h).$$

We state a discrete version of Proposition 3.1.2 and note that the proof is straightforward.

Proposition 3.1.5 *The pair $(p_h, u_h) \in [V^h_{mini}]^{n\times 2} \times \mathcal{A}(\mathcal{T}_h)$ is a discrete harmonic pair, subject to the boundary condition $u_h = u_{D,h}$ if and only if one of the following equivalent formulations holds*

1. *for all $(\sigma_h, v_h) \in [V^h_{mini}]^{n\times 2} \times \mathcal{F}[u_h]$ we have*

$$\begin{aligned} (p_h; \sigma_h) + (\operatorname{div}\sigma_h, u_h) &= \int_{\partial M} u_{D,h}\sigma_h \bullet \nu_{\partial M}\, dx, \\ (\operatorname{div} p_h, v_h) &= 0. \end{aligned}$$

2. *There exists $\lambda_h = (\lambda_h^{k+1}, \dots, \lambda_h^n) \in [\mathcal{S}^1(\mathcal{T}_h)]^{n-k}$ such that*

$$\begin{aligned} (p_h, \sigma_h) + (\operatorname{div}\sigma_h, u_h) &= \int_{\partial M} u_{D,h}\sigma_h \bullet \nu_{\partial M}\, dx, \\ (\operatorname{div} p_h, \eta_h) + \sum_{i=k+1}^{n} (\lambda_h^i, [\nu^i(u_h)]_h \bullet \eta_h)_h &= 0, \end{aligned}$$

for all $(\sigma_h, \eta_h) \in [V^h_{mini}]^{n\times 2} \times [\mathcal{S}^1_0(\mathcal{T}_h)]^n$, where $([\nu^i(u_h)]_h)_{i=k+1,\dots,n}$ are the discrete normal fields spanning $N_{u_h(z)}N$ at every node $z \in \mathcal{N}_h$.

Theorem 3.1.6 *Given $N, u_{D,h}$, $[V^h_{mini}]^{n\times 2}$ and $\mathcal{A}(\mathcal{T}_h)$ as above, there exist discrete harmonic pairs into N.*

Proof. We show the existence of saddle points. (i) Let $\alpha = n \operatorname{card}\mathcal{N}_h$ and $\beta = 2(\alpha + n \operatorname{card}\mathcal{T}_h)$. Then $[V^h_{mini}]^{n\times 2} \simeq \mathbb{R}^\beta$ and $\mathcal{A}(\mathcal{T}_h) \simeq \underbrace{N \times \cdots \times N}_{(\alpha/n)-times} =: K \subset \mathbb{R}^\alpha$, and K is compact. Any coordinate representation of $\widetilde{E}$ can be written as

$$(p, v) \mapsto \frac{1}{2}p^T Bp + p^T Dv + p^T c,$$

with $B \in \mathbb{R}^{\beta\times\beta}$ positiv definite, $D \in \mathbb{R}^{\beta\times\alpha}$ and $c \in \mathbb{R}^\beta$. Since the above expression is quadratic in p we have for every fixed $v \in K$ the existence of p_v such that

$$E(p_v, v) = \inf_{p\in\mathbb{R}^\beta} \widetilde{E}(p, v).$$

(ii) The mapping $v \mapsto p_v$ is continuous and so is $v \mapsto \widetilde{E}(p_v, v)$. To prove this claim we note that the following equation holds for p_v

$$\sigma^T Bp_v + \sigma^T Dv + \sigma^T c = 0 \quad \forall\sigma \in \mathbb{R}^\beta.$$

Hence, we obtain for $p_{v_1}, p_{v_2} \in \beta$

$$(p_{v_1} - p_{v_2})^T B(p_{v_1} - p_{v_2}) + (p_{v_1} - p_{v_2})^T D(v_1 - v_2) = 0.$$

If $\alpha > 0$ denotes the coercivity constant of B we arrive at

$$||p_{v_1} - p_{v_2}|| \leq \alpha^{-1}||D||_{op}||v_1 - v_2||,$$

that is, $v \mapsto p_v$ is continuous.
(iii) Since K is compact and finite dimensional there exists v^* satisying

$$\widetilde{E}(p_{v^*}, v^*) = \sup_{v \in K} \widetilde{E}(p_v, v) = \sup_{v \in K} \inf_{p \in \mathbb{R}^\beta} \widetilde{E}(p, v).$$

□

We focus now on the question under which assumptions accumulation points of discrete harmonic pairs $(p_h, u_h)_{h>0} \subset H(\mathrm{div}, \mathbb{R}^{n\times 2}) \times W^{1,2}(M; \mathbb{R}^n)$ are harmonic. In order to make use of the above stated convergence result we need to recover the antisymmetric structure in the discrete equation. In the continuous case this follows from Theorem I.2. in [68]. The $m-th$ component of the right-hand side of equation (3.1.2) equals

$$A_N^m(u)[\nabla u, \nabla u] = \sum_{\ell,i=1}^n A_N^m(u)_{\ell,i} \nabla u^i \bullet \nabla u^\ell.$$

Since $(A_N^m(u)_{\ell,i})_{m=1,\dots,n}$ is perpendicular to $T_u N$ for every ℓ and i, we have that

$$\forall \ell, i \in \{1, \dots, n\} \qquad \sum_{m=1}^n A_N^m(u)_{\ell,i} \nabla u^m = 0.$$

Thus, the right-hand side becomes

$$\sum_{\ell,i=1}^n A_N^m(u)_{\ell,i} \nabla u^i \bullet \nabla u^\ell = \sum_{\ell,i=1}^n (A_N^m(u)_{\ell,i} - A_N^\ell(u)_{m,i}) \nabla u^i \bullet \nabla u^\ell = \sum_{\ell=1}^n \Omega^{m\ell} \bullet \nabla u^\ell,$$

where

$$\Omega^{m\ell} := \sum_{i=1}^n (A_N^m(u)_{\ell,i} - A_N^\ell(u)_{m,i}) \nabla u^i. \tag{3.1.3}$$

We proceed with a discrete version of this calculation.

Lemma 3.1.7 *Let $(p_h, u_h) \in [V^h_{mini}]^{n\times 2} \times \mathcal{A}(\mathcal{T}_h)$ be a discrete harmonic pair. Introduce $\Omega_h \in L^2(M; so(n) \otimes \mathbb{R}^2)$ as*

$$\Omega_h^{m\ell} := \sum_{i=k+1}^n [\nu^i(u_h)]_{h,m} \nabla [\nu^i(u_h)]_{h,\ell} - [\nu^i(u_h)]_{h,\ell} \nabla [\nu^i(u_h)]_{h,m},$$

where $[\nu^i(u_h)]_{h,m} \in \mathcal{S}^1(\mathcal{T}_h)$ denotes the m-th component of $[\nu^i(u_h)]_h \in [\mathcal{S}^1(\mathcal{T}_h)]^n$. Furthermore, we define the functional $\Psi_h : [\mathcal{S}^1(\mathcal{T}_h)]^n \to \mathbb{R}$

$$\begin{aligned}
\Psi_h(\eta_h) := &- \sum_{z \in \mathcal{N}_{h_1}} \sum_{i=k+1}^n \int_M \eta_h(z) \bullet (\nu_i(u_h(z)) - [\nu_i(u_h)]_h) \nabla u_h : \nabla(\nu^i(u_h(z))\varphi_z) dx \\
&- \sum_{z \in \mathcal{N}_h} \sum_{i=k+1}^n \int_M (\eta_h(z) - \eta_h) \bullet [\nu_i(u_h)]_h \nabla u_h : \nabla(\nu^i(u_h(z))\varphi_z) dx \\
&- \sum_{z \in \mathcal{N}_h} \sum_{i=k+1}^n \int_M \eta_h \bullet \nu_i(u_h(z)) \nabla u_h : [\nu_i(u_h))]_h \otimes \nabla \varphi_z dx.
\end{aligned}$$

Then

$$(\mathrm{div}\, p_h, \eta_h) + (\Omega_h \bullet \nabla u_h, \eta_h) = (\nabla u_h - p_h, \nabla \eta_h^{nor}) + \Psi_h(\eta_h)$$

for all $\eta_h \in [\mathcal{S}^1(\mathcal{T}_h)]^n$.

Proof. We compute for $\eta_h = \eta_h^{tan} + \eta_h^{nor}$

$$(\operatorname{div} p_h, \eta_h) = (\operatorname{div} p_h, \eta_h^{tan}) + (\operatorname{div} p_h, \eta_h^{nor}) = -(\nabla u_h, \nabla \eta_h^{nor}) + (\nabla u_h - p_h, \nabla \eta_h^{nor}), \tag{3.1.4}$$

where $(\operatorname{div} p_h, \eta_h^{tan}) = 0$ since (p_h, u_h) is a discrete harmonic pair. With the definition (1.5.2) of η_h^{nor} we obtain

$$\begin{aligned}
(\nabla u_h, \nabla \eta_h^{nor}) &= \sum_{z\in\mathcal{N}_h} (\nabla u_h, \eta_h^{nor}(z) \otimes \nabla\varphi_z) \\
&= \sum_{z\in\mathcal{N}_h} \sum_{i=k+1}^{n} (\nabla u_h, \nu_i(u_h(z)) \bullet \eta_h(z)\nu_i(u_h(z)) \otimes \nabla\varphi_z) \\
&= \sum_{z\in\mathcal{N}_h} \sum_{i=k+1}^{n} \int_M \eta_h(z) \bullet \nu_i(u_h(z))\nabla u_h : \nabla(\nu^i(u_h(z))\varphi_z)\mathrm{d}x \\
&= \sum_{z\in\mathcal{N}_h} \sum_{i=k+1}^{n} \int_M \eta_h(z) \bullet [\nu_i(u_h))]_h\nabla u_h : \nabla(\nu^i(u_h(z))\varphi_z)\mathrm{d}x \\
&\quad + \sum_{z\in\mathcal{N}_h} \sum_{i=k+1}^{n} \int_M \eta_h(z) \bullet (\nu_i(u_h(z)) - [\nu_i(u_h))]_h)\nabla u_h : \nabla(\nu^i(u_h(z))\varphi_z)\mathrm{d}x \\
&= \sum_{z\in\mathcal{N}_h} \sum_{i=k+1}^{n} \int_M \eta_h \bullet [\nu_i(u_h))]_h\nabla u_h : \nabla(\nu^i(u_h(z))\varphi_z)\mathrm{d}x \\
&\quad + \sum_{z\in\mathcal{N}_h} \sum_{i=k+1}^{n} \int_M \eta_h(z) \bullet (\nu_i(u_h(z)) - [\nu_i(u_h))]_h)\nabla u_h : \nabla(\nu^i(u_h(z))\varphi_z)\mathrm{d}x \\
&\quad + \sum_{z\in\mathcal{N}_h} \sum_{i=k+1}^{n} \int_M (\eta_h(z) - \eta_h) \bullet [\nu_i(u_h))]_h\nabla u_h : \nabla(\nu^i(u_h(z))\varphi_z)\mathrm{d}x.
\end{aligned}$$

We incorporate the definition of Ψ_h

$$\begin{aligned}
(\nabla u_h, \nabla \eta_h^{nor}) &= \sum_{z\in\mathcal{N}_h} \sum_{i=k+1}^{n} \int_M \eta_h \bullet [\nu_i(u_h)]_h\nabla u_h : \nu^i(u_h(z)) \otimes \nabla\varphi_z\mathrm{d}x \\
&\quad - \sum_{z\in\mathcal{N}_h} \sum_{i=k+1}^{n} \int_M \eta_h \bullet \nu_i(u_h(z))\nabla u_h : [\nu_i(u_h)]_h \otimes \nabla\varphi_z\mathrm{d}x \\
&\quad - \Psi_h(\eta_h).
\end{aligned}$$

Next we recover the antisymmetric matrix Ω_h

$$\begin{aligned}
(\Omega_h \bullet \nabla u_h, \eta_h) &= \sum_{i=k+1}^{n} \sum_{m,\ell=1}^{n} \int_M \eta_h^m\, \Omega_h^{m\ell} \bullet \nabla u_h^\ell \,\mathrm{d}x \\
&= \sum_{i=k+1}^{n} \sum_{m,\ell=1}^{n} \int_M \eta_h^m \Big([\nu^i(u_h)]_{h,m}\nabla[\nu^i(u_h)]_{h,\ell} - [\nu^i(u_h)]_{h,\ell}\nabla[\nu^i(u_h)]_{h,m}\Big) \bullet \nabla u_h^\ell \,\mathrm{d}x \\
&= \sum_{i=k+1}^{n} \sum_{m,\ell=1}^{n} \sum_{z\in\mathcal{N}_h} \int_M \eta_h^m \Big([\nu^i(u_h)]_{h,m}\nu^i(u_h(z))_\ell \otimes \nabla\varphi_z \\
&\qquad\qquad - [\nu^i(u_h)]_{h,\ell}\nu^i(u_h(z))_m \otimes \nabla\varphi_z\Big) \bullet \nabla u_h^\ell \,\mathrm{d}x \\
&= \sum_{z\in\mathcal{N}_h} \sum_{i=k+1}^{n} \int_M \eta_h \bullet \Big([\nu_i(u_h)]_h\nabla u_h : \nu^i(u_h(z)) \otimes \nabla\varphi_z \\
&\qquad\qquad - \nu_i(u_h(z))\nabla u_h : [\nu_i(u_h)]_h \otimes \nabla\varphi_z\Big)\mathrm{d}x \\
&= (\nabla u_h, \nabla \eta_h^{nor}) + \Psi_h(\eta_h).
\end{aligned}$$

Combining this with (3.1.4) we deduce

$$\begin{aligned}(\operatorname{div} p_h, \eta_h) + (\Omega_h \bullet \nabla u_h, \eta_h) &= (\operatorname{div} p_h, \eta_h) + (\nabla u_h, \nabla \eta_h^{nor}) + \Psi_h(\eta_h)\\ &= (\nabla u_h - p_h, \nabla \eta_h^{nor}) + \Psi_h(\eta_h)\end{aligned}$$

□

The next three lemmas show that Ψ_h converges to a sum of Dirac measures and prove that the sequence of antisymmetric matrices $(\Omega_h)_h$ converges to Ω given in (3.1.3), provided that N is of class C^3. After recovering the second fundamental form in the limit matrix we deduce, that weak accumulation points of discrete harmonic pairs are harmonic.

Lemma 3.1.8 *Let $(A_h)_{h>0} \subset L^\infty(M;\mathbb{R}^{n\times n}) \cap W^{1,2}$ satisfy $||A_h||_{L^\infty} + ||A_h||_{W^{1,2}} \leq C_0$ and let $(u_h)_{h>0} \subset W^{1,2}(M;\mathbb{R}^n)$ satisfy $u_h \in \mathcal{A}(\mathcal{T}_h)$ for all $h > 0$ and $||\nabla u_h||_{L^2} \leq C_0$. We extend Ψ_h to a functional on $C(M;\mathbb{R}^n)$ through $\eta \mapsto \Psi_h(\mathcal{I}_h\eta)$. Then $(\Psi_h)_{h>0} \subset C(M;\mathbb{R}^n)^*$ is uniformly bounded and for $\eta \in C^1(M;\mathbb{R}^n)$ we have the estimate*

$$|\Psi_h([A_h^T\eta]_h)| \leq C'h||\nabla\eta||_{L^\infty} + C'' \sum_{z\in\mathcal{N}_h} \gamma_{h,z}^3 |\eta(z)|, \tag{3.1.5}$$

where for every $z \in \mathcal{N}_h$ we define

$$\gamma_{h,z} := \max\{||\nabla u_h||_{L^2(\omega_z)}, ||\nabla A_h||_{L^2(\omega_z)}\}.$$

*The constants $C' > 0$ and $C'' > 0$ depend on N, C_0, an inverse estimate and the geometry of $\mathcal{T}_h$. An application of the results from Appendix **??** shows that $(\Psi_h)_{h>0}$ converges to a sum of Dirac measures as $h \to 0$.*

Proof. We start with the uniform bound for $(\Psi_h)_{h>0}$. Using (1.5.1) we see that

$$\nabla u_h : \nu^i(u_h(z)) \otimes \nabla\varphi_z = \sum_{j=1}^{2} \partial_{x_j} u_h \bullet \nu^i(u_h(z))\partial_j\varphi_z \leq C_N|\nabla u_h|^2.$$

Moreover, since $\sum_{z\in\mathcal{N}_h} \nabla\varphi_z = 0$ we have for $\eta_h := \mathcal{I}_h\eta$ that

$$\sum_{z\in\mathcal{N}_h}\sum_{i=k+1}^{n} \int_M \eta_h \bullet [\nu_i(u_h)]_h \nabla u_h : [\nu_i(u_h))]_h \otimes \nabla\varphi_z \mathrm{d}x = 0. \tag{3.1.6}$$

We add (3.1.6) to $\Psi(\eta_h)$ and obtain the uniform bound

$$\begin{aligned}|\Psi_h(\eta_h)| \leq \quad & 2C_N||\eta_h||_{L^\infty} \sum_{z\in\mathcal{N}_h} \int_{\omega_z} |\nabla u_h|^2 \mathrm{d}x\\ & + \sum_{z\in\mathcal{N}_h} \int_{\omega_z} |\eta_h(z)||[\nu^i(u_h)]_h - \nu^i(u_h(z))||\nabla u_h||\nabla\varphi_z| \mathrm{d}x,\\ \leq \quad & CC_N||\nabla u_h||_{L^2}^2||\eta||_{L^\infty}.\end{aligned}$$

We split Ψ_h into three terms $\Psi_h = \Theta_h^1 + \Theta_h^2 + \Theta_h^3$ and consider the first one

$$\begin{aligned}|\Theta_h^1([A_h^T\eta]_h)| &= \left| \sum_{z\in\mathcal{N}_{h_1}}\sum_{i=k+1}^{n} \int_M [A_h^T\eta]_h(z) \bullet (\nu_i(u_h(z)) - [\nu_i(u_h)]_h)\nabla u_h : \nabla(\nu^i(u_h(z))\varphi_z)\mathrm{d}x \right|\\ &\leq C \sum_{z\in\mathcal{N}_h} \left|[A_h^T\eta]_h(z)\right| h \int_{\omega_z} |\nabla u_h|^3 \,\mathrm{d}x\\ &\leq C \sum_{z\in\mathcal{N}_h} ||\nabla u_h||_{L^2(\omega_z)}^3 |\eta(z)|.\end{aligned}$$

Where we use the L^∞-bound on A_h, (1.5.1) and the estimate on $[\nu_i(u_h)]_h$ from Lemma 1.5.3. For Θ_h^2 we compute

$$\begin{aligned}
|\Theta_h^2([A_h^T\eta]_h)| &\leq C\sum_{z\in\mathcal{N}_h}||[A_h^T\eta]_h(z)-[A_h^T\eta]_h||_{L^2(\omega_z)}||\nabla u_h||_{L^\infty(\omega_z)}||\nabla u_h||_{L^2(\omega_z)}\\
&\leq C\sum_{z\in\mathcal{N}_h}h_z^2||\nabla u_h||_{L^\infty(\omega_z)}||\nabla u_h||_{L^2(\omega_z)}||A_h||_{L^\infty(\omega_z)}||\nabla\eta||_{L^\infty(\omega_z)}\\
&\quad + C\sum_{z\in\mathcal{N}_h}h_z||\nabla u_h||_{L^\infty(\omega_z)}||\nabla u_h||_{L^2(\omega_z)}||\nabla A_h||_{L^2(\omega_z)}|\eta(z)|\\
&\leq Ch||\nabla u_h||_{L^2}^2||A_h||_{L^\infty}||\nabla\eta||_{L^\infty}+C\sum_{z\in\mathcal{N}_h}||\nabla A_h||_{L^2(\omega_z)}||\nabla u_h||_{L^2(\omega_z)}^2|\eta(z)|.
\end{aligned}$$

Here, we incorporate (1.5.1) and

$$||[A_h^T\eta]_h(z)-[A_h^T\eta]_h||_{L^2(\omega_z)}\leq C_{\mathcal{T}_h}\Big(h_z^2||A_h||_{L^\infty}||\nabla\eta||_{L^\infty}+h_z||\nabla A_h||_{L^2(\omega_z)}|\eta(z)|\Big)$$

from Lemma 1.5.3. We replace η_h through $[A_h^T]_h$ in (3.1.6) and add it to Θ_h^3 to obtain

$$\begin{aligned}
\Theta_3^h([A_h^T\eta]_h) = &\quad -\sum_{z\in\mathcal{N}_h}\sum_{i=k+1}^n\int_M[A_h^T\eta]_h\bullet\nu_i(u_h(z))\nabla u_h:[\nu_i(u_h))]_h\otimes\nabla\varphi_z\mathrm{d}x\\
= &\quad \sum_{z\in\mathcal{N}_h}\sum_{i=k+1}^n\int_M[A_h^T\eta]_h\bullet([\nu_i(u_h)]_h-\nu_i(u_h(z)))\nabla u_h:[\nu_i(u_h))]_h\otimes\nabla\varphi_z\mathrm{d}x\\
= &\quad \sum_{z\in\mathcal{N}_h}\sum_{i=k+1}^n\int_{\omega_z}\Big([A_h^T\eta]_h-[A_h^T\eta]_h(z)\Big)\bullet\Big(\nu_i(u_h(z))-[\nu_i(u_h)]_h\Big)\nabla u_h:[\nu_i(u_h)]_h\otimes\nabla\varphi_z\mathrm{d}x\\
&+\sum_{z\in\mathcal{N}_h}\sum_{i=k+1}^n\int_{\omega_z}[A_h^T\eta]_h(z)\bullet\Big(\nu_i(u_h(z))-[\nu_i(u_h)]_h\Big)\nabla u_h:[\nu_i(u_h)]_h\otimes\nabla\varphi_z\mathrm{d}x\\
= &\quad \sum_{z\in\mathcal{N}_h}\sum_{i=k+1}^n\int_{\omega_z}\Big([A_h^T\eta]_h-[A_h^T\eta]_h(z)\Big)\bullet\Big(\nu_i(u_h(z))-[\nu_i(u_h)]_h\Big)\nabla u_h:[\nu_i(u_h)]_h\otimes\nabla\varphi_z\mathrm{d}x\\
&+\sum_{z\in\mathcal{N}_h}\sum_{i=k+1}^n\int_{\omega_z}[A_h^T\eta]_h(z)\bullet\Big(\nu_i(u_h(z))-[\nu_i(u_h)]_h\Big)\nabla u_h:\Big([\nu_i(u_h)]_h-\nu_i(u_h(z))\Big)\otimes\nabla\varphi_z\mathrm{d}x\\
&+\sum_{z\in\mathcal{N}_h}\sum_{i=k+1}^n\int_{\omega_z}[A_h^T\eta]_h(z)\bullet\Big(\nu_i(u_h(z))-[\nu_i(u_h)]_h\Big)\nabla u_h:\nu_i(u_h(z))\otimes\nabla\varphi_z\mathrm{d}x.
\end{aligned}$$

We deduce by the same estimates as for Θ_h^1 and Θ_h^2 that

$$|\Theta_3^h([A_h^T\eta]_h)|\leq Ch||\nabla u_h||_{L^2}^2||A_h||_{L^\infty}||\nabla\eta||_{L^\infty}+C\sum_{z\in\mathcal{N}_h}||\nabla A_h||_{L^2(\omega_z)}||\nabla u_h||_{L^2(\omega_z)}^2|\eta(z)|.$$

Finally we combine the estimates on Θ_h^1,Θ_h^2 and Θ_h^3

$$\begin{aligned}
|\Psi_h([A_h^T\eta]_h)| &\leq |\Theta_1^h([A_h^T\eta]_h)|+|\Theta_2^h([A_h^T\eta]_h)|+|\Theta_3^h([A_h^T\eta]_h)|\\
&\leq C'h||\nabla\eta||_{L^\infty}+C''\sum_{z\in\mathcal{N}_h}\gamma_{h,z}^3|\eta(z)|.
\end{aligned}$$

□

Lemma 3.1.9 *Let $N\subset\mathbb{R}^n$ be a submanifold of class C^3, $(u_h)_{h>0}\subset W^{1,2}(M;\mathbb{R}^n)$ satisfy $u_h\in\mathcal{A}(\mathcal{T}_h)$ and $||\nabla u_h||_{L^2}\leq C_0$ for all $h>0$, and let $(\Omega_h)_{h>0}\subset L^2(M;so(n)\otimes\mathbb{R}^2)$ be defined as in*

Lemma 3.1.7. Then there exists a (not relabeled) subsequence $(\Omega_h)_{h>0}$ such that $\Omega_h \rightharpoonup \Omega$ in L^2, where $\Omega \in L^2(M; so(n) \otimes \mathbb{R}^2)$ is locally given by

$$\Omega^{m\ell} = \sum_{i=k+1}^{n} \nu_m^i(u)\nabla(\nu_\ell^i(u)) - \nu_\ell^i(u)\nabla(\nu_m^i(u)).$$

Proof. There exists a (not relabeled) subsequence $(u_h)_h$ that converges weakly in $W^{1,2}$ to some $u \in W^{1,2}(M;\mathbb{R}^n)$ and $u \in N$ almost everywhere. Then, by Rellich's compact embedding $W^{1,2}(M;\mathbb{R}^n) \hookrightarrow L^2(M;\mathbb{R}^n)$ we have that $u_h \to u$ in L^2 and again by taking a subsequence we deduce that $u_h \to u$ almost everywhere. We need to find a L^2-bound for $\nabla[\nu^i(u_h)]_h$, since this implies that $(\Omega_h)_h \subset L^2(M; so(n) \otimes \mathbb{R}^2)$ is uniformly bounded. The vector field ν^i is C^2 regular so that the Taylor series yields for $x \in \omega_z$ and $z \in \mathcal{N}_h$

$$\begin{aligned}\nu^i(\pi_N(u_h(x))) = &\quad \nu^i(u_h(z)) + (\pi_N(u_h(x)) - u_h(z))^T\nabla\nu^i(u_h(z)) + o(|\pi_N(u_h(x)) - u_h(z)|^2)\\ = &\quad \nu^i(u_h(z)) + (\pi_N(u_h(x)) - u_h(z))^T\nabla\nu^i(u_h(z)) + o(h_z^2|\nabla u_h(x)|^2).\end{aligned}$$

We estimate

$$\begin{aligned}\left|\nabla[\nu^i(u_h)]_h\right|^2 = &\quad \left|\sum_{z\in\mathcal{N}_h} \nu^i(u_h(z))\nabla\varphi_z\right|^2\\ = &\quad \left|\sum_{z\in\mathcal{N}_h} (\nu^i(u_h(z)) - \nu^i(\pi_N(u_h(x))))\nabla\varphi_z\right|^2\\ \le &\quad \left|\sum_{z\in\mathcal{N}_h} (u_h(x) - u_h(z))^T\nabla\nu^i(u_h(z))\nabla\varphi_z\right|^2 + \sum_{z\in\mathcal{N}_h} o(h_z^4|\nabla u_h(x)|^4)|\nabla\varphi_z|^2\\ \le &\quad C_{N,\mathcal{T}_h}|\nabla u_h(x)|^2 + o(h^2|\nabla u_h(x)|^4)\end{aligned}$$

Integrating both sides of the inequality yields

$$||\nabla[\nu^i(u_h)]_h||_{L^2}^2 \le C_{N,\mathcal{T}_h}(||\nabla u_h||_{L^2}^2 + ||\nabla u_h||_{L^2}^4).$$

The uniform bound on $(\Omega_h)_h$ yields the existence of a (not relabeled) subsequence and $\Omega \in L^2(M; so(n)\otimes \mathbb{R}^2)$ such that $\Omega_h \rightharpoonup \Omega$ in L^2. We show that

$$[\nu^i(u_h)]_{k,h}\nabla[\nu^i(u_h)]_{h,\ell} \to \nu_k^i(u)\nabla(\nu_\ell^i(u)) \quad \text{for} \quad h \to 0,$$

in the sense of distribution and recover Ω as claimed. For $g \in C_c^\infty(M;\mathbb{R}^n)$ such that $\pi_N(u_h(\operatorname{supp} g)) \subset U_j$ for some $j \in \{1,\dots,K\}$, where $(U_1,\dots,U_K)$ is the finite subcover on which we have a local moving frame. We compute

$$\begin{aligned}\int_M [\nu^i(u_h)]_{\ell,h}\nabla[\nu^i(u_h)]_{m,h} \bullet g\mathrm{d}x = &-\int_M \Big([\nu^i(u_h)]_{\ell,h} - \nu_\ell^i(u)\Big)\nabla[\nu^i(u_h)]_{m,h} \bullet g\mathrm{d}x\\ &+ \int_M \nu_\ell^i(u)\nabla[\nu^i(u_h)]_{m,h} \bullet g\mathrm{d}x.\end{aligned}$$

The convergence of $[\nu^i(u_h)]_{\ell,h} \to \nu_\ell^i(u)$ in L^2 can be established with Lemma 3.1.10. Together with the boundedness of $(\nabla[\nu^i(u_h)]_h)_{h>0}$ in L^2 we see that the first summand vanishes for $h \to 0$. For the second summand we have

$$\begin{aligned}\int_M \nu_\ell^i(u)\nabla[\nu^i(u_h)]_{m,h} \bullet g\mathrm{d}x = &-\int_M [\nu^i(u_h)]_{m,h}\mathrm{div}(\nu_\ell^i(u)g)\mathrm{d}x\\ &\to -\int_M \nu_m^i(u)\mathrm{div}(\nu_\ell^i(u)g)\mathrm{d}x = \int_M \nu_\ell^i(u)\nabla\nu_m^i(u) \bullet g\mathrm{d}x.\end{aligned}$$

Again, we use the convergence $[\nu^i(u_h)]_{m,h} \to \nu_m^i(u)$ in L^2 which we establish in Lemma 3.1.10. □

Lemma 3.1.10 *Let $F \in W^{1,\infty}(\mathbb{R}^n;\mathbb{R})$ and $(u_h)_{h>0} \subset [\mathcal{S}^1(\mathcal{T}_h)]^n$ such that $u_h \rightharpoonup u$ in $W^{1,2}(M;\mathbb{R}^n)$. For*

$$[F(u_h)]_h := \sum_{z\in\mathcal{N}_h} F(u_h(z))\varphi_z$$

there exists a (not relabeled) subsequence satisfying $[F(u_h)]_h \to F(u)$ in L^2 for $h \to 0$.

Proof. We have $|[F(u_h)]_h - F(u)| \le |[F(u_h)]_h - F(u_h)| + |F(u_h) - F(u)| \le |[F(u_h)]_h - F(u_h)| + ||F||_{W^{1,\infty}}|u_h - u|$. It suffices to show $|[F(u_h)]_h - F(u_h)| \to 0$ in L^2 since the convergence of the second summand follows by the pointwise convergence of a subsequence of $(u_h)_{h>0}$. We use $\sum_{z\in\mathcal{N}_h}\varphi_z = 1$ and compute pointwise

$$\begin{aligned} |[F(u_h)]_h - F(u_h)|^2 = &\quad |\sum_{z\in\mathcal{N}_h}(F(u_h(z)) - F(u_h))\varphi_z|^2 \\ \le &\quad \sum_{z\in\mathcal{N}_h}|(F(u_h(z)) - F(u_h))|^2|\varphi_z|^2 \\ \le &\quad ||F||^2_{W^{1,\infty}}\sum_{z\in\mathcal{N}_h}|u_h(z) - u_h|^2|\varphi_z|^2, \end{aligned}$$

and conclude

$$\begin{aligned} \int_M |[F(u_h)]_h - F(u_h)|^2\,\mathrm{d}x \le &\quad C||F||^2_{W^{1,\infty}}\sum_{z\in\mathcal{N}_h}\int_{\omega_z}|u_h - u_h(z)|^2|\varphi_z|^2\mathrm{d}x \\ \le &\quad C||F||^2_{W^{1,\infty}}\sum_{z\in\mathcal{N}_h}h_z^2||\nabla u_h||^2_{L^2(\omega_z)} \\ \le &\quad Ch^2||F||^2_{W^{1,\infty}}||\nabla u_h||^2_{L^2} \to 0 \end{aligned}$$

for $h \to 0$. □

We are finally able to prove the convergence result for discrete harmonic pairs. To emphasize the necessity of two meshes for the different variables we state Theorem 3.1.11 with triangulations $\mathcal{T}_{h_1}, \mathcal{T}_{h_2}$.

Theorem 3.1.11 *Let $M \subset \mathbb{R}^2$ be a polygonal Lipschitz domain and $\mathcal{T}_{h_1}, \mathcal{T}_{h_2}$ be two sequences of quasiuniform triangulations of M with mesh-sizes $h_2 = o(h_1)$. Suppose that (BC) holds and that $u_{D,h_1}(z) \in N$ for all $z \in \mathcal{N}_{h_1} \cap \partial M$. Let $(p_{h_2}, u_{h_1}) \subset H(\mathrm{div};\mathbb{R}^{n\times 2}) \times W^{1,2}(M;\mathbb{R}^n)$ be a sequence of discrete harmonic pairs that satisfy*

$$||p_{h_2}||_{H(\mathrm{div})} + ||u_{h_1}||_{W^{1,2}} \le C_0.$$

Then every weak accumulation point of $(p_{h_2}, u_{h_1})_{h_1,2}$ satisfies $p = \nabla u$ and $u \in W^{1,2}(M;\mathbb{R}^n)$ is a harmonic map into N subject to the boundary conditions $u|_{\partial M} = u_D$.

Proof. From Lemma 3.1.7 we know that $(p_{h_2}, u_{h_1}) \in [V^{h_2}_{mini}]^{n\times 2} \times \mathcal{A}(\mathcal{T}_{h_1})$ solves the system

$$\begin{aligned} (p_{h_2};\sigma_{h_2}) + (\mathrm{div}\,\sigma_{h_2}, u_{h_1}) &= \int_{\partial M} u_{D,h_1}\sigma_{h_2}\bullet\nu_{\partial M}\,\mathrm{d}x, \\ (\mathrm{div}\,p_{h_2}, \eta_{h_1}) + (\Omega_{h_{1,2}}\bullet\nabla u_{h_1}, \eta_{h_1}) &= (\nabla u_{h_1} - p_{h_2}, \nabla\eta^{nor}_{h_1}) + \Psi_{h_{1,2}}(\eta_{h_1}), \end{aligned}$$

for all $(\sigma_{h_2}, v_{h_1}) \in [V^{h_2}_{mini}]^{n\times 2} \times [\mathcal{S}^1_0(\mathcal{T}_{h_1})]^n$. The proof of convergence is mainly the same as in Theorem 2.2.1, except that we need to show that the right-hand side of the second equation converges to a sum of Dirac measures when we test with $[A^T_{h_{1,2}}\eta]_{h_1}$, where $\eta \in C^\infty_0(M;\mathbb{R}^n)$ and $(A_{h_{1,2}})_{h_{1,2}} \subset L^\infty(M;\mathbb{R}^{n\times n}) \cap W^{1,2}$ is the sequence of matrices provided by Theorem 2.1.3. This is stated in Lemma 3.1.8 and with the results from Lemma 3.1.9 we conclude that every weak limit $u \in W^{1,2}(M;\mathbb{R}^n)$ of the sequence $(u_{h_1})_{h_1}$ solves

$$-\Delta u^\ell = \sum_{m=1}^n \Omega^{\ell m}\bullet\nabla u^m = \sum_{i=k+1}^n\sum_{m=1}^n \Big(\nu^i_\ell(u)\nabla(\nu^i_m(u)) - \nu^i_m(u)\nabla(\nu^i_\ell(u))\Big)\bullet\nabla u^m$$

for $\ell = 1,\dots,n$ and is therefore harmonic. □

3.2. A compactness result for the P^1-method

In this section we give a new proof for the compactness result of harmonic maps with the P^1-method introduced in [13].

Definition 3.2.1 *A vector field $u_h \in [\mathcal{S}^1(\mathcal{T}_h)]^n$ is called a discrete harmonic map into N subject to the boundary data $u_{D,h}$ if and only if $u_h(z) = u_{D,h}(z)$ for all $z \in \mathcal{N}_h \cap \partial M$, $u_h(z) \in N$ for all $z \in \mathcal{N}_h$ and u_h is stationary for*

$$v_h \mapsto \frac{1}{2}\int_M |\nabla v_h|^2 \, dx$$

among all $v_h \in [\mathcal{S}^1(\mathcal{T}_h)]^n$ such that $v_h(z) = u_{D,h}(z)$ for all $z \in \mathcal{N}_h \cap \partial M$ and $v_h(z) \in N$ for all $z \in \mathcal{N}_h$.

As for the mixed formulation we can recover the antisymmetric structure in the Lagrangian multipliers.

Lemma 3.2.2 *Let $u_h \in \mathcal{A}(\mathcal{T}_h)$ be a discrete harmonic map. Introduce $\Omega_h \in L^2(M; so(n) \otimes \mathbb{R}^2)$ as*

$$\Omega_h^{m\ell} := \sum_{i=k+1}^{n} [\nu^i(u_h)]_{h,m} \nabla [\nu^i(u_h)]_{h,\ell} - [\nu^i(u_h)]_{h,\ell} \nabla [\nu^i(u_h)]_{h,m},$$

where $[\nu^i(u_h)]_{h,m} \in \mathcal{S}^1(\mathcal{T}_h)$ denotes the m-th component of $[\nu^i(u_h)]_h \in [\mathcal{S}^1(\mathcal{T}_h)]^n$. Furthermore, we define the functional $\Psi_h : [\mathcal{S}^1(\mathcal{T}_h)]^n \to \mathbb{R}$

$$\begin{aligned}
\Psi_h(\eta_h) := &- \sum_{z \in \mathcal{N}_{h_1}} \sum_{i=k+1}^{n} \int_M \eta_h(z) \bullet (\nu_i(u_h(z)) - [\nu_i(u_h)]_h) \nabla u_h : \nabla(\nu^i(u_h(z))\varphi_z) dx \\
&- \sum_{z \in \mathcal{N}_h} \sum_{i=k+1}^{n} \int_M (\eta_h(z) - \eta_h) \bullet [\nu_i(u_h)]_h \nabla u_h : \nabla(\nu^i(u_h(z))\varphi_z) dx \\
&- \sum_{z \in \mathcal{N}_h} \sum_{i=k+1}^{n} \int_M \eta_h \bullet \nu_i(u_h(z)) \nabla u_h : [\nu_i(u_h))]_h \otimes \nabla \varphi_z \, dx.
\end{aligned}$$

Then

$$(\nabla u_h, \nabla \eta_h) + (\Omega_h \bullet \nabla u_h, \eta_h) = \Psi_h(\eta_h)$$

for all $\eta_h \in [\mathcal{S}^1(\mathcal{T}_h)]^n$.

Proof. An analog computation to the one in Proposition 3.1.5 shows that $u_h \in [\mathcal{S}^1(\mathcal{T}_h)]^n$ is a discrete harmonic map, subject to the boundary conditions $u_h|_{\partial M} = u_{D,h}$ if and only if, $u_h(z) \in N$ for all $z \in \mathcal{N}_h$, $u_h(z) = u_{D,h}(z)$ for all $z \in \mathcal{N}_h \cap \partial M$ and u_h solves

$$(\nabla u_h, \nabla v_h) = 0,$$

for all $v_h \in \mathcal{F}[u_h]$. Thus, we compute for arbitrary $\eta_h \in [\mathcal{S}^1(\mathcal{T}_h)]^n$ as in the proof of Lemma 3.1.7

$$\begin{aligned}
(\nabla u_h, \nabla v_h) = &\quad (\nabla u_h, \nabla(\eta_h^{nor} + \eta_h^{tan})) \\
= &\quad (\nabla u_h, \nabla \eta_h^{nor}) \\
= &\quad \sum_{z \in \mathcal{N}_h} (\nabla u_h, \eta_h^{nor}(z) \otimes \nabla \varphi_z) \\
= &\sum_{z \in \mathcal{N}_h} \sum_{i=k+1}^{n} (\nabla u_h, \nu_i(u_h(z)) \bullet \eta_h(z) \nu_i(u_h(z)) \otimes \nabla \varphi_z) \\
= &-(\Omega_h \bullet \nabla u_h, \eta_h) + \Psi_h(\eta_h).
\end{aligned}$$

□

By Lemma 3.1.8 and Lemma 3.1.9 we know that Ψ_h converges to a sum of Dirac measures and that Ω_h converges locally to the second fundamental form. We are, therefore, able to state the convergence proof for the P^1 method.

Theorem 3.2.3 *Let M be a polygonal Lipschitz domain and $(\mathcal{T}_h)_h$ be a sequence of quasiuniform triangulations of M. Let $\theta > 0$ and $u_h \in [\mathcal{S}^1(\mathcal{T}_h)]^n$ be such that*

$$||\nabla u_h||_{L^{2+\theta}} \leq C_0,$$

where the constant $C_0 > 0$ is independent of the mesh-size $h > 0$. If in addition $u_h(z) = u_{D,h}(z)$ for all $z \in \mathcal{N}_h$ for $u_{D,h}$ from Assumption (BC) and

$$(\nabla u_h, \nabla v_h) = 0$$

for all $v_h \in [\mathcal{S}^1_0(\mathcal{T}_h)]^n$ satisfying $v_h(z) \in T_{u_h(z)}N$ for all $z \in \mathcal{N}_h$, then every weak accumulation point of the sequence $(u_h)_h$ is a harmonic map into N.

Proof. We know that u_h solves

$$(\nabla u_h; \nabla v_h) - (\Omega_h \bullet \nabla u_h, v_h) + \Psi_h(v_h) = 0,$$

and the error term Ψ_h causes no problems if we test the equation with $[A_h^T \eta]_h$. Then $||\Omega_h||_{L^{2+\theta}} \leq C$ if $||\nabla u_h||_{L^{2+\theta}} \leq C$ and we can apply Theorem 2.3.1. □

3.3. Iterative algorithm for harmonic pairs

Our method of choice to find discrete harmonic maps is a H^1-gradient flow in the u-variable, that is, we are looking for $(p, u) : (0, \infty) \times M \to \mathbb{R}^{n\times 2} \times N$ such that $(p(0, \cdot), u(0, \cdot)) = (p_0, u_0)$ and

$$\begin{aligned} (p\,;\,\sigma) \,+\, (\operatorname{div}\sigma, u) \quad &= \quad \int_{\partial M} u_D\, \sigma \bullet \nu_{\partial M}\, \mathrm{d}x \\ (\operatorname{div} p, \xi) \,-\, (\nabla \partial_t u\,;\, \nabla\xi) \quad &= \quad 0, \end{aligned}$$

for almost every $t \in (0, \infty)$, all $\sigma \in H(\operatorname{div}; \mathbb{R}^{n\times 2})$ and all $\xi \in L^2(M; \mathbb{R}^n)$ such that $\xi(x) \in T_{u(t,x)}N$ for almost every $(t, x) \in (0, \infty) \times M$.

Fully-discrete H^1-flow. *Input:* Triangulation $\mathcal{T}_h$ of M, stopping criterion $\varepsilon > 0$, time-step size $\tau > 0$ and $(p_h^0, u_h^0) \in [V^h_{mini}]^{n\times 2} \times \mathcal{A}(\mathcal{T}_h)$ such that $u_h^0(z) = u_{D,h}(z)$ for all $z \in \mathcal{N}_h \cap \partial M$. Set $i = 0$.

1. Compute $(\mu_h^i, w_h^i) \in [V^h_{mini}]^{n\times 2} \times \mathcal{F}[u_h^i]$ such that

$$\begin{aligned} \tau(\mu_h^i; \sigma_h) \,+\, \tau(\operatorname{div}\sigma_h, w_h^i) \quad &= \quad -\,(p_h^i; \sigma_h) + (\sigma_h, \nabla u_h^i) \\ \tau(\operatorname{div}\mu_h^i, \xi_h) \,-\, (\nabla w_h^i; \nabla\xi_h) \quad &= \quad -\,(\operatorname{div} p_h^i; \xi_h), \end{aligned}$$

   for all $\sigma_h \in [V^h_{mini}]^{n\times 2}$ and all $\xi_h \in \mathcal{F}[u_h^i]$.

2. Stop if $||\nabla w_h^i||_{L^2(M)} + ||\mu_h^i||_{L^2(M)} < \varepsilon$.

3. Set

$$p_h^{i+1} := p_h^i + \tau\mu_h^i,$$

   and

$$u_h^{i+1}(z) := \pi_N(u_h^i(z) + \tau w_h^i(z)),$$

   for all $z \in \mathcal{N}_h$.

4. Set $i = i + 1$ and go to (1).

Output: $(p_h^*, u_h^*) := (p_h^i, u_h^i)$.

Remark 3.3.1 *Since* $w_h^i(z) = 0$ *for all* $z \in \mathcal{N}_h \cap \partial M$ *it holds* $\int_{\partial M} u_{D,h}\sigma_h \bullet \nu dx = \int_{\partial M} u^i\, \sigma_h \bullet \nu dx$ *for all* $\sigma_h \in [V_{mini}^h]^{n\times 2}$ *and all* $i \in \mathbb{N}$. *Hence we compute*

$$-(\operatorname{div}\sigma_h, u_h^*) + \int_{\partial M} u_{D,h}\,\sigma_h \bullet \nu_{\partial M}\, dx = (\sigma_h; \nabla u_h^*),$$

and see that the boundary values are incorporated in the right hand-side of the first equation in step (1).

Remark 3.3.2 *Our scheme includes a projection in every iterative step. In a semi-discrete version, this was first used in [1] for the computation of stable configurations in the theory of liquid crystals. A fully discrete scheme due to the ideas in [1] was introduced in [11]. A finite element method for the p-harmonic flow into spheres using a projection step was developed and analyzed in [8]. A profound discussion of different gradient flow approaches and Newton iteration methods for the computation of stationary points of the Dirichlet energy can be found in [12].*

Lemma 3.3.3 *1. Let* $(p_h, u_h) \in [V_{mini}^h]^{n\times 2} \times \mathcal{A}(\mathcal{T}_h)$, *define* $\ell_1(\sigma_h) := (\nabla u_h - p_h; \sigma_h)$ *and* $\ell_2(\xi_h) := -(\operatorname{div} p_h, \xi_h)$. *Then there exists a unique solution* $(\mu_h, w_h) \in [V_{mini}^h]^{n\times 2} \times \mathcal{F}[u_h]$ *of*

$$\begin{aligned} \tau(\mu_h;\sigma_h) \;+\; \tau(\operatorname{div}\sigma_h, w_h) &= \ell_1(\sigma_h) \\ \tau(\operatorname{div}\mu_h, \xi_h) \;-\; (\nabla w_h; \nabla\xi_h) &= \ell_2(\xi_h), \end{aligned}$$

for all $(\sigma_h, \xi_h) \in [V_{mini}^h]^{n\times 2} \times \mathcal{F}[u_h]$.

2. Let $C_0 := ||\nabla u_h||_{L^2} + ||p_h||_{L^2}$, *then the following estimates hold for* (μ_h, w_h)

$$\begin{aligned} ||\mu_h||_{L^2}^2 &\le C_0^2\Big(2/\tau^2 + 1/(2\tau)\Big) \\ ||\nabla w_h||_{L^2}^2 &\le C_0^2\Big(1 + 1/\tau\Big) \end{aligned}$$

3. Let $C_{inv} > 0$ *be the constant from the inverse estimate* $||w_h||_{L^\infty} \le C_{inv}\log h_{min}^{-1}||\nabla w_h||_{L^2}$, *where* $h_{min} = \min\limits_{T\in\mathcal{T}_h} \operatorname{diam} T$. *Then the function* w_h *satisfies*

$$||w_h||_{L^\infty} \le CC_{inv}C_0 \log h_{min}^{-1}\sqrt{1 + 1/(2\tau)}.$$

For $\tau > 0$ *small enough the projection* $\pi_N(u_h(z) + \tau w_h(z))$ *is then well defined for all* $z \in \mathcal{N}_h$.

Remark 3.3.4 *Note that* $h_{min} = h_{1,min}$, *that is, we only need the inverse estimate on the coarser space* $[\mathcal{S}^1(\mathcal{T}_{h_1})]^n$.

Proof. (i) The functions (μ_h, w_h) are solutions of the following saddle-point problem:

Compute $(\mu_h, w_h, \lambda_h) \in [V_{mini}^h]^{n\times 2} \times [\mathcal{S}_0^1(\mathcal{T}_h)]^n \times [\mathcal{S}_0^1(\mathcal{T}_{h_1})]^{n-k}$ *such that*

$$\tau(\mu_h, \sigma_h) + \tau(\operatorname{div}\sigma_h, w_h) = \ell_1(\sigma_h), \tag{3.3.1}$$

$$\tau(\operatorname{div}\mu_h, \xi_h) - (\nabla w_h, \nabla\xi_h) + \sum_{i=k+1}^{n} (\lambda_h^i, [\nu^i(u_h)]_h \bullet \xi_h)_h = \ell_2(\xi_h), \tag{3.3.2}$$

$$\sum_{i=k+1}^{n} (\rho_h^i, [\nu^i(u_h)]_h \bullet w_h)_h = 0, \tag{3.3.3}$$

for all $(\sigma_h, \xi_h, \rho_h) \in [V_{mini}^h]^{n\times 2} \times [\mathcal{S}_0^1(\mathcal{T}_h)]^n \times [\mathcal{S}_0^1(\mathcal{T}_{h_1})]^{n-k}$. We define the bilinear forms

$$
\begin{aligned}
a:\ [V^h_{mini}]^{n\times 2} \times [V^h_{mini}]^{n\times 2} &\to \mathbb{R}, \quad (p_h,\sigma_h)\mapsto (p_h\,;\,\sigma_h),\\
b:\ [V^h_{mini}]^{n\times 2} \times [\mathcal{S}^1_0(\mathcal{T}_h)]^n &\to \mathbb{R}, \quad (\sigma_h,u_h)\mapsto (\operatorname{div}\sigma_h,u_h),\\
c:\ [\mathcal{S}^1_0(\mathcal{T}_h)]^n \times [\mathcal{S}^1_0(\mathcal{T}_h)]^n &\to \mathbb{R}, \quad (u_h,v_h)\mapsto (\nabla u_h\,;\,\nabla v_h).\\
d:\ [\mathcal{S}^1_0(\mathcal{T}_h)]^n \times [\mathcal{S}^1_0(\mathcal{T}_h)]^{n-k} &\to \mathbb{R}, \quad (u_h,\rho_h)\mapsto \sum_{i=k+1}^{n}(\rho^i_h,[\nu^i(u_h)]_h\bullet u_h)_h,
\end{aligned}
$$

so that the above system (3.3.1)-(3.3.3) is of the form

$$
\begin{bmatrix} A & B^T & 0\\ B & -C & D^T\\ 0 & D & 0\end{bmatrix}\begin{bmatrix} v_1\\ v_2\\ v_3\end{bmatrix}=\begin{bmatrix} l_1\\ l_2\\ l_3\end{bmatrix},
$$

where we use a coordinate representation as in Theorem 3.1.6 to define the matrices A, B, C and D. We first show the invertibility of $\begin{bmatrix} -C & D^T\\ D & 0\end{bmatrix}$. For $\rho_h\in[\mathcal{S}^1_0(\mathcal{T}_h)]^{n-k}$ we define $v^*_h\in[\mathcal{S}^1_0(\mathcal{T}_h)]^n$ through $v^*_h(z)=\sum\limits_{i=k+1}^{n}\nu^i(u_h(z))\rho^i_h(z)$ for all $z\in\mathcal{N}_h$. It follows

$$
\begin{aligned}
\sup_{v_h\in[\mathcal{S}^1_0(\mathcal{T}_h)]^n\setminus\{0\}}\frac{1}{||v_h||_{L^2(M)}}\sum_{i=k+1}^{n}(\rho^i_h,[\nu^i(u_h)]_h\bullet v_h)_h &\geq \frac{1}{||v^*_h||_{L^2(M)}}\sum_{i=k+1}^{n}(\rho^i_h,[\nu^i(u_h)]_h\bullet v^*_h)_h\\
&=\frac{1}{||v^*_h||_{L^2(M)}}\sum_{i=k+1}^{n}||\rho^i_h||^2_h\\
&\geq \beta||\rho_h||_{L^2(M)},
\end{aligned}
$$

where $\beta>0$ only depends on $\dim N=k$. Taking the infimum over all ρ_h on both sides leads to the inf-sup condition for D. For the regularity of the whole matrix we show that its kernel is trivial. Suppose that

$$
\begin{bmatrix} A & B^T & 0\\ B & -C & D^T\\ 0 & D & 0\end{bmatrix}\begin{bmatrix} v_1\\ v_2\\ v_3\end{bmatrix}=0,
$$

then it follows that $Av_1+B^Tv_2=0$, $Bv_1-Cv_2+D^Tv_3=0$ and $Dv_2=0$. Multiplying the three equations with v_1, v_2 and v_3 we get

$$
\begin{array}{lllll}
v_1^TAv_1 & + & v_1^TB^Ttv_2 & & = 0\\
v_2^TBv_1 & - & v_2^TCv_2 & + & v_2^TD^Tv_3 = 0\\
 & & v_3^TDv_2 & & = 0.
\end{array}
$$

This leads to $v_1^TAv_1+v_2^TCv_2=0$. Since A and C are positive definite matrices we have $v_1=v_2=0$. Together with the regularity of $\begin{bmatrix} -C & D^T\\ D & 0\end{bmatrix}$ we obtain $v_3=0$.

(ii) We test the system with (μ_h,w_h) and subtract the two equations to arrive at

$$
\tau||\mu_h||^2_{L^2}+||\nabla w_h||^2_{L^2}\leq||\nabla u_h-p_h||_{L^2}||\mu_h||_{L^2}+||p_h||_{L^2}||\nabla w_h||_{L^2}.
$$

To get an estimate for μ_h we use the following inequalities

$$
||\nabla u_h-p_h||_{L^2}||\mu_h||_{L^2}\leq\frac{1}{2\tau}||\nabla u_h-p_h||^2_{L^2}+\frac{\tau}{2}||\mu_h||^2_{L^2}\leq C_0^2/\tau+\tau/2||\mu_h||^2_{L^2},
$$

$$
||p_h||_{L^2}||\nabla w_h||_{L^2}\leq\frac{1}{4}||p_h||^2_{L^2}+||\nabla w_h||^2_{L^2},
$$

and obtain

$$
\tau/2||\mu_h||^2_{L^2}\leq C_0^2(1/\tau+1/4).
$$

The estimate for w_h follows by other weights in Young's inequality and the same procedure.
(iii) We use an inverse inequality for w_h

$$||w_h||_{L^\infty} \leq C_{inv} \log h_{min}^{-1} ||\nabla w_h||_{L^2},$$

and get by the results in (ii)

$$||w_h||_{L^\infty(M)} \leq C C_{inv} C_0 \log h_{min}^{-1} \sqrt{1 + 1/(2\tau)}.$$

Hence, for $\tau > 0$ small enough, such that $C C_0 \log h_{min}^{-1} \sqrt{\tau^2 + \tau/2} \leq \omega_N$, the projection of $u_h(z) + \tau w_h(z)$ onto N is well defined for all $z \in \mathcal{N}_h$. □

Lemma 3.3.5 *In addition to the above assumptions, suppose that N is a C^3 submanifold. There exists a constant $C > 0$ such that for $\tau \leq \frac{h_{min}}{C C_0} < 1$ and $\widetilde{C} := C C_0 \tau h_{min}^{-1} < 1$, we have for the sequence $(p_h^i, u_h^i)_{i=0,\dots,J}$, $J \in \mathbb{N}$, computed through the discrete H^1-flow, the following inequality*

$$\frac{\tau^2}{2} \sum_{i=0}^{J} ||\mu_h^i||_{L^2}^2 + (1 - \widetilde{C})\tau \sum_{i=0}^{J} ||\nabla w_h^i||_{L^2}^2 + \frac{1}{2}||p_h^{J+1}||_{L^2}^2 \leq \frac{1}{2}||p_h^0||_{L^2}^2,$$

where C_0 depends on $||p_h^0||_{L^2}$ and $||\nabla u_h^0||_{L^2}$.

Proof. Since π_N is a C^2 map we obtain for every $z \in \mathcal{N}_h$ the identity

$$u_h^{i+1}(z) = u_h^i(z) + \tau w_h^i(z) + \mathcal{O}(|\tau w_h^i(z)|^2).$$

Set $r_h^{i+1} := u_h^{i+1} - u_h^i - \tau w_h^i$ and obtain the estimates

$$||r_h^{i+1}||_{L^2(M)}^2 \leq ||r_h^{i+1}||_{L^4(M)}^4, \qquad ||\nabla r_h^{i+1}||_{L^2(M)}^2 \leq C\tau^4 h_{min}^{-2} ||\nabla w_h^i||_{L^2(M)}^4.$$

Testing the H^1-flow with (μ_h^i, w_h^i) and summing up the two equations we arrive at

$$(p_h^{i+1}, \mu_h^i) + ||\nabla w_h^i||_{L^2} + \{(p_h^{i+1}, \nabla w_h^i) - (\mu_h^i, \nabla(u_h^i + \tau w_h^i)\} = 0.$$

We investigate the last summand

$$\begin{aligned}
(\mu_h^i, \nabla(u_h^i + \tau w_h^i)) &= \frac{1}{\tau}[(p_h^{i+1}, \nabla(u_h^{i+1} - r_h^{i+1})) - ((p_h^i, \nabla(u_h^i + \tau w_h^i))] \\
&= \frac{1}{\tau}[(p_h^{i+1}, \nabla(u_h^{i+1} - r_h^{i+1})) - ((p_h^{i+1}, p_h^i)] \\
&= \frac{1}{\tau}[(p_h^{i+1}, \nabla(u_h^{i+1} - r_h^{i+1})) - ((p_h^{i+1}, \nabla(u_h^i - r_h^i))] \\
&= \frac{1}{\tau}[(p_h^{i+1}, \nabla(u_h^{i+1} - u_h^i - r_h^{i+1})) + (p_h^{i+1}, \nabla r_h^i)] \\
&= (p_h^{i+1}, \nabla w_h^i) + \frac{1}{\tau}(p_h^{i+1}, \nabla r_h^i),
\end{aligned}$$

and get

$$(p_h^{i+1}, \mu_h^i) + ||\nabla w_h^i||_{L^2} + \frac{1}{\tau}(p_h^{i+1}, \nabla r_h^i) = 0.$$

We estimate

$$\begin{aligned}
\frac{1}{\tau}(p_h^{i+1}, \nabla r_h^i) &= \frac{1}{\tau}(p_h^i, \nabla r_h^i) + (\mu_h^i, \nabla r_h^i) \\
&\leq C\tau^2 h_{min}^{-1} ||\nabla w_h^{i-1}||_{L^2}^2 \left(\frac{C_0}{\tau} + \frac{C_0\sqrt{1 + \tau/2}}{\tau} \right) \\
&\leq C C_0 \tau h_{min}^{-1} ||\nabla w_h^{i-1}||_{L^2}^2.
\end{aligned}$$

Using the binomial identity $b(b-a) = (b-a)^2/2 + (b^2-a^2)/2$ we get

$$\frac{\tau}{2}||\mu_h^i||_{L^2}^2 + ||\nabla w_h^i||_{L^2}^2 - CC_0\tau h_{min}^{-1}||\nabla w_h^{i-1}||_{L^2}^2 + \frac{1}{2\tau}(||p_h^{i+1}||_{L^2}^2 - ||p_h^i||_{L^2}^2) \leq 0. \tag{3.3.4}$$

For $\tau < \frac{h_{min}}{CC_0}$ we obtain after summation over $i = 0, \dots, J$ and setting $\widetilde{C} := CC_0\tau h_{min}^{-1} < 1$

$$\frac{\tau^2}{2}\sum_{i=0}^{J}||\mu_h^i||_{L^2}^2 + (1-\widetilde{C})\tau\sum_{i=0}^{J}||\nabla w_h^i||_{L^2}^2 + \frac{1}{2}||p_h^{J+1}||_{L^2}^2 \leq \frac{1}{2}||p_h^0||_{L^2}^2,$$

where we set $w_h^i := 0$ for $i < 0$. From (3.3.4) we see

$$||p_h^{i+1}||_{L^2}^2 + \widetilde{C}||\nabla w_h^i||_{L^2}^2 \leq ||p_h^i||_{L^2}^2 + \widetilde{C}||\nabla w_h^{i-1}||_{L^2}^2,$$

an inductive argument shows $||p_h^i||_{L^2}^2 \leq ||p_h^0||_{L^2}^2 \leq C_0^2$ for $i = 0, \dots, J$. We set $\sigma_h = \sum_T \nabla(u_h^i + \tau w_h^i)|_T b_T$ and deduce

$$(\sigma_h, \nabla(u_h^i + \tau w_h^i)) = \sum_T \int_T |\nabla(u_h^i + \tau w_h^i)|_T|^2 b_T \,\mathrm{d} = \sum_T \frac{|T|}{60}|\nabla(u_h^i + \tau w_h^i)|_T|^2 = \frac{1}{60}||\nabla(u_h^i + \tau w_h^i)||_{L^2}^2,$$

as well as

$$\begin{aligned}||\sigma_h||_{L^2}^2 = \sum_T \int_T |\sigma_h|_T|^2 |b_T|^2 \,\mathrm{d}x &= \sum_T |\nabla(u_h^i + \tau w_h^i)|_T|^2 \int_T |b_T|^2 \,\mathrm{d}x \\ &= \sum_T \frac{|T|}{2520}|\nabla(u_h^i + \tau w_h^i)|_T|^2 = \frac{1}{2520}||\nabla(u_h^i + \tau w_h^i)||_{L^2}^2.\end{aligned}$$

Therefore

$$||\nabla(u_h^i + \tau w_h^i)||_{L^2}^2 = 60(\sigma_h, \nabla(u_h^i + \tau w_h^i)) = 60(\sigma_h, p_h^{i+1}) \leq \frac{60}{\sqrt{2520}}||p_h^{i+1}||_{L^2}||\nabla(u_h^i + \tau w_h^i)||_{L^2}.$$

Combining this with $||\nabla u_h^{i+1}||_{L^2} \leq C_N||\nabla(u_h^i + \tau w_h^i)||_{L^2}$ results in

$$||\nabla u_h^{i+1}||_{L^2} \leq \tilde{C}_N||p_h^{i+1}||_{L^2},$$

where $\tilde{C}_N = \frac{60}{\sqrt{2520}}C_N$. This shows that $\tilde{C}_N^{-1}||\nabla u_h^{i+1}||_{L^2} + ||p_h^{i+1}||_{L^2} \leq C_0$ if $\tilde{C}_N^{-1}||\nabla u_h^i||_{L^2} + ||p_h^i||_{L^2} \leq C_0$ and justifies the above assumption on the bounds of $||\nabla u_h^i||_{L^2}$ and $||p_h^i||_{L^2}$. □

The following Theorem is an adaption of Theorem 3.2.7 from [13] to the mixed formulation. We only state the result, the proof is straightforward.

Theorem 3.3.6 *Suppose that the conditions of Lemma 3.3.5 are satisfied. Then our Algorithm terminates within a finite number of iterations and the output $(p_h^*, u_h^*) \in [V_{mini}^h]^{n\times 2} \times \mathcal{A}(\mathcal{T}_h)$ satisfies $u_h^*(z) = u_{D,h}(z)$ for all $z \in \mathcal{N}_h \cap \partial M$, and*

$$\begin{aligned}(p_h^*; \sigma_h) + (\operatorname{div}\sigma_h, u_h^*) &= \int_{\partial M} u_{D,h}\sigma_h \bullet \nu_{\partial M}\, dx + \mathcal{R}es_h^1(\sigma_h) \\ (\operatorname{div} p_h^*, v_h) &= \mathcal{R}es_h^2(v_h),\end{aligned}$$

for all $(\sigma_h, v_h) \in [V_{mini}^h]^{n\times 2} \times \mathcal{F}[u_h^*]$, where the linear functionals $\mathcal{R}es_h^1$ and $\mathcal{R}es_h^2$ satisfy

$$\mathcal{R}es_h^1(\sigma_h) + \mathcal{R}es_h^2(v_h) \leq \varepsilon(||\sigma_h||_{L^2} + ||\nabla v_h||_{L^2})$$

for all $(\sigma_h, v_h) \in [V_{mini}^h]^{n\times 2} \times \mathcal{F}[u_h^*]$. For a sequence $\varepsilon_J \to 0$ as $J \to \infty$, every accumulation point of the corresponding sequence of outputs $(p_h^{*,J}, u_h^{*,J})_{J\in\mathbb{N}}$ is a discrete harmonic map into N subject to the boundary data $u_{D,h}$.

3.4. Iterative algorithm for the P^1-method

We quickly recall the definition of the H^1-flow for the P^1-method proposed in **??**. We are looking for $u : (0,\infty) \times M \to N$ such that $u(0,\cdot) = u^0$ and

$$(\nabla \partial_t u_h, \nabla v_h) + (\nabla u_h; \nabla v_h) = 0$$

for almost every $t \in (0,\infty)$, and all $v \in W_0^{1,2}(M;\mathbb{R}^n)$ such that $v(x) \in T_{u(t,x)}N$ for almost every $(t,x) \in (0,\infty) \times M$ and $u^0|_{\partial M} = u_D$. The discrete H^1-flow then reads

Fully-discrete H^1-flow. *Input:* Triangulation $\mathcal{T}_h$ of M, stopping criterion $\varepsilon > 0$, time-step size $\tau > 0$ and $u_h^0 \in \mathcal{A}(\mathcal{T}_h)$ such that $u_h^0(z) = u_{D,h}(z)$ for all $z \in \mathcal{N}_h \cap \partial M$. Set $i = 0$.

1. Compute $w_h^i \in \mathcal{F}[u_h^i]$ such that

   $$(\nabla w_h^i, \nabla v_h) + (\nabla u_h^i; \nabla v_h) = 0,$$

   for all $v_h \in \mathcal{F}[u_h^i]$.
2. Stop if $||\nabla w_h^i||_{L^2(M)} < \varepsilon$.
3. Set

   $$u_h^{i+1}(z) := \pi_N(u_h^i(z) + \tau w_h^i(z)),$$

   for all $z \in \mathcal{N}_h$.
4. Set $i = i + 1$ and go to (1).

Output: $u_h^* := u_h^i$.

Remark 3.4.1 *(i) A stability proof for this algorithm can be achieved by the same methods as for the mixed method, see [13] for details.*
(ii) In [12] there are more schemes for the computation of discrete harmonic maps such as the L^2 flow or a coupling of a Newton-iteration and the H^1-flow.

3.5. Necessity of the projection step

In this section we discuss the necessity of the projection step in the H^1-flow. For the numerical realization we may suppose that N is given by the intersection of zero level sets of functions $f^{k+1}, \dots, f^n : \mathbb{R}^n \to \mathbb{R}$,

$$N := \{p \in \mathbb{R}^n : f^{k+1}(p) = \cdots = f^n(p) = 0\}.$$

Then, the normal space at $p \in N$ is given by

$$N_pN = \operatorname{span}\left\{ \frac{\nabla f^{k+1}(p)}{|\nabla f^{k+1}(p)|}, \dots, \frac{\nabla f^n(p)}{|\nabla f^n(p)|} \right\} =: \operatorname{span}\left\{\nu^{k+1}(p), \dots, \nu^n(p)\right\}.$$

Furthermore, we assume that f^m is defined on the whole $\mathbb{R}^n$ and $\nabla f^m \neq 0$ in a δ_N-neighborhood of N for $m = k+1, \dots, n$. In every step of the proposed numerical scheme we compute $(\mu_h^i, w_h^i) \in [V_{mini}^h]^{n\times 2} \times \mathcal{F}[u_h^i]$ satisfying

$$\begin{aligned} \tau(\mu_h^i; \sigma_h) \,+\, \tau(\operatorname{div} \sigma_h, w_h^i) \quad &= \quad -\,(p_h^i; \sigma_h) + (\sigma_h, \nabla u_h^i), \\ \tau(\operatorname{div} \mu_h^i, \xi_h) \,-\, (\nabla w_h^i; \nabla \xi_h) \quad &= \quad -\,(\operatorname{div} p_h^i; \xi_h), \end{aligned}$$

for all $\sigma_h \in [V_{mini}^h]^{n\times 2}$ and all $\xi_h \in \mathcal{F}[u_h^i]$. Then, a projection step is carried out

$$u_h^{i+1}(z) := \pi_N(u_h^i(z) + \tau w_h^i(z)),$$

for all $z \in \mathcal{N}_h$. The question is, can we bound the distance of the output $u_h^* \in [\mathcal{S}^1(\mathcal{T}_h)]^n$ to the submanifold N if we omit the projection step and update by $u_h^{i+1} := u_h^i + \tau w_h^i$? In [14] this question was answered in the affirmative for $N = \{\Phi = (\Phi_1, \Phi_2) \in \mathbb{R}^{3\times 2} : \Phi_1 \bullet \Phi_2 = 0 \text{ and } |\Phi_1| = |\Phi_2| = 1\}$. The subset $N \subset \mathbb{R}^{3\times 2}$ is used to describe isometries $u : \mathbb{R}^2 \to \mathbb{R}^3$ that satisfy $\partial_x u \bullet \partial_y u = 0$ and $|\partial_x u| = |\partial_y u| = 1$. A penalty term $t^{-2}||\Phi_h - \nabla u_h||$ is added to the energy and $\Phi_h \in [V_{mini}^h]^{3\times 2}$ satisfies the constraint $\Phi_h(z) \in N$ for all $z \in \mathcal{N}_h$. In every step of the gradient-flow the correction $\mathrm{d}_t\Phi_h^i \in [\mathcal{S}^1(\mathcal{T}_h)]^{3\times 2}$ is computed subject to the constraints

$$\mathrm{d}_t\Phi_{h,1}^i(z) \bullet \Phi_{h,2}^i(z) + \Phi_{h,1}^i(z) \bullet \mathrm{d}_t\Phi_{h,2}^i(z) = 0$$

and

$$\mathrm{d}_t\Phi_{h,1}^i(z) \bullet \Phi_{h,1}^i(z) = 0, \quad \mathrm{d}_t\Phi_{h,2}^i(z) \bullet \Phi_{h,2}^i(z) = 0,$$

for all $z \in \mathcal{N}_h$. An easy computation shows that

$$||\mathcal{I}_h[|\Phi_{h,1}^J|^2 - 1]||_{L^1} + ||\mathcal{I}_h[|\Phi_{h,2}^J|^2 - 1]||_{L^1} + ||\mathcal{I}_h[\Phi_{h,1}^J \bullet \Phi_{h,2}^J]||_{L^1} \leq C\tau^2 \sum_{i=1}^{J} ||\nabla \mathrm{d}_t\Phi_h^i||_{L^2}^2.$$

In light of the usual energy law $\tau \sum_{i=1}^J ||\nabla \mathrm{d}_t\Phi_h^i||_{L^2}^2 \leq CE(\Phi_h^0)$ this yields

$$||\mathcal{I}_h[|\Phi_{h,1}^J|^2 - 1]||_{L^1} + ||\mathcal{I}_h[|\Phi_{h,2}^J|^2 - 1]||_{L^1} + ||\mathcal{I}_h[\Phi_{h,1}^J \bullet \Phi_{h,2}^J]||_{L^1} \leq C\tau E(\Phi_h^0).$$

The same procedure can be applied to the general case if the above assumptions on the submanifold N hold true. We formulate the H^1-flow without projection step, state the now simplified stability result for the scheme and bound the disctance of the iterates from the manifold N.

Projectionless discrete H^1-flow. *Input:* Triangulation $\mathcal{T}_h$ of M, stopping criterion $\varepsilon > 0$, time-step size $\tau > 0$ and $(p_h^0, u_h^0) \in [V_{mini}^h]^{n\times 2} \times \mathcal{A}(\mathcal{T}_h)$ such that $u_h^0(z) = u_{D,h}(z)$ for all $z \in \mathcal{N}_h \cap \partial M$ and $u_0(z) \in N$ for all $z \in \mathcal{N}_h$. Set $i = 0$.

1. Compute $(\mu_h^i, w_h^i) \in [V_{mini}^h]^{n\times 2} \times [\mathcal{S}_0^1(\mathcal{T}_h)]^n$ such that $w_h^i(z) \bullet \nabla f^m(u_h^i(z)) = 0$ for all $z \in \mathcal{N}_h$ and all $m = k+1, \dots, n$, and satisfying

$$\begin{aligned} \tau(\mu_h^i; \sigma_h) \; + \; \tau(\operatorname{div} \sigma_h, w_h^i) \quad &= \quad -(p_h^i; \sigma_h) + (\sigma_h, \nabla u_h^i), \\ \tau(\operatorname{div} \mu_h^i, \xi_h) \; - \; (\nabla w_h^i; \nabla \xi_h) \quad &= \quad -(\operatorname{div} p_h^i; \xi_h), \end{aligned}$$

   for all $\sigma_h \in [V_{mini}^h]^{n\times 2}$ and all $\xi_h[\mathcal{S}_0^1(\mathcal{T}_h)]^n$ such that $\xi_h(z) \bullet \nabla f^m(u_h^i(z)) = 0$ for all $z \in \mathcal{N}_h$ and all $m = k+1, \dots, n$.

2. Stop if $||\nabla w_{h_1}^i||_{L^2(M)} + ||\mu_{h_2}^i||_{L^2(M)} < \varepsilon$.

3. Set $p_h^{i+1} := p_h^i + \tau\mu_h^i$ and $u_h^{i+1} := u_h^i + \tau w_h^i$.

4. Set $i = i + 1$ and go to (1).

Output: $(p_h^*, u_h^*) := (p_h^i, u_h^i)$.

Theorem 3.5.1 *Let $N \subset \mathbb{R}^n$ be a C^2 submanifold given by level set functions $f^{k+1}, \dots, f^n : \mathbb{R}^n \to \mathbb{R}$ that satisfy $\nabla f^m \neq 0$ in a δ_N-neighborhood of N for some $\delta_N > 0$ and $m = k+1 \dots, n$. Then, there exists a constant $C' > 0$ such that the sequence of iterates $(p_h^i, u_h^i)_{0\leq i\leq J}$, $J \in \mathbb{N}$, computed in step (1) of our numerical scheme satisfies*

$$\tau^2 \sum_{i=0}^{J-1} ||\mu_h^i||_{L^2}^2 + 2\tau \sum_{i=0}^{J-1} ||\nabla w_h^i||_{L^2}^2 + ||p_h^J||_{L^2}^2 = ||p_h^0||_{L^2}^2, \tag{3.5.1}$$

and if $u_h^0(z) \in N$ for all $z \in \mathcal{N}_h$, then

$$\sum_{m=k+1}^{n} ||\mathcal{I}_h[f^m(u_h^J)]||_{L^1} \leq C'\tau ||p_h^0||_{L^2}^2.$$

Proof. (i) We test with (μ_h^i, w_h^i) and obtain

$$(p_h^{i+1}, \mu_h^i) + ||\nabla w_h^i||_{L^2}^2 + \{(p_h^{i+1}, \nabla w_h^i) - (\mu_h^i, \nabla(u_h^i + \tau w_h^i))\} = 0.$$

We investigate the last summand

$$\begin{aligned}
(\mu_h^i, \nabla(u_h^i + \tau w_h^i)) &= (\mu_h^i, \nabla u_h^{i+1}) \\
&= \frac{1}{\tau}[(p_h^{i+1}, \nabla u_h^{i+1}) - (p_h^i, \nabla u_h^{i+1})] \\
&= \frac{1}{\tau}[(p_h^{i+1}, \nabla u_h^{i+1}) - (p_h^{i+1}, p_h^i)] \\
&= \frac{1}{\tau}[(p_h^{i+1}, \nabla u_h^{i+1}) - (p_h^{i+1}, \nabla u_h^i)] \\
&= \frac{1}{\tau}(p_h^{i+1}, \nabla u_h^{i+1} - u_h^i) \\
&= (p_h^{i+1}, \nabla w_h^i),
\end{aligned}$$

and get by the binomial identity $b(b-a) = (b-a)^2/2 + (b^2 - a^2)/2$ the local energy equality

$$\frac{\tau}{2}||\mu_h^i||_{L^2}^2 + \frac{1}{2\tau}\Big(||p_h^{i+1}||_{L^2}^2 - ||p_h^i||_{L^2}^2\Big) + ||\nabla w_h^i||_{L^2}^2 = 0.$$

Summing over $i = 0, \dots, J-1$ yields

$$\tau^2 \sum_{i=0}^{J-1} ||\mu_h^i||_{L^2}^2 + 2\tau \sum_{i=0}^{J-1} ||\nabla w_h^i||_{L^2}^2 + ||p_h^J||_{L^2}^2 = ||p_h^0||_{L^2}^2.$$

Note that $||p_h^i||_{L^2} \le ||p_h^0||_{L^2} \le C_0$ and $||\nabla u_h^i||_{L^2} \le C||p_h^i||_{L^2} \le CC_0$ for $i = 0, \dots, J$.
(ii) With the mass $\beta_z := \int_M \varphi_z \, \mathrm{d}x$ of a nodal basis function φ_z and points $\xi_z^m \in M$ for $m = k+1, \dots, n$ and $z \in \mathcal{N}_h$ we compute

$$\begin{aligned}
\sum_{m=k+1}^{n} ||\mathcal{I}_h[f^m(u_h^J)]||_{L^1} &= \sum_{m=k+1}^{n} \sum_{z \in \mathcal{N}_h} \beta_z |f^m(u_h^J(z))| \\
&= \sum_{m=k+1}^{n} \sum_{z \in \mathcal{N}_h} \beta_z \left| f^m(u_h^{J-1}(z)) + (u_h^J(z) - u_h^{J-1}(z))^T D^2 f^m(\xi_z^m)(u_h^J(z) - u_h^{J-1}(z)) \right| \\
&\le \sum_{m=k+1}^{n} \sum_{z \in \mathcal{N}_h} \beta_z \left(|f^m(u_h^{J-1}(z))| + C_{f^m} |u_h^J(z) - u_h^{J-1}(z)|^2 \right)
\end{aligned}$$

Where we use the constraint on w_h^J

$$(u_h^J(z) - u_h^{J-1}(z)) \bullet \nabla f^m(u_h^{J-1}(z)) = \tau w_h^J(z) \bullet \nabla f^m(u_h^{J-1}(z)) = 0.$$

An inductive argument shows that

$$\begin{aligned}
\sum_{m=k+1}^{n} ||\mathcal{I}_h[f^m(u_h^J)]||_{L^1} &\le C_N \sum_{j=1}^{J} \sum_{z \in \mathcal{N}_h} \beta_z |u_h^j(z) - u_h^{j-1}(z)|^2 \\
&\le CC_P C_N \tau^2 \sum_{j=1}^{J} ||\nabla w_h^j||_{L^2}^2 \\
&\le C' \tau ||p_h^0||_{L^2}^2,
\end{aligned}$$

where we used the fact that $\sum_z \beta_z |v_h(z)|^2 \le C||v_h||_{L^2}$ for $\mathcal{S}^1$-functions, the Poincaré estimate for $w_h^j \in [\mathcal{S}_0^1(\mathcal{T}_h)]^n$, for $j = 1, \dots, J$ and the energy estimate (3.5.1), which we proved in (i). □

Remark 3.5.2 *(i) The bound on the distance shows that* $\operatorname{dist}(u_h^i, N) \leq \delta_N$ *if* $\tau > 0$ *is small enough. This implies that* $\nabla f^m(u_h^i(z)) \neq 0$ *for* $z \in \mathcal{N}_h$ *and* $m = k+1, \ldots, n$*. Therefore, the pointwise constraint on* w_h^i *is well-defined for* $i = 0, \ldots, J$*.*
(ii) Note that we only need that N *is of class* C^2 *and not* C^3 *as in the stability proof of the* H^1*-flow with projection step.*

Chapter 4.

Surfaces of prescribed mean curvature

We start this section by introducing a special 2-form that leads to the equation for surfaces of prescribed mean curvature $H \in L^\infty$, namely

$$-\Delta u = 2H(u)\partial_x u \times \partial_y u. \tag{4.0.1}$$

Hereafter we present a discretization of (4.0.1) in mixed form suiting the convergence proof from Chapter 2. We end this section with an iterative algorithm to compute discrete parametrizations.

4.1. The volume functional

Consider $B_1(0) \subset \mathbb{R}^2$, $Q \in W^{1,\infty}(\mathbb{R}^3;\mathbb{R}^3)$ and $H := \frac{1}{3}\operatorname{tr} DQ \in L^\infty(\mathbb{R}^3;\mathbb{R})$. For functions $u \in L^\infty(B_1(0);\mathbb{R}^3) \cap W^{1,2}$ we define the volume functional

$$V(u) := \frac{2}{3}\int_{B_1(0)} Q(u) \bullet (\partial_x u \times \partial_y u)\mathrm{d}x.$$

If $Q(u) = H_0 u$, for $H_0 \in \mathbb{R}$, the integral is a multiple of the algebraic volume of the cone from the origin to the graph of u as we show now for piecewise affine functions. Let $z_0 = (0,0)$, $z_1 = (h,0)$, $z_2 = (0,h)$, $T = \operatorname{conv}\{(0,0),(0,h),(h,0)\}$ and $u_h \in [\mathcal{S}^1(T)]^3$. We compute

$$\partial_x u_h = h^{-1}(u_h(z_1) - u_h(z_0)), \quad \partial_y u_h = h^{-1}(u_h(z_2) - u_h(z_0))$$

and

$$\partial_x u_h \times \partial_y u_h = h^{-2}(u_h(z_1) - u_h(z_0)) \times (u_h(z_2) - u_h(z_0)) = \frac{2|u_h(T)|}{h^2}\nu_{u_h(T)} = \frac{|u_h(T)|}{|T|}\nu_{u_h(T)}.$$

Finally we set $\mathrm{m}_T = \frac{1}{3}(z_0 + z_1 + z_2)$ and conclude

$$\begin{aligned}\frac{1}{3}\int_T H_0 u_h \bullet \partial_x u_h \times \partial_y u_h \mathrm{d}x &= \frac{H_0}{3}\frac{|u_h(T)|}{|T|}\int_T u_h \bullet \nu_{u_h(T)}\mathrm{d}x \\ &= \frac{H_0}{3}\frac{|u_h(T)|}{|T|}|T|u_h(\mathrm{m}_T) \bullet \nu_{u_h(T)} = \frac{H_0}{3}|u_h(T)|h_{u_h(T)},\end{aligned}$$

where $h_{u_h(T)}$ denotes the height of the pyramid with base $u_h(T)$ and top $0 \in \mathbb{R}^3$. The last expression is H_0 times the volume of the pyramid and terminates our motivation. The next lemma provides the first variation of V both in the continuous case and for piecewise affine functions.

Lemma 4.1.1 *Let $B := B_1(0) \subset \mathbb{R}^2$ be the unit disk, B_h a polygonal approximation of B and $\mathcal{T}_h$ a quasiuniform triangulation of B_h. Let $u \in W^{1,2}(B,\mathbb{R}^3)$ and $Q \in W^{1,\infty}(\mathbb{R}^3,\mathbb{R}^3)$. For the volume functional $V : W^{1,2}(B,\mathbb{R}^3) \to \mathbb{R}$, defined through*

$$u \mapsto \frac{2}{3}\int_B Q(u) \bullet (\partial_x u \times \partial_y u)\,dx.$$

we have for $v \in W_0^{1,2}(B;\mathbb{R}^3)$ that

$$\frac{d}{d\varepsilon}\Big|_{\varepsilon=0} V(u+\varepsilon v) = 2\int_B H(u)v \bullet (\partial_x u \times \partial_y u)\,dx.$$

The same formula holds if we replave u, v and B by $u_h \in [\mathcal{S}^1(\mathcal{T}_h)]^3$, $v_h \in [\mathcal{S}^1_0(\mathcal{T}_h)]^3$ and B_h. Moreover let $u_h, \tilde{u}_h \in [\mathcal{S}^1(\mathcal{T}_h)]^3$ be such that $u_h(z) = \tilde{u}_h(z)$ for all $z \in \mathcal{N}_h \cap \partial B_h$ and set $w_h := \tau^{-1}(\tilde{u}_h - u_h) \in [\mathcal{S}^1_0(\mathcal{T}_h)]^3$. If $Q \in W^{2,\infty}(\mathbb{R}^3, \mathbb{R}^3)$ then

$$V(\tilde{u}_h) - V(u_h) - 2\tau(H(u_h)\partial_x u_h \times \partial_y u_h, w_h) \leq C\tau^2 \left(1 + \log h_{min}^{-1}\Big(||\nabla u_h|| + \log h_{min}^{-1}||\nabla u_h||^2\Big)\right) ||\nabla w_h||^2,$$

where $C > 0$ depends on $||Q||_{W^{2,\infty}}$ and C_{inv}.

Proof. (i) For the variation of the volume functional in the continuous case, see Lemma 1.2.11.
(ii) For the affine functions we have to carry out the integration by parts to show that no jump terms occur across inner edges. We suppress the index h in the following calculation and obtain

$$\begin{aligned}
&\int_B Q_1(\partial_x v_2 \partial_y u_3 - \partial_x v_3 \partial_y u_2)\,\mathrm{d}x + \int_B Q_1(\partial_x u_2 \partial_y v_3 - \partial_x u_3 \partial_y v_2)\,\mathrm{d}x \\
&\qquad = \sum_{T \in \mathcal{T}_h} \int_T Q_1(\partial_x v_2 \partial_y u_3 - \partial_x v_3 \partial_y u_2)\,\mathrm{d}x + \int_T Q_1(\partial_x u_2 \partial_y v_3 - \partial_x u_3 \partial_y v_2)\,\mathrm{d}x \\
&\qquad = -\int_B \partial_x u \bullet DQ_1(v_2 \partial_y u_3 - v_3 \partial_y u_2)\mathrm{d}x - \int_B \partial_y u \bullet DQ_1(v_3 \partial_x u_2 - v_2 \partial_x u_3)\mathrm{d}x \\
&\qquad\quad + \sum_{T \in \mathcal{T}_h} \int_{\partial T} Q_1(u)\big(v_2(\nu_1 \partial_y u_3 - \nu_2 \partial_x u_3) + v_3(\nu_2 \partial_x u_2 - \nu_1 \partial_y u_3\big)\,\mathrm{d}s \\
&\qquad = -\int_B \partial_x u \bullet DQ_1(v_2 \partial_y u_3 - v_3 \partial_y u_2)\mathrm{d}x - \int_B \partial_y u \bullet DQ_1(v_3 \partial_x u_2 - v_2 \partial_x u_3)\mathrm{d}x \\
&\qquad\quad + \sum_{T \in \mathcal{T}_h} \int_{\partial T} Q_1(u)\big(v_2(\tau \bullet \nabla u_3) - v_3(\tau \bullet \nabla u_3)\big)\,\mathrm{d}s,
\end{aligned}$$

and the sum over all boundaries ∂T for $T \in \mathcal{T}_h$ vanishes since the tangential component of the gradient of any function in $\mathcal{S}^1(\mathcal{T}_h)$ is continuous. The rest of the variation can then be computed as in the first part of the proof of Lemma 1.2.11.
(iii) Again, we suppress the index h. We use a Taylor expansion of Q and an inverse estimate to obtain

$$(Q(\tilde{u}) - Q(u), \partial_x u \times \partial_y u) \leq \tau(DQw, \partial_x u \times \partial_y u) + C_Q C_{inv} \tau^2 (\log h_{min}^{-1})^2 ||\nabla w||^2 ||\nabla u||^2.$$

Now, we compute the estimate for the difference of the volumes

$$\begin{aligned}
V(\tilde{u}) - V(u) &\leq \tau(Q(u), \partial_x u \times \partial_y w) + \tau(Q(u), \partial_x w \times \partial_y u) + \tau(DQw, \partial_x u \times \partial_y u) \\
&\quad + \tau(Q(\tilde{u}) - Q(u), \partial_x \tilde{u} \times \partial_y w) + \tau(Q(\tilde{u}) - Q(u), \partial_x w \times \partial_y u) \\
&\quad + \tau^2(Q(u), \partial_x w \times \partial_y w) + C_Q C_{inv} \tau^2 (\log h_{min}^{-1})^2 ||\nabla w||^2 ||\nabla u||^2 \\
&\leq 2\tau(H(u)\partial_x u \times \partial_y u, w) + \tau(Q(\tilde{u}) - Q(u), \partial_x \tilde{u} \times \partial_y w) \\
&\quad + \tau(Q(\tilde{u}) - Q(u), \partial_x w \times \partial_y u) + C_Q \tau^2 (1 + C_{inv} (\log h_{min}^{-1})^2 ||\nabla u||^2) ||\nabla w||^2 \\
&\leq 2\tau(H(u)\partial_x u \times \partial_y u, w) + C_Q \tau^2 \left(1 + C_{inv} \log h_{min}^{-1}\Big(||\nabla u|| + \log h_{min}^{-1}||\nabla u||^2\Big)\right) ||\nabla w||^2.
\end{aligned}$$

□

4.2. A Compactness result for surfaces of prescribed mean curvature

Given a smooth, embedded and possibly knotted boundary curve $\Gamma \subset \mathbb{R}^3$, $u_D : \partial B_1(0) \to \mathbb{R}^3$ satisfying $u_D(\partial B_1(0)) = \Gamma$ and $H \in L^\infty(\mathbb{R}^3)$, we look for a parametrization $u : B_1(0) \to \mathbb{R}^3$ such that

$$-\Delta u + 2H(u)\partial_x u \times \partial_y u = 0 \text{ in } B_1(0), \tag{4.2.1}$$

$$u = u_D \text{ on } \partial B_1(0). \tag{4.2.2}$$

We present a mixed formulation and introduce a gradient flow based algorithm to find small solutions of the problem. Our numerical tests show the same experimental order of convergence as in [33]. Convergence of the discretization can be established using the antisymmetric structure of the nonlinearity in the equation. From Lemma 4.1.1 we know that the right energy for the mixed formulation is

$$\widetilde{E}^H(p,u) = \frac{1}{2}\int_B |p|^2 + \int_B \operatorname{div} p \bullet u \,\mathrm{d}x + \frac{2}{3}\int_B Q(u) \bullet (\partial_x u \times \partial_y u)\,\mathrm{d}x - \int_{\partial B} u_D p \bullet \nu_{\partial B}\,\mathrm{d}x,$$

where $H = \frac{1}{3}\operatorname{tr} DQ$. Before we define the discrete energy we note that we consider polygonal approximations B_h of the unit disk B and assume that $\chi_{B_h} \nearrow \chi_B$ almost everywhere in $\mathbb{R}^2$ as $h \to 0$, where χ_{B_h} denotes the characteristic function of the set B_h. Two sequences of quasiuniform triangulations $\mathcal{T}_{h_1}$ and $\mathcal{T}_{h_2}$ with $h_2 = o(h_1)$ and $h_2 \leq h_1$ are always such that $\cup_{\mathcal{T}_{h_2}} T_{h_2} = \cup_{\mathcal{T}_{h_1}} T_{h_1} = B_{h_1}$. Furthermore we recall that $P_0^{h_2} : [\mathcal{L}^0(\mathcal{T}_{h_1})]^{3\times 2} \to [V_{mini}^{h_2}]^{3\times 2}$ is the L^2-projection on $[V_{mini}^{h_2}]^{3\times 2}$. We state everything in the remaining section with the different indices h_1 and h_2 and start with an assumption on the boundary values.

Assumption (BC)'. We assume that there exists $u_{D,h_1} \in [\mathcal{S}^1(\mathcal{T}_{h_1})]^3$ such that for $\sigma_{h_2} := \mathcal{J}_{h_2}\sigma$ with $\sigma \in C^\infty(B, \mathbb{R}^{3\times 2})$ we have

$$\int_{\partial B_{h_1}} u_{D,h_1}\sigma_{h_2} \bullet \nu_{\partial B_{h_1}}\mathrm{d}x \quad \to \quad \int_{\partial B} u_D \sigma \bullet \nu_{\partial B}\mathrm{d}x \qquad \text{for} \quad h_1 \to 0.$$

Lemma 4.2.1 *We define the discrete energy* $\widetilde{E}^H_{h_{1,2}} : [V_{mini}^{h_2}]^{3\times 2} \times [\mathcal{S}^1(\mathcal{T}_{h_1})]^3 \to \mathbb{R}$

$$(p_{h_2}, u_{h_1}) \mapsto \frac{1}{2}\int_{B_{h_1}} |p_{h_2}|^2 + \int_{B_{h_1}} \operatorname{div} p_{h_2} \bullet u_{h_1}\, dx + \frac{2}{3}\int_{B_{h_1}} Q(u_{h_1}) \bullet (\partial_x u_{h_1} \times \partial_y u_{h_1})\, dx - \int_{\partial B_{h_1}} u_{D,h_1} p_{h_2} \bullet \nu_{\partial B}\, dx,$$

and introduce $\Omega_{h_1} \in L^2(B_{h_1}, so(3) \otimes \mathbb{R}^2)$ *as*

$$\Omega_{h_1} := H(u_{h_1}) \begin{bmatrix} 0 & \nabla^\perp u^3_{h_1} & -\nabla^\perp u^2_{h_1} \\ -\nabla^\perp u^3_{h_1} & 0 & \nabla^\perp u^1_{h_1} \\ \nabla^\perp u^2_{h_1} & -\nabla^\perp u^1_{h_1} & 0 \end{bmatrix}.$$

Then the Euler-Lagrange equation corresponding to $\widetilde{E}^H_{h_{1,2}}$ *are: Find* $(p_{h_2}, u_{h_1}) \in [V_{mini}^{h_2}]^{3\times 2} \times [\mathcal{S}^1(\mathcal{T}_{h_1})]^3$ *satisfying*

$$\begin{aligned} (p_{h_2}; \sigma_{h_2}) + (\operatorname{div} \sigma_{h_2}, u_{h_2}) \qquad &= \int_{\partial B_{h_1}} u_{D,h_1}\sigma_{h_2} \bullet \nu_{\partial B_{h_1}}\, dx \\ (\operatorname{div} p_{h_2}, v_{h_1}) - (\Omega_{h_1} \bullet \nabla u_{h_1}, v_{h_1}) &= 0 \end{aligned}$$

for all $(\sigma_{h_1}, v_{h_1}) \in [V_{mini}^{h_2}]^{3\times 2} \times [\mathcal{S}_0(\mathcal{T}_{h_1})]^3$.

Proof. For the variation of the volume functional see Lemma 4.1.1. □

Theorem 4.2.2 *Consider two sequences of quasiuniform triangulations* $(\mathcal{T}_{h_1})_{h_1}, (\mathcal{T}_{h_2})_{h_2}$ *of* B_{h_1} *with* $h_2 = o(h_1)$. *Suppose that (BC)' and let* $(p_{h_2}, u_{h_1}) \subset H(\operatorname{div}; \mathbb{R}^{3\times 2}) \times L^2(B, \mathbb{R}^3)$ *be a sequence of saddle points of* $\widetilde{E}^H_{h_{1,2}}$ *that satisfy*

$$||p_{h_2}||_{H(\operatorname{div})} + ||u_{h_1}||_{W^{1,2}} \leq C_0.$$

Then every weak accumulation of $(p_{h_2}, u_{h_1})_{h_{1,2}}$ *satisfies* $p = \nabla u$ *and* $u \in W^{1,2}(M; \mathbb{R}^n)$ *is a solution of (4.2.1)-(4.2.2).*

Proof. (i) We have that $(\Omega_{h_1})_{h_1>0} \subset L^2(B_1(0); so(3) \otimes \mathbb{R}^2)$ is uniformly bounded since $(u_{h_1})_{h_1>0} \subset W^{1,2}(B_1(0); \mathbb{R}^3)$ is bounded and $H \in L^\infty(\mathbb{R}^3)$. Together with the uniform bound on $(p_{h_2})_{h_2}$ we can

apply Theorem 2.2.1.
(ii) It holds $\Omega_{h_1} \rightharpoonup \Omega$ in L^2 as $h_1 \to 0$ and $\Omega \in L^2(B_1(0); so(3) \otimes \mathbb{R}^2)$ is given by

$$\Omega := H(u) \begin{bmatrix} 0 & \nabla^\perp u^3 & -\nabla^\perp u^2 \\ -\nabla^\perp u^3 & 0 & \nabla^\perp u^1 \\ \nabla^\perp u^2 & -\nabla^\perp u^1 & 0 \end{bmatrix},$$

since $\nabla u_{h_1} \rightharpoonup \nabla u$ in L^2 and $H(u_{h_1}) \to H(u)$ almost everywhere in $B_1(0)$ for $h_1 \to 0$. □

Remark 4.2.3 *Convergence can also be established via Wente's Lemma and the methods of compensated compactness. However the formulation with an antisymmetric matrix is used in [68] to show, that the assumption $H \in L^\infty(\mathbb{R}^3)$ is enough to ensure continuity of the solution u.*

4.2.4. Iterative algorithm for Surfaces of prescribed mean curvature

We propose a method to compute discrete surfaces with a prescribed mean curvature and given boundary data, motivated as in the harmonic mapping case by a H^1-gradient flow. For a better readability we state everything in one mesh-size.

Fully-discrete H^1-flow. *Input:* Triangulation $\mathcal{T}_h$ of B_h, stopping criterion $\varepsilon > 0$, time-step size $\tau > 0$ and $(p_h^0, u_h^0) \in [V_{mini}^h]^{3\times 2} \times [\mathcal{S}^1(\mathcal{T}_h)]^3$ satisfying $u_h^0(z) = u_{D,h}(z)$ for all $z \in \mathcal{N}_h \cap \partial B_h$. Set $i = 0$.

1. Compute $(\mu_h^i, w_h^i) \in [V_{mini}^h]^{3\times 2} \times [\mathcal{S}_0^1(\mathcal{T}_h)]^3$ such that

$$\begin{aligned} (p_h^i + \tau\mu_h^i; \sigma_h) + (\operatorname{div}\sigma_h, u_h^i + \tau w_h^i) &= \int_{\partial B_h} u_{D,h}\sigma_h \bullet \nu_{\partial B_h}\,\mathrm{d}x \\ (\operatorname{div} p_h^i + \tau\mu_h^i, v_h) - (\nabla w_h^i, \nabla v_h) &= 2(H(u^i)\partial_x u_h^i \times \partial_y u_h^i, v_h) \end{aligned}$$

   for all $(\sigma_h, v_h) \in [V_{mini}^h]^{3\times 2} \times [\mathcal{S}_0^1(\mathcal{T}_h)]^3$.

2. Stop if $||\nabla w_h^i||_{L^2(M)} + ||\mu_h^i||_{L^2(M)} < \varepsilon$.

3. Set
$$p_h^{i+1} := p_h^i + \tau\mu_h^i \qquad \text{and} \qquad u_h^{i+1} := u_h^i + \tau w_h^i.$$

4. Set $i = i + 1$ and go to (1).

Output: $(p_h^*, u_h^*) := (p_h^i, u_h^i)$.

Definition 4.2.5 *We define the space of admissible pairs through*

$$\mathbb{V}_h := \big\{(p_h, u_h) \in [V_{mini}^h]^{3\times 2} \times [\mathcal{S}^1(\mathcal{T}_h)]^3 : u_h\big|_{\partial B_h} = u_{h,D},\ E_h^H(u_h) := \frac{1}{2}||P_0^h(\nabla u_h)||_{L^2}^2 + V(u_h) \geq 0\big\}.$$

We show that our algorithm terminates within a finite number of steps providing a discrete surface spanning $u_{D,h}$ with prescribed mean curvature.

Theorem 4.2.6 *Let $(p_h^i, u_h^i)_{0\leq i\leq J} \subset \mathbb{V}_h$ ($J \in \mathbb{N}$) be a sequence of functions computed in step (1) of our algorithm and let $C' := C\left(1 + \log h_{min}^{-1}\left(||\nabla u_h|| + \log h_{min}^{-1}||\nabla u_h||^2\right)\right)$ be the constant from Lemma 4.1.1. If $\tau^{-1} > C'$ then for all $J \geq 1$*

$$\frac{\tau^2}{2}\sum_{i=0}^{J}||\mu_h^i||_{L^2}^2 + (1 - C')\tau\sum_{i=0}^{J}||\nabla w_h^i||_{L^2}^2 + E_h^H(u_h^{J+1}) \leq E_h^H(u_h^0),$$

where $C' > 0$ depends on upper bounds for $||\nabla u_h^0||_{L^2}$, $||p_h^0||_{L^2}$ and $\log h_{min}^{-1}$.

Proof. (i) Subtract the first equation in step (1) for i and $i+1$ and test it with $\sigma_h = p_h^{i+1}$. In the second equation we use $v_h = w_h^i$ and subtract it from the first one to obtain

$$(\mu_h^i, p_h^{i+1}) + ||\nabla w_h^i||_{L^2} + (2H(u_h^i)\partial_x u_h^i \times \partial_y u_h^i, w_h^i) = 0.$$

Incorporating the results from Lemma 4.1.1 we see the local energy estimate

$$(\mu_h^i, p_h^{i+1}) + ||\nabla w_h^i||^2 + \tau^{-1}(V(u_h^{i+1}) - V(u_h^i)) \leq C'\tau||\nabla w_h^i||^2.$$

We use the binomial identity $b(b-a) = 1/2(b-a)^2 + 1/2(b^2 - a^2)$ and $p_h^i = P_0^h(\nabla u_h^i)$ to obtain

$$\frac{\tau}{2}||\mu_h^i||_{L^2} + (1 - C'\tau)||\nabla w_h^i||_{L^2}^2 + \tau^{-1}(E_h^H(u_h^{i+1}) - E^H(u_h^i)) \leq 0.$$

(ii) We take the sum over $i = 0, \ldots, J$ to deduce the energy inequality

$$\frac{\tau^2}{2}\sum_{i=0}^{J}||\mu_h^i||_{L^2}^2 + (1 - C'\tau\sum_{i=0}^{J}||\nabla w_h^i||_{L^2}^2 + E_h^H(u_h^{J+1}) \leq E_h^H(u_h^0).$$

Since $E_h^H(u_h^{J+1}) > 0$ for all $J \in \mathbb{N}$ we know that for $\varepsilon > 0$ there exists $J_\varepsilon \in \mathbb{N}$ such that $||\mu_h^i||_{L^2} + ||\nabla w_h^i||_{L^2} \leq \varepsilon$, and the algorithm terminates. □

Remark 4.2.7 *(i) Theorem 4.2.6 says that if the sequence of iterates stays in $\mathbb{V}_h$ then the algorithm terminates within a finite number of steps. However, for $|H|||u_{D,h}||_{L^\infty} < 1$ this theoretical drawback had no influence on the experiments. We note that the definition of $\mathbb{V}_h$ is inspired by the existence result in [72] that uses coerciveness of the energy $E_{H_0}(u) := \frac{1}{2}\int_B |\nabla u|^2\, dx + \frac{2}{3}\int_B H_0 u\partial_x u \times \partial_y u\, dx$ on the set*

$$\mathcal{M} := \left\{u \in W^{1,2}(B;\mathbb{R}^3) : u_{\partial B} = u_D,\, |H|||u||_{L^\infty(B)} < 1\right\}.$$

(ii) The existence of a solution $(\mu_h^i, w_h^i) \in [V_{mini}^h]^{3\times 2} \times [\mathcal{S}(\mathcal{T}_h)]^3$ in every time-step can be proved with the same methods as in the harmonic mapping case.

Chapter 5.

Numerical experiments for the mixed method

In this section we provide some numerical examples both for harmonic maps into submanifolds and surfaces of prescribed mean curvature.

5.1. Harmonic maps

5.1.1. Extinction of singularities

A model for liquid crystals. We consider an application from the theory of liquid crystals and start with a short introduction to a theoretical model. A configuration of the liquid crystal can be described by a vector field $m(x) \in \mathbb{R}^3$, $x \in V = (0,1)^3$ our vessel. It is natural to use statistical averages of m for the description of macroscopic characteristics. Since the molecules of the crystal have a so-called head-to-tail symmetry, that is $m(x) \simeq -m(x)$, all the odd moments have to vanish and the lowest order even moments yield a symmetrix matrix

$$G = \langle m \otimes m \rangle, \quad G \geq 0, \quad \mathrm{tr}G = 1,$$

where the brackets $\langle \cdot \rangle$ denote a certain statistical average, see [74] for a derivation of G. The de Gennes order parameter tensor is defined as the traceless, symmetric matrix $Q := G - \frac{1}{3}\mathrm{id}$. In the uniaxial case it is assumed that Q has two equal eigenvalues and admits therefore a representation $Q = s(n \otimes n - \frac{1}{3}\mathrm{id})$, where $n \in \mathbb{S}^2$ is the optical axis and $s \in [-1/2, 1]$ is the orientation order parameter. The orientational order s takes values between $s = -\frac{1}{2}$ (all molecules are in a plane perpendicular to the optical axis) and $s = 1$ (all molecules are perfectly aligned). We note, however, that in practice it is observed that the orientational order of the liquid crystal is constant almost everywhere with values between 0.6 and 0.8. Using Q-fields to describe liquid crystals has become more popular in recent years, see e.g. [5], and for a substantial treatment of liquid crystals see [58, 74] and the references therein.

We restrict ourselves here to the classical Oseen-Frank model that assumes $s = const$ and a dependence of the bulk energy on the orientation vector field $n : V \to \mathbb{S}^2$. Symmetries of the molecules are taken into account by the fact that the free energy density σ satisfies

$$\sigma(n, \nabla n) = \sigma(-n, -\nabla n), \quad \sigma(Rn, R\nabla n R^T) = \sigma(n, \nabla n) \quad \text{for} \quad R \in O(3).$$

Based on this conditions and certain physical considerations Oseen and Frank came up with the free energy density

$$\sigma(n, \nabla n) := k_1 |\mathrm{div}\, n|^2 + k_2 |n \bullet \mathrm{curl}\, n|^2 + k_3 |n \times \mathrm{curl}\, n|^2 + (k_2 + k_4)(|\nabla n|^2 - |\mathrm{div}\, n|^2),$$

with material constants $k_1, \ldots, k_4 \in \mathbb{R}$. For a derivation of the energy density see [74]. The most simple energy in the Oseen Frank theory, which we will use here, is then

$$E(n) := \frac{1}{2} \int_V |\nabla n|^2 \, \mathrm{d}x.$$

It is true that the molecules of the liquid crystal tend to align themselves parallel to the boundary when they contact other materials. These boundary conditions are often referred to as partial constraint or planar angchoring conditions and they are the natural choice. When the surface is worked in a special manner the liquid crystal aligns with the treatment and can be specified. Then one speaks about strong or homeotropic angchoring conditions. In the partial constraint case defects at the boundary can be observed leading to so called Schlieren textures. There are different types of defects (disclinations) and each type is assigned a number and a sign. Some of them may cancel each other out if they come into contact. We consider the upper boundary $M := (0,1)^2 \times \{1\}$ of V and simulate the annihilation of opposite degree-1 and degree-2 singularities as our algorithm is running. The preference of the alignment parallel to the surface M is modelled by the use of a Ginzburg-Landau penalty term. Thus, we consider

$$E(n) = \frac{1}{2}\int_M |\nabla n|^2 \,\mathrm{d}x + \frac{1}{2\varepsilon^2}\int_M |n_3|^2 \,\mathrm{d}x.$$

Penalizing the out of plane component is physically consistent since the alignment parallel to M is favored but not forced. Mathematically this is crucial since the singularities in the plane have infinite Dirichlet energy. Then, the domain M and the parameters ε, h and τ are given by

$$M = (-1,1)^2,\ \varepsilon = 10^{-1},\ h = \sqrt{2}2^{-6},\ \tau = h/10.$$

Construction of the initial data. In our first experiment we examine the extinction of two opposite degree-1 singularities. We set $\varphi(r) := \tanh(r)$ and use this function to regularize the singularities. Let $d = 0.35$ and $(r_\pm, \phi_\pm)$ be polar coordinates about $(\pm d, 0)$. We set

$$\begin{aligned} n_+^0(z) &:= -\big(\varphi(r/\varepsilon)\cos(-\phi_+/2), \varphi(r/\varepsilon)\sin(-\phi_+/2), (1-\varphi(r/\varepsilon)^2)^{1/2}\big),\\ n_-^0(z) &:= \ \ \big(\varphi(r/\varepsilon)\cos(\phi_-/2), \varphi(r/\varepsilon)\sin(\phi_-/2), (1-\varphi(r/\varepsilon)^2)^{1/2}\big),\\ n_D(z) &:= \ \ \big(-1,0,0\big) \end{aligned}$$

for all $z \in \mathcal{N}$ and introduce a partition of unity on M to assemble the initial data $n^0 \in [\mathcal{S}^1(\mathcal{T}_h)]^3$. See Figure 5.1 on the left where we plot the first two components of the vector fields n_+^0, n_-^0 and n_D. We define the piecewise affine linear functions

$$\psi(t) = -|t| + 1,$$

$$\psi_-(t) := \begin{cases} (1+t)/(1-d), & -1 \le t \le -d \\ (d-t)/(2d), & -d < t < d \\ 0, & d \le t \le 1 \end{cases},$$

$$\psi_+(t) := \begin{cases} 0, & -1 \le t \le -d \\ (d+t)/(2d), & -d < t < d \\ (1-t)/(1-d), & d \le t \le 1 \end{cases},$$

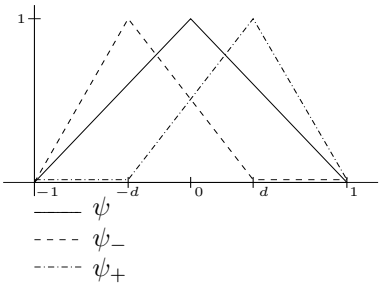

and set $\eta_\pm(x_1,x_2) := \psi_\pm(x_1)\psi(x_2)$ as well as $\eta_D = 1 - \eta_+ - \eta_-$. See Figure 5.1 on the right where we plot the functions η_+, η_- and η_D. Finally we set

$$\widetilde{n}^0 := \mathcal{I}_h[\eta_+ n_+^0] + \mathcal{I}_h[\eta_- n_-^0] + \mathcal{I}_h[\eta_D n_D],$$

and define n^0 through $n^0(z) := \widetilde{n}^0(z)/|\widetilde{n}^0(z)|$ for all $z \in \mathcal{N}$. We remark, that we rotated the negative degree-1 singularity in the experiment by π to match the vector field smoothly at $x_1 = 0$, see Figure 5.1 on the bottom for a plot of n^0. The auxiliary variable is defined as $p_h^0 := P_h^0 \nabla n^0 \in [V_{mini}^h]^{3\times 2}$. In a second experiment we plant two negative degree-1 singularities at $(0.6, 0)$ and $(-0.7, 0)$ and one positive degree-2 singularity at $(0.2, 0)$, see Figure 5.2. The setup for the third experiment is analogous to the second one with opposite signs of the singularities.

Discussion of the experiments. Snapshots of the evolution and decay of the discrete energy $E_h := \frac{1}{2}||p_h||^2_{L^2(M)} + \frac{1}{2\varepsilon^2}||n_3||^2_{L^2(M)}$ can be seen in Figure 5.3, Figure 5.5 and Figure 5.6 for the first, second and third experiment respectively. We observe that singularities are resolved reliably by our

mixed method. The evolution under the H^1-gradient flow in the n_h-variable leads to a fast extinction of the singularities and stopps at the absolute minimum obtained for $n_h = n_D$ and $p_h = 0$. We note that the choice of $\tau = O(h)$ yields stable simulations as predicted by the theory. When singularities meet during the evolution blow-ups in the L^∞-norm of $p_h \sim \nabla u_h$ can occur. In the first experiment we observe a finite time blow-up near the origin, see Figure 5.4 for details. While the energy decreases continuously during the evolution the L^∞-norm of p_h takes its maximum value at time $t = 28.64$.

5.1.2. Projection versus no projection

We compare the H^1-flow with and without employing a projection step for the mixed method and the $P1$-method. We use the stereographic projection to examine an example for which we know the exact solution.

Definition 5.1.3 (Stereographic projection) *Let $H_0 \in \mathbb{R}$, $R = \frac{1}{H_0}$, $a = \sqrt{R^2 - 1}$ and $\delta = R + a$. Let $N = [0, 0, \delta]^T$ be the 'north pole' of the sphere $\partial B_R(c)$ with radius R and center $c = [0, 0, a]^T$. The stereographic projection Φ^R_{sp} from N to the sphere $\partial B_R(c)$ is defined as*

$$\Phi^R_{sp} : \mathbb{R}^2 \to \partial B_R(c), \quad (x_1, x_2) \mapsto \left[\frac{2R\delta x_1}{|x|^2 + \delta^2}, \frac{2R\delta x_2}{|x|^2 + \delta^2}, \delta \frac{|x|^2 + \delta^2 - 2R\delta}{|x|^2 + \delta^2} \right].$$

See Figure 5.9 for a sketch of the geometry that leads to the formula of Φ^R_{sp}. For $R = 1$ we obtain the standard stereographic projection $\Phi_{sp} := \Phi^1_{sp} : \mathbb{R}^2 \to \mathbb{S}^2$,

$$\Phi_{sp} : \mathbb{R}^2 \to \mathbb{S}^2, \quad (x_1, x_2) \mapsto \left[\frac{2x_1}{1 + |x|^2}, \frac{2x_2}{1 + |x|^2}, \frac{-1 + |x|^2}{1 + |x|^2} \right]^T.$$

Proposition 5.1.4 *Let $M := (-\frac{1}{\sqrt{2}}, \frac{1}{\sqrt{2}})^2 \subset \mathbb{R}^2$,*

$$V := \{ v \in W^{1,2}(M; \mathbb{R}^3) : v \in \mathbb{S}^2 \text{ a.e. and } v|_{\partial M} = \Phi_{sp}|_{\partial M} \}$$

and $E : V \to \mathbb{R}$,

$$v \mapsto \frac{1}{2} \int_M |\nabla v|^2 \, dx.$$

Then, Φ_{sp} is a stationary point of E.

Proof. For $\Phi_{sp} := \left[\Phi_{sp,1}, \Phi_{sp,2}, \Phi_{sp,3} \right]^T$ we compute

$$-\Delta \Phi_{sp,1} = \frac{16x_1}{(1 + x_1^2 + x_2^2)^3}, \quad -\Delta \Phi_{sp,2} = \frac{16x_2}{(1 + x_1^2 + x_2^2)^3} \quad \text{and} \quad -\Delta \Phi_{sp,3} = \frac{8(-1 + x_1^2 + x_2^2)}{(1 + x_1^2 + x_2^2)^3}.$$

Combining this with

$$|\nabla \Phi_{sp}|^2 = \sum_{i=1}^{3} \sum_{j=1}^{2} (\partial_j \Phi_{sp,i})^2 = \frac{8}{(1 + x_1^2 + x_2^2)^2} \tag{5.1.1}$$

yields $-\Delta \Phi_{sp}(x) = \Phi_{sp}(x) \, |\nabla \Phi_{sp}(x)|^2$, which is exactly the Euler-Lagrange equation corresponding to the energy E. □

Setting of the experiment. *The sequence of triangulations $\mathcal{T}_\ell$ of M is generated by ℓ uniform refinements (division of each triangle into four congruent ones) of the initial triangulation $\mathcal{T}_0$ of M which consists of two triangles obtained by dividing M along the diagonal $x_1 = x_2$. Hence, the mesh-size h_ℓ is given by $h_\ell = 2^{-\ell}$, $\ell = 2, \ldots, 6$. We set $\tau_\ell = h_\ell^2$ and $u^0_{h_\ell}(z) = \Phi_{sp}(z)$ for all $z \in \mathcal{N}_{h_\ell} \cap \partial M$. At the interior nodes we set*

$$u^0_{h_\ell}(z) = \Phi_{sp}(z) + 0.25 \mathrm{rand}_{h_\ell}(z),$$

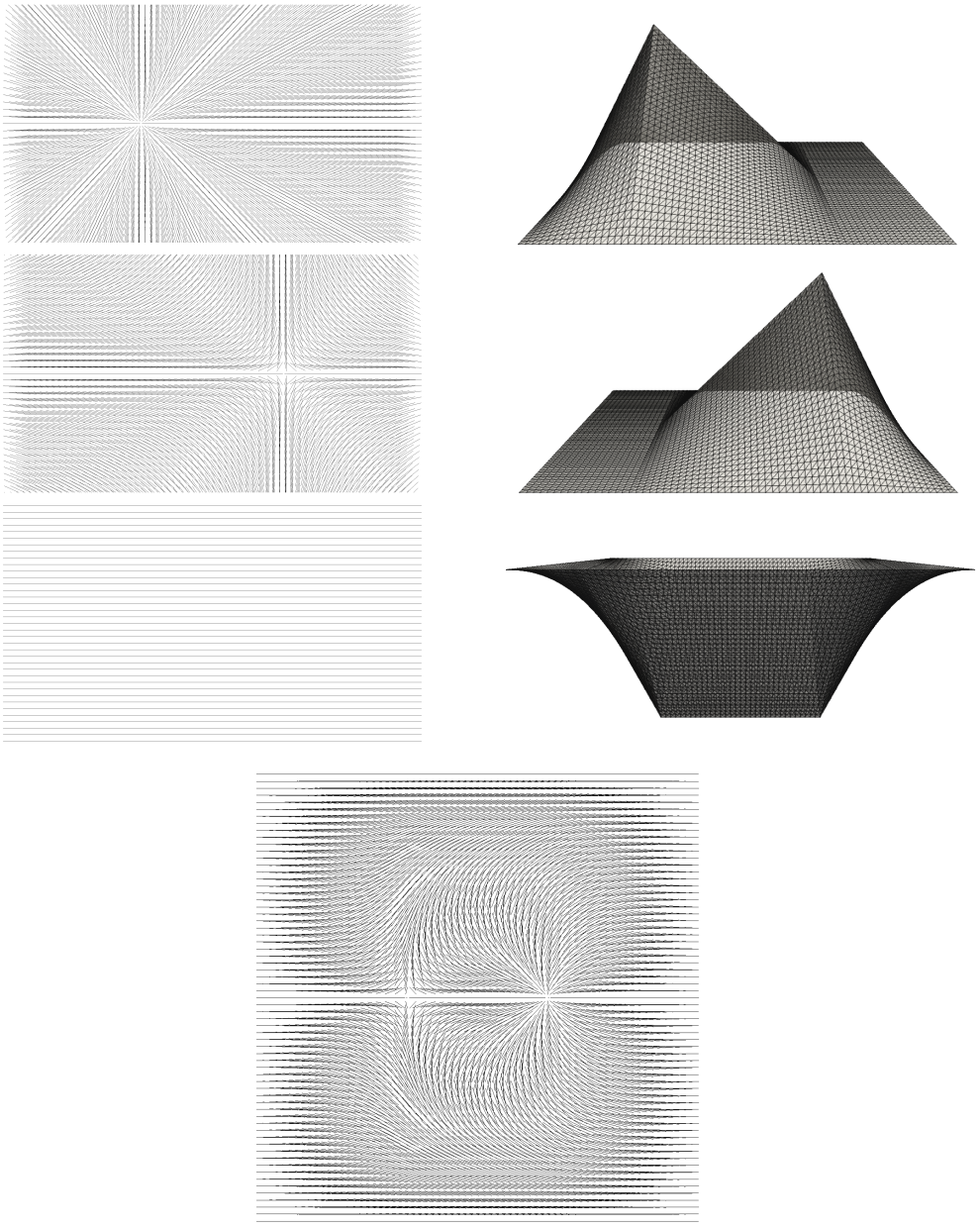

Figure 5.1.: Assembling the initial vector field with two degree-1 defects of opposite sign. We plot the first two components of n_+^0, n_-^0 and n_D in a strip around $x_2 = 0$ (three upper plots on the left) and the corresponding partition of unity consisting of η_+, η_- and η_D (three upper plots on the right). On the bottom we see the initial data n^0 for the first experiment. At every node $z \in \mathcal{N}$ we have $m(z) \in \mathbb{S}^2$ for $m \in \{n_+^0, n_-^0, n_D, n^0\}$ and we plot the first two components of $\{z + tm(z) : z \in \mathcal{N}, t \in (-1/10, 1/10)\}$.

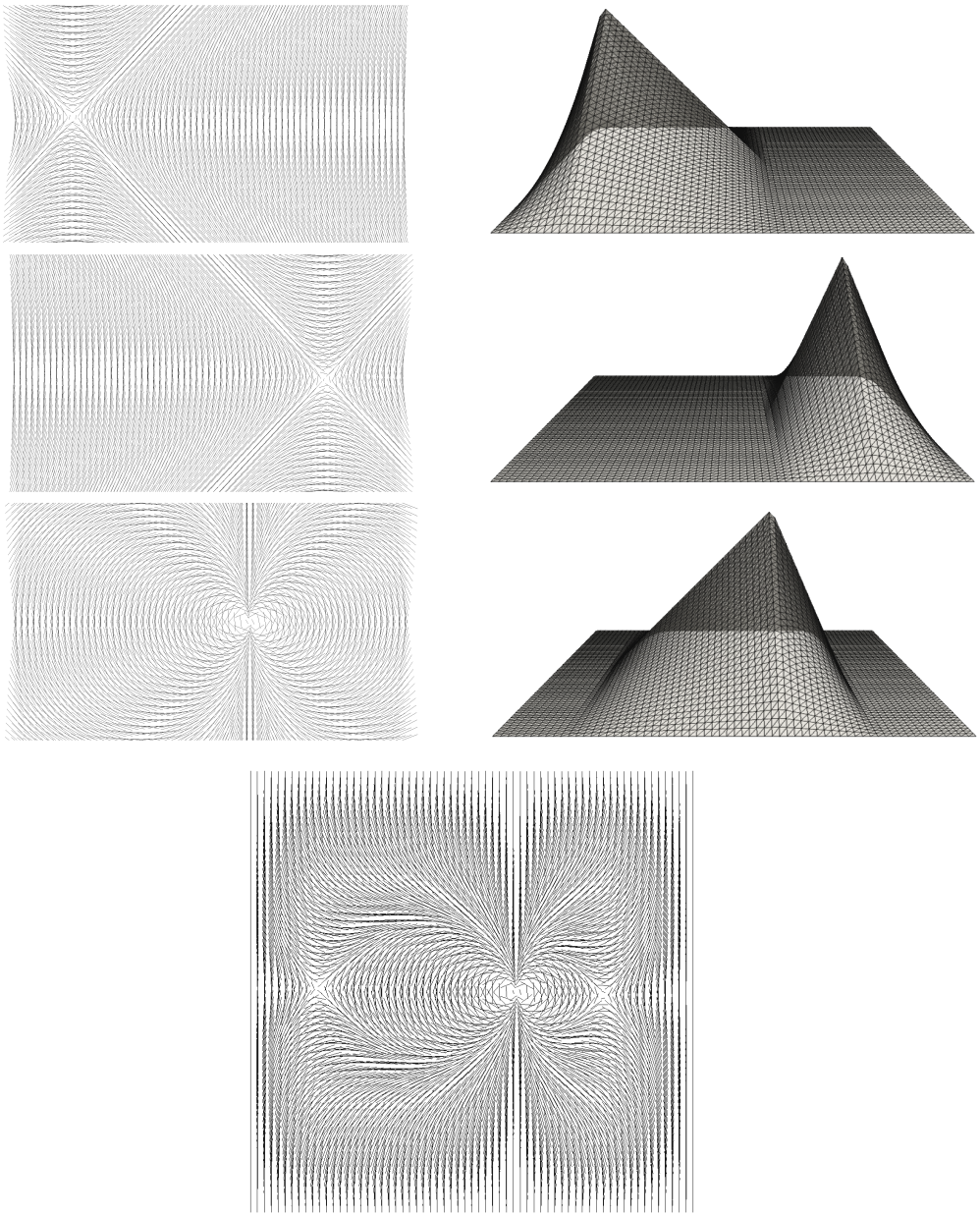

Figure 5.2.: Assembling the initial vector field n^0 with two negative degree-1 defects located at $x_1 = 0.6$ and $x_1 = -0.7$ and one positive degree-2 defect located at $x_1 = 0.2$. We depict n^0_+, n^0_- and n_D as well as the corresponding partition of unity in the upper plots and n^0 at the bottom.

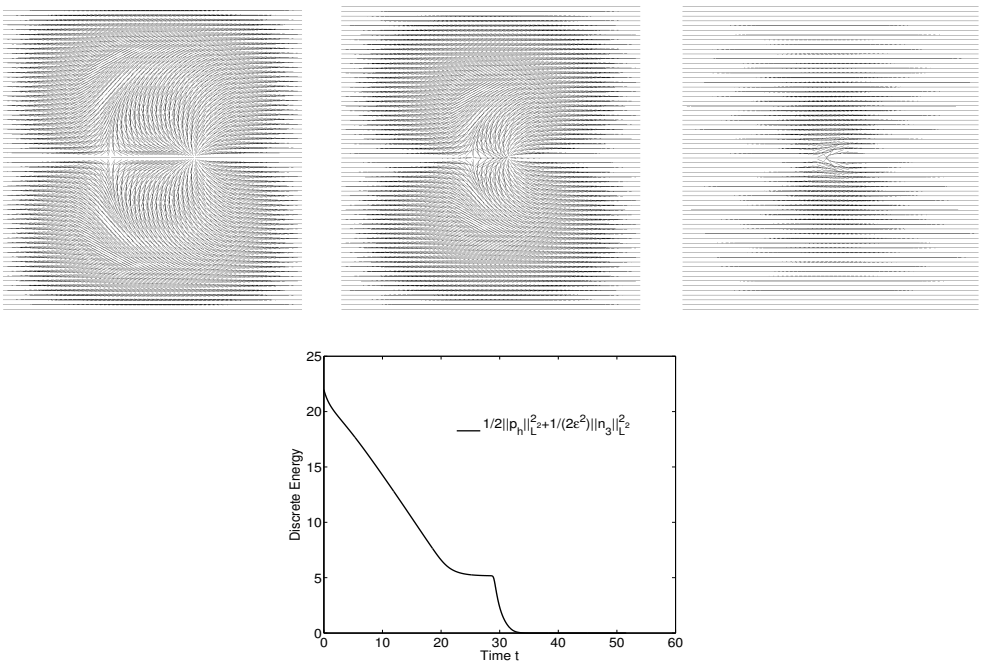

Figure 5.3.: Extinction of two opposite degree-1 singularities during the computation and an energy plot demonstrating the decay of energy: Snapshots of the evolution at times $t = 2.21, 11.04$ and 22.09. The energy shows a strong decay when the attracting defects eventually annihilate.

where $\text{rand}_{h_\ell} \in [\mathcal{S}^1(\mathcal{T}_{h_\ell})]^3$ *takes random values in* $(-0.5, 0.5)^3$. *For the mixed method we use* $p^0_{h_\ell} = P_0^{h_\ell} \nabla u_{h_\ell}$ *and as a stopping criterion we set* $\varepsilon = 10^{-5}$.

We emphasize that all results on the experimental order of convergence for harmonic maps have to be taken with a pinch of salt. We do not have a uniqueness result for discrete harmonic maps, however, from the continuous setting we know by [50] that solutions are unique if the image of the map as a subset of the target manifold N satisfies the cut locus condition. The latter means that every pair of points in the image can be joint be exactly one minimizing geodesic arc of N. Clearly $\Phi_{sp}(M)$ satisfies the cut-locus conditions, thus, we suppose that the output of any of our testet schemes is an approximation of Φ_{sp}. Based on this assumption we compute different errors and experimental orders of convergence.

The question of performing a projection step or not clearly hinges on the target manifold and on the energy one wants to minimize. If, for example, the target manifold is the unit sphere and the gradient flow yields a discretization for which an energy inequality can be shown under the restraint $\tau \sim h$, then, of course, it makes sense to embed the projection step. This renormalization of the iterate is quite fast and the whole scheme is then stable for $\tau \sim h$. However, in our experiments both versions provided good approximations as can be seen in the Tables 5.1, 5.2, 5.3 and 5.4, and the proof of the energy inequality in the mixed formulation is much easier without the projection step.

5.2. Surfaces of prescribed mean curvature

We start with a discussion of starting values, since this is a delicate issue in the computation of surfaces of prescribed mean curvature. In the second part we study the experimental order of convergence for a model problem where we know the exact solution. Finally we present some numerical results for the Enneper surface and more difficult and knotted boundary curves.

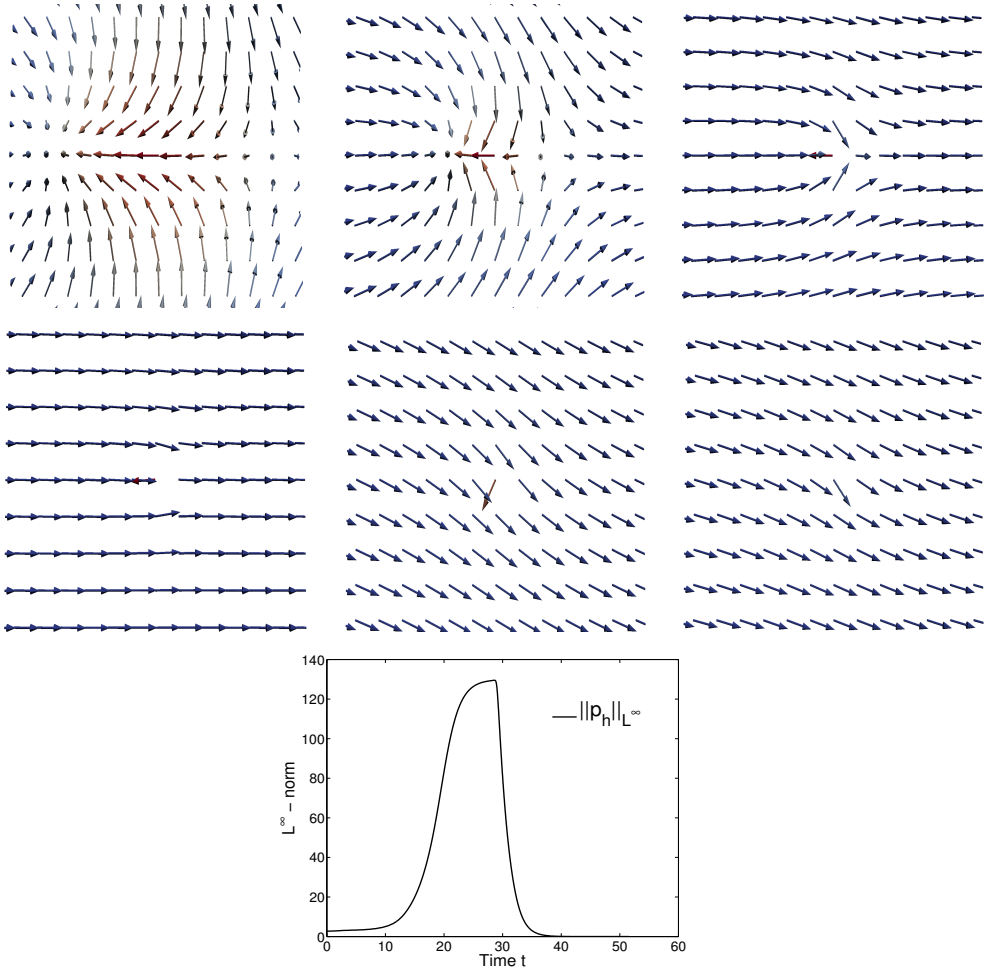

Figure 5.4.: Zoom to the origin $x_1 = x_2 = 0$ where the auxiliary variable p_h takes its maximum value during the evolution (top). Snapshots at time $t = 11.04, 16.57, 22.09, 28.64, 29, 83$ and $t = 32.04$ show the vector field in the neighborhood of the origin. The vector field is colored by the absolute value of p_h, where blue corresponds to small and red to large values. There is a finite time blow-up in the L^∞-norm of p_h at time $t = 28.64$ (bottom).

	Mixed-method -projection-		Mixed-method -no projection-		$P1$-method -projection-		$P1$-method -no projection-	
h	err_{H^1}	eoc	err_{H^1}	eoc	err_{H^1}	eoc	err_{H^1}	eoc
0.25	$1.85 * 10^{-1}$	–	$1.85 * 10^{-1}$	–	$6.26 * 10^{-2}$	–	$6.26 * 10^{-2}$	–
0.125	$5.10 * 10^{-2}$	1.86	$5.09 * 10^{-2}$	1.86	$1.59 * 10^{-2}$	1.97	$1.59 * 10^{-2}$	1.97
0.0625	$1.34 * 10^{-2}$	1.93	$1.34 * 10^{-2}$	1.93	$4.01 * 10^{-3}$	1.99	$4.01 * 10^{-3}$	1.99
0.03125	$3.68 * 10^{-3}$	1.86	$3.68 * 10^{-3}$	1.86	$1.00 * 10^{-3}$	2.00	$1.01 * 10^{-3}$	2.00
0.015625	$1.10 * 10^{-3}$	1.77	$1.08 * 10^{-3}$	1.77	$2.51 * 10^{-4}$	2.00	$2.52 * 10^{-4}$	1.99

Table 5.1.: H^1-error and experimental order of convergence for the different schemes.

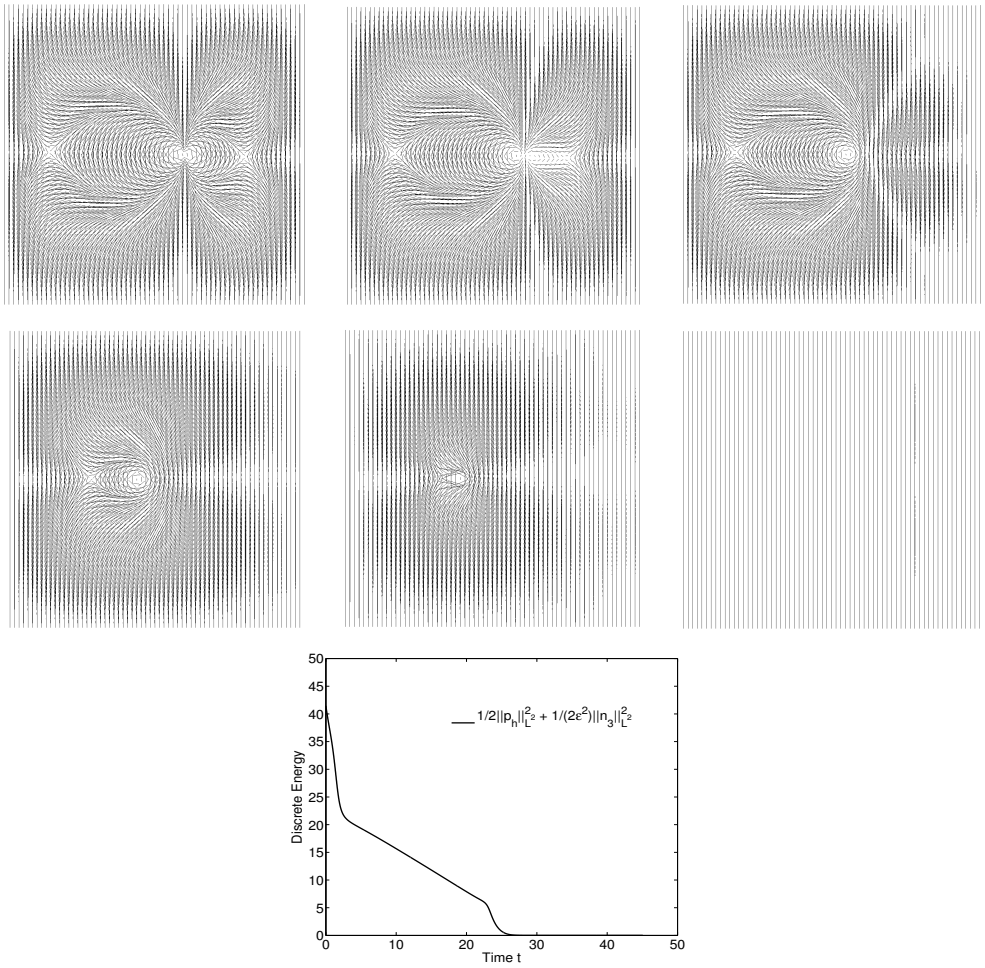

Figure 5.5.: Extinction of three singularities during the computation and an energy plot demonstrating the decay of energy: Snapshots of the evolution of the first two components at times $t = 0, 1.10, 2.20, 11.04, 18.78$ and 33.14. The nearby negative degree-1 and positive degree-2 singularities come together and result in a rotated positive degree-1 defect. Then, as in the first experiment an annihilation takes place when the remaining singularities meet. The energy shows strong decays when the annihilations take place.

	Mixed-method -projection-		Mixed-method -no projection-		$P1$-method -projection-		$P1$-method -no projection-	
h	err_{L^2}	eoc	err_{L^2}	eoc	err_{L^2}	eoc	err_{L^2}	eoc
0.25	$3.37 * 10^{-2}$	–	$3.37 * 10^{-2}$	–	$1.17 * 10^{-2}$	–	$1.17 * 10^{-2}$	–
0.125	$9.37 * 10^{-3}$	1.85	$9.37 * 10^{-3}$	1.85	$3.11 * 10^{-3}$	1.92	$3.11 * 10^{-3}$	1.91
0.0625	$2.35 * 10^{-3}$	2.00	$2.35 * 10^{-3}$	2.00	$7.96 * 10^{-4}$	1.97	$7.95 * 10^{-4}$	1.97
0.03125	$5.82 * 10^{-4}$	2.01	$5.82 * 10^{-4}$	2.01	$2.00 * 10^{-4}$	1.99	$2.00 * 10^{-4}$	1.99
0.015625	$1.45 * 10^{-4}$	2.01	$1.45 * 10^{-4}$	2.01	$5.01 * 10^{-5}$	2.00	$5.02 * 10^{-5}$	2.00

Table 5.2.: L^2-error and experimental order of convergence for the different schemes.

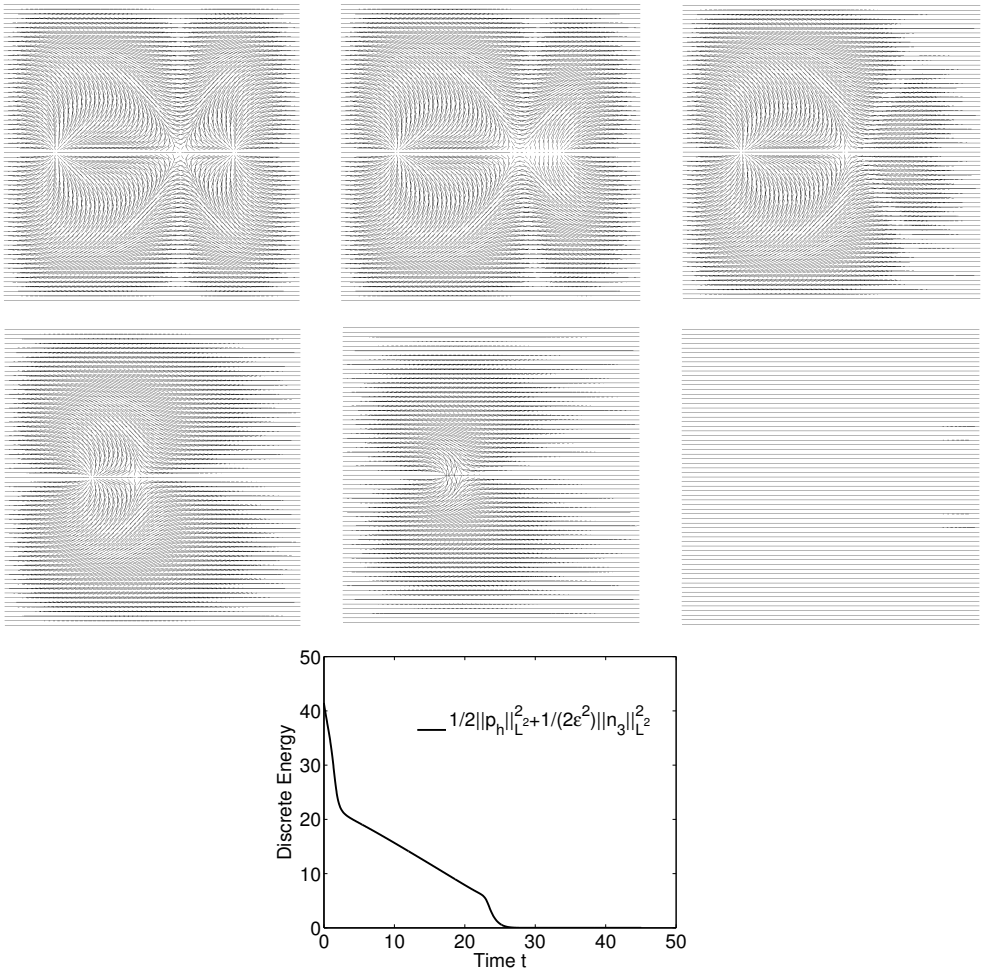

Figure 5.6.: Extinction of three singularities during the computation and an energy plot demonstrating the decay of energy: Snapshots of the evolution of the first two components at times $t = 0, 1.10, 2.20, 11.04, 18.78$ and 33.14. The nearby negative degree-2 and positive degree-1 singularities come together and result in a negative degree-1 defect. Then, as in the first experiment an annihilation takes place when the remaining singularities meet. The evolution shows strong analogies to the one of the second simulation. For the piecewise constant functions $E_h^i : t \mapsto \frac{1}{2}||p_h(t)||_{L^2}^2 + \frac{1}{2\varepsilon^2}||n_3(t)||_{L^2}^2$, where $i = 2, 3$ indicates the number of the experiment, we compute $\sup_t |E_h^2(t) - E_h^3(t)| = 1.78 * 10^{-14}$.

	Mixed-method -projection-		Mixed-method -no projection-		$P1$-method -projection-		$P1$-method -no projection-	
h	err_{L^∞}	eoc	err_{L^∞}	eoc	err_{L^∞}	eoc	err_{L^∞}	eoc
0.25	$5.15 * 10^{-2}$	–	$5.14 * 10^{-2}$	–	$1.49 * 10^{-2}$	–	$1.49 * 10^{-2}$	–
0.125	$1.20 * 10^{-2}$	2.11	$1.20 * 10^{-2}$	2.11	$3.42 * 10^{-3}$	2.13	$3.42 * 10^{-3}$	2.13
0.0625	$2.96 * 10^{-3}$	2.02	$2.96 * 10^{-3}$	2.01	$8.74 * 10^{-4}$	1.97	$8.73 * 10^{-4}$	1.97
0.03125	$7.33 * 10^{-4}$	2.01	$7.36 * 10^{-4}$	2.01	$2.20 * 10^{-4}$	1.99	$1.89 * 10^{-4}$	2.00
0.015625	$1.82 * 10^{-4}$	2.01	$1.82 * 10^{-4}$	2.01	$5.55 * 10^{-5}$	1.98	$5.51 * 10^{-5}$	1.99

Table 5.3.: L^∞-error and experimental order of convergence for the different schemes.

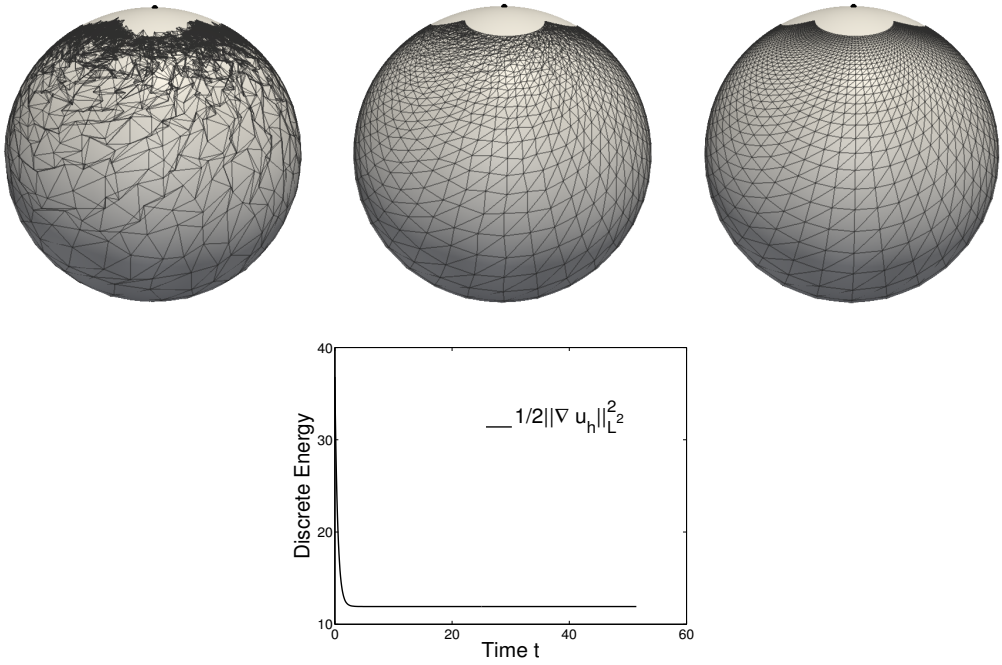

Figure 5.7.: Computation of the stereographic projection as a stationary point of the Dirichlet energy. Snapshots of the evolution at times $t = 0$, $t = 1.7$ and $t = 57,7$. At time $t = 57,7$ the discrete energy of the output u_h^* is $E(u_h) = 11.922$ and the difference from the exact solution is $|E(\Phi_{sp}) - E(u_h)| = 0.034$, where we use formula (5.1.1) to compute $E(\Phi_{sp})$. Starting point for the H^1-flow is a perturbation of Φ_{sp} and we set $M = (-4, 4)^2$ as well as $\tau = h = 2^{-4}\sqrt{2}$ in this experiment. We use the $P1$-method with projection step for this computation. Note, that the cut-locus condition is not fulfilled for $\Phi_{sp}((-4, 4)^2)$.

	h	0.25	0.125	0.0625	0.03125	0.015625
Mixed-method	$\|\|1 - \|u_{h_\ell}\|\|\|_{h_\ell, L^\infty}$	$1.84 * 10^{-4}$	$3.20 * 10^{-5}$	$8.75 * 10^{-6}$	$2.98 * 10^{-6}$	$7.12 * 10^{-7}$
$P1$-method	$\|\|1 - \|u_{h_\ell}\|\|\|_{h_\ell, L^\infty}$	$1.13 * 10^{-4}$	$3.60 * 10^{-5}$	$1.39 * 10^{-5}$	$3.41 * 10^{-6}$	$9.38 * 10^{-7}$

Table 5.4.: Maximal distance to the sphere expressed in the norm $||f||_{h,L^\infty} = \max_{z \in \mathcal{N}_h} |f(z)|$.

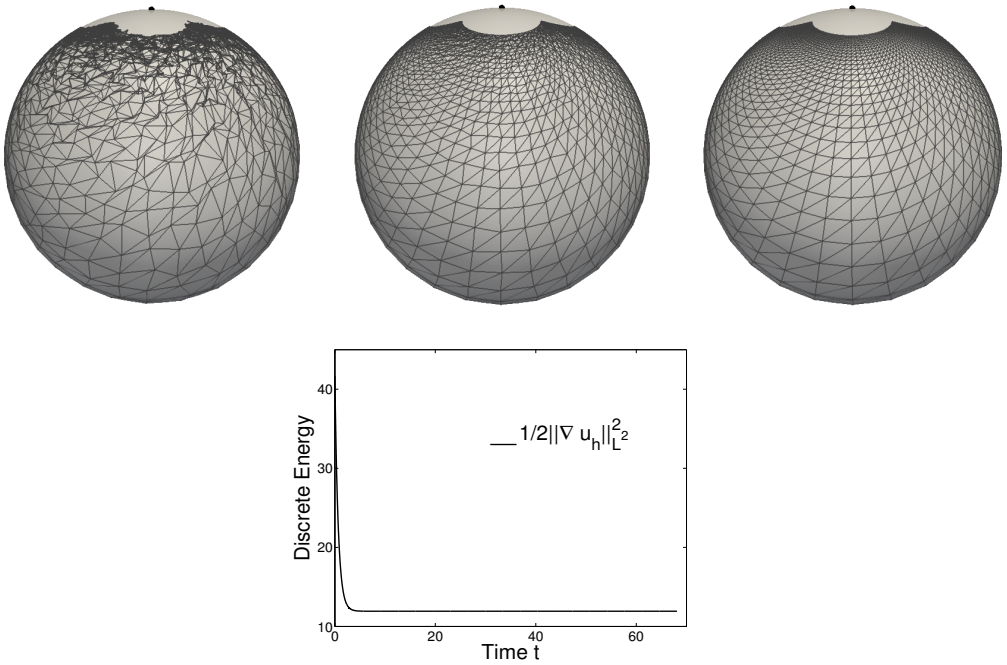

Figure 5.8.: Same experiment as in Figrue 5.7, using the mixed-method without projection step. Snapshots of the evolution at times $t = 0.78$, $t = 2.73$ and at the end time $t = 68.09$. Then, the discrete energy of the output u_h^* is $E(u_h^*) = 11.924$ and the difference from the exact solution is $|E(\Phi_{sp}) - E(u_h^*)| = 0.031$. As above the starting point for the H^1-flow is a perturbation of Φ_{sp} and we set $M = (-4, 4)^2$ as well as $\tau = h^2 = 2^{-7}$. Furthermore, we compute for u_h^* that $\max_{z \in \mathcal{N}_h} \text{dist}(u_h^*(z), \mathbb{S}^2) = 2.33 * 10^{-5}$.

5.2.1. Discussion of Starting values

Given a boundary curve Γ and $u_D \in C(\overline{B_1(0)}, \mathbb{R}^3)$ satisfying $u_D(\partial B_1(0)) = \Gamma$ we want to find a map $u_h^0 \in [\mathcal{S}^1(\mathcal{T}_h)]^3$ satisfying the boundary conditions $u_h^0(z) = u_D(z)$ for all $z \in \mathcal{N}_h \cap \partial B_h$ and being an appropriate starting point for the H^1-gradient flow. We propose the following iterative scheme for the computation of such a u_h^0: Let $i_{max} \in \mathbb{N}$ be the number of steps of the iteration and $U_h^0 = \mathrm{id}_h \in [\mathcal{S}^1(\mathcal{T}_h)]^3$ the discrete identity on B_h. Let $U_h^1 \in [\mathcal{S}^1(\mathcal{T}_h)]^3$ satisfy $U_h^1(z) = u_D(z)$ for all $z \in \mathcal{N}_h \cap \partial B_h$ and let U_h^1 be arbitrary at the inner nodes. We define a discrete homotopy from U_h^0 to U_h^1 by functions $U_h^i \in [\mathcal{S}^1(\mathcal{T}_h)]^3$, that is

$$U_h^i = (1 - i/i_{max})U_h^0 + i/i_{max}U_h^1,\ i = 0, \dots, i_{max},$$

and give the scheme:

1. Set $i = 0$ and $u_h^{0,i} = \mathrm{id}_h \in [\mathcal{S}^1(\mathcal{T}_h)]^3$.
2. Compute a discrete solution $u_h^{*,i}$ with the H^1-flow from Chapter 4, with starting value $u_h^{0,i}$ and $p_h^{0,i} = P_0^h(\nabla u_h^{0,i})$.
3. Set $i = i + 1$, $u_h^{0,i}(z) = u_h^{*,i-1}(z)$ for all $z \in \mathcal{N}_h \setminus \partial B_1(0)$ and $u_h^{0,i}(z) = U_h^i(z)$ for all $z \in \mathcal{N}_h \cap \partial B_1(0)$.
4. Stop if $i = i_{max}$ otherwise go to (2).

Output: $(p_h^*, u_h^*) = (p_h^{*,i_{max}}, u_h^{*,i_{max}})$.

Remark. *For $i < i_{max}$ we may set $H = 0$ and compute discrete minimal surfaces satisfying the boundary conditions in every step. The so obtained surface $u_h^{0,i_{max}}$ serves well as initial data for the last step and its computation is faster.*

5.2.2. Determination of the experimental order of convergence

We choose polygonal approximations of $B_1(0)$ with different mesh-sizes, varrying from $h = 0.420$ to $h = 0.011$. We set $B = B_1(0)$, $u|_{\partial B} = \mathrm{id}$ and $H_0 = 3/4$. As starting values we take the identity for u_h^0 and $p_h^0 = P_0^h(\nabla u_h^0)$. The exact solution of (4.0.1) is a conformally parametrized spherical cap of a ball with radius $R = 4/3$, that means $u_{ex} = \Phi_{sp}^{4/3}$. Since u_{ex} is smooth on $B_1(0)$ we work with one mesh $h = h_1 = h_2$. This is also justified by the experimental order of convergence for the L^2-error of $p_h - \nabla u_h$ as can be seen in Figure 5.10. Our starting point for the algorithm is the identity map on $B_1(0)$, the stopping criterion is $\varepsilon = 10^{-6}$ and the time-step size is $\tau = h$. We compute the errors $\mathrm{err}_{\ell,Y} := ||u_h^* - X||_Y$ for $Y = L^2, L^\infty$ or $W^{1,2}$, where ℓ denotes the refinement step of the mesh. Expecting an estimate of the form $\mathrm{err}_{\ell,Y} \sim h_\ell^{\mathrm{eoc}_Y}$ we can compute the experimental order of convergence using

$$\mathrm{eoc}_Y = \frac{\log(err_{\ell+1,Y}/err_{\ell,Y})}{\log(h_{\ell+1}/h_\ell)}.$$

For the proposed model problem we compute

$$eoc_{H^1} \sim 1, \quad eoc_{L^2} \sim 2 \quad \text{and} \quad eoc_{L^\infty} \sim 2,$$

as can be seen in Figure 5.10. This is comparable to the results stated in **??**. However, we emphasize that we have no error estimates for our method.

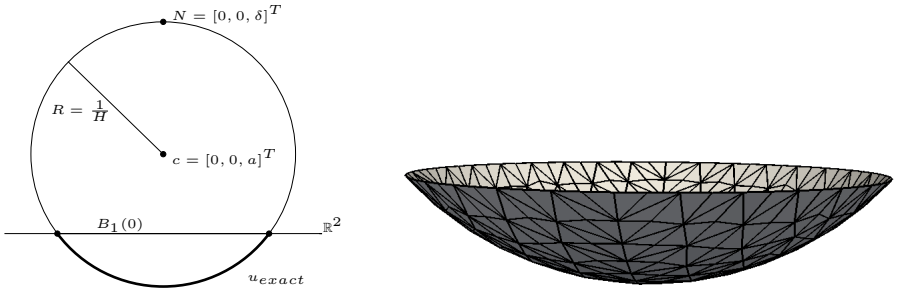

Figure 5.9.: Stereographic projection of $B_1(0)$ from N to the ball $B_R([0,0,a])$ as exact solution: A sketch of the geometry that leads to the formula for u_{ex} and an output from our numerical algorithm with $H = 0.75$ and 289 nodes.

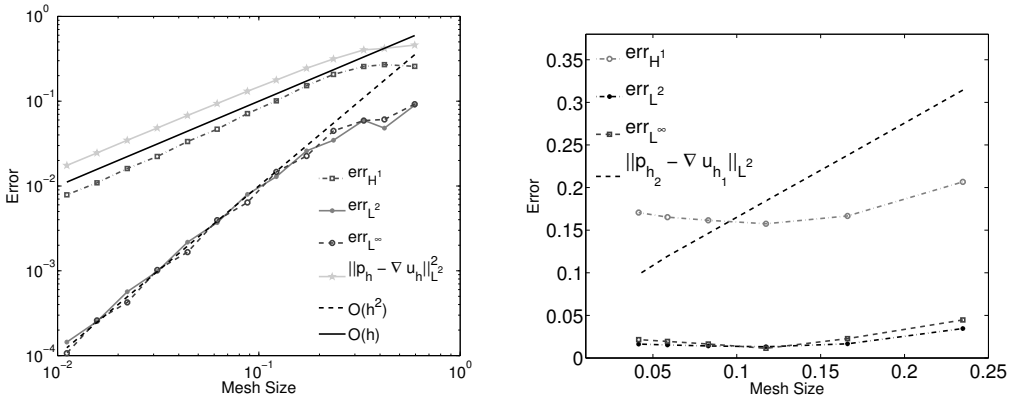

Figure 5.10.: Errors for a sequence of triangulations and $H = 0.75$ (left). Note that the experimental order of convergence of $||p_h - \nabla u_h||$ is one. Same setting ($H = 0.75$) with fixed $h_1 = 0.332$ and varying h_2 (right). The error $||p_{h_2} - \nabla u_{h_1}||$ becomes smaller for $h_2 < h_1$ while the L^2-, H^1- and L^∞-error stay almost the same. Thus, in this case it is not worth working with a finer grid for the auxiliary variable.

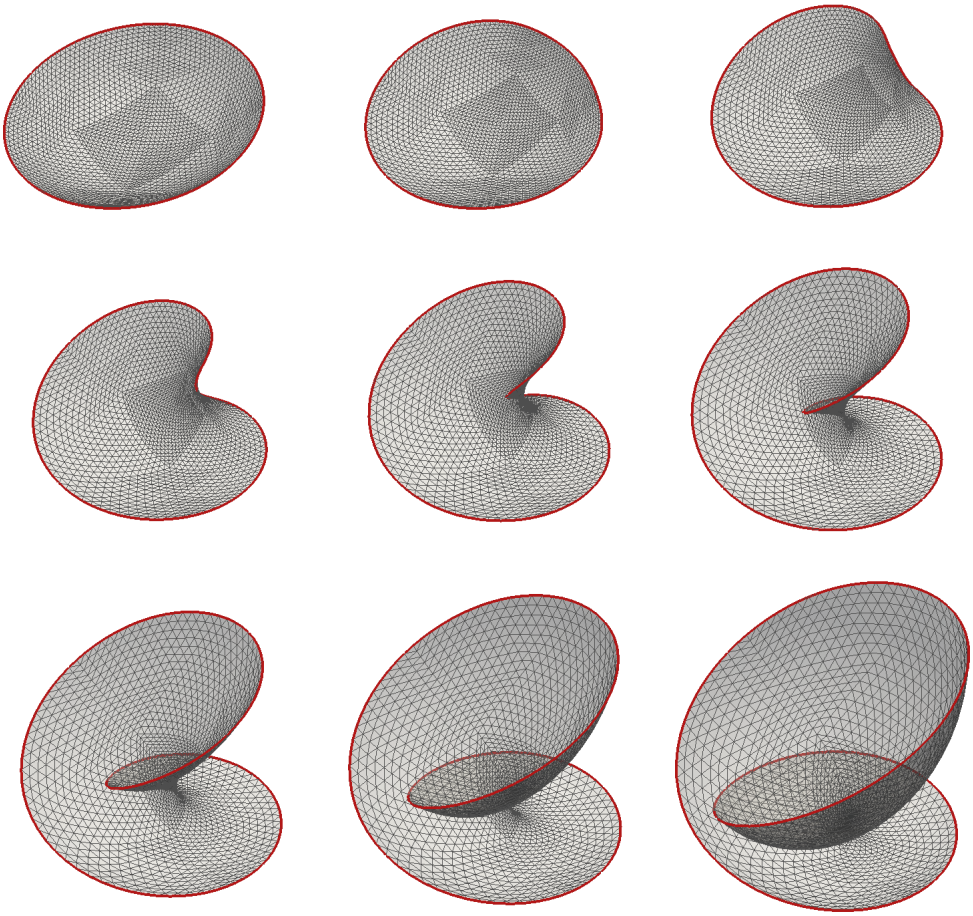

Figure 5.11.: Homotopy of the boundary curve from $\partial B_1(0)$ to $\Gamma = \gamma([0, 2\pi])$ for γ given by (5.2.1) and discrete surface spanning Γ: Snapshots of the homotopy at the iteration steps $i = 5k$ for $k = 0, \ldots, 8$.

5.2.3. More involved boundary curves

In this section we discuss the performance of our algorithm for different boundary curves $\Gamma \subset \mathbb{R}^3$ and different values of $H = H_0 \in \mathbb{R}$. We start with the curve

$$\gamma : [0, 2\pi] \to \mathbb{R}^3, t \mapsto \Big((1 + 0.1\cos 3t)\cos 2t,\ (1 + 0.1\cos 3t)\sin 2t,\ \sin t\Big) \tag{5.2.1}$$

for $H_0 = 0.8$. We use $i_{max} = 40$, a triangulation of $B_1(0)$ with $h = 0.016$ and $\tau = h$. Although we cannot guarantee conformality of the output we observe a good mesh quality with no degenerating elements. Snapshots of the evolution can be seen in Figure 5.11.

In a second experiment we use the curve

$$\gamma : [0, 2\pi] \to \mathbb{R}^3, t \mapsto \Big(R\cos t - \frac{R^3}{3}\cos 3t,\ R\sin t + \frac{R^3}{3}\sin 3t, R^2\cos 2t\Big) \tag{5.2.2}$$

for $R = 2.0$ and $H_0 = 0.15$. As above we set $i_{max} = 40$, use a triangulation of $B_1(0)$ with $h = 0.016$ and we set $\tau = h$. Snapshots of the evolution can be seen in Figure 5.13. Both boundary curves have also been investigated in [33] with different values for H_0.

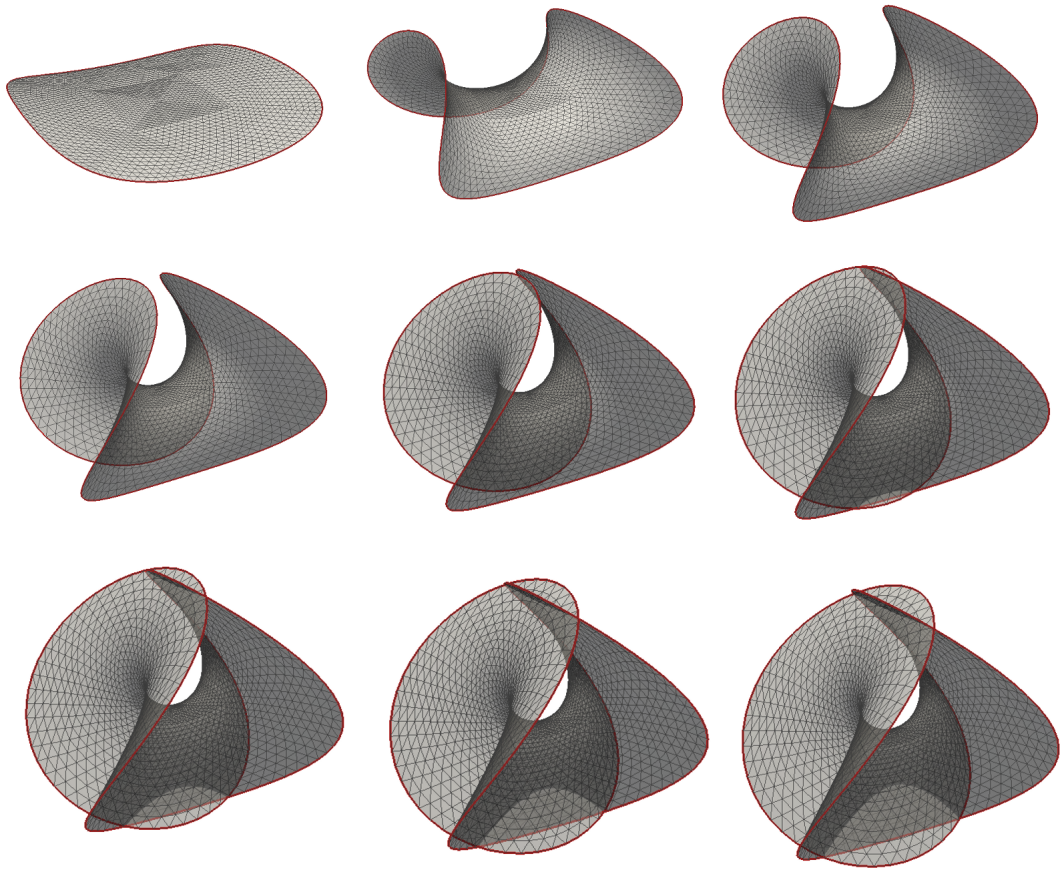

Figure 5.12.: Homotopy of the boundary curve from $\partial B_1(0)$ to $\Gamma = \gamma([0, 2\pi])$ for γ given by (5.2.2) and discrete surface spanning Γ: Scaled snapshots of the homotopy at the iteration steps $i = 5k$ for $k = 0, \ldots, 8$.

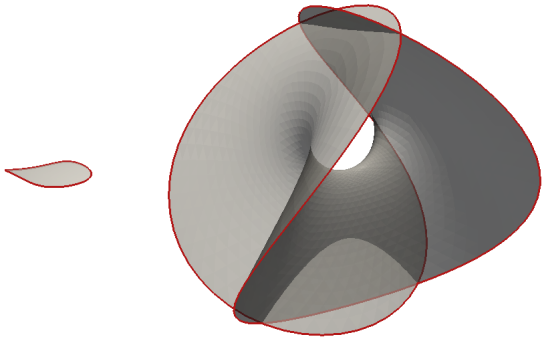

Figure 5.13.: Homotopy from the identity to $\Gamma = \gamma([0, 2\pi])$ for γ given by (5.2.2): Snapshots after the first iteration step (left) and at the end of the algorithm (right), now unscaled, to stress the different sizes.

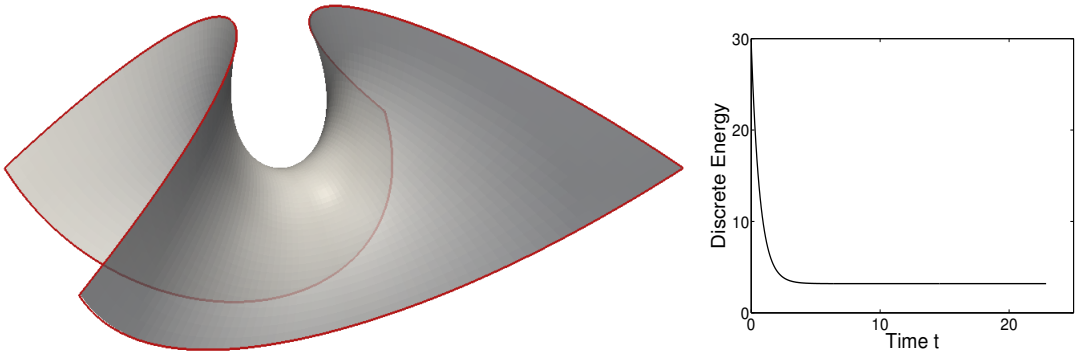

Figure 5.14.: Approximation of the Enneper surface $\Gamma = X(M)$ for $M = (-1.25, 1.25)^2$ and the parametrization X from (5.2.3) and energy curve during the simulation. Starting point for our computation is a perturbation of $\mathcal{I}_h X$ as defined in the setting of the experiment. Here, we use a uniform triangulation of M with mesh-size $h = 5\sqrt{2}2^{-8}$, time-step size $\tau = h$ and $\varepsilon = 10^{-6}$ as stopping criterion for the mixed H^1-flow. At the end of the computation we have $||u_h^* - \mathcal{I}_h X||_{L^\infty} = 1.42 * 10^{-4}$. A rapid decay of the initial energy is due to the non-smooth initial data. We remark that the energy is always positive and conclude that the sequence of outputs stays in $\mathbb{V}_h$ as required for the termination of the algorithm.

5.2.4. The Enneper surface

At the end of this section we perform another experiment for which we know the exact solution. The Enneper surface is a minimal surface ($H = 0$) and can be parametrized by

$$X : (\xi_1, \xi_2) \mapsto \left[\frac{\xi_1}{3}(1 - \frac{\xi_1^2}{3} + \xi_2^2), -\frac{\xi_2}{3}(1 - \frac{\xi_2^2}{3} + \xi_1^2), \frac{\xi_1^2 - \xi_2^2}{3}\right]^T. \tag{5.2.3}$$

To see that $X(M)$, $M \subset \mathbb{R}^2$ a bounded domain, is minimal we use the definitions of the first and second fundamental form as well as the formula for the mean curvature from Chapter 1 and compute

$$X_1 := \frac{\partial X}{\partial \xi_1} = \frac{1}{3}[1 - \xi_1^2 + \xi_2^2, -2\xi_1\xi_2, 2\xi_1]^T, \quad X_2 := \frac{\partial X}{\partial \xi_2} = \frac{1}{3}[2\xi_1\xi_2, -1 - \xi_1^2 + \xi_2^2, 2\xi_2]^T.$$

We conclude that

$$X_1 \bullet X_2 = 0 \quad \text{as well as} \quad |X_1|^2 = |X_2|^2.$$

Therefore,

$$g = |X_1|^2 \mathrm{id}_{2\times 2} \quad \text{and} \quad g^{-1} = |X_1|^{-2} \mathrm{id}_{2\times 2}.$$

Note, that $|X_1|^2 = 0$ would imply that $\xi_1 = 0$ and then $1 + \xi_2^2 = 0$. For $\xi_2 \in \mathbb{R}$ this is not possible and, therefore, $g^{-1} : M \to \mathbb{R}^{2\times 2}$ is well-defined. A more lengthy computation results in

$$A = \begin{bmatrix} \frac{\partial \nu}{\partial \xi_1} \bullet X_1 & \frac{\partial \nu}{\partial \xi_1} \bullet X_2 \\ \frac{\partial \nu}{\partial \xi_2} \bullet X_1 & \frac{\partial \nu}{\partial \xi_2} \bullet X_2 \end{bmatrix} = \begin{bmatrix} \frac{2}{3} & 0 \\ 0 & -\frac{2}{3} \end{bmatrix},$$

where we use that $\nu = \frac{X_1 \times X_2}{|X_1 \times X_2|}$. Finally, we obtain that

$$H = \sum_{i,j} g^{ij} A_{ij} = |X_1|^2 \left(\frac{2}{3} - \frac{2}{3}\right) = 0.$$

Setting of the experiment. For a sequence of uniform triangulations of the square $M = (-1.25, 1.25)^2$ with mesh-sizes $h_\ell = 5\sqrt{2}2^{-\ell}$ for $\ell = 4, \dots, 9$ we compute approximations of the

	$\|\|u_h^* - \mathcal{I}_h X\|\|_{L^2}$		$\|\|u_h^* - \mathcal{I}_h X\|\|_{L^\infty}$		$\|\|u_h^* - \mathcal{I}_h X\|\|_{W^{1,2}}$	
h	err_{L^2}	eoc	err_{L^∞}	eoc	$err_{W^{1,2}}$	eoc
0.44194174	$2.538 * 10^{-2}$		$2.004 * 10^{-2}$		$9.306 * 10^{-2}$	
0.22097087	$9.120 * 10^{-3}$	1.476	$6.156 * 10^{-3}$	1.703	$4.432 * 10^{-2}$	1.070
0.11048543	$2.646 * 10^{-3}$	1.785	$1.865 * 10^{-3}$	1.723	$1.774 * 10^{-2}$	1.320
0.05524272	$7.065 * 10^{-4}$	1.905	$5.250 * 10^{-4}$	1.829	$6.633 * 10^{-3}$	1.420
0.02762136	$1.821 * 10^{-4}$	1.956	$1.423 * 10^{-4}$	1.883	$2.403 * 10^{-3}$	1.465
0.01381067	$4.618 * 10^{-5}$	1.979	$3.769 * 10^{-5}$	1.916	$8.573 * 10^{-4}$	1.487

Table 5.5.: Different errors and experimental orders of convergence for the Enneper surface defined through (5.2.3).

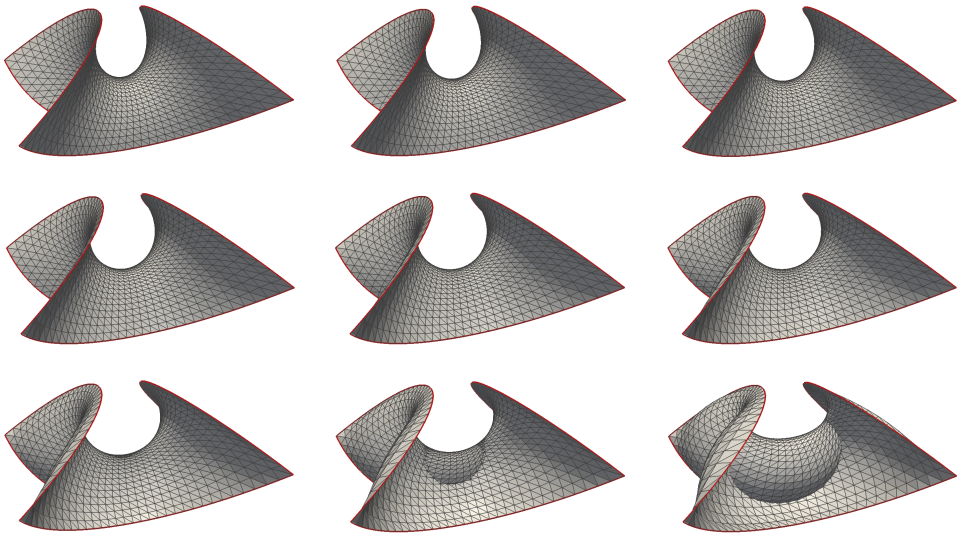

Figure 5.15.: Various solutions for the boundary curve $\Gamma := X(\partial M)$ for X given by (5.2.3) and $M = (-1.25, 1.25)^2$. We use a uniform triangulation of M with mesh-size $h = 5\sqrt{2}2^{-7}$, a perturbation of $\mathcal{I}_h X$ in the interior of M as initial data, $\tau = h$ and $\varepsilon = 10^{-6}$ as stopping criterion. Stationary points of the discrete energy $E^h_{H_0}(p_h, u_h)$ for $H_0 = 0.2, 0.4, \ldots, 1.8$ are displayed from top to bottom and left to right. We observe that for $H_0 > 1.8$ the algorithm does not terminate.

Enneper surface. For the initial data we use the function $\text{rand}_{h_\ell} \in [\mathcal{S}^1_0(\mathcal{T}_{h_\ell})]^3$ which takes random values in $(-0.1, 0.1)^3$ and set

$$u_0^{h_\ell}(z) = \mathcal{I}_h X + \text{rand}_{h_\ell}(z) \quad \text{for all} \quad z \in \mathcal{N}_{h_\ell} \setminus \partial M,$$

as well as $p^0_{h_\ell} := P_0^{h_\ell}(\nabla u_{h_\ell})$ and $H_0 = 0$. We hereafter compute the errors $\text{err}_{\ell,Y} := ||u_h^* - X||_Y$ for $Y = L^2, L^\infty$ or $W^{1,2}$ and the experimental orders of convergence, see Table 5.5.

Chapter 6.

Geometric Flows and Applications from Biology

In this chapter we discuss finite element methods for geometric flows which attracted a great many numerical analysists in the last years, see for example [10, 21, 27, 31, 36, 37, 66]. We are mainly interested in the L^2-gradient flow for energies of the form

$$E(\Gamma) = \int_\Gamma \frac{\kappa_0}{2}(H - H_0)^2 + \frac{\kappa_G}{2} K \,\mathrm{d}\sigma. \tag{6.0.1}$$

Here H is the mean curvature and K the Gauss curvature of a closed surface $\Gamma \subset \mathbb{R}^3$ and κ_0 and κ_G are the associated moduli of elasticity. By Gauss-Bonnet, the integral of K is a topological constant on a closed surface and can be neglected for evolutions in one topological class of surfaces. The quantity H_0 is usually referred to as *spontaneous curvature* and describes the preferred value of curvature induced by the ambient space on a membrane in equilibrium. Furthermore, we impose constraints on the enclosed volume $V(\Gamma)$ and on the surface area $A(\Gamma)$. First we discuss two main settings:

- $H_0 = 0$, $\kappa_0 = 1$ and $\kappa_G = 0$: The Willmore energy.
- $H_0 = 0$, $\kappa_0 = 1$, $\kappa_G = 0$, $V(\Gamma) = V_0$ and $A(\Gamma) = A_0$: The Helfrich energy [45].

Afterwards we present our results from [16] where we discuss a model for the shape of lipid bilayer membranes which takes into account the coupling with a surfactant distributed on the surface.

We give a quick introduction to surface finite elements and the numerical treatment of the Willmore- and Helfrich-flow as it was introduced in [21] and [10]. Equiped with these techniques we proceed with our model for surfactants and biomembranes.

6.1. Willmore- and Helfrich-flow

We start with the energy (6.0.1) for $H_0 = const$, $\kappa_0 = 1$ and $\kappa_G = 0$. We compute the first variation, using Lemma 1.2.10

$$\frac{\mathrm{d}}{\mathrm{d}s}\Big|_{s=0} E(\Gamma_s) = \int_{\Gamma_t} (H - H_0)(\Delta_{\Gamma_t}\phi + \phi|\nabla_{\Gamma_t}\phi|^2)\,\mathrm{d}\sigma - \frac{1}{2}\int_{\Gamma_t}(H - H_0)^2 H\phi\,\mathrm{d}\sigma.$$

We want to compute stationary points of (6.0.1) and consider the L^2-gradient flow. We denote by $v = v(t) : \Gamma_t \to \mathbb{R}$ the normal velocity of the evolving surface $\Gamma_t \subset \mathbb{R}^3$ at time $t \in [0, T)$ and solve

$$(v, \phi)_{\Gamma_t} = -\frac{\mathrm{d}}{\mathrm{d}s}\Big|_{s=t} E(\Gamma_s) = -(\nabla_{\Gamma_t} H, \nabla_{\Gamma_t}\phi)_{\Gamma_t} + ((H - H_0)|\nabla_{\Gamma_t}\nu|^2, \phi)_{\Gamma_t} - \frac{1}{2}((H - H_0)^2 H, \phi)_{\Gamma_t},$$

for all $\phi \in C_c^\infty(\Gamma_t; \mathbb{R})$ and $t \in [0, T)$. Here $(\cdot, \cdot)_{\Gamma_t}$ denotes the L^2-inner product on Γ_t. If we consider the Helfrich energy, then the velocity v must satisfy

$$\int_{\Gamma_t} v\,\mathrm{d}\sigma = 0 \quad \text{and} \quad \int_{\Gamma_t} Hv\,\mathrm{d}\sigma = 0. \tag{6.1.1}$$

We have two possibilities at hand to ensure conservation of volume and surface area numerically. One is to compute the Lagrangian multipliers explicitly, as it was proposed in [10], the other is to compute v in such a way that equations (6.1.1) are satisfied. This can be done via a Newton iteration which guarantees conservation of these quantities up to machine precission.

6.1.1. Finite elements on surfaces

The time discretization of the gradient flow leads to a family of surfaces $(\Gamma^j)_{j\in\mathbb{N}}$ related to the time-steps t_j. Let Γ_h^j be a polyhedral approximation of Γ^j consisting of flat triangles with maximal diameter less than $h>0$. Since Γ_h^j is the union of triangles $T\in\mathcal{T}^j$, we identify the triangulation $\mathcal{T}^j$ and the discrete surface Γ_h^j. Let $\mathbb{V}^j=\mathbb{V}(\Gamma_h^j)$ be the space of all continuous functions on Γ_h^j whose restriction to the triangles are affine. Moreover let $\mathbb{C}_0^j=\mathbb{C}_0(\Gamma_h^j)$ denote the space of all functions that are constant on every triangle and define the averaging operator $\mathcal{A}^j:\mathbb{C}_0^j\to\mathbb{V}^j$, $v\mapsto\sum_a v_a\varphi_a$, where $v_a:=\frac{1}{|\omega_a|}\int_{\omega_a}v(x)\mathrm{d}x$ and $(\varphi_a)_{a\in\mathcal{N}^j}$ is the standard nodal basis of $\mathbb{V}^j$. Here $\mathcal{N}^j=\mathcal{N}(t_j)=\{a_1(t_j),\dots,a_N(t_j)\}$ is the set of all nodes in Γ_h^j, $\omega_a=\mathrm{supp}\varphi_a$, and the map $t_j\mapsto a(t_j)\in\mathbb{R}^3$ is the trajectory on which a node $a\in\mathcal{N}$ moves in time as the surface is changing its shape. If $\widetilde{\nu}^j\in\mathbb{C}_0^j$ stands for the the piecewise constant outer normal to Γ_h^j, then

$$\nu^j:=\mathcal{A}^j(\widetilde{\nu}^j)\in[\mathbb{V}^j]^3 \tag{6.1.2}$$

is a piecewise linear reconstruction of $\widetilde{\nu}^j$. For a given function $\phi^{j-1}\in\mathbb{V}^{j-1}$ we define $G^j\circ\phi^{j-1}\in\mathbb{V}^j$ by $(G^j\circ\phi^{j-1})(a(t_j))=\phi^{j-1}(a(t_{j-1}))$ for all $a\in\mathcal{N}^j$. For a better readability we will denote $G^j\circ\phi^{j-1}$ also by ϕ^{j-1} if no confusion is possible.

6.1.2. Discretization

We start with the time discretization. Given the surface $\Gamma^{j-1}\subset\mathbb{R}^3$ at time t_{j-1} we follow the ideas in [30] to parametrize Γ^j at time t_j over Γ^{j-1}. We thus look for $X^j:\Gamma^{j-1}\to\mathbb{R}^3$ and set $\Gamma^j=X^j(\Gamma^{j-1})$. As in [10], we approximate the normal velocity via

$$v^j\approx\frac{1}{\tau}\big(X^j-\mathrm{id}_{\Gamma^{j-1}}\big)\bullet\nu^{j-1},$$

where $\nu^{j-1}:\Gamma^{j-1}\to\mathbb{S}^2$ is the outer unit normal to Γ^{j-1}. Now, again, using an idea from [30] to compute H^j we discretize the crucial geometric identity $\Delta_\Gamma X=H\nu$ [30, 31]:

$$\Delta_{\Gamma^{j-1}}X^j=H^j\nu^{j-1}.$$

Notice that we compute the scalar mean curvature H^j, as in [10], and not the mean curvature vector, as in [21, 31]. We define the semi-implicit discretization $\Psi_E^{j-1,j}:=\Psi_E^{j-1,j}(H^j,H^{j-1},\nu^{j-1})\in\mathbb{V}^{j-1}$ of the gradient of the energy given by

$$\Big(\Psi_E^{j-1,j},\phi\Big)_{\Gamma_h^{j-1}}:=-\Big(\nabla_\Gamma H^j,\nabla_\Gamma\phi\Big)_{\Gamma_h^{j-1}}-\frac{1}{2}\Big(H^j(H^{j-1}-H_0)^2,\phi\Big)_{\Gamma_h^{j-1}}+\Big((H^{j-1}-H_0)|\nabla_\Gamma\nu^{j-1}|^2,\phi\Big)_{\Gamma_h^{j-1}}$$

for all $\phi\in\mathbb{V}^{j-1}$.

6.1.3. Volume and mass constraints

We recall a method for the conservation of area and volume proposed in [21]. We introduce the extended energy

$$F(\Gamma)=E(\Gamma)+\rho_1\left(V(\Gamma)-V_0\right)+\rho_2\left(A(\Gamma)-A_0\right),$$

and compute the first variation with respect to Γ:

$$\Big\langle\frac{\delta F}{\delta\Gamma},\phi\Big\rangle=\Big\langle\frac{\delta E}{\delta\Gamma},\phi\Big\rangle+\rho_1\int_\Gamma\phi\mathrm{d}\sigma-\rho_2\int_\Gamma H\phi\mathrm{d}\sigma.$$

The normal velocity of the Helfrich flow at time $t\in[0,T)$ is defined by $(v_{Hel},\phi)_{\Gamma_t}=-\Big\langle\frac{\delta F}{\delta\Gamma},\phi\Big\rangle$. We split it into three parts

$$v_{Hel}=v_E+\rho_1v_V+\rho_2v_A,$$

and compute in each time-step v_E^j, v_V^j, v_A^j:

$$(v_E^j,\phi_h)_{\Gamma_h^{j-1}} = -\Big(\Psi_E^{j-1,j},\phi_h\Big)_{\Gamma_h^{j-1}},\quad (v_V^j,\phi_h)_{\Gamma_h^{j-1}} = -(1,\phi_h)_{\Gamma_h^{j-1}},\quad (v_A^j,\phi_h)_{\Gamma_h^{j-1}} = (H^j,\phi_h)_{\Gamma_h^{j-1}}.$$

The idea is to find ρ_1^j and ρ_2^j so that volume and area are conserved. We define the function

$$f^j:\mathbb{R}^2\to\mathbb{R}^2,\quad (\rho_1,\rho_2)\mapsto \begin{bmatrix} V(\Gamma_h^j(\rho_1,\rho_2)) - V(\Gamma_h^{j-1}) \\ A(\Gamma_h^j(\rho_1,\rho_2)) - A(\Gamma_h^{j-1}) \end{bmatrix},$$

for $\Gamma_h^j(\rho_1,\rho_2) = X(\Gamma_h^{j-1},\rho_1,\rho_2)$, $X = X^{j-1} + \tau(v_E^j + \rho_1 v_V^j + \rho_2 v_A^j)$. Now we use a Newton iteration to compute a solution (ρ_1^j,ρ_2^j) of $f(\rho_1,\rho_2) = 0$ and set $X^j = X^{j-1} + \tau(v_E^j + \rho_1^j v_V^j + \rho_2^j v_A^j)$ and $\Gamma_h^j = X^j(\Gamma_h^{j-1})$.

6.1.4. Semi-implicit fully discrete Helfrich flow

We start with an initial polyhedral surface Γ_h^0 and a time-step size $\tau > 0$. We set $j := 1$ and iterate on j the following steps:

1. Compute $(\widetilde{X}^j, H^j) \in [\mathbb{V}^{j-1}]^3 \times \mathbb{V}^{j-1}$ satisfying

$$\frac{1}{\tau}\Big((\widetilde{X}^j - X^{j-1})\bullet\nu^{j-1},\phi\Big)_{\Gamma_h^{j-1}} = -\Big(\Psi_E^{j-1,j},\phi\Big)_{\Gamma_h^{j-1}},$$
$$\Big(\nabla_{\Gamma_h^{j-1}}\widetilde{X}^j,\nabla_{\Gamma_h^{j-1}}\eta\Big)_{\Gamma_h^{j-1}} = -\Big(H^j,\eta\bullet\nu^{j-1}\Big)_{\Gamma_h^{j-1}},$$

   for all $\phi\in\mathbb{V}^{j-1}$ and all $\eta\in\mathbb{V}(\Gamma_h^{j-1};\mathbb{R}^3)$.

2. Set

$$v_E = \frac{1}{\tau}\big(\widetilde{X}^j - X^{j-1}\big)\bullet\nu^{j-1},\quad v_V = -1,\quad v_A = H^j,$$

   and compute (ρ_1^j,ρ_2^j) such that $f^j(\rho_1^j,\rho_2^j) = 0$. Set

$$X^j = X^{j-1} + \tau(v_E + \rho_1^j v_V + \rho_2^j v_A)\nu^{j-1}\quad\text{and}\quad \Gamma_h^j = \{X^j(x) :\, x\in\Gamma_h^{j-1}\}.$$

3. Set $X^j := G^j\circ X^j = \mathrm{id}_{\Gamma_h^j}$, $j = j+1$ and go to (1).

Remark 6.1.5 *(i) As a stopping criterion for the discrete evolution we use that the change of the discrete energy*

$$E_h(\Gamma_h^j) := \int_{\Gamma_h^j}\frac{1}{2}(H^j - H_0)^2\,d\sigma$$

in two consecutive time-steps is less than 10^{-5}.
(ii) If we denote by $\mathbf{H} = H\nu$ *the mean curvature vector, then [21] it is possible to show that the variation of the Willmore energy can be expressed as follows*

$$\frac{d}{ds}\Big|_{s=0}E(\Gamma_s) = \int_\Gamma \nabla_\Gamma(\phi\nu):\nabla_\Gamma\mathbf{H}\,d\sigma - \int_\Gamma(\nabla_\Gamma X + \nabla_\Gamma X^T)\nabla_\Gamma(\phi\nu):\nabla_\Gamma\mathbf{H} + \int_\Gamma \mathrm{div}_\Gamma(\phi\nu)\mathrm{div}_\Gamma\mathbf{H}.$$

Note that this formulation circumvents the computation of $|\nabla_\Gamma\nu|^2$.

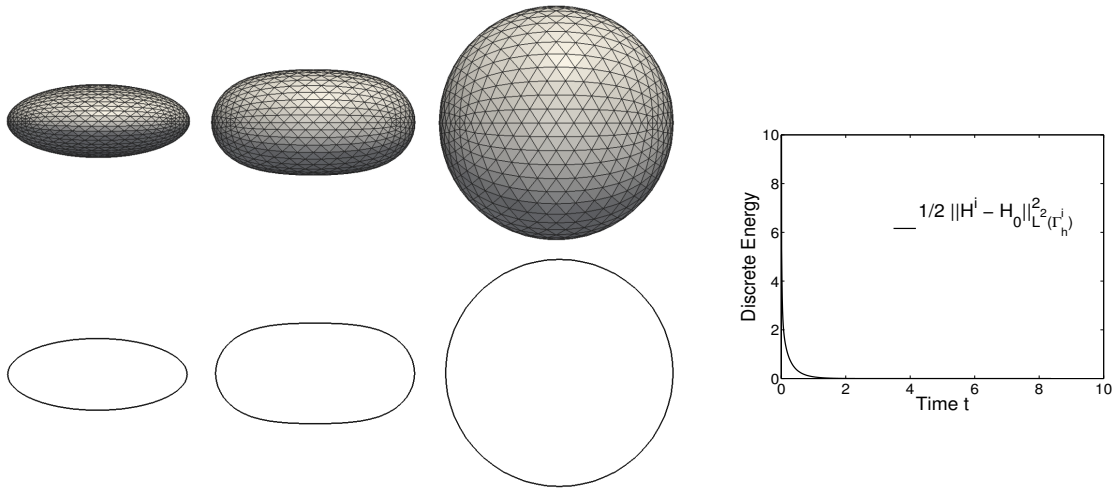

Figure 6.1.: Evolution from a prolate ellipsoid to a sphere of radius $R = \frac{4}{3}$ corresponding to the spontaneous curvature $H_0 = \frac{3}{2}$: Snapshots of the evolution at times $t = 0.00$, $t = 0.01$ and $t = 1.00$. Whole discrete surface (upper row) and cut through the plane $x_1 = 0$ (lower row). For a triangulation of the unit sphere, consisting of card $\mathcal{T} = 2048$ elements and card $\mathcal{N} = 1026$ nodes we use the initial surface $\Gamma_h^0 := \{\tilde{a} : \tilde{a} = a_1 e_1 + a_2 e_2 + 0.4 a_3 e_3,\ a \in \mathcal{N}\}$. Furthermore, we use the time-step size $\tau = 10^{-2}$ and as a stopping criterion we set $\varepsilon = 10^{-6}$. The right plot depicts the decay of the discrete energy $E_h^i = \frac{1}{2}||H^i - H_0||^2_{L^2(\Gamma_h^i)}$ during the evolution. At the end time $t = 8.37$ we have a discrete energy $E_h^* = 2.58 * 10^{-10}$.

6.2. FEM for director fields on flexible surfaces - Introduction and discussion of the proposed model

We turn to the question of how to predict the shape of a cell bounded by a lipid bilayer membrane. Modelling this has inspired a significant body of research in the past twenty years ranging from purely mechanical descriptions to advanced mathematical analysis. We refer, e.g., to the papers [23, 45, 38, 51] for the discussion of the shape of a red blood cell and the basic models developed for this purpose. Excellent reviews of the topic can be found in [69, 60]. Almost all of these models share the basic structure given by an energy functional of the form (6.0.1). Where again we may neglect the summand with the Gaussian curvature because we stay in one topological class.

In the first part of this chapter we considered H_0 constant, the usual choice, but it might also depend on another variable such as the bilipid concentration [19, 28, 37, 36, 61, 76]. Alternatively, H_0 might be induced by an underlying director field as in [55] and our models below. The shape derivative of (6.0.1) is given in [10] for H_0 constant and in [29] for H_0 depending on the position.

In a broader context, the question to find the shape of a cell is surprisingly similar to the related problem of determining the shape of an interface between two immiscible liquids with or without surfactants. The prediction of the structure and the elastic properties of such interfaces is still a challenging problem in applied mathematics and physics and has been investigated by a wide range of techniques reaching from molecular dynamics simulations to continuum descriptions in coarse grained models; see [55] that inspired this work. These similarities motivate to explore model energies for membranes which combine classical elasticity terms like those present in (6.0.1) with terms which couple the local orientation of the surfactants or the lipid molecules with the curvature of the interface or the membrane, respectively; a related publication, which was the starting point for this work is [15]. These energy contributions are relevant in the gel phase of the membrane. We investigate a novel model for the shape of a lipid bilayer membrane which takes into account a coupling between the

curvature $H = -\mathrm{div}_\Gamma \nu$ of the membrane Γ and the local orientation of the lipid molecules, described by a director field n. The nonlinear model is governed by the energy

$$E(\Gamma, n) = \int_\Gamma \Big(\frac{1}{2} \big| \mathrm{div}_\Gamma \nu - \delta \mathrm{div}_\Gamma n \big|^2 + \frac{\lambda}{2} \big| \nabla_\Gamma n \big|^2 \Big) \mathrm{d}\sigma, \tag{6.2.1}$$

where div_Γ and ∇_Γ are the tangential divergence and gradient operators and $\lambda > 0$. Comparing with (6.0.1), we can interpret $H_0 = -\delta \mathrm{div}\, n$ with $\delta \in \mathbb{R}$ as an induced spontaneous curvature on Γ due to the coupling with n. In order to develop an effective approximation scheme, we first linearize this model locally in a flat region of Γ and represent Γ as a graph with height u (Monge gauge). The resulting model is a special case of that introduced by Laradji and Mouritsen [55].

We study this model, propose a practical FEM for an L^2-gradient flow of this functional, and state a priori estimates, which lead to existence of a limiting solution pair (u, n). We also explore the dynamics of defects using our FEM. Since this part of the paper was mainly done by the co-authors we focus here on the nonlinear functional (6.2.1), derive an L^2-gradient flow, use the ideas from the previous sections and show simulations of defects. The insight gathered from the linearized graph case turns out to be useful in understanding the nonlinear regime.

6.2.1. A model for surfactants

The starting point of our analysis is the Ginzburg-Landau model in Laradji and Mouritsen [55] which was originally developed for surfactant monolayers at liquid-liquid interfaces with a locally varying density of surfactants ϕ. The formulation assumes that this interface is given by a two-dimensional surface Γ in the three-dimensional ambient space described by a height function $u : \Omega \to \mathbb{R}$. The model in [55], which is discussed below, is an attempt to match deviations from the bending energy model (6.0.1) with $H_0 = 0$ for low wave numbers, which were detected via molecular dynamics computations. The total energy of a configuration is assumed to be given by (see Appendix A in [55])

$$\begin{aligned} \mathcal{F}(u, \phi, n) \;=\; \int_\Omega \Big(& \xi \sqrt{1 + |\nabla u|^2} + \frac{\kappa}{2} |\operatorname{div} \nu|^2 + \frac{a}{2}\, \phi^2 + \frac{c}{2}\, |\nabla \phi|^2 - \mu_s \phi \\ & + \frac{g(\phi)}{2}\, |n|^2 - h(\phi) \nu \bullet n + \frac{k(\phi)}{2} |\operatorname{div} n|^2 - \frac{\ell(\phi)}{2}\, \operatorname{div} \nu \operatorname{div} n \Big) \mathrm{d}x \end{aligned}$$

with suitable constants ξ, κ, a, c, μ_s and nonnegative functions ϕ, h, g, k, and ℓ. Here ∇ and div denote the planar differential operators gradient, i.e., $\nabla z = (\partial_1 z, \partial_2 z)$ for a scalar function z, and divergence, i.e., $\operatorname{div} F = \partial_1 F_1 + \partial_2 F_2$ for a vectorfield $F = (F_1, F_2, F_3)$, whereas $\nu = (-\nabla u, 1)/\sqrt{1 + |\nabla u|^2}$ is the normal to the graph of u. In [55] it is shown that the surface tension ξ is vanishingly small for densities ϕ close to one. Therefore we may assume that $\xi \approx 0$ and that ϕ is nearly equal to 1 and discard all terms depending on ϕ and ξ in $\mathcal{F}$. As a further simplification and in order to focus on the interaction of orientation and curvature, we assume that n is a unit vector and we omit for the moment the term proportional to $\nu \bullet n$ which favors alignment of n along ν. This leads to the following model which contains the essential features

$$\mathcal{F}(u, n) \;=\; \int_\Omega \Big(\frac{\kappa}{2} |\operatorname{div} \nu|^2 + \frac{k}{2} |\operatorname{div} n|^2 - \frac{\ell}{2}\, \operatorname{div} \nu \operatorname{div} n \Big) \mathrm{d}x,$$

with constant parameters κ, k, ℓ. Upon completing the square, one obtains

$$\mathcal{F}(u, n) \;=\; \int_\Omega \Big(\frac{\kappa}{2} \Big(\operatorname{div} \nu - \frac{\ell}{2\kappa}\, \operatorname{div} n \Big)^2 + \Big(\frac{k}{2} - \frac{\ell^2}{8\kappa} \Big) \, |\operatorname{div} n|^2 \Big) \mathrm{d}x.$$

Comparing with (6.0.1) and (6.2.1), we interpret this formula as saying that the local arrangement of the surfactants leads to a (position dependent) spontaneous curvature

$$H_0 = -\frac{\ell}{2\kappa}\, \operatorname{div} n\,,$$

which becomes less important for large values of the bending rigidity κ. We finally observe that in order to bound the energy it is sufficient to assume that

$$\frac{k}{2} - \frac{\ell^2}{8\kappa} \geq 0\,.$$

The corresponding positive convex term $|\operatorname{div} n|^2$ in the energy gives us coercivity of the functional $\mathcal{F}(u,n)$ but it is insufficient for devising a practical numerical scheme, deriving a priori bounds for discrete solutions which allow passing to the limit, and showing existence of a minimizing pair (u,n). We thus modify the model upon replacing $|\operatorname{div} n|^2$ with the usual Frank energy $|\nabla n|^2$ of the director field n, which is ubiquitous in the theory of liquid crystals. As the maximal mesh size tends to zero we may pass to the limit for n, in view of the enhanced H^1 regularity, as well as to enforce the unit length constraint on n via a projection method due to Alouges [1], and extended in [11] to FEM. Such a projection does not increase the energy of the Dirichlet integral, but the analogous assertion is not true for the energy of the divergence.

6.2.1.1. A model for biomembranes

Our interest in augmented Canham-Helfrich models originates in the search for models that allow one to predict the experimentally observed coarsening mechanisms in membranes in the gel phase based on recombination of topological defects [52]. Related models, based on the assumption that this recombination is driven by an interaction between the director field and the curvature, have been proposed in [73] and analyzed in [15]. See also [39] for a closely related approach.
In the model in [73] the lipid monolayer is considered in the gel phase and it is assumed that the director field is oriented in a fixed angle relative to the surface normal [65]. Therefore it suffices to study the tangential part m of the director field which is itself a vector field of fixed length. The related energy functional in a linearized setting is

$$E(u,m) = \frac{\kappa}{2}\int_\Omega |\Delta u|^2 \mathrm{d}x + \frac{C_q}{2}\int_\Omega |\nabla m|^2 \mathrm{d}x - \delta \int_\Omega D^2 u : (m\otimes m - \frac{1}{2}\,I)\mathrm{d}x,$$

subject to a length constraint for m. Our numerical experiments for a rigidly imposed length constraint show that the coupling between u and m is too weak in the regime of parameters which define a well-posed minimization problem in order to simulate the observed recombination of defects [15]. The coupling proposed in the present model is stronger in the sense that it involves one more derivative. It also allows a direct extension to the nonlinear model (6.2.1) on closed surfaces; cf. Section 6.2.5.

6.2.2. Linear model on graphs

We give a linearized version of (6.2.1) for surfactants and augment the obtained energy by a term which penalizes deviations of the out of plane component from a given value to model biomembranes. We focus on the local situation in which the surface Γ is described by the graph of a function $u\colon \Omega \to \mathbb{R}^3$ with $\Omega \subset \mathbb{R}^2$ convex. Moreover, we assume that the displacements are small,

$$|\nabla u| \ll 1.$$

This yields $\sqrt{1+|\nabla u|^2} \approx 1$ as well as $\nu \approx (-\nabla u, 1)$, whence $\operatorname{div}_\Gamma \nu \approx -\Delta u$. Moreover, we have

$$\nabla_\Gamma n \approx \nabla n, \qquad \operatorname{div}_\Gamma n \approx \operatorname{div} n_p,$$

where n_p stands for the tangential part of the director field $n = (n_1, n_2, n_3)$, that is, $n_p = (n_1, n_2)$, and ∇, div are the planar differential operators. We are now ready to write the linearized energy: find $u \in H^2(\Omega)$ with $u = u_D$ on $\partial\Omega$, $u_D \in H^2(\Omega)$, $n \in H^1(\Omega;\mathbb{R}^3)$ with $n = n_D$ on $\partial\Omega$, $n_D \in H^1(\Omega;\mathbb{S}^2)$ and $\mu \in L^1(\Omega)$ as stationary points of the integral

$$E(u,n,\mu) = \frac{1}{2}\int_\Omega |\Delta u + \delta \operatorname{div} n_p|^2 \mathrm{d}x + \frac{1}{2}\int_\Omega |\nabla n|^2 \mathrm{d}x + \frac{1}{2}\int_\Omega \mu\big(|n|^2 - 1\big)\mathrm{d}x - \int_{\partial\Omega} g\partial_\nu u \mathrm{d}S\,. \quad (6.2.2)$$

Note that $\mu \in L^1(\Omega)$ is the Lagrange multiplier for the nonlinear constraint $n \in \mathbb{S}^2$ and that g is related to the boundary values for the mixed method we discuss below. This model captures the essential features of the simplified linear model of Section 6.2.1.1 with energy $\mathcal{F}(u, n)$.
To model surfactants we do not impose an angle between ν and n, which typically tend to align in the gel phase of the membrane. To model biomembranes, instead, we penalize the deviation of $\nu \bullet n \approx n_3$ from a prescribed value ξ_0 via

$$\frac{1}{2\varepsilon^2} \int_\Omega \left(|n_3|^2 - \xi_0^2\right)^2,$$

with small parameter $\varepsilon > 0$. This term being lower order does not cause difficulties in the numerical method or the passage to the limit and will thus be ignored for the subsequent discussion until Section 6.6.

6.2.3. Relaxation dynamics for surfactants

To detect critical points we suggest a relaxation dynamics given by an L^2-gradient flow, i.e., we assume that there exist constants Γ_u and $\Gamma_n > 0$ such that

$$\begin{aligned} \langle \partial_t u, v\rangle &= -\Gamma_u \langle \frac{\delta E}{\delta u}, v\rangle \qquad \text{for all } v \in H^2(\Omega) \cap H_0^1(\Omega)\,, \\ \langle \partial_t n, m\rangle &= -\Gamma_n \langle \frac{\delta E}{\delta n}, m\rangle \qquad \text{for all } m \in H_0^1(\Omega, \mathbb{R}^3)\,. \end{aligned}$$

For simplicity we assume in the following that the units are chosen in such a way that $\Gamma_u = \Gamma_n = 1$. If we include the equilibrium condition for the Lagrange multiplier in our equations, then we obtain the following coupled system of partial differential equations: for all $v \in H^2(\Omega) \cap H_0^1(\Omega)$, for all $m \in H_0^1(\Omega; \mathbb{R}^3)$, and for all $\eta \in L^1(\Omega)$,

$$\begin{aligned} \langle \partial_t u, v\rangle &= -\big(\Delta u + \delta \operatorname{div} n_p, \Delta v\big) + \int_{\partial\Omega} g \partial_\nu v \mathrm{d}S\,, \\ \langle \partial_t n, m\rangle &= -\big(\Delta u + \delta \operatorname{div} n_p, \delta \operatorname{div} m_p\big) - (\nabla n, \nabla m) - (\mu n, m)\,, \\ 0 &= \frac{1}{2}\left(\eta, |n|^2 - 1\right). \end{aligned} \tag{6.2.3}$$

Hereafter we write for simplicity $(\cdot, \cdot)$ for the inner product in L^2. We impose the following boundary conditions provided by the setting of the model,

$$u = u_D,\ n = n_D \ \text{ on } \partial\Omega\,,$$

and we need to choose a second boundary condition for the fourth order equation involving u. Such a condition is implicit in the equation for u_t above because integration by parts gives formally $\tilde{z} = g$ with

$$\tilde{z} = \Delta u + \delta \operatorname{div} n_p.$$

Despite the fact that this quantity is a priori only in L^2, we prove that there exists a solution with $\tilde{z} \in H^1$ so that the boundary condition $\tilde{z} = g$ is well-posed. Note that this is a natural condition at first sight in the energy minimization but it becomes essential for the operator splitting: we use a mixed method for the variables u and $z = \tilde{z} - g$ with homogeneous Dirichlet boundary conditions. Finally we collect the equations in their strong form:

$$\tilde{z} = \Delta u + \delta \operatorname{div} n_p\,, \qquad \tilde{z}\big|_{\partial\Omega} = g\,, \tag{6.2.4}$$

$$\partial_t u = -\Delta \tilde{z}\,, \qquad u\big|_{\partial\Omega} = u_D\,, \tag{6.2.5}$$

$$\partial_t n_p = \delta \nabla \tilde{z} + \Delta n_p - \mu n_p\,, \qquad n_p\big|_{\partial\Omega} = n_{D,p}\,, \tag{6.2.6}$$

$$\partial_t n_3 = \Delta n_3 - \mu n_3\,, \qquad n_3\big|_{\partial\Omega} = n_{D,3}\,, \tag{6.2.7}$$

$$|n|^2 - 1 = 0\,, \qquad \text{a.e. in } \Omega\,. \tag{6.2.8}$$

The essential difference with respect to the model proposed by Uchida [73], and analyzed in [15] for a rigid constraint $|n| = 1$, is the additional derivative of $\operatorname{div} n_p$ in the coupling term $\tilde{z}$. This leads to additional difficulties in the stability analysis of the numerical scheme as compared to [15]. We propose in Section 6.7.5 a semi-implicit algorithm for the computation of approximate solutions in finite element spaces and prove uniform bounds for a suitable energy of the system. We then present in Section 6.6 several numerical experiments displaying quite interesting dynamics of defects. Note, that the L^2-gradient flow for biomembranes is obtained by adding the term $\frac{1}{\varepsilon^2}(|n_3|^2 - \xi_0^2)n_3$ to the equation (6.2.7).

6.2.4. Qualitative analysis of defect-shape interaction

In order to understand the interaction of defects and shape in the biomembrane case, i.e., when the angle between the director and surface normal is fixed, we consider in Sections 6.3 and 6.6 a decomposition of the director field n into a tangential and normal part. The normal part is a fixed multiple of the surface normal and the tangential, planar part n_p has a fixed length. This decomposition allows us to construct in Section 6.3 formal stationary solutions with $-\Delta u = \operatorname{div} n_p$. The proposed director fields are (infinite energy) limits of energy-minimizing configurations for a Ginzburg-Landau regularization of the Frank energy $\int_\Omega |\nabla n_p|^2 \mathrm{d}x$ subject to their own boundary data, cf. [20]. This approach allows a precise characterization of the shape corresponding to different defects and provides insight on the long time asymptotics of (u, n). In the numerical experiments for the linear model on graphs reported in Section 6.6 we allow the tangential part of the director field to develop an out-of-plane component, so that the full director field violates the angle condition and finite energy minimizers are possible. We observe that for defects of degree ± 1 the asymptotic behavior is dictated by the solutions found in Section 6.3. It is important to realize that, in contrast to [15], our new model with rigid constraint $|n| = 1$ admits defects in the limit because n_p is allowed to go out of plane near point singularities, a feature fully documented in Section 6.6. The numerical results for the full model on closed surfaces reported in Section 6.8 show that the theoretical and practical predictions of the interaction of defects with the membrane shape in the simplified case explain the interesting dynamics occurring in the full biomembrane model for which the presence of defects is unavoidable if the angle between ν and n is fixed.

6.2.5. Nonlinear model on closed surfaces

For a smooth embedded surface $\Gamma \subset \mathbb{R}^3$, a director field $n : \Gamma \to \mathbb{S}^2$ and constants δ, ε and λ, we consider the energy (6.2.1) augmented as follows

$$E(\Gamma, n) = \frac{1}{2}\int_\Gamma |\operatorname{div}_\Gamma \nu - \delta \operatorname{div}_\Gamma n|^2 \mathrm{d}\sigma + \frac{\lambda}{2}\int_\Gamma |\nabla_\Gamma n|^2 \mathrm{d}\sigma + \frac{1}{2}\int_\Gamma \mu(|n|^2 - 1)\mathrm{d}\sigma + \frac{1}{2\varepsilon^2}\int_\Gamma f(n \bullet \nu)\mathrm{d}\sigma,$$

where μ is the Lagrange multiplier for the rigid constraint $|n| = 1$ and f is given by $f(x) = (x^2 - \xi_0^2)^2$, for $\xi_0 \in [0, 1]$. The last term penalizes the deviation of the three-dimensional director field n from the cone of all vectors that have a given angle with respect to the unit normal ν to the surface, as discussed already in Section 6.2.3. Thus, for $\varepsilon = \infty$, which corresponds to neglecting the last term, we obtain the surfactant case, while $\varepsilon \ll 1$ results in the modelling of biomembranes. In Section 6.7, we derive a variation of the energy with respect to Γ and n, which is the first step on the way to discover critical points of $E(\Gamma, n)$. We also introduce a semi-implicit algorithm based on parametric finite elements of Barrett, Garcke and Nünberg [10] to model the L^2-gradient flow of $E(\Gamma, n)$, see also [6]. As we are interested in the simulation of cells and biomembranes, side conditions like conservation of the enclosed volume and/or the surface area are important. For this purpose we use a Newton-iteration method, as proposed in [21]. In Section 6.8 we explore the behavior of the nonlinear model via simulations. We first show that for $\delta = 1$ and without angle penalization, the vectors ν and n tend to align since this minimizes $(\operatorname{div}_\Gamma(\nu - n))^2$. We also display the dynamics of defects of degree ± 1 and observe that locally the membrane shape is similar to that discovered earlier in the graph case. We conclude that defects of the director field n have a dramatic effect on the shape of Γ, as observed in experiments, e.g., reported in [53].

6.3. Qualitative Behavior of Graphs

To build intuition about the mechanisms introduced by the coupling term in the model, we fix stationary tangential director fields n_p of unit length and compute a function $u \in H_0^1(\Omega)$ for which the first term in (6.2.1) vanishes. For ease of readability we omit the subscript p throughout this section. We thus impose that the auxiliary variable

$$\tilde{z} = \Delta u + \operatorname{div} n$$

vanishes, thereby giving the relation

$$-\Delta u = \operatorname{div} n.$$

Motivated by experimental observations we are particularly concerned with the surface structure when the director field represents a defect of positive or negative degree-one, i.e.,

$$n = \exp(\pm i\theta) = \cos\theta \pm i \sin\theta$$

in polar coordinates (r, θ) and complex notation. Notice that for such a field n we have $\int_\Omega |\nabla n|^2 \mathrm{d}x = \infty$, so n cannot be a minimizer of the energy which involves the Dirichlet integral of n, but it arises as the limit of minimizers of a corresponding Ginzburg-Landau regularization that penalizes the unit-length constraint, cf. [20]. Therefore our calculations are only meant to explain the structures observed in our experiments of Section 6.6 which necessarily involve regularizations of the corresponding fields. We first compute the divergence

$$\operatorname{div} n = \partial_x \cos\theta \pm \partial_y \sin\theta = -\sin\theta\ \partial_x\theta \pm \cos\theta\ \partial_y\theta,$$

and recall that $\theta = \arctan y/x$, whence

$$\partial_x\theta = \frac{-y}{x^2+y^2}\,, \qquad \partial_y\theta = \frac{x}{x^2+y^2}\,.$$

We insert this result into the expression for $\operatorname{div} n$ and obtain

$$\operatorname{div} n = \frac{y^2 \pm x^2}{r^3} = \frac{\sin^2\theta \pm \cos^2\theta}{r}.$$

6.3.1. Positive degree-one defects

We now take $n = \exp(i\theta) = \cos\theta + i\sin\theta$. We thus seek u such that the inhomogeneous equation (in polar coordinates)

$$\Delta u = \frac{1}{r}\partial_r\Big(r\partial_r u\Big) + \frac{1}{r^2}\partial_\theta^2 u = -\frac{1}{r}$$

holds. It is natural to look for a radial solution $u(r) = -r^\alpha$ and the expression for Δu implies the necessary condition $\alpha = 1$ and the cone-like surface (see Figure 6.2 (left)):

$$u(r) = -r.$$

Consider now the director field $n = e^{i(\theta+\pi/2)}$ rotated by an angle $\pi/2$. Such an n satisfies $\operatorname{div} n = 0$, whence $u = 0$; this is depicted in the right plot of Figure 6.2. Any other rotation $n = e^{i(\theta+\theta_0)}$ by an angle θ_0 can be expressed as $n = \cos\theta_0\, n_1 + \sin\theta_0\, n_2$ with n_1, n_2 the director fields in Figure 6.2. The corresponding solution is thus

$$u = -r\cos\theta_0.$$

6.3.2. Negative degree-one defects

We now take $n = \exp(-i\theta) = \cos\theta - i\sin\theta$. We thus seek u as a solution of the inhomogeneous equation

$$\Delta u = \frac{1}{r}\partial_r\Big(r\partial_r u\Big) + \frac{1}{r^2}\partial_\theta^2 u = -\frac{\sin^2\theta - \cos^2\theta}{r} = -\frac{\cos(2\theta)}{r}\,.$$

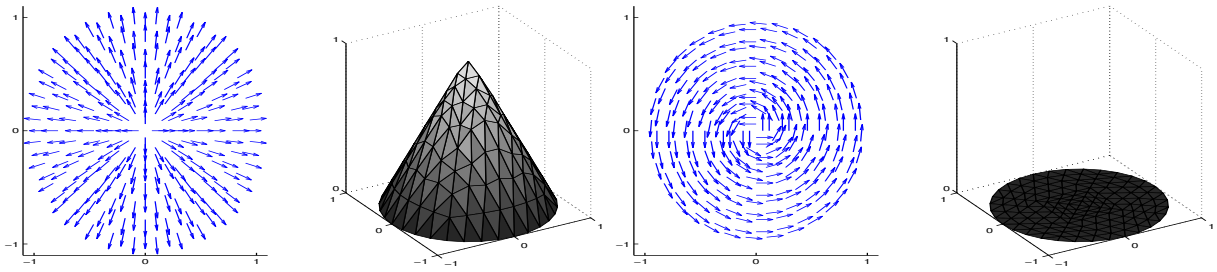

Figure 6.2.: Positive degree-one defect: director field $n = e^{i\theta}$ and cone-like surface $u = 1 - r$ (left), and rotated director field $n = e^{i(\theta+\pi/2)}$ and function $u = 0$ (right) related by (finite element discretizations of) $-\Delta u = \operatorname{div} n$ with $u|_{\partial\Omega} = 0$.

We try a solution of the form $u(r,\theta) = Cr^\alpha \cos(2\theta)$ for suitable constants C, α and evaluate the partial differential equation to obtain the necessary condition

$$\Delta u = C\big(\alpha^2 - 4\big) r^{\alpha-2} \cos(2\theta) = -\frac{\cos(2\theta)}{r},$$

whence $\alpha = 1, C = 1/3$ and

$$u(r,\theta) = \frac{1}{3}\, r \cos(2\theta).$$

This solution is a saddle and is depicted in Figure 6.3 (left). Consider now the director field $n = e^{-i(\theta-\theta_0)}$ which can be written as $n = e^{-i(\theta-\theta_0/2)} e^{i\theta_0/2}$. We thus realize that the value of n at θ results from reading the value at $\theta - \theta_0/2$ and rotating clockwise by $\theta_0/2$, an effective rotation of $e^{-i\theta}$ by the angle $\theta_0/2$. The corresponding solution thus reads

$$u(r,\theta) = \frac{1}{3}\, r \cos(2\theta - \theta_0).$$

Figure 6.3 (right) displays such a pair (u, n) for $\theta_0 = \pi/2$.

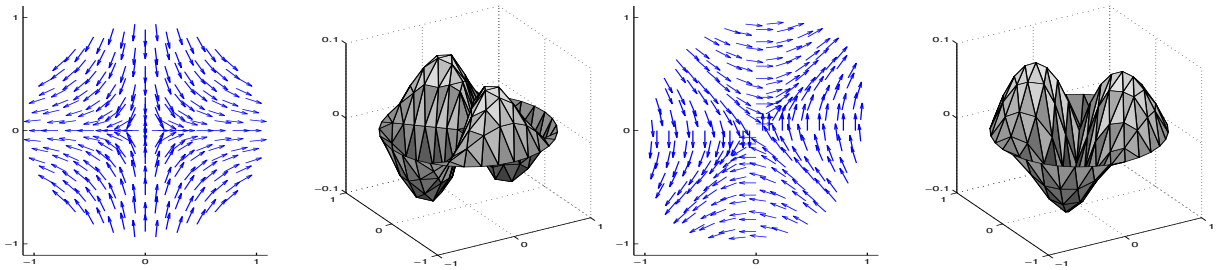

Figure 6.3.: Negative degree-one defect: director field $n = e^{-i\theta}$ and saddle-like surface $u(r,\theta) \approx \frac{1}{3} r \cos(2\theta)$ (left), and rotated director field $n = e^{-i(\theta-\pi/2)}$ and corresponding rotated saddle-like surface $u(r,\theta) \approx \frac{1}{3} r \cos(2\theta - \pi/2)$ (right) related by (finite element discretizations of) $-\Delta u = \operatorname{div} n$ and $u|_{\partial\Omega} = 0$. Due to the boundary condition u mimics the exact saddle structure only in a neighborhood of the origin.

6.4. A semi-implicit scheme for graphs

For simplicity we suppress in this section the index h in connection with all finite element spaces and functions, that is, we write e.g., $\mathcal{T}$, $\mathbb{V}$ and (u, n) instead of $\mathcal{T}_h$, $\mathbb{V}_h$ and (u_h, n_h), respectively. We use upper indices for the functions at discrete time steps. In particular $n^0 \in \mathbb{V}$ is a suitable approximation of the initial data n_D. Since we use time-independent boundary conditions we may assume that we

are given approximations $n^0 \in [\mathbb{V}]^3$ and $u^0 \in \mathbb{V}^0$ of n_D and u_D with $|n^0(a)| = 1$ for all $a \in \mathcal{N}$. Moreover we replace the additional variable $\tilde{z} = \Delta u + \delta \operatorname{div} n_p$, which has a Dirichlet boundary value g, by $z = \tilde{z} - g$, which has vanishing trace. Given $n^0 \in [\mathbb{V}]^3$ and $u^0 \in \mathbb{V}^0$, we let $z^0 \in \mathbb{V}^0$ be an approximation to $z(0)$ defined as

$$(z^0, y) = -(g, y) - (\nabla u^0, \nabla y) - \delta(n_p^0, \nabla y) \quad \text{for all } y \in \mathbb{V}^0\,, \tag{6.4.1}$$

and observe that the right-hand side in this equality defines a continuous linear form on $\mathbb{V}$. Since the L^2 inner product is a norm on $\mathbb{V}^0$ (with zero Dirichlet conditions), existence of a unique solution z^0 follows from the Lax-Milgram lemma.
In the numerical analysis of our proposed scheme we will need to control $\|\nabla z^0\|$. For this we assume for simplicity that $\Delta u^0\big|_{\partial\Omega} = 0$. Then, we define the discrete Laplacian Δ^0 with zero boundary values for a finite element function v to be the unique element $\Delta^0 v \in \mathbb{V}_0$ that satisfies

$$(\Delta^0 v, w) = -(\nabla v, \nabla w) \quad \text{for all } w \in \mathbb{V}_0$$

and let Π^0 denote the L^2 projection onto $\mathbb{V}_0$. We then have that

$$z^0 = -\Pi^0(g - \delta \operatorname{div} n_p^0) + \Delta^0 u^0$$

and

$$\|\nabla z^0\| \leq \|\nabla\big[- \Pi^0(g - \delta \operatorname{div} n_p^0) + \Delta^0 u^0\big]\|. \tag{6.4.2}$$

The assumption $\Delta u^0\big|_{\partial\Omega} = 0$ can be avoided by appropriately splitting $g = \Delta u(0)\big|_{\partial\Omega} + \tilde{g}$ and replacing g by $\tilde{g}$ in the above discussion.

We propose a semi-implicit method for (6.2.3) in which the computation of the director field is naturally decoupled from the calculation of u^j and z^j. We set $\widetilde{n}^0 = n^0$ and seek for $j \geq 1$ and given u^{j-1}, $\widetilde{n}^{j-1}$, n^{j-1} functions

$$u^j \in \mathbb{V}_0\,, \quad z^j \in \mathbb{V}_0\,, \quad \widetilde{\mathrm{d}}_t n^j \in \mathcal{F}[n^{j-1}]$$

such that

$$(z^j, y) + (\nabla u^j, \nabla y) + \delta(\widetilde{n}_p^{j-1}, \nabla y) = -(g, y) \qquad \text{for all } y \in \mathbb{V}_0\,, \tag{6.4.3}$$

$$(\,\mathrm{d}_t u^j, v) - (\nabla z^j, \nabla v) = (\nabla g, \nabla v) \qquad \text{for all } v \in \mathbb{V}_0\,, \tag{6.4.4}$$

$$(\,\widetilde{\mathrm{d}}_t n^j, m) - \delta(\nabla z^j, m_p) + \big(\nabla \widetilde{n}^j, \nabla m\big) = \delta(\nabla g, m_p) \quad \text{for all } m \in \mathcal{F}[n^{j-1}], \tag{6.4.5}$$

where $\widetilde{n}^j = n^{j-1} + \tau\, \widetilde{\mathrm{d}}_t n^j$ and $u^j = u^{j-1} + \tau\, \mathrm{d}_t u^j$. Now set

$$n^j(a) = \frac{\widetilde{n}^j(a)}{|\widetilde{n}^j(a)|} = \frac{n^{j-1}(a) + \tau\, \widetilde{\mathrm{d}}_t n^j(a)}{|n^{j-1}(a) + \tau\, \widetilde{\mathrm{d}}_t n^j(a)|}, \quad \text{for all } a \in \mathcal{N}.$$

We remark that the system (6.4.3)-(6.4.4) has the structure of a saddle-point problem, that is similar to a hybrid formulation of the bilaplacian (with penalty term), i.e., (6.4.3)-(6.4.4) can be rewritten as

$$\begin{aligned}(z^j, y) + (\nabla u^j, \nabla y) &= -(g, y) - \delta(\widetilde{n}_p^{j-1}, \nabla y) \qquad \text{for all } y \in \mathbb{V}_0\,,\\ (\nabla z^j, \nabla v) - \tau^{-1}(u^j, v) &= -\tau^{-1}(u^{j-1}, v) - (\nabla g, \nabla v) \quad \text{for all } v \in \mathbb{V}_0\,.\end{aligned}$$

Owing to the essential boundary conditions imposed on z^j and u^j a $P1 - P1$ discretization is stable. The Lax-Milgram lemma implies the unique solvability of (6.4.5) on the non-empty linear space $\mathcal{F}[n^{j-1}]$.

6.5. Stability analysis and weak solution in the graph case

We refer the reader to [16] for a proof of the results stated in this section. It is possible to verify bounds (uniform in τ) for the following quantities:

$$A(J) = \frac{1}{4}\|\nabla z^J\|^2 + \frac{1}{2}\sum_{j=1}^{J}\tau\|\,\mathrm{d}_t\nabla u^j\|^2 + \frac{\tau}{2}\sum_{j=1}^{J}\tau\|\,\mathrm{d}_t\nabla z^j\|^2\,,$$

$$B(J) = \frac{1}{2}\|z^J\|^2 + \frac{1}{2}\|\nabla n^J\|^2 + \frac{1}{2}\sum_{j=1}^{J}\tau\Big(\|\,\mathrm{d}_t u^j\|^2 + \|\,\widetilde{\mathrm{d}}_t n^j\|^2\Big) + \frac{\tau}{2}\sum_{j=1}^{J}\tau\Big(\|\,\mathrm{d}_t z^j\|^2 + \|\,\widetilde{\mathrm{d}}_t\nabla n^j\|^2\Big),$$

for all $J \geq 1$. That is, we prove that if τ is chosen appropritaly and the triangulation $\mathcal{T}$ is weakly acute, then $A(J)$ and $B(J)$ are bounded uniformly by constants depending on the starting values, the boundary values and the end time $T \in \mathbb{R}$. We recall the definition (6.4.1) of $z^0 \in \mathbb{V}^0$ and assume

$$u_D \in H^3(\Omega), \qquad n_D \in H^2(\Omega), \qquad g \in H^2(\Omega). \tag{6.5.1}$$

Combined with (6.4.1), this implies that $\|\nabla z^0\|$ is uniformly bounded with respect to h.

The mentioned a priori estimates allow us to establish the existence of a weak solution of the continuous L^2-gradient flow that satisfies an energy inequality. We now state precisely the notion of solution already introduced in (6.2.3) and refer the reader to [15] for details about passing to the limit.

Definition 6.5.1 (weak solution) *Let $\Omega \subset \mathbb{R}^2$ be a bounded and convex Lipschitz domain and fix $T > 0$. We call a pair (u, n) a weak solution of (6.2.3) in the time interval $I = (0, T)$ if the following assertions are true:*

(i) $n \in H^1(I; L^2(\Omega;\mathbb{R}^2)) \cap L^\infty(I; H^1(\Omega;\mathbb{R}^2))$, $u \in H^1(I; L^2(\Omega)) \cap L^\infty(I; H^2(\Omega))$;

(ii) $|n(t,x)| = 1$ *for almost every* $(t,x) \in I \times \Omega$;

(iii) $n(0,\cdot) = n_D$, $u(0,\cdot) = u_D$ *with* $u_D \in H^3(\Omega)$ *and* $n_D \in H^2(\Omega)$;

(iv) $n(t,\cdot)|_{\partial\Omega} = n_D$ *and* $u(t,\cdot)|_{\partial\Omega} = u_D$ *in the sense of traces for almost every* $t \in I$;

(v) $\Delta u + \delta\,\mathrm{div}\, n_p \in L^2(I; H^1(\Omega))$ *and satisfies for a.e.* $t \in I$ *that* $(\Delta u + \delta\,\mathrm{div}\, n_p)\big|_{\partial\Omega} = g$ *with* $g \in H^2(\Omega)$ *given;*

(vi) for all $(m, v) \in L^2(I; H_0^1(\Omega;\mathbb{R}^2)) \times L^2\big(I; H^2(\Omega) \cap H_0^1(\Omega)\big)$ *satisfying* $m \bullet n = 0$ *almost everywhere in* $I \times \Omega$ *we have*

$$\int_I \big\{(\partial_t u, v) + (\Delta u + \delta\,\mathrm{div}\, n_p, \Delta v)\big\}\mathrm{d}t - \int_{\partial\Omega} g\partial_\nu v \mathrm{d}S = 0\,,$$
$$\int_I \big\{(\partial_t n, m) + (\Delta u + \delta\,\mathrm{div}\, n_p, \delta\,\mathrm{div}\, m_p) + (\nabla n, \nabla m)\big\}\mathrm{d}t = 0\,.$$

Remark 6.5.2 *We note that the discrete a priori estimates allows one to deduce the existence of a solution (u, n) that satisfies the energy inequality*

$$\frac{1}{2}\|\Delta u + \delta\,\mathrm{div}\, n_p\|^2 + \frac{1}{2}\|\nabla n\|^2 + \int_0^T \big(\|\partial_t u\|^2 + \frac{1}{2}\|\partial_t n\|^2\big)\mathrm{d}t$$
$$\leq \frac{1}{2}\|\Delta u_D + \delta\,\mathrm{div}(n_D)_p\|^2 + \frac{1}{2}\|\nabla n_D\|^2 + \delta^2 T\|\nabla g\|^2 + \frac{T}{2}\|\Delta g\|^2\,.$$

We refer the reader to [71] for related existence theories in the context of the harmonic map heat flow.

6.6. Numerical Experiments for Graphs

In this section we report on various numerical experiments carried out with the scheme devised and analyzed in the previous sections. Since we want to illustrate the interaction of defects and shape we consider the case of a membrane in the gel phase where the director field prefers to have a fixed angle with respect to the normal to the surface, say $\pi/2$ for convenience. As in Section 6.3 the director field n has unit length but is allowed to develop an out-of-plane component to accommodate for topological defects; we omit the index p throughout this section for the tangential part n_p of n. We thus augment the system of equations discussed in Section 6.4 by the term $\varepsilon^{-2}(\widetilde{n}_3^j, m_3)$, where the subscript 3 refers to the third, or out-of-plane, component of a vectorfield, in (6.4.5), i.e., for the evolution of the director field we employ the equation

$$(\widetilde{\mathrm{d}}_t n^j, m) - \delta(\nabla z^j, m_p) + \big(\nabla \widetilde{n}^j, \nabla m\big) + \varepsilon^{-2}(\widetilde{n}_3^j, m_3) = 0\,.$$

This modification corresponds to the additional penalty term

$$\frac{1}{2\varepsilon^2}\int_\Omega |n_3|^2\,\mathrm{d}x$$

in the energy, i.e., our energy functional is

$$E[u,z,n] = \frac{1}{2}\int_\Omega |z|^2\mathrm{d}x + \frac{1}{2}\int_\Omega |\nabla n|^2\mathrm{d}x + \frac{1}{2\varepsilon^2}\int_\Omega |n_3|^2\mathrm{d}x$$

subject to the relation $z = \Delta u + \delta\mathrm{div}(n_1, n_2)$, the pointwise constraint $|n| = 1$, and Dirichlet boundary conditions for u, z, and n. We remark that the inclusion of an implicit treatment of the convex penalty term in the stability analysis for the numerical scheme in Section 6.4 poses no difficulties.
The goal of this section is to explore the qualitative behavior of the evolution for specific initial conditions with defects. Here, the terminology of a defect refers to a singularity in the renormalized planar part of the director field which is also called vortex. This evolution typically shows an initial phase with a significant change of the shape in order for the system to adjust to the given initial and boundary values which is followed by a slower evolution towards an equilibrium shape. In the figures we display typical intermediate shapes and states which are close to an equilibrium. In our simulations the domain Ω and the parameters δ, T, and ε are given by

$$\Omega = (-1/2, 1/2)^2, \quad \delta = 1, \quad T = 1, \quad \varepsilon = 10^{-2}\,.$$

We denote by (r, ϕ) the usual polar coordinates in $\mathbb{R}^2$ (with respect to the origin). The function φ which is used in the extension of a function given on $\partial\Omega$ to Ω is equal to $\varphi(r) = \tanh(r)$. The initial values are always chosen to be

$$u_0 = 0, \quad g = \mathcal{I}_h[\mathrm{div}\, n_0]$$

for different choices of n_0 and where $\mathcal{I}_h$ is the nodal interpolation operator. The sequence of triangulations $\mathcal{T}_\ell$ is generated by ℓ uniform refinements (division of each triangle into four congruent ones) of the initial triangulation $\mathcal{T}_0$ of Ω which consists of two triangles obtained by dividing Ω along the diagonal $x_1 = x_2$. Hence the mesh-size h_ℓ is given by $h_\ell = \sqrt{2}2^{-\ell}$. Moreover we used $\tau_\ell = h_\ell/(8\sqrt{2})$ as time-step size.

6.6.1. Positive degree-one defect

We choose boundary conditions which correspond to a defect of degree one, i.e.,

$$n_0|_{\partial\Omega}(x_1, x_2) = n_0|_{\partial\Omega}(r\cos\phi, r\sin\phi) = \big(\cos(\phi), \sin(\phi), 0\big) = \big(e^{i\phi}, 0\big)\,, \quad (x_1, x_2) \in \partial\Omega$$

(in complex notation). Note that these boundary data do not allow for a continuous, purely planar extension, since any such extension would necessarily contain topological defects of infinite energy. Thus it is expected that the numerical solution will develop an out-of-plane component of the vectorfield despite the penalization of this component in the energy in order to accommodate the length

constraint. For energetic reasons, there should be only one point in the domain where such a defect-like structure is observed. Therefore we define the extension of n_0 which is needed for the numerical scheme at all interior nodes $a \in \mathcal{N}$ with the help of polar coordinates (r_2, ϕ_2) about $(-1/4, -1/4)$ by

$$n_0(a) = n_0(r_2\cos\phi_2, r_2\sin\phi_2) = \big(\varphi(r_2/\varepsilon)\cos(\phi_2), \varphi(r_2/\varepsilon)\sin(\phi_2), (1-\varphi(r_2/\varepsilon)^2)^{1/2}\big)\,.$$

Thus there is such a defect-like structure already present in the initial data but it is not located at the origin where it is expected to move during the evolution of the system.
The snapshots of the evolution in Figure 6.4 show indeed that this initial vortex moves slowly towards the origin, which is an energetically favorable configuration. At the same time, the surface develops a profile which is a smoothed version of the cone described in Section 6.3. The location of the maximal height moves together with the vortex towards the origin. The initially strong energy decay shown in the bottom plot of Figure 6.4 is related to the incompatibility of the initial data in the sense that $\Delta u_0 + \delta \operatorname{div} n_0$ is large.

6.6.2. Negative degree-one defect

We employ

$$n_0|_{\partial\Omega}(r\cos\phi, r\sin\phi) = \big(\cos(-\phi), \sin(-\phi), 0\big) = \big(e^{-i\phi}, 0\big)$$

with an extension to Ω so that the defect is located at $x = (-1/4, -1/4)$ as above. A defect of negative degree-one in the planar part of the director field is favored by the boundary conditions and already present in the extension of $n_0|_{\partial\Omega}$ to Ω. The corresponding evolution is shown in Figure 6.5. As in the case of a positive degree-one defect we observe that the defect of negative degree-one moves towards the center of the domain. The surface adjusts to the defect by developing a saddle-shape and follows its motion. Eventually we observe a stationary configuration with a saddle as predicted in Section 6.3. In accordance, the energy shows a rapid decay in the beginning and then only decreases moderately. We point out that in order to match smoothly the director field at $x_1 = 0$ the negative degree-one defect is that of Section 6.6.2 rotated by π.

6.7. The nonlinear model on closed surfaces

In this section we return to the nonlinear model of Section 6.2.5, which corresponds to the energy

$$E(\Gamma, n) := \frac{1}{2}\int_\Gamma (\operatorname{div}_\Gamma \nu - \delta \operatorname{div}_\Gamma n)^2 \mathrm{d}\sigma + \frac{\lambda}{2}\int_\Gamma |\nabla_\Gamma n|^2 \mathrm{d}\sigma + \int_\Gamma \mu\big(|n|^2 - 1\big)\mathrm{d}\sigma + \frac{1}{2\varepsilon^2}\int_\Gamma f(n \bullet \nu)\mathrm{d}\sigma. \quad (6.7.1)$$

To formulate the gradient flow of $E(\Gamma, n)$ we need the first variation of $E(\Gamma, n)$. Therefore, we repeat again some basics in differential geometry and expand it to the present setting. Then, we follow with a discretization of the gradient flow using parametric finite element methods.

6.7.1. Elementary differential geometry, part II

Let $\mathcal{U} \subset \mathbb{R}^2$ be open and $X : \mathcal{U} \to \mathbb{R}^3$, $(u_1, u_2) \mapsto X(u_1, u_2)$ be a local parametrization of Γ. If $X_i = \partial_{u_i} X$, then the induced metric on Γ is given by $g_{ij} = X_i \bullet X_j$. The inverse of g_{ij} is g^{ij} and the square root of the matrix g^{ij} is $g_{ij}^{(-1/2)}$, i.e., $\sum_k g_{ik}^{(-1/2)} g_{jk}^{(-1/2)} = g^{ij}$. If $g = \det(g_{ij})$, then the volume element on Γ is given by $\mathrm{d}\sigma = \sqrt{g}\mathrm{d}u_1\mathrm{d}u_2$. The unit normal is $\nu = \frac{X_1 \times X_2}{|X_1 \times X_2|}$, and the second fundamental form is $h_{ij} = -\partial_i \nu \bullet X_j$. If f and F are scalar- and vector-valued functions on Γ and $\tilde{f}, \tilde{F}$ are arbitrary extensions then the tangential gradient and divergence on Γ are given by

$$\nabla_\Gamma f = \nabla \tilde{f} - (\nu \bullet \nabla \tilde{f})\nu, \qquad \operatorname{div}_\Gamma F = \operatorname{div} \tilde{F} - \nu^T D\tilde{F}\nu.$$

In the local coordinates defined above these operators are

$$(\nabla_\Gamma f) \circ X = \sum_{i,j} g^{ij}\partial_j (f \circ X) X_i, \qquad (\operatorname{div}_\Gamma F) \circ X = \sum_{i,j} g^{ij}\partial_i (F \circ X) \bullet X_j. \quad (6.7.2)$$

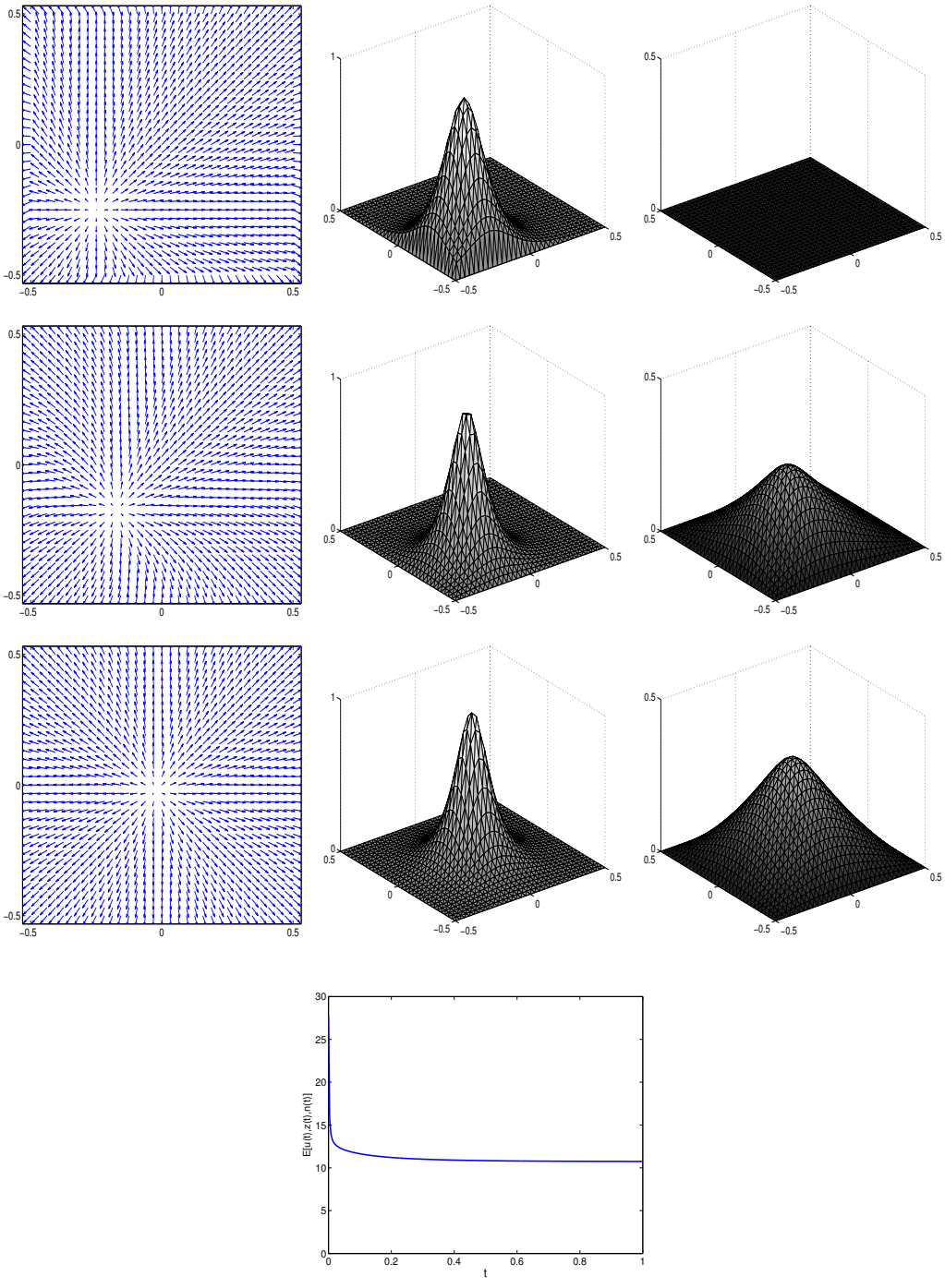

Figure 6.4.: Positive degree-one defect: in-plane component of the director field (left), out-of-plane component of the director field (middle), and height function (right) after $n = 0, 32, 256$ time steps. The surface develops a smoothed out cone and follows the motion of the defect. The energy shows a rapid initial decay when the surface adjusts to the defect.

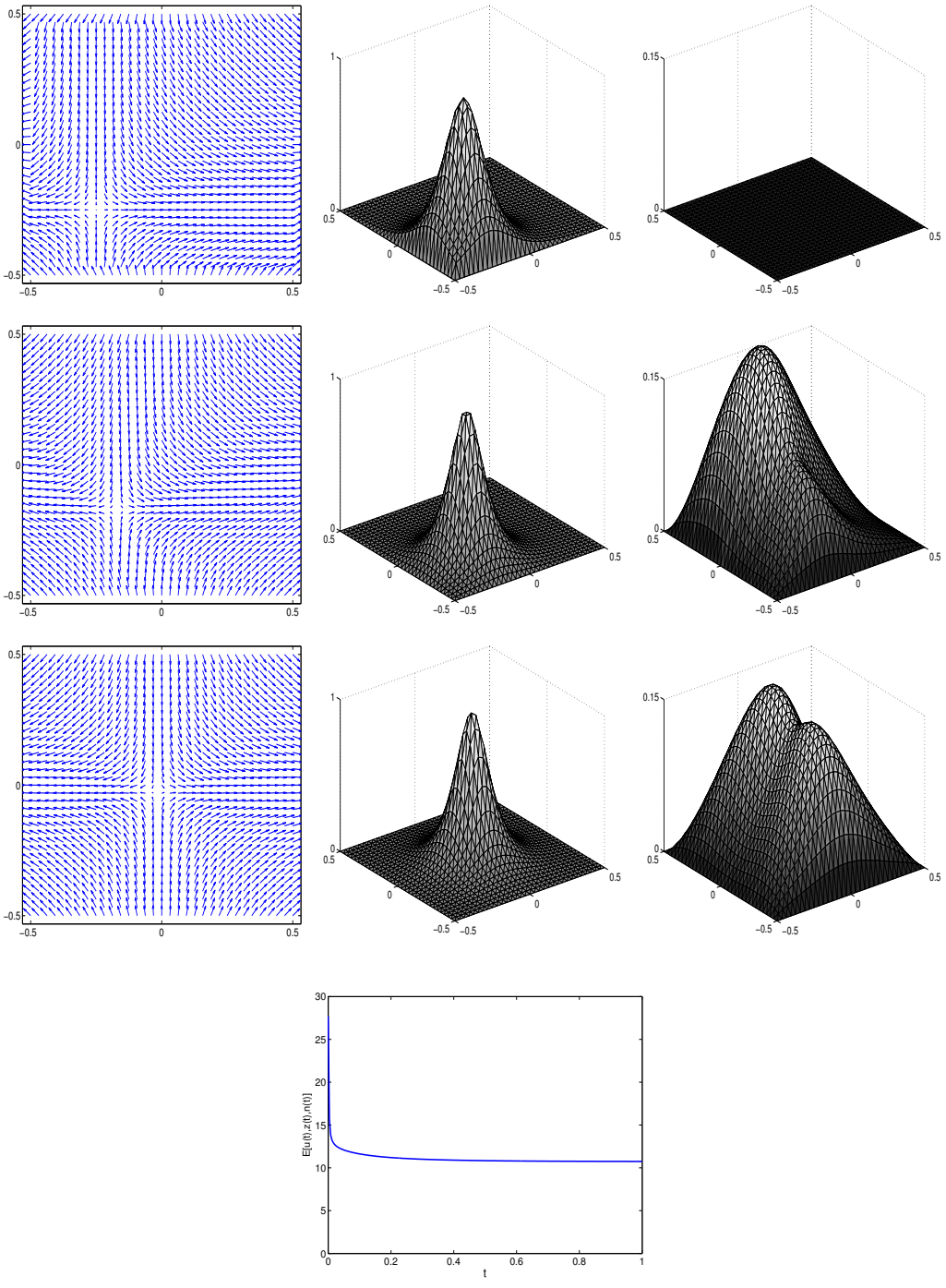

Figure 6.5.: Negative degree-one defect: in-plane component of the director field (left), out-of-plane component of the director field (middle), height function (right) after $n = 0, 8, 16$ time steps. The height function shows a saddle shape in a neighborhood of the defect and this configuration is stable. The energy decays rapidly during the first time steps and remains almost constant subsequently.

For $F = \nu$ we obtain the mean curvature, i.e.,

$$H = -\operatorname{div}_\Gamma \nu = \sum_{i,j} g^{ij} h_{ij}.$$

With this definition the unit sphere $\mathbb{S}^2$ has mean curvature -2. It is now easy to check for all functions f, f_1, and f_2 the identities

$$(\nabla_\Gamma f_1 \bullet \nabla_\Gamma f_2) \circ X = \sum_{i,j} g^{ij} \partial_i (f_1 \circ X) \partial_j (f_2 \circ X), \qquad X_i \bullet (\nabla_\Gamma f) \circ X = \partial_i (f \circ X). \tag{6.7.3}$$

We note that the tangential gradient $\nabla_\Gamma F$ of a vector field F is a square matrix in $\mathbb{R}^{3\times 3}$ whose i-th row is the tangential gradient of the i-th component of F. If F is tangential, then it can be equivalently written as

$$F = \sum_k (V_k \bullet F) V_k = \sum_{i,j,k} g_{ik}^{(-1/2)} g_{jk}^{(-1/2)} F \bullet X_i X_j = \sum_{i,j} g^{ij} F \bullet X_i X_j.$$

Applying this expression to the tangential vector $\partial_k \nu$ yields the Weingarten equations

$$\partial_k \nu = -\sum_{i,j} g^{ij} h_{ki} X_j. \tag{6.7.4}$$

The Laplace-Beltrami operator $\Delta_\Gamma f = \operatorname{div}_\Gamma \nabla_\Gamma f$ has the following expression in local coordinates

$$\Delta_\Gamma f = \frac{1}{\sqrt{g}} \sum_{i,j} \partial_i (\sqrt{g} g^{ij} \partial_j f). \tag{6.7.5}$$

Let ϕ be a smooth real-valued function on Γ and $s \in (-\xi, \xi)$, $\xi > 0$ small enough. A normal variation of Γ is given by the map

$$X_s(u_1, u_2) = X(u_1, u_2) + s\phi(X(u_1, u_2))\nu$$

with values in a tubular neighborhood of Γ. The first variation of E in (6.7.1) with respect to Γ is now defined as

$$\langle \delta_\Gamma E, \phi \rangle := \frac{\mathrm{d}}{\mathrm{d}s}\Big|_{s=0} E(\Gamma_s, n).$$

We write $\psi' := \partial_s|_{s=0} \psi_s$ for a quantity that depends on s and recall the basic geometric identities from Lemma 1.2.9

$$g'_{ij} = -2\phi h_{ij}, \quad (g^{ij})' = 2\phi \sum_{k,\ell} g^{jk} g^{i\ell} h_{\ell k}, \quad \nu' = -\nabla_\Gamma \phi, \quad \mathrm{d}\sigma' = -\phi H \mathrm{d}\sigma, \quad H' = \Delta_\Gamma \phi + \phi |\nabla_\Gamma \nu|^2. \tag{6.7.6}$$

For the side conditions we define the area and volume function as

$$A : \Gamma \mapsto \int_\Gamma 1 \,\mathrm{d}\sigma, \quad V : \Gamma \mapsto \frac{1}{3} \int_\Gamma x \bullet \nu \,\mathrm{d}\sigma.$$

6.7.2. First variation of the energy and gradient flow

In the following we identify n with its constant extension in the normal direction so that $n_s = n$ and therefore $n' = 0$. Notice that the variation of $E(\Gamma, n)$ with respect to Γ does depend on the particular extension. This choice is not arbitrary: biomembranes are made of lipid bilayers and thus have a small thickness across which it is reasonable to assume no variation of the physical quantities such as n.

Lemma 6.7.3 *For a normal variation of Γ defined by a function ϕ as in Section 6.7.1 we have*

$$\partial_s|_{s=0} \operatorname{div}_{\Gamma_s} n = -\phi \nabla_\Gamma n : \nabla_\Gamma \nu + \nu^T \nabla_\Gamma n \nabla_\Gamma \phi, \tag{6.7.7}$$

$$\partial_s|_{s=0} |\nabla_{\Gamma_s} n|^2 = -2\phi (\nabla_\Gamma n)^T : \nabla_\Gamma \nu (\nabla_\Gamma n). \tag{6.7.8}$$

Proof. Using the expression (6.7.2) for the tangential divergence $\operatorname{div}_\Gamma n$, we obtain

$$\partial_s|_{s=0}(\operatorname{div}_{\Gamma_s} n) = \partial_s|_{s=0}\Big(\sum_{i,j} g_s^{ij}\partial_i n \bullet X_{s,j}\Big) = \sum_{i,j}(g^{ij})'\partial_i n \bullet X_j + g^{ij}\partial_i n' \bullet X_j + g^{ij}\partial_i n \bullet X_j'.$$

Since $n' = 0$ the middle term vanishes. For the first term we use (6.7.6) to write

$$\sum_{i,j}(g^{ij})'\partial_i n \bullet X_j = 2\phi \sum_{i,j,k,\ell} g^{jk}g^{i\ell}h_{\ell k}\partial_i n \bullet X_j = 2\phi\sum_{i,\ell} g^{i\ell}\partial_i n \bullet \sum_{j,k} g^{jk}h_{\ell k}X_j.$$

We invoke the Weingarten equations (6.7.4) to identify the last factor with $-\partial_\ell \nu$, and (6.7.3) to get

$$\sum_{i,j}(g^{ij})'\partial_i n \bullet X_j = -2\phi\sum_{i,\ell} g^{i\ell}\partial_i n \bullet \partial_\ell \nu = -2\phi\nabla_\Gamma n : \nabla_\Gamma \nu.$$

To manipulate the remaining term, we first observe that $X_j' = \partial_j\phi\nu + \phi\partial_j\nu$. In view of (6.7.3) we see that

$$\sum_{i,j} g^{ij}\partial_i n \bullet X_j' = \sum_k \nu_k \nabla_\Gamma n_k \bullet \nabla_\Gamma\phi + \phi\nabla_\Gamma n : \nabla_\Gamma\nu.$$

Since $\sum_k \nu_k\nabla_\Gamma n_k \bullet \nabla_\Gamma\phi = \nu^T\nabla_\Gamma n\nabla_\Gamma\phi$, collecting the last two expressions leads to (6.7.7). To prove (6.7.8) we use (6.7.3) for $|\nabla_\Gamma n|^2$, combined with $n' = 0$, to arrive at

$$\partial_s|_{s=0}|\nabla_{\Gamma_s} n|^2 = \partial_s|_{s=0}\Big(\sum_{i,j} g_s^{ij}\partial_i n \bullet \partial_j n\Big) = \sum_{i,j}(g^{ij})'\partial_i n \bullet \partial_j n.$$

We replace $(g^{ij})'$ with the expression from (6.7.6), and next use (6.7.3) to write $h_{\ell k} = -X_k \bullet \nabla_\Gamma \nu X_\ell$, whence

$$\begin{aligned}\partial_s|_{s=0}|\nabla_{\Gamma_s} n|^2 &= 2\phi\sum_{i,j,k,\ell} g^{jk}g^{i\ell}h_{\ell k}\sum_m \partial_i n_m \partial_j n_m \\ &= -2\phi\sum_m \Big(\sum_{j,k} g^{jk}\partial_j n_m X_k\Big)\bullet\nabla_\Gamma\nu\Big(\sum_{i,\ell} g^{i\ell}\partial_i n_m X_\ell\Big).\end{aligned}$$

The equivalent representation (6.7.2) of the surface gradient yields

$$\partial_s|_{s=0}|\nabla_{\Gamma_s} n|^2 = -2\phi\sum_m \nabla_\Gamma n_m \bullet \nabla_\Gamma\nu\nabla_\Gamma n_m = -2\phi(\nabla_\Gamma n)^T : \nabla_\Gamma\nu\nabla_\Gamma n,$$

and completes the proof. □

To compute the first variation of the energy (6.7.1) we recall the differentiation rule

$$\frac{\mathrm{d}}{\mathrm{d}s}\Big|_{s=0}\int_{\Gamma_s}\psi_s \mathrm{d}\sigma_s = \int_\Gamma \psi' \mathrm{d}\sigma - \int_\Gamma \psi H\phi \mathrm{d}\sigma.$$

We abreviate the first variation of the four terms in (6.7.1) with I,II,III and IV and deduce for I

$$\frac{\mathrm{d}}{\mathrm{d}s}\Big|_{s=0}\left(\frac{1}{2}\int_{\Gamma_s}\big(H_s + \delta\operatorname{div}_{\Gamma_s} n\big)^2\mathrm{d}\sigma_s\right) = \int_\Gamma \big(H + \delta\operatorname{div}_\Gamma n\big)\big(H' + \delta\partial_s|_{s=0}\operatorname{div}_{\Gamma_s} n\big)\mathrm{d}\sigma - \frac{1}{2}\int_\Gamma \big(H + \delta\operatorname{div}_\Gamma n\big)^2 H\phi\mathrm{d}\sigma.$$

In light of (6.7.6) and (6.7.7), we can expand I as follows:

$$\begin{aligned}I &= \int_\Gamma \big(H + \delta\operatorname{div}_\Gamma n\big)\big(\Delta_\Gamma\phi + \phi|\nabla_\Gamma\nu|^2 - \delta\phi\nabla_\Gamma n : \nabla_\Gamma\nu + \delta\nu^T\nabla_\Gamma n \bullet \nabla_\Gamma\phi\big)\mathrm{d}\sigma \\ &= -\big(\nabla_\Gamma H, \nabla_\Gamma\phi\big) + \big(H|\nabla_\Gamma\nu|^2, \phi\big) - \delta\big(H(\nabla_\Gamma n : \nabla_\Gamma\nu), \phi\big) + \delta\big(H(\nu^T\nabla_\Gamma n), \nabla_\Gamma\phi\big) \\ &\quad - \delta\big(\nabla_\Gamma(\operatorname{div}_\Gamma n), \nabla_\Gamma\phi\big) + \delta\big(\operatorname{div}_\Gamma n|\nabla_\Gamma\nu|^2, \phi\big) - \delta^2\big(\operatorname{div}_\Gamma n(\nabla_\Gamma n : \nabla_\Gamma\nu), \phi\big) \\ &\quad + \delta^2\big(\operatorname{div}_\Gamma n(\nu^T\nabla_\Gamma n), \nabla_\Gamma\phi\big) - \frac{1}{2}\big(H(H + \delta\operatorname{div}_\Gamma n)^2, \phi\big).\end{aligned}$$

For II we apply (6.7.8) to arrive at

$$II = \frac{\mathrm{d}}{\mathrm{d}s}\Big|_{s=0} \int_{\Gamma_s} |\nabla_{\Gamma_s} n|^2 \mathrm{d}\sigma = -2\int_\Gamma \phi(\nabla_\Gamma n)^T : \nabla_\Gamma \nu \nabla_\Gamma n \mathrm{d}\sigma - \int_\Gamma |\nabla_\Gamma n|^2 H\phi \mathrm{d}\sigma.$$

Then III gives no contribution because $|n| = 1$ on Γ and $n' = 0$, namely

$$III = \frac{\mathrm{d}}{\mathrm{d}s}\Big|_{s=0} \int_{\Gamma_s} \Big(\mu\big(|n|^2 - 1\big)\Big)\mathrm{d}\sigma = \int_\Gamma \Big(\mu'\big(|n|^2-1\big) + 2\mu n \bullet n'\Big)\mathrm{d}\sigma - \int_\Gamma \mu\big(|n|^2-1\big)\phi H \mathrm{d}\sigma = 0.$$

Finally, since (6.7.6) implies $(n \bullet \nu)' = n \bullet \nu' = -n \bullet \nabla_\Gamma \phi$, we can compute for IV

$$IV = \frac{\mathrm{d}}{\mathrm{d}s}\Big|_{s=0} \int_{\Gamma_s} f(n \bullet \nu_s)\mathrm{d}\sigma = -\int_\Gamma f'(n\bullet\nu) n \bullet \nabla_\Gamma \phi \mathrm{d}\sigma - \int_\Gamma f(n\bullet\nu) H\phi \mathrm{d}\sigma.$$

We are now in a position to write $\delta_\Gamma E$. Collecting all previous expressions I - IV we obtain for all $\phi \in C^\infty(\Gamma)$

$$\begin{aligned}\Big\langle \frac{\delta E}{\delta \Gamma}, \phi\Big\rangle = &-\Big(\nabla_\Gamma H, \nabla_\Gamma \phi\Big) + \Big(H|\nabla_\Gamma \nu|^2, \phi\Big) - \delta\Big(H(\nabla_\Gamma n : \nabla_\Gamma \nu), \phi\Big) + \delta\Big(H(\nu^T \nabla_\Gamma n), \nabla_\Gamma \phi\Big)\\
&- \delta\Big(\nabla_\Gamma(\mathrm{div}_\Gamma n), \nabla_\Gamma \phi\Big) + \delta\Big(\mathrm{div}_\Gamma n |\nabla_\Gamma \nu|^2, \phi\Big) - \delta^2\Big(\mathrm{div}_\Gamma n(\nabla_\Gamma n : \nabla_\Gamma \nu), \phi\Big)\\
&+ \delta^2\Big(\mathrm{div}_\Gamma n(\nu^T \nabla_\Gamma n), \nabla_\Gamma \phi\Big) - \frac{1}{2}\Big(H(H + \delta \mathrm{div}_\Gamma n)^2, \phi\Big) - \lambda\Big((\nabla_\Gamma n)^T : D\nu(\nabla_\Gamma n), \phi\Big)\\
&- \frac{\lambda}{2}\Big(H|\nabla_\Gamma n|^2, \phi\Big) - \frac{1}{2\varepsilon^2}\Big(f'(n\bullet\nu)n, \nabla_\Gamma \phi\Big) - \frac{1}{2\varepsilon^2}\Big(Hf(n\bullet\nu), \phi\Big),\end{aligned}$$

The variation with respect to n is given by

$$\Big\langle \frac{\delta E}{\delta n}, m\Big\rangle = \delta\Big(H + \delta \mathrm{div}_\Gamma n, \mathrm{div}_\Gamma m\Big) + \lambda\Big(\nabla_\Gamma n, \nabla_\Gamma m\Big) + \Big(2\mu n, m\Big) + \frac{1}{2\varepsilon^2}\Big(f'(n\bullet\nu), m\bullet\nu\Big),$$

for all $m \in C^\infty(\Gamma; \mathbb{R}^3)$. This expression simplifies if we impose tangential variations $m \in C^\infty(\Gamma; T_n\mathbb{S}^2) := \{v \in C^\infty(\Gamma;\mathbb{R}^3) : v(x) \in T_{n(x)}\mathbb{S}^2 \text{ a.e. } x \in \Gamma\}$ so that $(\mu n, m) = 0$.
We simulate the evolution of Γ and n via a relaxation dynamics, which is an *L^2-gradient flow*. If v denotes the normal velocity of Γ, we then have to solve the following system of PDE on Γ

$$\begin{aligned}\langle v, \phi\rangle &= -\Big\langle \frac{\delta E}{\delta \Gamma}, \phi\Big\rangle \quad \text{for all } \phi \in C^\infty(\Gamma),\\
\langle \partial_t n, m\rangle &= -\Big\langle \frac{\delta E}{\delta n}, m\Big\rangle \quad \text{for all } m \in C^\infty(\Gamma; T_n\mathbb{S}^2),\end{aligned}$$

subject to the constraint that $n(t,x) \in \mathbb{S}^2$ for almost every (t,x).

Remark 6.7.4 *Let $\Phi : [0,T) \times \mathbb{R}^3 \to \mathbb{R}^3$ be the flow of the evolution of $\Gamma(t)$ for $t \in [0,T)$, that is, $\Phi(0,\cdot)|_{\Gamma(0)} = \mathrm{id}|_{\Gamma(0)}$ and $\partial_t \Phi(t,x) = v(t,\Phi(t,x))\nu(t,\Phi(t,x))$. Then*

$$\frac{d}{ds}\Big|_{s=t} E(\Gamma(s), n(s,\Phi(s,\cdot))) = \Big\langle \frac{\partial E}{\partial \Gamma}, v\Big\rangle + \Big\langle \frac{\partial E}{\partial n}, \frac{d}{ds}\Big|_{s=t} n(s,\Phi(s,\cdot))\Big\rangle.$$

Since n is constant in normal direction we have that

$$\frac{d}{ds}\Big|_{s=t} n(s,\Phi(s,x)) = \partial_t n(t,\Phi(t,x)) + \nabla n(t,\Phi(t,x)) \bullet \nu(t,\Phi(t,x)) v(t,\Phi(t,x)) = \partial_t n(t,\Phi(t,x)).$$

Although, we do not prove a discrete energy law for the L^2-gradient flow in the closed surface case we have that

$$\frac{d}{ds}\Big|_{s=t} E(\Gamma(s), n(s,y(s))) = -\langle v, v\rangle - \langle \partial_t n, \partial_t n\rangle \le 0,$$

and expect a discrete energy reduction in the numerical experiments.

6.7.5. Discretization

As in Section 6.1.2 we start with the time discretization. Given the surface $\Gamma^{j-1} \subset \mathbb{R}^3$ at time t_{j-1} we follow the ideas in [30] to parametrize Γ^j at time t_j over Γ^{j-1}. We thus look for $X^j : \Gamma^{j-1} \to \mathbb{R}^3$ and set $\Gamma^j = X^j(\Gamma^{j-1})$. As in [10], we approximate the normal velocity via

$$v^j \approx \frac{1}{\tau}\big(X^j - \mathrm{id}_{\Gamma^{j-1}}\big) \bullet \nu^{j-1},$$

where $\nu^{j-1} : \Gamma^{j-1} \to \mathbb{S}^2$ is the outer unit normal to Γ^{j-1}. Now, again, using an idea from [30] to compute H^j we discretize the crucial geometric identity $\Delta_\Gamma X = H\nu$ [30, 31]:

$$\Delta_{\Gamma^{j-1}} X^j = H^j \nu^{j-1}.$$

For the evolution of n we use the techniques from [11]. In order to formulate the fully discrete evolution concisely we set $\mathrm{Div}_{\Gamma_h^{j-1}} n^{j-1} := \mathcal{A}^j(\mathrm{div}_{\Gamma_h^{j-1}} n^{j-1})$, denote by $(\cdot,\cdot)_{\Gamma_h^{j-1}}$ the standard L^2-inner product on Γ_h^{j-1}, and we define $\Psi_{\delta_\Gamma E}^{j-1,j} = \Psi_{\delta_\Gamma E}^{j-1,j}(H^j, H^{j-1}, \nu^{j-1}, n^{j-1}) \in \mathbb{V}^{j-1}$ to be the representation of a semi-implicit discretization of $\frac{\delta E}{\delta \Gamma}$ given by

$$\begin{aligned}
\Big(\Psi_{\delta_\Gamma E}^{j-1,j}, \phi\Big) = &-\Big(\nabla_{\Gamma_h^{j-1}} H^j, \nabla_{\Gamma_h^{j-1}}\phi\Big)_{\Gamma_h^{j-1}} + \Big(H^{j-1}|\nabla_{\Gamma_h^{j-1}}\nu^{j-1}|^2, \phi\Big)_{\Gamma_h^{j-1}} - \delta\Big(H^j(\nabla_{\Gamma_h^{j-1}} n^{j-1} : \nabla_{\Gamma_h^{j-1}}\nu^{j-1}), \phi\Big)_{\Gamma_h^{j-1}} \\
&+ \delta\Big(H^j((\nu^{j-1})^T\nabla_{\Gamma_h^{j-1}} n^{j-1}), \nabla_{\Gamma_h^{j-1}}\phi\Big)_{\Gamma_h^{j-1}} - \delta\Big(\nabla_{\Gamma_h^{j-1}}(\mathrm{Div}_{\Gamma_h^{j-1}} n^{j-1}), \nabla_{\Gamma_h^{j-1}}\phi\Big)_{\Gamma_h^{j-1}} \\
&+ \delta\Big(\mathrm{Div}_{\Gamma_h^{j-1}} n^{j-1}|\nabla_{\Gamma_h^{j-1}}\nu^{j-1}|^2, \phi\Big)_{\Gamma_h^{j-1}} - \delta^2\Big(\mathrm{Div}_{\Gamma_h^{j-1}} n^{j-1}(\nabla_{\Gamma_h^{j-1}} n^{j-1} : \nabla_{\Gamma_h^{j-1}}\nu^{j-1}), \phi\Big)_{\Gamma_h^{j-1}} \\
&+ \delta^2\Big(\mathrm{Div}_{\Gamma_h^{j-1}} n^{j-1}((\nu^{j-1})^T\nabla_{\Gamma_h^{j-1}} n^{j-1}), \nabla_{\Gamma_h^{j-1}}\phi\Big)_{\Gamma_h^{j-1}} - \frac{1}{2}\Big(H^j(H^{j-1} + \delta\mathrm{Div}_{\Gamma_h^{j-1}} n^{j-1})^2, \phi\Big)_{\Gamma_h^{j-1}} \\
&- \lambda\Big((\nabla_{\Gamma_h^{j-1}} n^{j-1})^T : \nabla_{\Gamma_h^{j-1}}\nu^{j-1}(\nabla_{\Gamma_h^{j-1}} n^{j-1}), \phi\Big)_{\Gamma_h^{j-1}} - \frac{\lambda}{2}\Big(H^j|\nabla_{\Gamma_h^{j-1}} n^{j-1}|^2, \phi\Big)_{\Gamma_h^{j-1}} \\
&- \frac{1}{2\varepsilon^2}\Big(f'(n^{j-1}\bullet\nu^{j-1})n^{j-1}, \nabla_{\Gamma_h^{j-1}}\phi\Big)_{\Gamma_h^{j-1}} - \frac{1}{2\varepsilon^2}\Big(H^j f(n^{j-1}\bullet\nu^{j-1}), \phi\Big)_{\Gamma_h^{j-1}},
\end{aligned}$$

for all $\phi \in \mathbb{V}^{j-1}$.

6.7.6. Semi-implicit fully discrete gradient flow with constraints

We start with an initial polyhedral surface Γ_h^0, time-step size $\tau > 0$, parameters $\varepsilon, \delta, \lambda$, and an initial director field $n^0 \in [\mathbb{V}^0]^3$ with $|n^0(a)| = 1$ for all $a \in \mathcal{N}_h^0$. We set $j := 1$ and iterate on j the following steps:

1. Compute $(\widetilde{X}^j, H^j) \in [\mathbb{V}^{j-1}]^3 \times \mathbb{V}^{j-1}$ satisfying

$$\begin{aligned}
\frac{1}{\tau}\Big((\widetilde{X}^j - X^{j-1})\bullet\nu^{j-1}, \phi\Big)_{\Gamma_h^{j-1}} &= -\Big(\Psi_{\delta_\Gamma E}^{j-1,j}, \phi\Big)_{\Gamma_h^{j-1}}, \\
\Big(\nabla_{\Gamma_h^{j-1}}\widetilde{X}^j, \nabla_{\Gamma_h^{j-1}}\eta\Big)_{\Gamma_h^{j-1}} &= -\Big(H^j, \eta\bullet\nu^{j-1}\Big)_{\Gamma_h^{j-1}},
\end{aligned}$$

   for all $\phi \in \mathbb{V}^{j-1}$ and all $\eta \in \mathbb{V}(\Gamma_h^{j-1}; \mathbb{R}^3)$.

2. Set

$$v_E = \frac{1}{\tau}\big(\widetilde{X}^j - X^{j-1}\big)\bullet\nu^{j-1}, \quad v_V = -1, \quad v_A = H^j,$$

   and compute (ρ_1^j, ρ_2^j) such that $f^j(\rho_1^j, \rho_2^j) = 0$. Set

$$X^j = X^{j-1} + \tau(v_E + \rho_1^j v_V + \rho_2^j v_A)\nu^{j-1}, \quad \Gamma_h^j = \{X^j(x) : x \in \Gamma_h^{j-1}\}, \quad n^{j-1} := G^j \circ n^{j-1}.$$

3. Compute $\widetilde{\mathrm{d}}_t n^j \in \mathbb{F}[n^{j-1}]$ with

$$\Big(\widetilde{\mathrm{d}}_t n^j, m\Big)_{\Gamma_h^j} + \tau\lambda\Big(\nabla_{\Gamma_h^j}\widetilde{\mathrm{d}}_t n^j, \nabla_{\Gamma_h^j} m\Big)_{\Gamma_h^j} = -\lambda\Big(\nabla_{\Gamma_h^j} n^{j-1}, \nabla_{\Gamma_h^j} m\Big)_{\Gamma_h^j} - \delta\Big(H^j + \delta \mathrm{Div}_{\Gamma_h^{j-1}} n^{j-1}, \mathrm{div}_{\Gamma_h^j} m\Big)_{\Gamma_h^j} - \frac{1}{2\varepsilon^2}\Big(f'(n^{j-1}\bullet\nu^j), m\bullet\nu^j\Big)_{\Gamma_h^j},$$

for all $m \in \mathbb{F}[n^{j-1}]$, where the latter is the space of vector-valued continuous piecewise linear functions that are orthogonal to n^{j-1} at the nodes $\mathcal{N}^{j-1}$.

4. For all $a \in \mathcal{N}^j$ set

$$n^j(a) = \frac{n^{j-1}(a) + \tau\,\widetilde{\mathrm{d}}_t n^j(a)}{|n^{j-1}(a) + \tau\,\widetilde{\mathrm{d}}_t n^j(a)|}.$$

5. Set $X^j := G^j \circ X^j = \mathrm{id}_{\Gamma_h^j}$, $j = j+1$ and go to (1).

Remark 6.7.7 *(i) Setting $(\rho_1^j, \rho_2^j) = 0$ in 2 reduces the iteration to an L^2-flow for $E(\Gamma, n)$.*
(ii) Solvability of the system in Step (1) can be established by arguing as in [10]; see also [6].

6.8. Numerical experiments for the nonlinear model

In our numerical experiments for the model on closed surfaces we distinguish the cases $\varepsilon = \infty$ and $\varepsilon \ll 1$, where $\varepsilon = \infty$ means that the term penalizing variations of n from a prescribed angle relative to the surface normal, i.e., the term including f in $E(\Gamma, n)$, is omitted. The realization of the volume and area constraints via the Newton iteration outlined above allowed us to satisfy the conservation of these quantities up to machine precision. As a stopping criterion for the discrete evolutions we used that the change of the discrete energy

$$E_h(\Gamma_h, n_h) := \frac{1}{2}\int_{\Gamma_h}(H + \delta\mathcal{A}(\mathrm{div}_{\Gamma_h} n_h))^2 \mathrm{d}\sigma + \frac{\lambda}{2}\int_{\Gamma_h}|\nabla_{\Gamma_h} n_h|^2 \mathrm{d}\sigma + \frac{1}{2\varepsilon^2}\int_{\Gamma_h} f(n_h \bullet \nu)\mathrm{d}\sigma$$

in two consecutive time-steps was less than 10^{-5}. For significantly smaller stopping criteria we observed in some of our experiments that the evolution became unstable which is related to unfavorable tangential motions on the surface which eventually lead to singularities in the mesh. Given that there is no stability analysis for the closed surface case an optimal time-step size can not be computed and in our simulations we mainly use $\tau = h^4$. Moreover we work only on two different meshes so there is no evidence for assuming a scaling or special asymptotics for τ. We believe that by employing mesh regularization techniques such as those in [6, 21] we could use larger time steps and a smaller stopping criterion. The evolution equation for the director field n on Γ is a second order parabolic equation and should therefore also work for $\tau \sim h^2$ as was shown in [32]. Our proposed algorithm was implemented in Matlab and all experiments were carried out on a standard desktop (Intel Core (TM) 2 Quad CPU Q6600 @ 2.40GHz). The CPU-time needed for the calculation of one step with 2048 elements including the assembly of the system matrices was around 0.05 seconds. In all figures displayed below the color scale was chosen so that low values of a quantity are represented by dark and large values by bright colors. All displayed arrows have unit length and are scaled for graphical purposes.

6.8.1. Surfactants

To simulate surfactants we omit the penalty term which corresponds to the choice $\varepsilon = \infty$.

Perturbed sphere with volume constraint. We set $\delta = 1$, $\lambda = 5$, $\tau = h^4$, choose as initial surface Γ_h^0 a perturbation of the unit sphere, and as initial director field n^0 a perturbation of the discrete outer unit normal ν^0. The perturbations were realized by displacing the nodes of a triangulation $\mathcal{T}$ of the unit sphere with 2048 elements in normal direction and the unit normals by random vectors

with magnitudes bounded by 0.1 and 0.05, respectively. The first summand of the continuous energy functional $E(\Gamma, n)$ vanishes for $n = \nu$ and this director field is stationary for the Dirichlet energy subject to a unit-length constraint, i.e., the outer unit normal of the sphere is a harmonic map into the unit sphere. Therefore, we expect that the pair $(\mathbb{S}^2, \nu)$ is a stationary point for $E(\Gamma, n)$ subject to a volume constraint. The snapshots of the discrete evolution shown in Figure 6.6 confirm this expected behavior and the monotone energy decay displayed in the right plot of Figure 6.6 suggests that the chosen discretization parameters are sufficiently small to compute a stable and accurate approximation of the exact evolution. When we stopped our calculations the discrete energy was $E_h = 62.8516$, which is an accurate approximation of the value $E(\mathbb{S}^2, \nu) = 20\pi$, i.e., the absolute error is $|E_h - E(\mathbb{S}^2, \nu)| < 0.02$. The alignment of the director field n describing the orientation of the surfactant molecules and the surface normal is visualized by the coloring of the displayed arrows and is an effect which is frequently observed for surfactants. We remark that our simulations showed that for larger values of λ we could use larger time steps.

4-4-1 Ellipsoid with area and volume constraint. We set $\delta = 1$, $\lambda = 1$, and $\tau = h^3$. To define the initial surface Γ^0 we employ a triangulation $\mathcal{T}$ of the unit sphere with 768 elements and deform the triangulated sphere by mapping its nodes contained in $\mathcal{N}$ onto a 4-4-1 ellipsoid, i.e., we set

$$\mathcal{N}^0 = \{\widetilde{a} : \widetilde{a} = 4a_1e_1 + 4a_2e_2 + e_3 \text{ for } a = (a_1, a_2, a_3) \in \mathcal{N}\},$$

and this defines a triangulation Γ_h^0 of the ellipsoid. The initial director field was defined by setting $n^0 = \nu^0$. Incorporating volume and area constraints in the evolution allows us to compare the qualitative behavior of our model with well known observations for the Helfrich flow which is included in our model and corresponds to the uncoupled flow defined through $\delta = 0$, i.e., without spontaneous curvature. The upper row in Figure 6.7 displays a cut through the discrete surfaces at different times within the evolution for $\delta = 1$. We observe that the surface develops the shape of a discocyte. Qualitatively, such shapes have been observed to be stationary for the Helfrich flow and we plotted in the second row of Figure 6.7 the discrete surfaces for this model, i.e., for our scheme with $\delta = 0$. We observe that the coupling with the director field leads to a deceleration and the shape of the discocyte is not as pronounced as in the uncoupled case. The plots including the director field in Figure 6.8 of the nearly stationary configuration in the coupled case show that the director field is aligned with the surface normal in regions where the surface can be approximated by a sphere, i.e., in regions where the unit normal is a harmonic map.

6.8.2. Biomembranes

In our second set of experiments for the full model on closed surfaces we use $\varepsilon = 1/\sqrt{20}$ and consider initial director fields on the sphere with different topological properties. In the gel phase the director field prefers to have a fixed angle with respect to the normal to the surface. As in the flat case we restrict ourselves to $\pi/2$, which corresponds to $\xi_0 = 0$. Throughout the first subsection the underlying triangulation of the unit sphere consists of 8192 elements, we always chose $\tau = h^4$, $\lambda = 1$, and we enforce conservation of the enclosed volume. For the last experiment we use a finer triangulation, consisting of 12288 elements, while τ and λ remain unchanged. To magnify relevant effects of the coupling between the director field an the curvature of the surface we employ different values of δ.

Positive degree-one defects. Given a point $a = (a_1, a_2, a_3)$ on the sphere we let (r, θ) be the polar coordinates of the first two components of a, i.e., $(a_1, a_2) = r(\cos\theta, \sin\theta)$. Since deviations of $n \bullet \nu$ from 0 are penalized by a Ginzburg Landau term we use the characteristic profile of tanh to regularize the initial singularities. Thus, we set $\varphi_\varepsilon(r) = \tanh(r/\varepsilon)$ and use this function in the extension of a director field in the neighborhood of a singularity. Then the transition of $n \bullet \nu$ from 0 to 1 is on an annulus of width ε around the center of the singularity where the value 1 is taken. Note that ε has to be chosen big enough so that the transition can be resolved properly by the mesh. We define three initial director fields n_0 that have defects of positive degree-one at the north and south pole as follows.

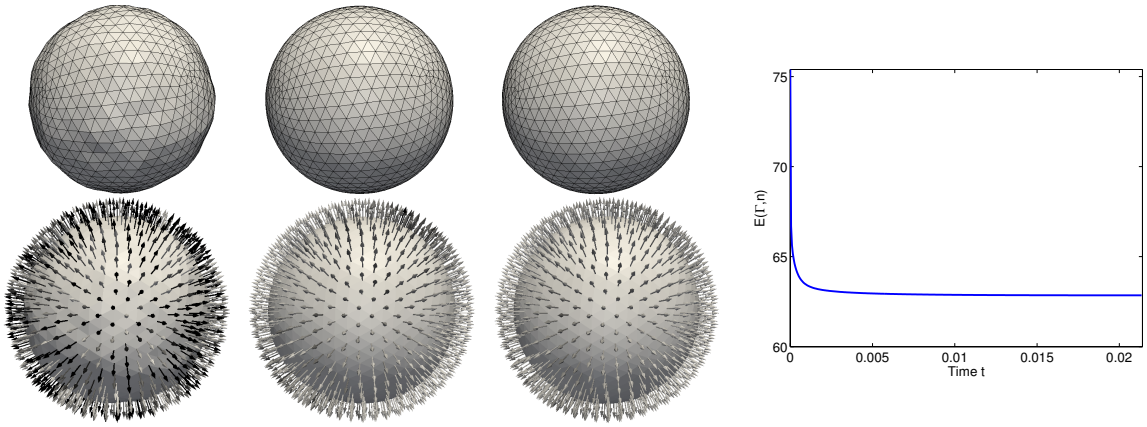

Figure 6.6.: Evolution from a perturbed sphere in the surfactant case with volume constraint: snapshots of the evolution after $n = 1, 50$ and 400 time-steps. The arrows are colored by $n \bullet \nu$. The surface normal and the director field align and the surface attains a stable state that coincides with a sphere. The right plot depicts the decay of the energy during the evolution.

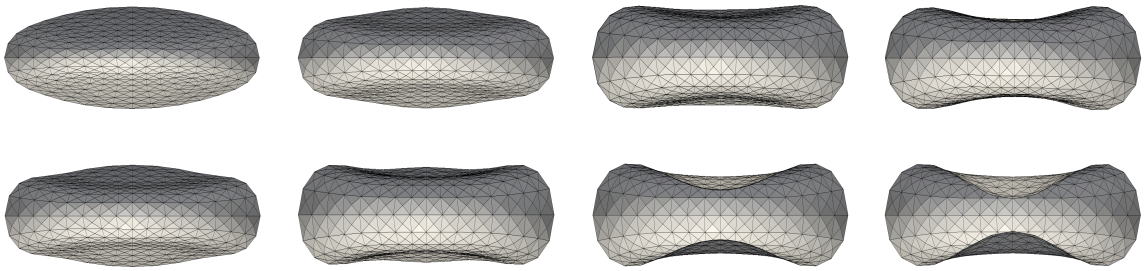

Figure 6.7.: Evolution from a prolate 4-4-1 ellipsoid in the surfactant case with volume and area constraint: snapshots of the evolution after $n = 50, 200, 600$ and 1200 time-steps. The upper plots show the evolution in the presence of surfactants ($\delta = 1$) while the second row shows the Helfrich-flow ($\delta = 0$). The coupling of the surface and the director field decelerates the evolution and leads to a less pronounced shape.

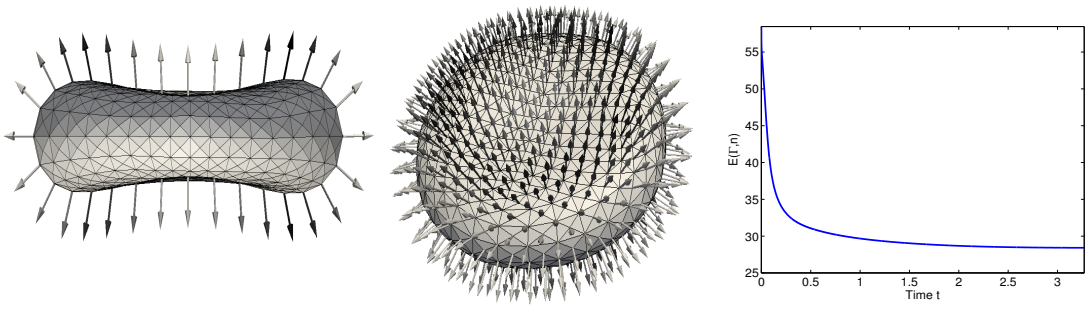

Figure 6.8.: Evolution from a prolate 4-4-1 ellipsoid in the surfactant case with volume and area constraint: snapshots of the final state of the evolution in the presence of surfactants ($\delta = 1$). The director field is colored by the deviation of $n \bullet \nu$ from 1 and we observe that in regions where the surface is approximated by a sphere the director aligns with the surface normal. A monotone decay of the energy can be observed in the right plot.

(i) *Two outward pointing defects:*

$$n^0(a) = \big(\varphi_\varepsilon(r)\cos(\theta), \varphi_\varepsilon(r)\sin(\theta), \mathrm{sign}(a_3)(1-\varphi_\varepsilon(r)^2)^{1/2}\big).$$

(ii) *Two* $90°$*-rotated defects:*

$$n^0(a) = \big(\varphi_\varepsilon(r)\cos(\theta+\pi/2), \varphi_\varepsilon(r)\sin(\theta+\pi/2), \mathrm{sign}(a_3)(1-\varphi_\varepsilon(r)^2)^{1/2}\big).$$

(iii) *Inward and outward pointing defect:*

$$n(a) = \frac{(0,0,1) - \varphi_\varepsilon(r)a_3 a}{|(0,0,1) - \varphi_\varepsilon(r)a_3 a|}.$$

The initial director fields are shown from different perspectives in the rows of Figure 6.9 for (i)-(iii), respectively. We use $\delta = 0.5$, $\delta = 1$, and $\delta = 0.75$ for the settings defined by (i), (ii), and (iii), respectively, in order to enhance the effect of the different defects on the shape of the surface.

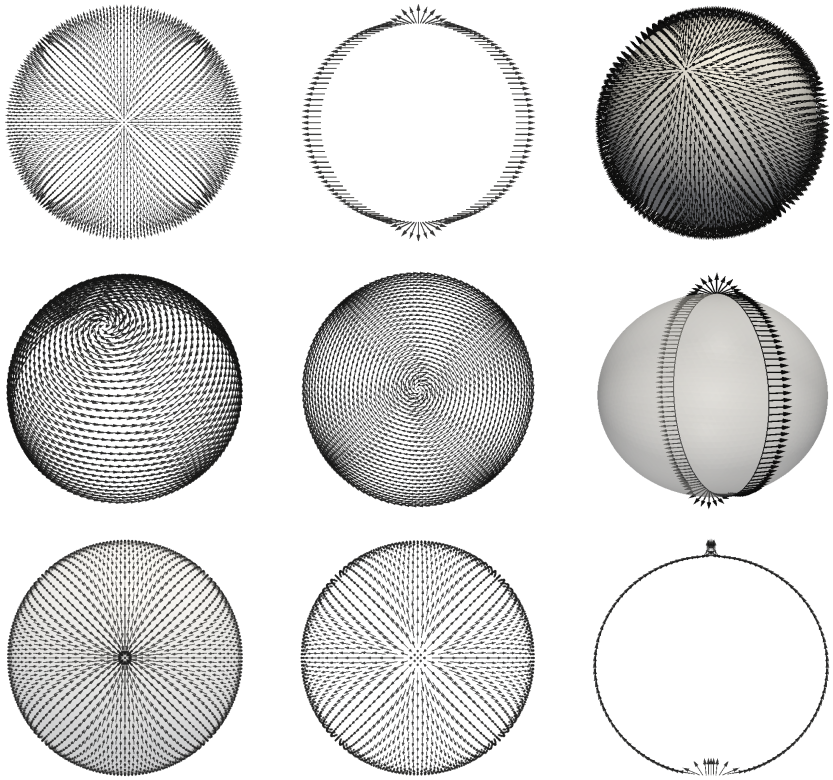

Figure 6.9.: Initial director fields with two defects of positive degree-one. Upper row: outward pointing defects at north and south pole defined in (i). Middle row: $90°$-rotated defects at north and south pole defined in (ii). Lower row: Inward and outward pointing defects at north and south pole defined in (iii).

Snapshots of the surface and the director field during the discrete evolutions defined with the initial data from (i) and (iii) are shown in Figure 6.10 and 6.11, respectively. The observed results are in very good agreement with our theoretical predictions from Section 6.3: the surface develops outward cones of negative curvature at defects for which the tangential part of the director field points away from the defect and inward cones if the director field points towards the defect. These configurations show certain analogies with stomatocyte and echinocyte shapes observed in experiments, cf., e.g., [53]. For the initial data defined in (i) and the corresponding snapshots displayed in Figure 6.10 we see that

the surface also develops large curvature in a neighborhood of the equator. This is related to the fact that the tangential component of the director field changes its sign along this line leading to a large contribution from the penalty term which induces local curvature. In the plots shown in Figure 6.11 where the initial director field from (iii) is tangential along the equator the surface does not develop such effects. For the initial data defined in (ii) we did not observe changes of the initial surface which again matches our earlier observation that a 90°-rotated defect of positive degree one is divergence free and hence does not enforce local curvature. We finally remark that the qualitative behavior of the surfaces with initial director fields defined in (i)-(iii) was nearly independent of the choice of the preferred angle ξ_0. This justifies the earlier discussed simplification of the previous sections to consider only the tangential part of the director field and to analyze its influence on the local shape of the surfaces. In Figure 6.12 we see the monotone decay of energy during the evolutions.

Negative degree-one defects. To analyze the effect of negative degree-one defects onto the local curvature we let again denote (r, θ) polar coordinates of the components (a_1, a_2) for a point $a = (a_1, a_2, a_3)$ on the sphere and define the initial director field by

$$\tilde{n}^0(a) = \big(\varphi_\varepsilon(r)\cos(-\theta), \varphi_\varepsilon(r)\sin(-\theta), \operatorname{sign}(a_3)(1-\varphi_\varepsilon(r)^2)^{1/2}\big),$$

$$n^0(a) = \frac{\tilde{n}^0(a) - 0.9(\tilde{n}^0(a) \bullet a)a}{|\tilde{n}^0(a) - 0.9(\tilde{n}^0(a) \bullet a)a|},$$

and set $\delta = 1$. The director field is displayed in Figure 6.13 from two different perspectives and along two geodesics through the north and south pole that intersect at those points in a right angle. By the Poincaré-Hopf index formula the sum of the degrees of the defects equals the Euler-Characteristic χ of the surface. Since $\chi(\mathbb{S}^2) = 2$ we expect other defects of positive degrees. For our choice of n^0 we obtain four defects of positive degree-one sitting on the equator. Two of them are outward- and two of them are inward-pointing. However at these points, the director field varies smoothly and ε-independently so that they do not have a strong effect on the local curvature. From the final states displayed in the plots in Figure 6.14 we see that within the evolution the surface adjusts to the director field by forming saddles at the poles. This is again in good agreement with our predictions in the simplified setting discussed in Section 6.3.

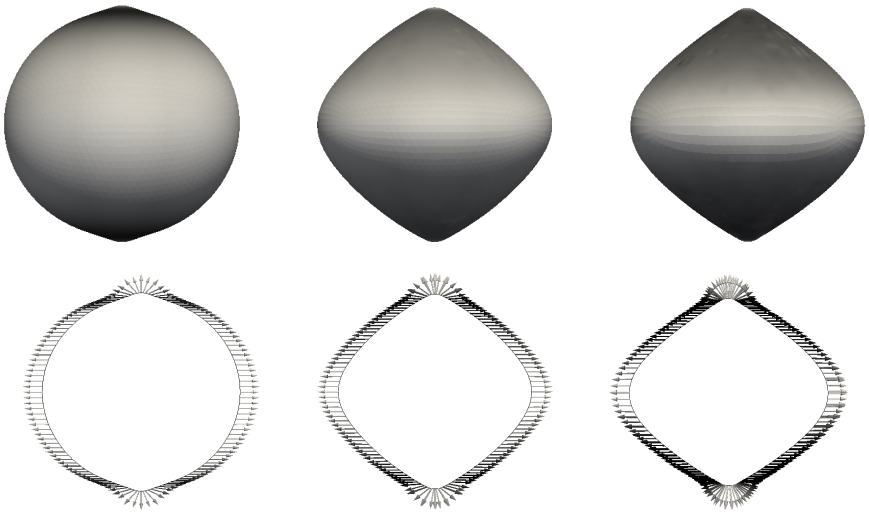

Figure 6.10.: Biomembrane case with two outward pointing defects of positive degree one: Snapshots of the evolving surface and of the director field along a (deformed) geodesic through the north and south pole after $n = 50, 1000, 4800$ time steps. The surface develops a cone-like shape at the poles while the director field remains nearly unchanged during the evolution. The surface and the director field are colored by $n \bullet \nu$.

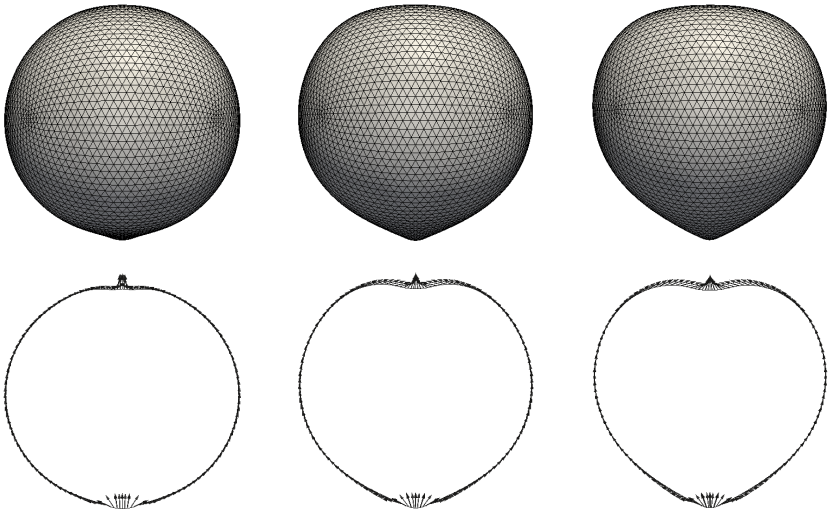

Figure 6.11.: Biomembrane case with inward and outward pointing defects of positive degree one: Snapshots of the surface and the director field along a (deformed) geodesic through the north and south pole after $n = 50, 500, 1400$ time steps. The surface develops inward and outward cones at the poles while the director field remains nearly unchanged during the evolution.

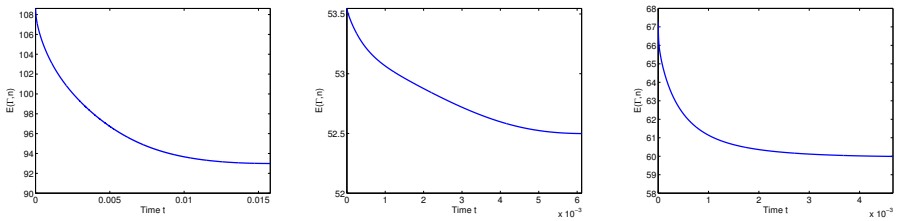

Figure 6.12.: Decay of energy during the evolution of the positive degree-one defects: Energies for the initial director fields defined through $(i), (ii)$ and (iii) (from left to right).

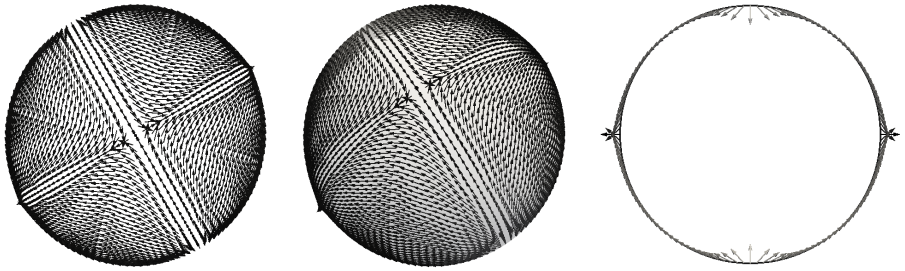

Figure 6.13.: Initial director field with negative degree-one defects at the north and south pole from different perspectives and the director field along the equator with 4 defects of positive degree-one.

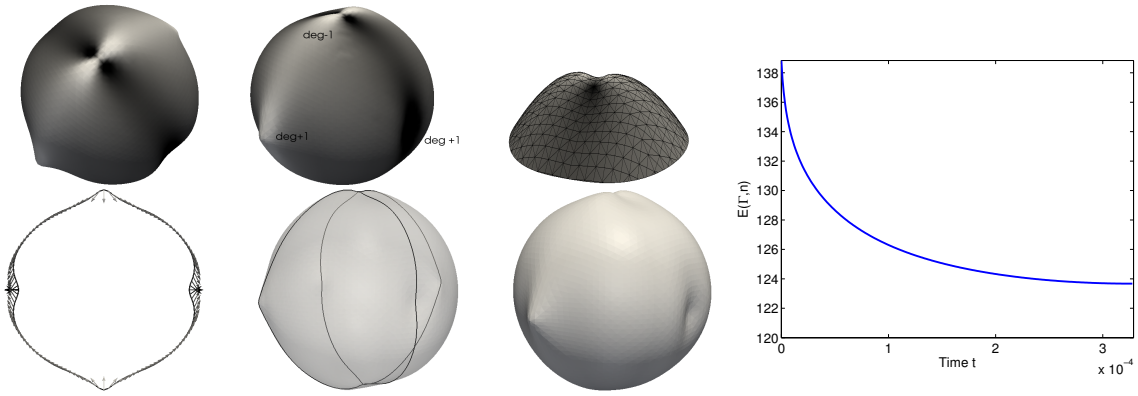

Figure 6.14.: Final states in the biomembrane case that develop from a director field with two negative degree-one defects at the poles: As in the linearized case the surface forms saddle-shapes at the places where defects are located (see the zoom to the north-pole in the upper-right picture). The cut through the equator shows cone like bowings due to the positive degree-one defects. The right plot shows the monotone decay of the energy during the evolution. The surface and the director field are colored by $\mathrm{div}_\Gamma n$.

Appendix A.

MATLAB Codes and Paraview Data

In this chapter we provide some MATLAB codes that we use in the numerical realization of the proposed schemes. Systems of linear equations are always solved by MATLAB's backslash operator. Most of the programms contain the function `nodal_basis` which provides a vector area_T $\in \mathbb{R}^{nE}$ and a matrix Dphi_T $\in \mathbb{R}^{3nE\times 3}$, where $nE = \operatorname{card}\mathcal{T}_h$ is the number of triangles in the given triangulation. The entries of the two outputs are `area_T`$(j) = |T_j|$ and

$$\text{Dphi\_T} = \left[\text{Dphi}_{T_1}, \text{Dphi}_{T_2}, \cdots \text{Dphi}_{T_{nE}}\right]^T$$

where $\text{Dphi}_{T_j} \in \mathbb{R}^{3\times 3}$ is defined as

$$\text{Dphi}_{T_j} := \left[\nabla\varphi_{j_1}\Big|_{T_j}, \nabla\varphi_{j_2}\Big|_{T_j}, \nabla\varphi_{j_3}\Big|_{T_j}\right]^T.$$

Here $\varphi_{j_1}, \varphi_{j_2}, \varphi_{j_3} \in \mathcal{S}^1(\mathcal{T}_h)$ are the nodal basis functions on the triangle $T_j \in \mathcal{T}_h$ with nodes z_{j_1}, z_{j_2} and $z_{j_3} \in \mathcal{N}_h$ for $j = 1, \ldots, nE$.

The visualization of our numerical experiments is performed by PARAVIEW. We give a sample of a `vtk`-File which we use for the visualization and present a programm that can be used to export MATLAB data to PARAVIEW.

Listing A.1: Assembling stiffness matrices for the mixed formulation

```
function [grad_1,grad_1bb,div_1,div_1bb] = divgrad_matrices(n4e,c4n)
% ---
[area_T,Dphi_T] = nodal_basis(c4n,n4e);
% ------------------------------------------------------------------
% --- P1-gradient and -divergence matrices-----------------------------
% ------------------------------------------------------------------
I=zeros(54*nE,1);J=I;X_grad=I;X_div=I;idx=1:6*nE;
for k = 1:3
    grad_k = Dphi_T(3*(0:nE-1)+k,:);
    for ell = 1:3
        grad_ell = P_Dphi_T(3*(0:nE-1)+ell,:);
        I(idx) = [  6*n4e(:,k)- 5;6*n4e(:,k)- 4;6*n4e(:,k)- 3;
                    6*n4e(:,k)- 2;6*n4e(:,k)- 1;6*n4e(:,k)- 0];
        J(idx) = [  3*n4e(:,ell)-2;3*n4e(:,ell)-1;3*n4e(:,ell)-0;
                    3*n4e(:,ell)-2;3*n4e(:,ell)-1;3*n4e(:,ell)-0];
        X_div(idx) = [  repmat(1/3*area_T.*grad_k(:,1),3,1);
                        repmat(1/3*area_T.*grad_k(:,2),3,1)];
        X_grad(idx) = [ repmat(1/3*area_T.*grad_ell(:,1),3,1);
                        repmat(1/3*area_T.*grad_ell(:,2),3,1)];
        idx = idx+6*nE;
    end
end
grad_1 = sparse(I,J,X_grad); div_1 = sparse(I,J,X_div);
% ------------------------------------------------------------------
% --- P1-bubble-gradient and -divergence matrices-------------------
% ------------------------------------------------------------------
I=zeros(18*nE,1);J=I;X_grad_bb=I;X_div_bb=I;idx=1:6*nE;
for ell = 1:3
```

```
29      grad_ell = Dphi_T(3*(0:nE-1)+ell,:);
30      I(idx) = [  6*(1:nE)- 5,6*(1:nE)- 4,6*(1:nE)- 3,...
31                  6*(1:nE)- 2,6*(1:nE)- 1,6*(1:nE)- 0];
32      J(idx) = [  3*n4e(:,ell)- 2;3*n4e(:,ell)- 1;3*n4e(:,ell)- 0;
33                  3*n4e(:,ell)- 2;3*n4e(:,ell)- 1;3*n4e(:,ell)- 0];
34      X_div_bb(idx)  = [  repmat(-1/60*area_T.*grad_ell(:,1),3,1);
35                          repmat(-1/60*area_T.*grad_ell(:,2),3,1)];
36      X_grad_bb(idx) = [  repmat(1/60*area_T.*grad_ell(:,1),3,1);
37                          repmat(1/60*area_T.*grad_ell(:,2),3,1)];
38      idx = idx+6*nE;
39  end
40  grad_1bb = sparse(I,J,X_grad_bb); div_1bb = sparse(I,J,X_div_bb);
```

MATLAB optimized assembling of the stiffness matrices `div` and `grad` that are needed for the mixed formulation. The matrices realize the following L^2-inner products

$$(\mathrm{div}\sigma_h, \xi_h) \quad \text{and} \quad (\sigma_h, \nabla\xi_h)$$

for $\xi_h \in [\mathcal{S}^1(\mathcal{T}_h)]^3$, $\sigma_h \in [\mathcal{S}^1(\mathcal{T}_h)]^{3\times 2}$ and $\sigma_h \in [\mathcal{B}^3(\mathcal{T}_h)]^{3\times 2}$ respectively.

- Lines 9 and 11: Extract $\mathrm{grad\_k}(j,:) = \nabla\varphi_k\Big|_{T_j}$ and $\mathrm{grad\_ell}(j,:) = \nabla\varphi_\ell\Big|_{T_j}$ where $k, \ell = 1, 2, 3$ correspond to the nodes of $T_j \in \mathcal{T}_h$.

- Lines 7−23: For $[\mathcal{S}^1(\mathcal{T}_h)]^3$ and $[\mathcal{S}^1(\mathcal{T}_h)]^{3\times 2}$ we have base vectors $(\varphi_k e_n)_{k\in\{1,\dots,nC\}}^{n\in\{1,\dots,6\}}$ and $(\varphi_\ell e_m)_{\ell\in\{1,\dots,nC\}}^{m\in\{1,2,3\}}$ where $(e_n)_{n=1,\dots 6}$ and $(e_m)_{m=1,2,3}$ denote the standard basis of $\mathbb{R}^6$ and $\mathbb{R}^3$, respectively. Then, the following pairings occure in the product $(\sigma_h, \nabla\xi_h)$ for $\xi_h \in [\mathcal{S}^1(\mathcal{T}_h)]^3$ and $\sigma_h \in [\mathcal{S}^1(\mathcal{T}_h)]^{3\times 2}$:

$$\begin{aligned}
\mathrm{grad_1}(6n4e(j,k)-5, 3n4e(j,\ell)-2) &= ((\partial_x\varphi_k), \varphi_\ell) = \mathrm{grad_k}(j,1) * \frac{1}{3}\mathrm{area_T}(j),\\
\mathrm{grad_1}(6n4e(j,k)-4, 3n4e(j,\ell)-1) &= ((\partial_x\varphi_k), \varphi_\ell) = \mathrm{grad_k}(j,1) * \frac{1}{3}\mathrm{area_T}(j),\\
\mathrm{grad_1}(6n4e(j,k)-3, 3n4e(j,\ell)-0) &= ((\partial_x\varphi_k), \varphi_\ell) = \mathrm{grad_k}(j,1) * \frac{1}{3}\mathrm{area_T}(j),\\
\mathrm{grad_1}(6n4e(j,k)-2, 3n4e(j,\ell)-2) &= ((\partial_y\varphi_k), \varphi_\ell) = \mathrm{grad_k}(j,2) * \frac{1}{3}\mathrm{area_T}(j),\\
\mathrm{grad_1}(6n4e(j,k)-1, 3n4e(j,\ell)-1) &= ((\partial_y\varphi_k), \varphi_\ell) = \mathrm{grad_k}(j,2) * \frac{1}{3}\mathrm{area_T}(j),\\
\mathrm{grad_1}(6n4e(j,k)-0, 3n4e(j,\ell)-0) &= ((\partial_y\varphi_k), \varphi_\ell) = \mathrm{grad_k}(j,2) * \frac{1}{3}\mathrm{area_T}(j).
\end{aligned}$$

  The first indices `6n4e(j,k)-5,...,6n4e(j,k)-0` are stored in `I` and the second ones in `J`. Using MATLAB's sparse command produces `grad_1 = sparse(I,J,X_grad_1)` via `grad_1(I(k),J(k)) = X_grad_1(k)` for $k = 1, \dots, 54nE$ in this case. Note, that repeating indices are summed up in the sparse command.

- Lines 27 − 40: Same procedure for $\sigma_h \in [\mathcal{B}^3(\mathcal{T}_h)]^{3\times 2}$. We employ elementwise integration by parts since $\sigma_{bb}\Big|_{\partial T_j} = 0$ for $\sigma_{bb} \in \mathcal{B}^3(\mathcal{T}_h)$ and $j = 1, \dots, nE$. Then for $j \in \{1, \dots, nE\}$ and $\ell \in \{1, \dots, nC\}$ we have that

$$(\partial_x b_{T_j}, \varphi_\ell) = -(b_{T_j}, \partial_x\varphi_\ell) = -\frac{|T_j|}{60}\partial_x\varphi_\ell \quad \text{and} \quad (\partial_y b_{T_j}, \varphi_\ell) = -(b_{T_j}, \partial_y\varphi_\ell) = -\frac{|T_j|}{60}\partial_y\varphi_\ell.$$

Listing A.2: H^1-flow for surfaces of prescribed mean curvature

```
1  function [U,energy] = h1_flow_plateau
2  % ---
3  addpath('auxiliary/','triangulation/');
4  % ---
5  [c4n,n4e,Db,¬,h] = mesh(ref);
6  nC = size(c4n,1); nE = size(n4e,1); tau = h;
7  % ---
8  dirichlet = unique(Db);
9  diriNodes_3 = [3*dirichlet - 2; 3*dirichlet - 1; 3*dirichlet - 0];
10 freeNodes = setdiff(1:(9*nC+6*nE),6*(nC+nE)+diriNodes_3);
11 % --- assemble matrices and initial data
12 [s,m,m_1bb,m_bb,grad_1,grad_1bb,div_1,div_1bb] = mixed_matrices(n4e,c4n);
13 [p,p_bb,u] = initial_data_plateau(n4e,c4n,Db,k);
14 % ---
15 while norm_corr > 1E-6
16     % --- assemble volume form
17     rhs_H = volume_form(n4e,c4n,u,H);
18     % --- compute correction
19     B =    tau*[m_6x6     m_1bb        div_1;
20                 m_1bb'    m_bb         div_1bb;
21                 div_1'    div_1bb'    -tau^(-1)*s];
22     y = -[ m_6x6*p+m_1bb*p_bb-grad_1*u;
23           m_1bb'*p+ m_bb*p_bb-grad_1bb*u;
24           div_1'*p+div_1bb'*p_bb-rhs_H];
25     x(freeNodes) = B(freeNodes,freeNodes)\y(freeNodes);
26     % --- update
27     mu = x(1:6*nC);
28     mu_bb = x((6*nC+1):(6*nC+6*nE));
29     w  = x((6*nC+6*nE+1):(6*nC+6*nE+3*nC));
30     p = p + tau*mu;
31     p_bb = p_bb + tau*mu_bb;
32     u = u + tau*w;
33     % --- compute norm of correction and discrete energy
34     norm_corr = sqrt(mu'*m_6x6*mu) + sqrt(mu_bb'*m_bb*mu_bb) + sqrt(w'*s*w);
35     energy(num+1) = 1/2*p'*m_6x6*p + 1/2*p_bb'*m_bb*p_bb + 1/3*rhs_H'*u;
36     % --- export surface
37     U = [u(1:3:3*nC) u(2:3:3*nC) u(3:3:3*nC)];
38     exportvtk('pictures/plateau_', n4e,U,num);
39 end
```

MATLAB code for the H^1-flow for surfaces of prescribed mean curvature. The computation of the nonlinearity in line 17 is sourced out to the function `volume_form.m`, see A.3.

Listing A.3: Volume form

```
function val = volume_form(n4e,c4n,u,H)
nC = size(c4n,1);nE = size(n4e,1);
[area_T,Dphi_T] = nodal_basis(c4n,n4e);
% --- compute piecewise gradient on elements
U = [u(1:3:3*nC) u(2:3:3*nC) u(3:3:3*nC)];
nabla_u_1 = zeros(nE,3); nabla_u_2 = zeros(nE,3); nabla_u_3 = zeros(nE,3);
for k = 1 : 3
nabla_u_1 = nabla_u_1 + (U(n4e(:,k),1)*ones(1,3)).*P_Dphi_T(k:3:3*nE,:);
nabla_u_2 = nabla_u_2 + (U(n4e(:,k),2)*ones(1,3)).*P_Dphi_T(k:3:3*nE,:);
nabla_u_3 = nabla_u_3 + (U(n4e(:,k),3)*ones(1,3)).*P_Dphi_T(k:3:3*nE,:);
end
% --- assemble partial derivatives and cross product
dx_u = [nabla_u_1(:,1) nabla_u_2(:,1) nabla_u_3(:,1)];
dy_u = [nabla_u_1(:,2) nabla_u_2(:,2) nabla_u_3(:,2)];
cross_elem = reshape(repmat(area_T/3,1,3)',3*nE,1).*reshape(cross(dx_u,dy_u)',3*nE,1);
X_cross_1 = repmat(cross_elem(1:3:3*nE),1,3);
X_cross_2 = repmat(cross_elem(2:3:3*nE),1,3);
X_cross_3 = repmat(cross_elem(3:3:3*nE),1,3);
% --- use accumarray for load vector defined by volume form
diag_1 = accumarray(n4e(:),X_cross_1(:),[nC,1]);
diag_2 = accumarray(n4e(:),X_cross_2(:),[nC,1]);
diag_3 = accumarray(n4e(:),X_cross_3(:),[nC,1]);
diag_rhs = reshape([diag_1,diag_2,diag_3]',3*nC,1);
val = 2*H*diag_rhs;
```

The function `volume_form` provides the load vector

$$\mathrm{val}(k) := 2\int_{B_h} H_0 \partial_x u_h^i \times \partial_y u_h^i \varphi_k \,\mathrm{d}x,$$

for $k = 1, \ldots, nC$ using the MATLAB function `accumarray`.

Listing A.4: Helfrich flow

```
function helfrich
format long
addpath('auxiliary','triangulations');
% --- get triangulation of the sphere
[c4n,n4e] = sphere_mesh;
nC = size(c4n,1)
tau = 1E-2; eps = 1E-5;
% --- compute initial curvature
kappa = comp_ini_kappa(c4n,n4e);
X = reshape(c4n',3*nC,1);
l2_v = inf; number = 1;
while l2_v > eps
    % --- assemble stiffness matrix and solve linear system
    w = averaged_normal(c4n,n4e);
    [m,s,S,M_nu,m_w] = helfrich_matrices(c4n,n4e,w);
    m_kappa = spdiags(diag(m).*kappa.^2,0,nC,nC);
    A = [M_nu',-tau*(s+m_kappa/2);S,M_nu];
    b = [-tau*m_w*kappa+M_nu'*X;zeros(3*nC,1)];
    xx = A\b;
    % --- compute velocities (V_W,V_V,V_A)
    V_W = (xx(1:3*nC)-X)/tau;
    V_V = -reshape(w',3*nC,1);
    kappa_vec = repmat(kappa,1,3).*w;
    V_A =  reshape(kappa_vec',3*nC,1);
    % --- use newton's method to compute normal velocity
    rho = newton_av(c4n,n4e,V_W,V_V,V_A,tau);
    V = V_W + rho(1)*V_A + rho(2)*V_V;
    v = sum(reshape(V',3,nC)'.*w,2);
    % --- update surface and curvature
    kappa = xx(3*nC+(1:nC));
    X = X+tau*V;
    c4n = reshape(X',3,nC)';
    % --- compute energy and normal velocity and export surface
    l2_surf = sqrt(v'*m*v);
    energy(number+1) = 1/2 kappa'*m*kappa;
    exportvtk('pictures/helfrich_', n4e,c4n,number,kappa);
    number = number+1;
end
```

MATLAB realization of the Helfrich-flow. The matrices `M_nu` and `m_w` provided by the function `helfrich_matrices` correspond to

$$(X_h \bullet \nu_h^i, v_h) \quad \text{and} \quad (\xi_h |\nabla \nu_h^i|^2, v_h),$$

for $\xi_h, v_h \in \mathcal{S}^1(\mathcal{T}_h)$, $X_h \in [\mathcal{S}^1(\mathcal{T}_h)]^3$ and the averaged unit normal $\nu_h^i \in [\mathcal{S}^1(\mathcal{T}_h)]^3$. We compute the velocities `V_W`, `V_V` and `V_A` as explained in Section 6.1.3 and `rho` using Newton's method to update $X_h^{i+1} = X_h^i + \tau(V_W + \rho(1) * V_A + \rho(2) * V_V)$.

Listing A.5: Export data for visualization with Paraview

```
function exportvtk(surfactant_,n4e,c4n,vector_field,kappa,num)
nC = size(c4n,1); nE = size(n4e,1);
num = num2str(num);
% --- open surfactant_num.vtk and write header
fid = fopen([file_ num '.vtk'],'wt');
fprintf(fid,'# vtk DataFile Version 3.0\n');
fprintf(fid,'vtk output\n');
fprintf(fid,'ASCII\n');
fprintf(fid,'DATASET POLYDATA\n');
% --- export c4n and n4e
fprintf(fid,'POINTS %d float\n' , nC);
fprintf(fid,'%3.9f   %3.9f   %3.9f\n',reshape(c4n',3*nC,1));
fprintf(fid,'\n \nPOLYGONS %d %d\n', nE,4*nE);
fprintf(fid,'3   %d   %d   %d\n',reshape((n4e-1)',3*nE,1));
% --- add point data
fprintf(fid,'\nPOINT_DATA %d\n', nC);
fprintf(fid,'SCALARS kappa float 1\n');
fprintf(fid,'LOOKUP_TABLE my_table\n');
% --- add vector field and close file
fprintf(fid,'%3.5f\n',kappa);
fprintf(fid,'VECTORS director_field float\n');
fprintf(fid,'LOOKUP_TABLE my_table\n');
fprintf(fid,'%3.5f %3.5f %3.5f\n', vector_field);
fclose(fid);
```

Listing A.6: Sample of a Paraview-file

```
# vtk DataFile Version 3.0
vtk output
ASCII
DATASET POLYDATA
POINTS 1026 float
 0.677052347   -0.665897812   -0.002517212
 0.677916766    0.670060037    0.008580416
 ...
-0.798207066   -0.061880697   -0.521678825
-0.738116809    0.001172313   -0.608059816

POLYGONS 2048 8192
3     0   258   260
3     1   263   264
...
3   281   280     5
3   280   279     5

POINT_DATA 1026
SCALARS kappa float 1
LOOKUP_TABLE my_table
-2.20045
-2.29372
...
-2.09172
-2.11694

VECTORS director float
 0.75465  -0.65589   0.01783
 0.70858   0.70508   0.02766
...
-0.83928  -0.03745  -0.54241
-0.77389   0.02983  -0.63262
```

Sample of a `vtk`-file for a mesh with $nC = \operatorname{card}\mathcal{N}_h = 1026$ and $nE = \operatorname{card}\mathcal{T}_h = 2048$. To every node two values are assigned: A scalar `kappa` and a three dimensional vector field `director`.

Bibliography

[1] Alouges, F. A new algorithm for computing liquid crystal stable configurations: the harmonic mapping case. *SIAM J. Numer. Anal. 34*, 5 (1997), 1708–1726.

[2] Alt, H.-W. Vorlesung Analysis III. *Skript der Vorlesung im WS 2001/02*. Institut für Angewandte Mathematik, Universität Bonn.

[3] Alt, H. W. *Lineare Funktionalanalysis*. Springer-Verlag Berlin Heidelberg, 2006.

[4] Arnold, D. N., Brezzi, F., and Fortin, M. A stable finite element for the Stokes equations. *Calcolo 21*, 4 (1984), 337–344 (1985).

[5] Ball, J. M., and Zarnescu, A. Orientability and energy minimization for liquid crystal models. *Mol. Cryst. Liq. Cryst. 495* (2008), 573–585.

[6] Bänsch, E., Morin, P., and Nochetto, R. H. A finite element method for surface diffusion: the parametric case. *J. Comput. Phys. 203*, 1 (2005), 321–343.

[7] Barrett, J. W., Bartels, S., Feng, X., and Prohl, A. A convergent and constraint-preserving finite element method for the p-harmonic flow into spheres. *SIAM J. Numer. Anal. 45*, 3 (2007), 905–927.

[8] Barrett, J. W., Bartels, S., Feng, X., and Prohl, A. A convergent and constraint-preserving finite element method for the p-harmonic flow into spheres. *SIAM J. Numer. Anal. 45*, 3 (2007), 905–927.

[9] Barrett, J. W., Garcke, H., and Nürnberg, R. On the parametric finite element approximation of evolving hypersurfaces in $\mathbb{R}^3$. *J. Comput. Phys. 227*, 9 (2008), 4281–4307.

[10] Barrett, J. W., Garcke, H., and Nürnberg, R. Parametric approximation of Willmore flow and related geometric evolution equations. *SIAM J. Sci. Comput. 31*, 1 (2008), 225–253.

[11] Bartels, S. Stability and convergence of finite-element approximation schemes for harmonic maps. *SIAM J. Numer. Anal. 43*, 1 (2005), 220–238 (electronic).

[12] Bartels, S. *Finite element approximation of harmonic maps betweeen surfaces*. Habilitation thesis, Humboldt Universität zu Berlin, Berlin, Germany, 2009.

[13] Bartels, S. Numerical analysis of a finite element scheme for the approximation of harmonic maps into surfaces. *Math. Comp. 79*, 271 (2010), 1263–1301.

[14] Bartels, S. Finite element approximation of large bending isometries. 2011.

[15] Bartels, S., Dolzmann, G., and Nochetto, R. H. A finite element scheme for the evolution of orientational order in fluid membranes. *M2AN Math. Model. Numer. Anal.* (2009).

[16] Bartels, S., Dolzmann, G., Nochetto, R. H., and Raisch, A. Finite element methods for director fields on flexible surfaces. 2011.

[17] Bartels, S., and Prohl, A. Constraint preserving implicit finite element discretization of harmonic map flow into spheres. *Math. Comp. 76*, 260 (2007), 1847–1859 (electronic).

[18] Bauer, M., and Kuwert, E. Existence of minimizing Willmore surfaces of prescribed genus. *Int. Math. Res. Not.*, 10 (2003), 553–576.

[19] Baumgart, T., Hess, S. T., and Webb, W. W. Imaging co-existing domains in biomembrane models coupling curvature and tension. *Nature 425* (2003), 832–824.

[20] Bethuel, F., Brezis, H., and Hélein, F. *Ginzburg-Landau vortices*. Progress in Nonlinear Differential Equations and their Applications, 13. Birkhäuser Boston Inc., Boston, MA, 1994.

[21] Bonito, A. N. R. H., and Pauletti, M. S. Parametric fem for geometric biomembranes. *Comput. Phys. 229* (2010), 3171–3188.

[22] Braess, D. *Finite elements*, third ed. Cambridge University Press, Cambridge, 2007. Theory, fast solvers, and applications in elasticity theory, Translated from the German by Larry L. Schumaker.

[23] Canham, P. B. The minimum energy of bending as a possible explanation of the biconcave shape of the human red blood cell. *J. Theort. Biol. 26* (1970), 61–81.

[24] Ciarlet, P. G. *The finite element method for elliptic problems*, vol. 40 of *Classics in Applied Mathematics*. Society for Industrial and Applied Mathematics (SIAM), Philadelphia, PA, 2002. Reprint of the 1978 original [North-Holland, Amsterdam; MR0520174 (58 #25001)].

[25] Coifman, R., Lions, P.-L., Meyer, Y., and Semmes, S. Compensated compactness and Hardy spaces. *J. Math. Pures Appl. (9) 72*, 3 (1993), 247–286.

[26] Deckelnick, K., Dziuk, G., and Elliott, C. M. Computation of geometric partial differential equations and mean curvature flow. *Acta Numer. 14* (2005), 139–232.

[27] Droske, M., and Rumpf, M. A level set formulation for Willmore flow. *Interfaces and Free Boundaries 6*, 3 (2004), 361–378.

[28] Du, Q., Liu, C., and Wang, X. A phase field approach in the numerical study of the elastic bending energy for vesicle membranes. *J. Comput. Phys. 198*, 2 (2004), 450–468.

[29] Dǒgan, G., and Nochetto, R. H. First variation of the general curvature-dependent surface energy. *Model. Math. Anal. Numer.* (2011).

[30] Dziuk, G. An algorithm for evolutionary surfaces. *Numer. Math. 58* (1991), 603–611.

[31] Dziuk, G. Computational parametric Willmore flow. *Numer. Math. 111*, 1 (2008), 55–80.

[32] Dziuk, G., and Elliott, C. M. Finite elements on evolving surfaces. *IMA J. Numer. Anal. 27*, 2 (2007), 262–292.

[33] Dziuk, G., and Hutchinson, J. E. Finite element approximations to surfaces of prescribed variable mean curvature. *Numer. Math. 102*, 4 (2006), 611–648.

[34] Eells, J., and Lemaire, L. Another report on harmonic maps [Bull. London Math. Soc. 20 (1988), no. 5, 385–524; MR0956352 (89i:58027)]. 69–208.

[35] Eells, J., and Lemaire, L. A report on harmonic maps [Bull. London Math. Soc. 10 (1978), no. 1, 1–68; MR0495450 (82b:58033)]. 1–68.

[36] Elliott, C. M., and Stinner, B. Modeling and computation of two phase geometric biomembranes using surface finite elements. *J. Comput. Phys. 229*, 18 (2010), 6585–6612.

[37] Elliott, C. M., and Stinner, B. A surface phase field model for two-phase biological membranes. *SIAM J. Appl. Math. 70*, 8 (2010), 2904–2928.

[38] Evans, E. Bending resistance and chemically induced moments in membrane bilayers. *Biophys. J. 14* (1974), 923–931.

[39] Fournier, J. B., and Galatoa, P. Sponges, tubules and modulated phases of paraantinematic membranes. *J. Phys. II 7* (1997), 1509–1520.

[40] Freire, A., Müller, S., and Struwe, M. Weak compactness of wave maps and harmonic maps. *Ann. Inst. H. Poincaré Anal. Non Linéaire 15*, 6 (1998), 725–754.

[41] Gulliver, I. R. D. Regularity of minimizing surfaces of prescribed mean curvature. *Ann. of Math. (2) 97* (1973), 275–305.

[42] Harbrecht, H. On the numerical solution of Plateau's problem. *Appl. Numer. Math. 59*, 11 (2009), 2785–2800.

[43] Heinz, E. Über die Regularität schwacher Lösungen nichtlinearer elliptischer Systeme. *Nachr. Akad. Wiss. Göttingen Math.-Phys. Kl. II*, 1 (1986), 1–15.

[44] Hélein, F. *Harmonic maps, conservation laws and moving frames*, second ed., vol. 150 of *Cambridge Tracts in Mathematics*. Cambridge University Press, Cambridge, 2002. Translated from the 1996 French original, With a foreword by James Eells.

[45] Helfrich, W. Elastic properties of lipid bilayers: theory and possible experiments. *Z. Naturforsch. C 28* (1973), 693–703.

[46] Hildebrandt, S. Nonlinear elliptic systems and harmonic mappings. In *Proceedings of the 1980 Beijing Symposium on Differential Geometry and Differential Equations, Vol. 1, 2, 3 (Beijing, 1980)* (Beijing, 1982), Science Press, pp. 481–615.

[47] Hildebrandt, S. Quasilinear elliptic systems in diagonal form. In *Systems of nonlinear partial differential equations (Oxford, 1982)*, vol. 111 of *NATO Adv. Sci. Inst. Ser. C Math. Phys. Sci.* Reidel, Dordrecht, 1983, pp. 173–217.

[48] Hu, Q., Tai, X.-C., and Winther, R. A saddle point approach to the computation of harmonic maps. *SIAM J. Numer. Anal. 47*, 2 (2009), 1500–1523.

[49] Isenberg, C. *The science of soap films and soap bubbles*. Dover science book. Dover Publications, 1992.

[50] Jäger, W., and Kaul, H. Uniqueness and stability of harmonic maps and their Jacobi fields. *Manuscripta Math. 28*, 1-3 (1979), 269–291.

[51] Jenkins, J. T. The equations of mechanical equilibrium of a model membrane. *SIAM J. Appl. Math. 32*, 4 (1977), 755–764.

[52] Johnson, M. A., and Decca, R. S. Dynamics of topological defects in the l_β' phase of 1, 2-dipalmitoyl phosphatidylcholine bilayers. *Optics Communications 281* (2008), 1870–1875.

[53] Khairy, K., Foo, J., and Howard, J. Shapes of red blood cells: Comparison of 3d confocal images with the bilayer-couple model. *Cellular and Molecular Bioengineering 1* (2008), 173–181. 10.1007/s12195-008-0019-5.

[54] Kuwert, E., and Schätzle, R. The Willmore flow with small initial energy. *J. Differential Geom. 57*, 3 (2001), 409–441.

[55] Laradji, M., and Mouritsen, O. G. Elastic properties of surfactant monolayers at liquid-liquid interfaces: A molecular dynamics study. *J. Chem. Phys. 112*, 19 (2000), 8621–8630.

[56] Lee, J. M. *Riemannian manifolds*, vol. 176 of *Graduate Texts in Mathematics*. Springer-Verlag, New York, 1997. An introduction to curvature.

[57] Lee, J. M. *Introduction to smooth manifolds*, vol. 218 of *Graduate Texts in Mathematics*. Springer-Verlag, New York, 2003.

[58] Lin, F., and Liu, C. Static and dynamic theories of liquid crystals. *J. Partial Differential Equations 14*, 4 (2001), 289–330.

[59] Lions, P.-L. The concentration-compactness principle in the calculus of variations. The limit case. I and II. *Rev. Mat. Iberoamericana 1*, 2 (1985), 45–121.

[60] Lipowsky, R., Döbereiner, H.-G., Hiergeist, C., and Indrani, V. Membrane curvature induced by polymers and colloids. *Physica A 249* (1998), 536–543.

[61] Lowengrub, J. S., Rätz, A., and Voigt, A. Phase-field modeling of the dynamics of multicomponent vesicles: spinodal decomposition, coarsening, budding, and fission. *Phys. Rev. E (3) 79*, 3 (2009), 0311926, 13.

[62] Mayer, U. F., and Simonett, G. A numerical scheme for axisymmetric solutions of curvature-driven free boundary problems, with applications to the Willmore flow. *Interfaces Free Bound. 4*, 1 (2002), 89–109.

[63] Müller, S., and Rumpf, M. A course on analysis and computation of nonlinear pde. *Lecture Notes, Winter Term 2010/11*. Institute for Numerical Simulation, Universität Bonn.

[64] Müller, S., Struwe, M., and Šverák, V. Harmonic maps on planar lattices. *Ann. Scuola Norm. Sup. Pisa Cl. Sci. (4) 25*, 3-4 (1997), 713–730 (1998). Dedicated to Ennio De Giorgi.

[65] Nagle, S. T.-N. J. F. Structure of lipid bilayers. *Biochim. Biophys. Acta 1469* (2000), 159–195.

[66] Olischläger, N., and Rumpf, M. Two step time discretization of Willmore flow. accepted at IMA Conference on the Mathematics of Surfaces.

[67] Raviart, P.-A., and Thomas, J. M. A mixed finite element method for 2nd order elliptic problems. In *Mathematical aspects of finite element methods (Proc. Conf., Consiglio Naz. delle Ricerche (C.N.R.), Rome, 1975)*. Springer, Berlin, 1977, pp. 292–315. Lecture Notes in Math., Vol. 606.

[68] Rivière, T. Conservation laws for conformally invariant variational problems. *Invent. Math. 168*, 1 (2007), 1–22.

[69] Seifert, U. Configurations of fluid membranes and vesicles. *Adv. Phys. 46* (1997), 13–137.

[70] Simon, L. Existence of surfaces minimizing the Willmore functional. *Comm. Anal. Geom. 1*, 2 (1993), 281–326.

[71] Struwe, M. Geometric evolution problems. In *Nonlinear partial differential equations in differential geometry (Park City, UT, 1992)*, vol. 2 of *IAS/Park City Math. Ser.* Amer. Math. Soc., Providence, RI, 1996, pp. 257–339.

[72] Struwe, M. *Variational methods*, fourth ed., vol. 34 of *Ergebnisse der Mathematik und ihrer Grenzgebiete. 3. Folge. A Series of Modern Surveys in Mathematics [Results in Mathematics and Related Areas. 3rd Series. A Series of Modern Surveys in Mathematics]*. Springer-Verlag, Berlin, 2008. Applications to nonlinear partial differential equations and Hamiltonian systems.

[73] Uchida, N. Dynamics of orientational ordering in fluid membranes. *Phys. Rev. E 66*, 4 (Oct 2002), 040902.

[74] Virga, E. G. *Variational theories for liquid crystals*, vol. 8 of *Applied Mathematics and Mathematical Computation*. Chapman & Hall, London, 1994.

[75] Wang, C. A compactness theorem of n-harmonic maps. *Ann. Inst. H. Poincaré Anal. Non Linéaire 22*, 4 (2005), 509–519.

[76] Wang, X., and Du, Q. Modelling and simulations of multi-component lipid membranes and open membranes via diffuse interface approaches. *J. Math. Biol. 56*, 3 (2008), 347–371.

[77] Willmore, T. J. *Riemannian geometry*. Oxford Science Publications. The Clarendon Press Oxford University Press, New York, 1993.

Zusammenfassung der Arbeit

Finite Element Methods for Geometric Problems

Alexander Raisch
Bonn, May 2012

In dieser Arbeit beschäftigen wir uns mit geometrischen partiellen Differentialgleichungen und deren Diskretisierung unter Verwendung von Finite Elemente Methoden. Geometrische partielle Differentialgleichungen treten in einer Vielzahl von physikalischen, technischen und biologischen Anwendungen auf und deren mathematische Behandlung erfreut sich seit einigen Jahren einer großen Beliebtheit.

Thematisch lässt sich die Arbeit in zwei Blöcke aufteilen. Im ersten Teil der die Kapitel zwei bis fünf umfasst geht es um die Approximation stationärer Punkte konform invarianter, nichtlinearer, elliptischer Energiefunktionale. Das Hauptaugenmerk liegt dabei auf einem Kompaktheitsresultat für Häufungspunkte der diskretisierten Energiefunktionale.
Die Euler Lagrange Gleichungen sind elliptisch und von zweiter Ordnung. Sie beinhalten kritische Nichtlinearitäten welche quadratisch von den ersten Ableitungen abhängen. Dies führt dazu, dass Häufungspunkte von Lösungen der diskretisierten Gleichung nicht zwangsläufig Lösungen der ursprünglichen Gleichung sind. Wir leiten eine schwache Formulierung der Gleichung in gemischter Form her und wählen stabile Finite Elemente Paare für die Diskretisierung. Zunächst zeigen wir, dass Lösungen der diskreten gemischten Formulierung Sattelpunkte eines erweiterten diskreten Energiefunktionals sind und schließen daraus auf die Existenz diskreter Lösungen. Um zu beweisen, dass Häufungspunkte der diskreten Sattelpunkte tatsächlich Lösungen der schwachen Formulierung sind bedienen wir uns eines Kompaktheitsresultats aus [68]. Dabei treten Fehlerterme diskreter Natur auf die mit Hilfe einiger Techniken aus [13] kontrolliert werden können. Schließlich stellen wir einen iterativen Algorithmus für die numerische Realisierung auf und führen mehrere Simulationen durch. Theoretische Stabilitätsergebnisse für den Algorithmus werden dabei numerisch bestätigt.

Im zweiten Teil stehen die Herleitung von Gradientenflüssen von Flächenfunktionalen (*shape functional*) sowie deren Diskretisierung unter Verwendung von Parametrischen Finite Elemente Methoden im Mittelpunkt.
Wir betrachten zunächst die sogenannte Willmore Energie einer zweidimensionalen Fläche im dreidimensionalen Raum und bestimmen deren erste Variation. Anschliessend formulieren wir den zugehörigen Gradientenfluss in schwacher Form und diskutieren eine Diskretisierung mittels parametrischer Finite Elemente. Dabei verwenden wir hauptsächlich ein in [10] entwickeltes Verfahren. Im weiteren Verlauf diskutieren wir die Modellierung von Zellmembranen und die Wirkung von oberflächenaktiven Substanzen, sogenannten Surfactants, auf die Form von Zellen. Zunächst untersuchen wir eine Linearisierung des Modells und treffen qualitative Aussagen über das Verhalten der Membrane in charakteristischen Fällen. Wir leiten eine geeignete schwache Formulierung der linearisierten Gleichung her und diskretisieren diese. Simulationen bestätigen die Vorhersagen der qualitativen Analyse. Dem nichtlinearen Fall zukehrend verwenden wir die Kenntnisse über parametrische Finite Elemente die wir zu Beginn des Abschnitts gewinnen konnten um eine geeignete Diskretisierung des Gradientflusses zu formulieren. Anschließende numerische Simulationen mit geschlossenen Flächen liefern viel versprechende Resultate und geben Anlass zu weiteren Forschungsarbeiten in diesem Bereich.